SEISMIC BEHAVIOR AND VULNERABILITY OF INDIAN RC FRAME BUILDINGS WITH URM INFILLS

Ph.D. THESIS

by

PUTUL HALDAR

DEPARTMENT OF EARTHQUAKE ENGINEERING
INDIAN INSTITUTE OF TECHNOLOGY ROORKEE
ROORKEE - 247667 (INDIA)
JULY, 2013

SEISMIC BEHAVIOR AND VULNERABILITY OF INDIAN RC FRAME BUILDINGS WITH URM INFILLS

A THESIS
Submitted in partial fulfilment of the requirements for the award of the degree of

DOCTOR OF PHILOSOPHY
in
EARTHQUAKE ENGINEERING

by

PUTUL HALDAR

DEPARTMENT OF EARTHQUAKE ENGINEERING
INDIAN INSTITUTE OF TECHNOLOGY ROORKEE
ROORKEE - 247667 (INDIA)
JULY, 2013

INDIAN INSTITUTE OF TECHNOLOGY ROORKEE
ROORKEE

CANDIDATE'S DECLARATION

I hereby certify that the work which is being presented in the thesis entitled "**SEISMIC BEHAVIOR AND VULNERABILITY OF INDIAN RC FRAME BUILDINGS WITH URM INFILLS**" in partial fulfilment of the requirements for the award of the Degree of Doctor of Philosophy and submitted in the Department of Earthquake Engineering of the Indian Institute of Technology Roorkee, Roorkee is an authentic record of my own work carried out during a period from August, 2008 to July, 2013 under the supervision of **Dr. Yogendra Singh,** Professor, and **Dr. D. K. Paul**, Emeritus Fellow, Department of Earthquake Engineering, Indian Institute of Technology Roorkee, Roorkee.

The matter presented in this thesis has not been submitted by me for the award of any other degree of this or any other Institute.

(PUTUL HALDAR)

This is to certify that the above statement made by the candidate is correct to the best of our knowledge.

(D. K. PAUL)
Supervisor

(YOGENDRA SINGH)
Supervisor

Date: July 08, 2013

The Ph. D. Viva-Voce Examination of **Ms. Putul Haldar**, Research Scholar, has been held on ……

Signature of Supervisors **Chairman, SRC** **External Examiner**

Head of the Department/Chairman, ODC

ABSTRACT

Reinforced Concrete (RC) framed buildings with Un-Reinforced Masonry (URM) infills are the most popular structural systems for multistory buildings in India and many other parts of the world. These buildings have shown poor performance during past earthquakes and suffered severe damage or collapse, even under moderate earthquakes. It is general practice to ignore the infills in design as the uncertainty in infill-frame interaction results in complex modes of failure, rendering the simulation of seismic behavior of infilled frames a challenging task. The behavior is further affected by the construction sequence of infilled frames, as the infills are usually added after completion of the frame, and it results in a gap between the infill and soffit of the beam above. Despite significant research effort dedicated to such buildings in the past decades, the understanding of seismic behavior of infilled frames is still not adequate and guidelines for modeling and analysis are lacking in the design codes. In this Thesis, a stock of available earthquake damage survey reports, experimental studies, analytical models and design codes, is taken to identify various failure modes of such buildings. A review of available models for estimating the strength of infills and frame members in various failure modes is also presented with an objective to identify the most reliable models.

A statistical exercise is carried out to select a representative building plan, based on the analysis of 50 buildings selected from a field survey, conducted earlier (DEQ 2009). The effect of infills and their construction sequence, on the seismic performance of generic RC buildings with the selected plan and designed as per relevant Indian Standards is studied. A comparative study of the available 1-, 2-, and 3-strut models is performed to examine their capability to predict the failure modes observed in post earthquake damage surveys and experimental studies. It is found that the single eccentric diagonal strut model has higher reliability in predicting the observed failure modes.

A macro-model is proposed to simulate the seismic behavior of URM infilled frames, which can be easily implemented on available software. The infills are modeled as eccentric diagonal struts connected to columns, with stiffness as defined in ASCE-41 (2007) and strength in various modes of failure is considered. Nonlinear ‘Gap’

elements are used to simulate the gap between the infill and the beam and to release the struts in tension. Sequential analysis is performed to take into account the construction sequence of infill panels relative to frames. It is observed that conventional simultaneous analysis ignoring the construction sequence may be highly erroneous and can almost nullify the effect of infills in some cases.

The complex behavior of infilled frames under lateral loading gets further complicated when infills are placed irregularly in plan and/or elevation to maximize the usage of available space. Mixed occupancy, lack of enforcement, and inadequate guidelines have resulted in a huge stock of seismically deficient irregular buildings throughout India. A survey (DEQ 2009) of multistorey buildings in the New Okhla Industrial Development Authority (NOIDA), a model township in the National Capital Region (NCR) in India, revealed that 95% of the surveyed buildings have ground storey open (without partitions) for parking and as many as 62% buildings suffer torsion irregularity. Taking a note of the widespread failure of buildings having irregularly placed infills, the seismic behavior and vulnerability of the three most common configurations of RC frames with irregular placement of infills, viz. open ground storey, front bay open in the ground storey, and three bays open in the ground storey, are studied.

Nonlinear Static Pushover analysis is performed to compare the seismic performance of Indian code designed RC frame buildings with and without URM infills. It is observed that the buildings, designed for gravity loads only, as per Indian Standards can generally survive seismic excitation up to MCE of Indian Seismic Zone IV (PGA = 0.24g), without collapse. However, inclusion of infills deteriorates the performance of RC frames significantly and the collapse of the gravity load designed infilled frame buildings is caused by brittle shear failure of column. It is observed that the open ground storey buildings designed for code (i.e. ground storey columns and beams designed for 2.5 times the normal base shear) is able to attain the stiffness and strength close to those of the corresponding uniformly infilled frame buildings and the estimated performance of such buildings is slightly better than the uniformly infilled frame buildings, indicating the adequacy of the code provisions for open ground storey buildings.

To study the seismic performance of buildings with asymmetric placement of infills in the ground storey, Incremental Dynamic Analysis is carried out using bi-directional

ground motions with a wide range of source and site parameters. The static capacity spectra are convoluted with the demand spectra to compare these with the dynamic capacity spectra. The convoluted static and dynamic capacity spectra match well and the ultimate drift ratio obtained from the two curves remain mostly the same, indicating that the strength and displacement parameters derived from static pushover curves, are comparable with IDA results.

Fragility curves of the studied buildings are developed using the different variabilities defined in HAZUS. Capacity of structure against “Incipient Collapse” damage state and variability in seismic demand are determined from the results of Incremental Dynamic Analysis. The comparative study of the fragility curves and Damage Probability Matrices suggest that URM infills result in significant increase in seismic vulnerability of RC frames. The vulnerability of infilled frames is further increased due to irregular placement of infills.

A comparative study of risk assessment methodologies based on macroseismic intensity and response spectrum approaches is also carried out. To facilitate the comparative study, a spreadsheet-based software tool ‘SeisVARA’ is developed using the vulnerability functions for Indian RC frames buildings with and without URM infills, developed in this Thesis. In this open software tool, seismic hazard can be specified either in terms of macroseismic intensity, or Peak Ground Acceleration in combination with the spectral shapes and soil amplification models of various earthquake design codes, or in terms of inelastic response spectra using the ‘Next Generation Attenuation Relationships’. A comparison of these different approaches is conducted for a typical city in northern India. Effect of different parameters, e.g. level of PGA, spectral shape, source-site parameters, and soil amplification models, on estimated loss, is also studied. It is observed that not only the different approaches result in widely varying damage and loss estimates, but also the variation of parameters within a given approach can result in considerable differences.

ACKNOWLEDGEMENT

I am taking this opportunity to express my deepest gratitude to the individuals without whose help, support and encouragement it would not have been possible to complete my thesis work.

At the very outset, I wish to thank my supervisor **Dr. Yogendra Singh**, Professor, Department of Earthquake Engineering, IIT Roorkee, for the support and encouragement I received from him at every stage of my research work. He has been the perfect teacher to me with his in-depth knowledge combined with a perspicacious approach, incisive criticism and a clear foresight. His every intervention has motivated me towards working hard and achieving my goals during the course of this thesis.

I wish to thank my co-supervisor **Dr. D. K. Paul**, Professor Emeritus, Department of Earthquake Engineering, IIT Roorkee, for his liberal guidance which I received in abundance. I could not have asked for a better role model, inspirational, supportive, and patient.

I wish to thank **Dr. Ajay Gairola**, Head, Centre of Excellence in Disaster Mitigation & Management, IIT Roorkee, **Dr. H. R. Wason**, Professor and former Head of the Department, and **Dr. M. L. Sharma**, Professor and Head, Department of Earthquake Engineering, IIT Roorkee, for extending their help in the best possible manner for carrying out my research work.

I sincerely acknowledge the financial support provided by **Ministry of Human Resource Development**, Govt. of India for this research work.

I would also like to thank **Dr. Dominik. H. Lang**, Senior Researcher, NORSAR International Centre of Geohazards (ICG), for his useful suggestions and help at various stages of my research work. I wish to express my gratitude to **Dr. Claus Milkereit,** GFZ German Research Centre for Geosciences, Helmholtz Centre Potsdam, for his spontaneous help whenever solicited.

I would like to thank **Dr. Vijay Namdev Khose**, **Mr. Phani Kumar Gade** and **Mr. Veereswara Rao Yeluguri** for their help and valuable discussion during my research work.

The members of the **Tea Club** have contributed immensely to my personal and professional time at IIT Roorkee. I would like to thank our Tea Club members Dr. Vijay Namdev Khose, **Dr. Ratnesh Kumar**, **Dr. J. S. R. Prasad** and our supervisor Dr. Yogendra Singh**,** who were always there with their warm, helpful and encouraging presence**.** Our rejuvenating evening tea breaks together were always a welcome break from the busy schedule.

I will always cherish the friendship and fond memories of my fellow research scholars. My special thanks are due to **Dr. Sumana Basu**, **Dr. Susmita Ghosh**, **Ms. Shreya Das**, **Ms. Arundhati Biswas**, **Mr. Sachin Kadam**, **Dr. Atanu Bhattacharya**, **Mr. Prabhat Kumar**, **Mr. Narshima D. S.**, **Mr. Govardhan**, **Mr. Rajeev Sachadeva**, **Mr. Anshu Tomar**, **Mr. Ranjit Das**, **Mr. S. Madni**, **Mr. H. Rangawala**, **Ms. Nivedita Mandal**, **Mr. Shounak Mitra** who have always helped me to face the hard work with a smile.

It is beyond my literary capability to express my indebtedness to my beloved parents **Smt. Sephali Halder** and **Shri Ganga Dhar Halder**, uncle **Shri Shankar Das Halder**, and aunt **Smt. Hena Halder**. These few words would not be sufficient to express my indebtedness to them for keeping faith on me. Their enormous support, constant inspiration, and unconditional love have always provided me a high mental support. Acknowledgement will not be complete without thanking my best friend **Waliul** for the very special person he is.

Finally, I wish to express my gratitude to all those well-wishers whose name are not mentioned here but have provided their unwavering support during my tenure at IIT Roorkee. This thesis would not have been a reality without any one of you. Thank you all for being with me with all your support whenever I needed.

Dated: July 08, 2013 (PUTUL HALDAR)

CONTENTS

LIST OF FIGURES

LIST OF TABLES

NOTATIONS

Symbols	Explanation
a	Equivalent width of the infill panel
A_c	Total effective area of the masonry infills
A_g	Gross cross-sectional area
A_i	Effective cross-sectional area of the masonry infills
A_n	Net grouted area of infill panel
a_s	Site class factor
A_v	Spacing of transverse reinforcement
b	Plan dimension of building perpendicular to the direction of ground motion
b_j	Effective width of joint
B_i	Observed median demand drift
C_i	Power law predicted median demand drift
C	Compressive force
C_0	Modification factor to relate spectral displacement of an equivalent single degree of freedom (SDOF) system to the roof displacement of the building
C_1	Modification factor to relate expected maximum inelastic displacements to displacements calculated for linear elastic response
C_2	Modification factor to represent the effect of pinched hysteresis shape, cyclic stiffness degradation on maximum displacement response
d	Depth of column
D	Base dimension of building
d_m	Diagonal length of the infill
ds	Particular damage state for a given spectral displacement
D_u	Ultimate displacements

Symbols	Explanation
D_y	Yield displacements
E_c	Modulus of elasticity of concrete
E_s	Modulus of elasticity of steel
E_{fe}	Expected modulus of elasticity of frame material (concrete)
E_{me}	Expected modulus of elasticity of infill material
e	Static eccentricity
e_d	Design eccentricity
e_a	Accidental eccentricity
e_s	Static eccentricity due to non coincidence of centre of mass and centre of stiffness
E_s	Modulus of elasticity of steel
E_c	Modulus of elasticity of concrete
E_f	Young's modulus of infill material
E	Modulus of elasticity of concrete
f_a	Compressive strength of infill
f'_{bs}	Bond shear strength between the masonry and mortar
f_{ck}	Characteristic strength of concrete
f'_c	Concrete compressive strength (cylinder)
f'_m	Compressive strength of infill material
f_s	Stress in reinforcing steel
f_y	Yield stress in reinforcing steel
f'_t	Tensile strength of infills
f'_v	Shear strength of masonry
f_{st}	Vertical compressive stress

Symbols	Explanation
f_{yv}	Yield strength of transverse reinforcement
g	Acceleration due to gravity
h	Height of column between center line of beams
h'	Height of infill panel
H	Height of the building
h_c	Depth of joint
h_{col}	Column height between centerlines of beams
$h_{\inf}$	Height of infill panel
I	Importance factor
I_{col}	Moment of inertia of column
I_g	Moment of inertia of gross concrete cross section
L	Total length of frame in the considered direction
l	Length of frame
$L_{\inf}$	Length of infill panel
l_{wi}	Length of the i^{th} infill in the first storey
L_s	Radius of gyration of the floor in plan
M_b	Nominal flexural strength of beam
M_c	Nominal flexural strength of column
M_{pb}	Plastic moment capacity of beam
M_{pc}	Plastic moment capacity of column
M_{ij}	Mean value of intensity for a given damage state *i* and building type *j*
σ_{ij}	Standard deviation for a given damage state *i* and building type *j*
M/V	Largest ratio of moment to shear under design loadings for the column
$M-R$	Magnitude-distance pair
n	Number of storeys

Symbols	Explanation
N	Number of ground motion records
N_d	Number of sample demand data points
P	Axial load on column
P_0	Axial force on column under gravity load alone
$P / A_g f'_c$	Axial Load Ratio
q	Behavior factor
r	Torsional radius
R_1	Reduction factor for presence of opening in infill panel
R_2	Reduction factor for existing damage in infilled frame
r_{inf}	Diagonal length of infill panel
R	Response reduction factor
R_c	Strength of infills in diagonal compression
R_{cr}	Strength of infills in corner crushing
R_s	Diagonal force to initiate bed-joint sliding in infill panel
R_t	Strength of infills in diagonal tension
$R\cos\theta$	Shear force exerted by infill
$R_{\mu d}$	Response reduction factor for ductility
s^2	Standard error
S	Spacing of transverse reinforcement
S_a	Spectral acceleration
S_{ay}	Yield spectral acceleration
S_{au}	Ultimate spectral acceleration
S_d	Spectral displacement
$\overline{S}_{d,ds}$	Median value of spectral displacement

Symbols	Explanation
S_{di}	Inelastic spectral displacement
S_{dy}	Yield spectral displacement
S_{du}	Ultimate spectral displacement
S_s	Shear span
t	Thickness of infill panel
t_{inf}	Thickness of infill panel and equivalent strut
T	Tensile force
T_a	Period or initial period
T_1	Fundamental period of a structure
T_e	Effective fundamental period
V_B	Base shear obtained analytically
$\overline{V_B}$	Base shear calculated using the empirical design period
V_{Ed}	Seismic shear forces acting on vertical primary seismic members of a storey
V_c	Shear force in column
V_{jh}	Shear force in joint
V_n	Shear strength of column
V_s	Shear strength provided by the hoops
V_y	Yield base shear corresponding to yield displacement
V_u	Ultimate base shear corresponding to ultimate displacement
$V_{s,30}$	Average shear wave velocity in the top 30 m
W	Effective seismic weight
W_i	Weight lumped at i^{th} element
Z	Zone factor

Symbols	Explanation
α	Contact length between frame and infill
α_b	Normalized contact length of beam-infill
α_c	Normalized contact length of column-infill
α_m	Modal mass participation factor
μ	Coefficient of internal friction between the masonry and mortar
λh	Stiffness of frame relative to infill
μ_d	Ductility
μ_s	Maximum storey ductility demand
β	Dispersion from the median of ground motion records
β_M	Modelling uncertainty
$\beta_{M(ds)}$	Variability associated with the discrete threshold of the damage state
β_D	Variability associated with the demand spectrum
β_C	Variability associated with capacity curve
β_{ds}	Lognormal standard deviation parameter that describes the total variability of damage state
$\beta_{D(S_a)}$	Seismic demand uncertainty
β_T	Total uncertainty
γ	Nominal strength coefficient based on joint geometry and amount of transverse reinforcement
γ_1	Coefficients to account for anchorage efficiency in beam reinforcement
γ_2	Coefficients to account for axial force in column
γ_3	Coefficients to account for slenderness of joint
Δ	Roof displacement
ϕ_{roof}	Modal shape coefficient for roof
ϕ_i	Modal shape coefficient for i^{th} floor

Symbols	Explanation
Δ_{eff} / h_{eff}	Drift ratio
Δ_{roof}	Target displacement at roof level
Δ_y	Yield displacement obtained from idealized bi-linear pushover curve
$\delta_{\max}$	Maximum storey drift
δ_{avg}	Average storey drift
ΔV_{RW}	Total reduction in the resistance of masonry walls
η	Amplification factor to consider non-uniform distribution of infills
ψ	PSI intensity
σ	Standard deviation of the cube strength of concrete
θ	Slope of equivalent diagonal strut from horizontal
θ'	Sloping angle of masonry diagonal strut at shear failure
Φ	Standard normal cumulative probability distribution function
Γ	Modal participation factor for the pushover mode
ρ_w	Area of flexural tension reinforcement
λ_c	Natural logarithm of median drift capacity for a given limit state
λ_{D/S_a}	Natural logarithm of calculated median demand drift for given spectral acceleration
υ	Basic shear strength of bed joints of masonry
K_{xi} , K_{yi}	Stiffness of i^{th} lateral load resisting frame/element in longitudinal and transverse directions
x_i, y_i	Coordinates of the centre of the i^{th} load resisting frame/element along longitudinal and transverse directions
r_x , r_y	Torsional radius along longitudinal and transverse direction
$\bar{x}_i$, $\bar{y}_i$	Distances of the i^{th} load resisting element from the centre of stiffness
X_r , Y_r	Coordinates of center of stiffness
X_m , Y_m	Coordinates of center of mass

ABBREVIATIONS

Symbols	Explanation
ADRS	Acceleration-Displacement Response Spectrum
ATC	Applied Technology Council
BL	Bilinear
C	Conforming
CONV	Convolution
COV	Coefficient of Variation
CP	“Collapse Prevention” performance level
CS	Cracked Section
CSM	Capacity Spectrum Methodology
DBD	Displacement-Based Design
DBE	Design Basis Earthquake
DCM	Displacement Coefficient Method
DM	Damage Measure
DMM	Displacement Modification Method
DPM	Damage Probability Matrix
EL	Equivalent Linearization
ELE	Earthquake Loss Estimation
ELM	Equivalent Linearization Method
EMS	European Macroseismic Scale
EPGA	Effective Peak Ground Acceleration
ERD	Earthquake Resistant Design
FBD	Force-Based Design
GLD	Gravity Load Designed
GMPE	Ground Motion Prediction Equation
GS	Gross Section

Symbols	Explanation
IC	Incipient Collapse
IDA	Incremental Dynamic Analysis
IM	Intensity Measure
IMRF	Intermediate Moment Resisting Frames
IO	"Immediate Occupancy" performance level
ISE	Inelastic Spectrum Estimation
IVARA	Seismic **V**ulnerability **A**nd **R**isk **A**ssessment of **I**ndian Housing
LS	"Life Safety" performance level
MBT	Model Building Type
MCE	Maximum Considered Earthquake
MCFT	Modified Compression Field Theory
MSK	Medvedev-Sponheuer-Karnik scale
NC	Nonconforming
NCR	National Capital Region
NDA	Nonlinear Dynamic Analysis
NGA	Next Generation Attenuation Relationships
NOIDA	New Okhla Industrial Development Authority
NSA	Nonlinear Static Analysis
NSP	Nonlinear Static Procedure
O1B	Open Front Bay in the Ground Storey
O3B	Open Three Bays in the Ground Storey
OG	Open Ground Storey
OG (C)	Open Ground Storey Designed as SMRF with Considering Provisions of BIS (2002) for Open Ground Storey Buildings
OG (NC)	Open Ground Storey Designed as SMRF without Considering Provisions of BIS (2002) for Open Ground Storey Buildings
OMRF	Ordinary Moment Resisting Frame
PBD	Performance-Based Design
PGA	Peak Ground Acceleration

Symbols	Explanation
PSI	Parameterless scale of Seismic Intensity
RC	Reinforced Concrete
SDOF	Single Degree of Freedom
SeisVARA	**Sei**smic **V**ulnerability **A**nd **R**isk **A**ssessment
SMRF	Special Moment Resisting Frame
SRSS	Square-Root-of-Sum-of-the Squares
UI	Uniform Infills
URM	Un-Reinforced Masonry

Chapter 1

INTRODUCTION

1.1 GENERAL

Reinforced Concrete (RC) moment-resisting frame buildings, with Un-Reinforced Masonry (URM) infills for interior and exterior partitions, are one of the most popular structural systems for multi-storey buildings in India and in many other parts of the world. Despite the fact that URM infills are very inhomogeneous in nature, leading to behavioral complexity and highly unpredictable failure mechanism of infilled frame buildings (Paulay and Priestley 1992), URM is the most preferred partition material by the virtue of its mould-ability, effective thermal, moisture, and acoustic insulation properties, ease of construction, and cost effectiveness.

Although, it is widely recognized for long (Smith 1966; Schriver 1989; Paulay and Priestley 1992; Singh et al. 1998; Sahota and Riddington 2001) that URM infills interact with and modify the seismic behavior of frame buildings, in usual design practice, URM infills are treated as non-structural elements and their stiffness, strength, and interaction with frames are often ignored. A number of factors are responsible for this practice, mostly related to the uncertainty and difficulty in simulating the behavior of infilled frames. These include highly variable mechanical properties of infill materials, variable infill-frame interaction (Shing et al. 1992; Mehrabi et al. 1996) leading to complex failure mechanism of infilled frames under lateral loading, absence of computation and time inexpensive modeling guidelines for infills, and moreover, the misleading assumption that infills will only provide additional strength, stiffness and damping, which will result in improved performance. Considering the complexity of infill-frame interaction, most of the design codes are silent about modeling and design of infilled frames. Interestingly, infills do not affect the behavior of the buildings under gravity load, as these do not participate in resisting gravity load. However, it is evident from past earthquakes (GSI 1995; DEQ 1999; EERI 2002; GSI 2003) that the behavior of the frames under lateral loads gets totally changed due to infills, and mostly leads to undesired structural performance in the event of an earthquake.

The behavior of RC frame with URM infills is further affected by the construction sequence of infilled frames. Traditionally, infill panels in framed buildings are provided after the frame is completed, at least for a few storeys. The construction sequence of infill panels relative to RC frame, followed in India is shown in Fig. 1.1. Figs. 1.1 (a) shows an intermediate stage of construction of infill panels in RC frames, whereas Figs. 1.1 (b) shows the final stage.

(a) (b)

(c)

Fig. 1.1 Photographs showing typical construction sequence of an infilled frame building: (a) intermediate stage, (b) final stage of construction, (c) gap between infills and beam due to construction sequence of infilled frames.

The construction sequence of infilled frames leads to a gap between the infill panel and the beam above. This gap spares the infill panels from resisting any gravity load

coming to the frame. Even relatively small initial gap can have significant effect on the structural behavior of infilled frames (Riddington 1984). According to Moghaddam and Dowling (1987), parameters like initial lack of fit between infill and frame, and workmanship might have even higher impact on the strength of infilled frame than the parameters like strength and stiffness of infills.

The complex behavior of infilled frame under lateral loading gets further complicated when infills are placed irregularly in plan and/or elevation to maximize the usage of available space. Mixed occupancy, lack of enforcement, and inadequate guidelines have resulted in a huge stock of seismically deficient irregular buildings throughout India. A Pilot survey (DEQ 2009) of multistorey buildings in the New Okhla Industrial Development Authority (NOIDA), a model township in the National Capital Region (NCR) in India, revealed that 95% of the surveyed buildings have ground storey open (without partitions) for parking (Fig. 1.2). Taking a note of the widespread failure of open ground storey buildings (Fig. 1.2 (b)) during Bhuj earthquake of January 26, 2001 like many other parts of the world (Naiem 1989; Wallace 1999; MCEER 2000; Sezen et al. 2003; Dogangun 2004; Inel et al. 2008), the Indian standard revised in 2002 (BIS 2002) included an amendment requiring the beams and columns of the open ground storeys to be designed for 2.5 times the design base shear for corresponding uniformly infilled frame buildings. However, the efficacy of this provision needs to be examined.

(a) (b)

Fig. 1.2 (a) Typical Indian multi-storey buildings with ground storey kept open for parking; (b) failure due to soft/weak storey phenomenon in an open ground storey building during 2001 Bhuj earthquake.

(a) (b)

Fig. 1.3 Typical Indian multi-storey residential cum commercial buildings: (a) front kept open for commercial purpose; (b) front kept open and no interior partitions in the ground story, to provide larger spaces for storage.

Due to lack of regulations, a sizeable number of the residential buildings in India are also being used for mixed occupancy, where the ground storey is used for commercial purpose and the upper storeys for residential purpose. The commercial usage demands for larger free spaces without partitions, and open front and/or sides (Fig. 1.3). This makes the buildings highly irregular, resulting in excessive torsion leading to ground storey failure (Fig. 1.4).

(a) (b)

Fig. 1.4 (a) Failure of buildings due to irregular placement of infills during 2011 Sikkim earthquake; (b) ground story failure due to torsion effect during 2007 Peru earthquake (Johansson et al. 2007).

The widespread failure of URM infilled RC frame buildings and consequent extensive physical and social losses, during the 2001 Bhuj earthquake, the first large earthquake in India affecting urban areas, highlighted the need for vulnerability assessment of the huge existing stock of such buildings in Indian cities. As systematic data on damage of such buildings during past earthquakes, is lacking, analytical investigation based on reliable estimation of capacity of such buildings is the only available option. In spite of intensive research effort of several decades (Ockleston 1955; Klinger and Bertero 1978; Paulay and Priestley 1992; Mehrabi and Shing 1994; Al-Chaar 2002; Asteris et al. 2011) to understand the behaviour of RC frames with URM infills, assessing the seismic performance of masonry-infilled RC frames remains a challenging task, because of difficulties in modeling the complex infill-frame interaction. Uncertainties in estimation of strength and ductility of URM infills in different failure modes, change in axial force and consequent change in stiffness and strength of columns with lateral sway, and strength and stiffness degradation under lateral loading, make the task of simulation of seismic behavior of infilled frames even more challenging. In developing countries like India, the challenge is further increased due to strength and detailing deficiencies in the existing (as well as newly constructed) buildings, resulting in several undesired modes of failure. Many of these buildings are not designed for earthquake forces at all, whereas in some other cases, earthquake forces might have been considered in analysis but detailing and construction do not comply with the standard specifications.

The present study has attempted to identify different failure modes in URM infilled RC frame buildings, based on the observations from past earthquakes and experimental studies. Various models for estimating capacity of RC frame members, infills, and infilled frames, in different modes are also examined and the models resulting in realistic prediction of failure modes are identified. The chosen models are used to estimate the capacity curves and fragility functions for URM infilled frames with different design levels as per Indian codes, and having design, detailing, and configurationally deficiencies prevalent in Indian constructions. Finally, the estimated fragility functions have been implemented in a user-friendly software tool for estimating seismic risk. The software closely follows the HAZUS methodology (FEMA 1999, 2003, 2006) and can be used to estimate seismic risk for any hazard scenario represented by Macro-seismic Intensity, or PGA/spectrum, or source site

parameters in the Next Generation Attenuation (NGA) relationships (Bozorgnia et al. 2010a; Bozorgnia et al. 2010b).

1.2 NEED FOR THE STUDY

Seismic safety of the built environment in seismically active regions has been on the national and international agenda, since earthquakes have been identified to be a serious threat to human development. As URM infilled RC frame buildings constitute the majority of the existing building stock in urban India, study of seismic behavior and consequent vulnerability of such buildings is an important task in this direction. Keeping in mind the increasing number of RC frames with irregular placement of infills in plan and/or elevation, such buildings have also been considered in the present study.

A review of available literature revealed that only a limited number of studies are available world-over, on seismic vulnerability of URM infilled RC Frame buildings. Although India has suffered several devastating earthquakes (1897 Great Assam earthquake, 1991 Uttarkashi earthquake, 1993 Killari earthquake, 1997 Jabalpur earthquake, 1999 Chamoli earthquake, 2001 Bhuj earthquake, and 2005 Kashmir earthquake) in the past, most of the earlier earthquakes affected mainly rural areas having predominantly masonry buildings. Further, systematic information on building damage during past earthquakes that would allow development of empirical fragility functions for Indian buildings is not available. Testing facilities required for experimental simulation of full scale multistory buildings are also not available in the country and the cost of such simulations is prohibitive. Further, a large variation in the design and construction of such buildings is observed. In such circumstances, analytical simulation of seismic behavior of these buildings is the most attractive alternative, as influence of large number of parameters and deficiencies observed in Indian construction can be studied with relatively smaller cost and effort.

This Thesis is an attempt to develop modeling guidelines for RC frames with and without URM infills and to develop a reliable, cost effective methodology for seismic risk assessment of existing Indian urban habitat. Particular focus is on evaluation of capacity curve parameters and fragility functions of existing RC frame buildings with and without URM infills, considering all possible failure modes of infill panels and surrounding frame members. Possible shear failure of joints is also considered in the

present study. As the assessment of earthquake risk for a region or community is a costly and time-consuming task, there is need to develop user-friendly, efficient tools and procedures for estimation of seismic risk in order to plan short term and long-term mitigation measures to reduce risk from future earthquakes. Further, adequate information on hazard and vulnerability is not available, at present, for all the regions of India. Therefore, software has been developed to make use of the information available in various forms, viz. Macro-seismic Intensity scales, design codes, and fragility functions obtained analytically and from studies on comparable building typologies in other parts of the world.

1.3 RESEARCH OBJECTIVES

The primary aim of this Thesis is to develop an analytical model for URM infilled RC frame buildings simulating various failure modes. The developed analytical model is used to study the effect of infill-frame interaction and major design and detailing deficiencies observed in Indian RC frame buildings, on their seismic performance. The study also attempts to estimate representative capacity curve parameters for RC frame buildings, with and without infills. The specific objectives of the study are as following:

1. To identify various failure modes of infills and frame members in URM infilled RC frame buildings based on observations during past earthquakes and experimental studies.

2. To review the available models for estimating strength of infills and RC frame members in the identified failure modes.

3. To develop analytical models for simulating the observed failure modes in RC frame buildings with and without URM infills.

4. To study the effect of URM infills on failure modes and seismic performance of RC frame buildings.

5. To study the effect of design and detailing deficiencies prevailing in Indian construction on seismic performance of RC frame buildings with and without URM infills.

6. To study the seismic behavior of RC frame buildings with irregular placement of URM infills and examine the adequacy of Indian code provisions for design of open ground storey buildings.

7. To develop fragility functions for representative Indian RC frame buildings with and without URM infills.

8. To develop an open source software tool for seismic risk assessment using different methodologies and incorporating the developed fragility functions.

9. To compare the losses estimated using different methodologies for a case-study of a typical north Indian city.

1.4 SCOPE OF THE STUDY

The present study is focused on estimation of capacity curve parameters for typical Indian RC frame buildings with and without URM infills. The study also identifies the influence of infill-frame interaction and common design and detailing deficiencies on the seismic performance and vulnerability of infilled frame buildings. The scope of the present study is limited to RC bare frames and RC frames with solid infills, designed and constructed as per Indian codes and practices. However, the models and conclusions drawn about behavior of URM infilled RC buildings are applicable to other parts of the world, as well.

There exists a large variation in design and construction practices of RC frames in India. Despite Indian standard codes for seismic design of buildings being in existence for the last half century, buildings are still being constructed without any consideration of earthquake actions, even in zones of high seismicity. Further, due to lack of regulations, buildings are being used for mixed occupancies, which results in horizontal and vertical irregularities in the buildings. Therefore, the buildings designed for gravity loads alone, with and without irregular placement of infills have been given special attention in this study. There is large variation in material properties, particularly those of masonry, in different parts of India. In the present study, the material properties reported in literature, for typical north-Indian construction have been used.

The study is based on 3D frame modeling of buildings, simulating the infills as equivalent diagonal struts. Various failure modes of beams, columns, and beam-column joints have been considered. As Indian code does not provide any guidelines for modeling beam-column joints, in the present study RC beam-column joints have been explicitly modelled in case of buildings designed and detailed without any consideration of earthquake resistant design provisions of BIS (1993, 2002), whereas in all the other cases the equivalent stiffness of RC beam-column joints has been modelled using the guidelines of ASCE-41 (2007) and ASCE/SEI-41 Supplement-1 (2007). Lumped plasticity models for frames and infills with hinge properties obtained from section analyses duly calibrated with the ASCE-41 (2007) guidelines have been used. Effect of soil and foundation flexibility on the seismic response of buildings has been ignored. However, the effect of soil amplification on ground motion has been considered.

In case of URM infills, both in-plane and out-of-plane actions are important. Generally, it is observed that infills cracks in in-plane action and ultimately failure occurs due to out-of–plane action. However, analytical approaches considering both the effects in a single model are not available, at present. Further, it is the in-plane action of the infills which results in infill-frame interaction and is responsible for significantly altering the behavior and failure modes of RC frames. The out-of-plane action can be dealt with separately and out-of-plane failure of infills can be avoided using simple measures. Therefore, the present study has been limited to in-plane action of URM infills only.

For reliable estimation of representative capacity curve parameters, the ideal way is to carry out nonlinear analysis of each and every building (or at least a large number of buildings) of the considered class and generate the statistical data to evaluate median values and dispersion to account for the variability in capacity. Since it is a very tedious and a time expensive exercise to evaluate a large number of existing buildings, in the present study, representative building configurations have been selected from a survey in a model township in the National Capital Region (NCR) (DEQ 2009) of India. The selection is based on the statistical evaluation of structural parameters such as range of building dimensions, number of frames in each direction, range of beam spans, redundancy in two directions, period of vibration, etc. The

variability in different parameters of fragility curves has been considered using the guidelines provided in HAZUS (FEMA 1999, 2003, 2006). Further, the survey focused on residential and office buildings. Commercial structures, having large spans, low strength partitions, and large shear walls/shear cores are beyond the scope of this study.

The case study on seismic risk assessment, presented in this Thesis is basically focused on comparison of the loss estimates from three different approaches, viz. macroseismic intensity, PGA with choice of spectral shapes and soil amplification models of various seismic building codes (BIS 2002); Eurocode-8 (2004); (NZS-1170.5 2004; ASCE-7 2006), and inelastic displacement spectra using the NGA relationships (Bozorgnia et al. 2010b)), using a common building inventory, rather than presenting the most reliable risk estimates for the test bed city, as the detailed inventory of the building stock and geotechnical data for the city is not available. The main emphasis of the present study is use of a common building inventory for the three approaches of seismic loss evaluation, to bring out the extent of variation and sensitivity of the estimated losses to different parameters.

1.5 ORGANISATION OF THE THESIS

The work reported in the present Thesis is organized in the following chapters:

Chapter-1 briefly describes various issues related with seismic behavior of URM infilled RC frame buildings. The Chapter introduces the challenges in modeling the seismic behavior of URM infilled RC frame buildings, and the construction practices in India resulting in different types of deficiencies and irregularities affecting seismic performance of such buildings. This Chapter also describes the need, objectives and scope of the present study.

Chapter-2 presents a review of available elastic and inelastic modeling techniques for RC frame members and their strength in various failure modes. This Chapter also takes a stock of the modeling techniques for URM infill panels, available in literature and some of the major national codes (BIS 2002); Eurocode-8 (2004); (NZS-4230 2004; ASCE-7 2006; ASCE-41 2007). A simple macro-model has been identified to simulate the interaction of infills with the surrounding frames, based on its ability to

reliably predict the observed failure modes. Effect of construction sequence on the seismic behavior of URM infilled RC frame buildings, is studied with the help of an analytical study carried out on four storey and ten storey buildings for two different design levels.

Chapter-3 investigates the possibility of different modes of failure of infills and frame members in URM infilled RC frame buildings under combined action of gravity and lateral loading. A generic set of representative buildings is also developed based on the observations of a field survey. Using the macro-model for URM infills, identified in the previous Chapter, the possibility of various failure modes is examined in buildings with different design and reinforcement detailing, as per Indian codes and construction practices. The effect of infills on axial forces and bending moment in columns, and demand-capacity ratios in different failure modes in various elements, including beam-column joints is investigated to identify the probable (and improbable) failure modes.

Chapter-4 presents the design philosophy of RC frame buildings with and without URM infills in different seismic design codes, viz. BIS (2002); Eurocode-8 (2004); NZS-1170.5 (2004); NZS-4230 (2004); ACI 318 (2005); ASCE-7 (2006); ASCE-41 (2007) and deals with the effect of URM infills on the estimated performance of RC frames. The model of infills developed in Chapter 2 has been used to study the effect of infills on seismic performance of RC frame buildings with different design levels and number of storeys. Failure patterns and seismic performance of RC frame buildings with and without URM infills and having common design and detailing deficiencies, have been presented in this Chapter.

Chapter-5 presents the behavior of RC frame buildings with irregular placement of infills. Particular focus is on the seismic performance of open ground storey buildings and buildings with asymmetric placement of infills. Adequacy of Indian code provisions for design of open ground storey buildings is also examined. Effect of deficient detailing with inadequate reinforcement and confinement, on seismic performance of RC frame buildings is also examined.

Chapter-6 focuses on the estimation of fragility curves for different design levels and placement of infills in RC frame buildings, to be used for seismic risk evaluation.

Fragility curves are developed for RC frame buildings with and without URM infills, RC frame buildings with open ground storey and asymmetric placing of infills, and with two different design levels and number of storeys. Effect of different deficiencies on the seismic vulnerability has also been discussed.

Chapter-7 presents the developed spread-sheet based software tool 'SeisVARA' (**Seis**mic **V**ulnerability **A**nd **R**isk **A**ssessment) for seismic risk assessment of the housing stock existing in a geographical unit. The tool has been used to perform a comparative study of different risk assessment methodologies using a common building inventory and loss model, while specifying the seismic demand in any of the three forms, i.e. macroseismic intensity, PGA with choice of spectral shapes and soil amplification models of various seismic building codes (BIS 2002); Eurocode-8 (2004); (NZS-1170.5 2004; ASCE-7 2006), and inelastic displacement spectra using the NGA relationships (Bozorgnia et al. 2010b).

Chapter-8 summarizes the major conclusions drawn from the present study and presents the scope of further research.

Chapter 2

MODELING OF URM INFILLED RC FRAME BUILDINGS

2.1 INTRODUCTION

Earthquake Resistant Design of structures has developed greatly, since the initial ideas took shape in early twentieth century. Invention of accelerograph and development of concept of Response Spectrum are among the most important steps in the history of ERD. The other most important development, at philosophical level, is understanding of the role of the three key parameters, viz. stiffness, strength and ductility, in estimating seismic response of structures. This requires realistic simulation of inelastic behavior of structures. Simulation of seismic behaviour of URM infilled RC frames is a complicated task due to the complex infill-frame interaction. Despite research efforts of several decades (Ockleston 1955; Smith 1968; Paulay and Priestley 1992; Mehrabi et al. 1996; Crisafulli 1997; Hashemi and Mosalam 2007), no consensus method for modeling of infilled frames is available, and most of the design codes are silent about modeling and design of infilled frames. Further, several deficiencies in building configuration, design, detailing and construction are commonly found in these buildings, making the simulation of seismic behavior of URM infilled RC frames a very challenging task.

Realistic simulation of inelastic behavior of a structure requires reliable estimation of member properties, such as effective stiffness, strength, ductility, and strength and stiffness degradation under cyclic loading. This Chapter, first, takes a stock of the available models for estimating various member properties for RC frames and URM infills. A comprehensive review on modeling of stiffness, strength and ductility of RC beams, columns, beam-column joints, and URM infills is presented. Different available models for simulation of the stiffness and strength of infill panels are evaluated in comparison with the experimental results and observations during past earthquakes. Limitations of the conventional ‘simultaneous’ analysis are identified and effect of construction sequence on the overall behaviour is studied. A realistic model of infills has been selected from the comparative study and a macro-model based simulation of the URM infilled RC frames with ‘initial lack of fit’ and

'sequential construction' of infills is proposed, which is used in the subsequent Chapters for study of seismic behavior and fragility of such structures.

2.2 EFFECTIVE STIFFNESS OF RC MEMBERS

Under seismic loading, RC members are expected to yield to dissipate energy imparted to the structure. This results in significant cracking of the members. Reliable estimation of effective/cracked stiffness of RC members under seismic loading is a crucial issue, not only in nonlinear analysis but also in traditional Force-Based Design (FBD) followed in design codes, as the dynamic characteristics (period of vibration and deflected shape) and hence spectral acceleration and design forces depend on the estimated stiffness. In Performance Based Design (PBD), the damage (indicated by displacement, interstorey-drifts, and plastic rotations in members) in the structure is largely governed by the realistic choice of effective stiffness. A widely varied opinion on the issue of magnitude and about the parameters governing the effective stiffness, exists among the research fraternity as well as in design codes (Kumar and Singh 2010). Researchers discovered that effective stiffness of RC members depends not only on the axial load (ASCE/SEI-41 Supplement-1 2007) but also on the reinforcement ratio (Khuntia and Ghosh 2004), eccentricity ratio (Mirza 1990; Khuntia and Ghosh 2004), yield strength of longitudinal reinforcement (NZS-3101:Part2 2006; Elwood and Eberhard 2009), bond slip of reinforcement bars (Elwood and Eberhard 2009), and shear span (Mirza 1990; Elwood and Eberhard 2009) of the member. Consideration of all of these parameters in analysis makes the design process cumbersome and iterative. Considering the uncertainty in estimation of effective stiffness of RC members, Indian Standard (BIS (2002)), US American (ASCE-7 (2010)) and New Zealand standard (NZS-1170.5 2004) recommend a capping on the design period of buildings, ensuring design for a minimum base shear as a safeguard against unrealistic stiffness estimates.

The design codes differ significantly on the issue of effective stiffness of RC members. Eurocode-8 (2004) specifies 50% reduced gross moment of inertia to be considered as effective for all RC elements while ACI 318 (2008) recommends 35% and 70% of gross moment of inertia to be considered as effective for beams and columns, without any consideration for degree of axial loading, and no recommendation has been made for effective stiffness of beam-column joints (ACI-

352R-02 2002). However, it is to be kept in mind that the stiffness recommendations of (ACI 318 2008) do not deal with seismic loading and have been primarily developed to account for the buckling of columns. FEMA-356 (2000)/ASCE-41 (2007) considers the effect of axial loading on the effective stiffness of columns and recommends effective stiffness of RC members considering flexure, shear and axial action. Elwood and Eberhard (2006) revealed that FEMA-356 (2000)/ASCE-41 (2007) guidelines can significantly overestimate the stiffness of columns with low axial loads, mainly because of the inadequate consideration of flexibility resulting from slip of the longitudinal reinforcement from adjacent beam-column joints (Elwood and Eberhard 2009) and proposed a more refined three component approach for estimating effective stiffness considering flexure, slip, and shear. Using the three component approach, Kumar and Singh (Kumar and Singh 2010) developed a model for realistic stiffness of RC members for the range of parameters, commonly found in the Indian RC frame buildings. At low axial forces, the model yields results close to the ASCE/SEI-41 Supplement-1 (2007). Table 2.1 summarizes the different effective stiffness models of RC members in various design standards/documents.

2.3 INELASTIC MODELING OF RC MEMBERS

Two approaches are available for nonlinear modeling of skeletal frame members. In Distributed Plasticity Approach, it is assumed that yielding is distributed over a finite length of the member. The structural characteristics of the member are calculated by assuming a displaced shape of the member axis, with internal forces calculated at various sections, from the resulting curvatures and axial strains. On the other hand, in Lumped Plasticity Approach, it is assumed that yielding takes place only at generalized plastic hinges of zero length, and the member between these hinges is assumed to be linearly elastic. Multidimensional action-deformation relationships are specified for the hinges. Lumped plasticity models are particularly suitable for analysis of building frames under seismic loading, because plastic action in such structures is usually confined to small lengths at beam and column ends. The lumped plasticity models simplify the computational effort significantly without compromising with accuracy (Chen and Powell 1982; Powell and Chen 1986).

Table 2.1

Overview of effective stiffness models for RC members, considered in the study

RC Member	Eurocode-8 (2004)	ACI 318 (2005, 2008)	FEMA-356 (2000)/ ASCE-41 (2007)	ASCE/SEI-41 Supplement-1 (2007)
Non-prestressed Beam	$0.5E_cI_g$	$0.35E_cI_g$	$0.5E_cI_g$	$0.3E_cI_g$
Columns with design gravity loads $\geq 0.5A_gf_c'$		$0.7E_cI_g$	$0.7E_cI_g$	$0.7E_cI_g$
Columns with design gravity loads $\leq 0.3A_gf_c'$			$0.5E_cI_g$	Linear interpolation
Columns with design gravity loads $\leq 0.1A_gf_c'$ or with tension			-	$0.3E_cI_g$
Beam-column joint with $\frac{\sum M_c}{\sum M_b} < 0.8$		-	Rigid	Rigid beam end zones with the column flexibility extending to the joint centerline
Beam-column joint with $0.8 \leq \frac{\sum M_c}{\sum M_b} \leq 1.2$				Rigid column end zones with the beam flexibility extending to the joint centerline
Beam-column joint with $\frac{\sum M_c}{\sum M_b} > 1.2$				50% of the end zones of both beam and column within the joint extents are rigid

where, E_c is Modulus of elasticity of concrete, I_g is moment of inertia of gross concrete section, A_g is gross cross sectional area, f_c' is compressive strength of concrete, M_c and M_b are nominal flexural strength of column and beam, respectively.

2.3.1 Modeling of Flexural Yielding and Axial Force-Moment Interaction

The generalized force-deformation behavior in lumped plasticity model for flexural action in RC beams and columns represents the back-bone curve (FEMA-273 1997) of the cyclic load-deformation relationship for the member. A typical generalized force-deformation curve is shown in Fig 2.1, where line AB represents linear elastic behavior and the slope from A to B represents the effective elastic stiffness of the member at yield. It is generally represented by the secant stiffness at first yield

(Priestley 2003; Priestley et al. 2007). Point B represents the expected yield strength of the member and until this point, no deformation occurs in the plastic hinge. The expected yield strength is obtained from equivalent bi-linearization of the moment-curvature curve for the RC section (Priestley 2003). It is usually considered as the expected moment capacity of the RC section corresponding to extreme concrete fiber strain of 0.4% (Priestley et al. 2007; CALTRANS 2010). The line BC represents strain hardening and the slope from B to C is generally considered such that the ultimate capacity at point C is 0-10% higher than the yield capacity. The line CD represents the initial failure of the component which may occur due to fracture of longitudinal reinforcement, spall of concrete or shear failure. The line DE represents residual strength of member where point E is considered as failure of the member. However, the resistance to the lateral load beyond point C is usually unreliable and ignored.

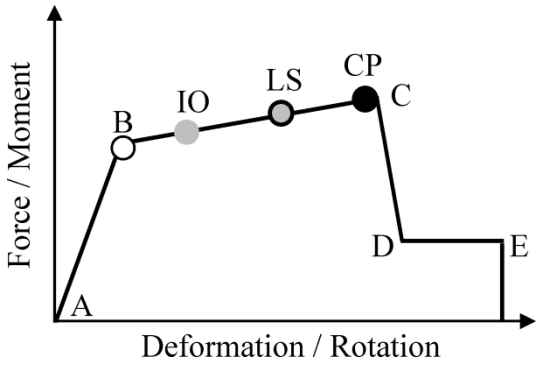

Fig. 2.1 Generalized force-deformation behavior of a typical RC member to define performance limit states under flexure as per ASCE-41 (2007).

In the present study, the flexural capacity of the RC beams and columns has been calculated using section analysis, considering the expected strengths of concrete and steel. The Indian RC design code (BIS 2000) defines the nominal strength (termed as characteristic strength, f_{ck}) as 95% confidence level cube crushing strength. Therefore, the expected cylinder strength for concrete has been considered as $0.8(f_{ck}+1.64\sigma)$, where, σ is the standard deviation of the cube strength, with values given in BIS (2000). The expected strength of the reinforcing steel has been considered as 1.25 times the nominal or minimum specified strength, according to ASCE-41 (2007), as values of standard deviation in strength of steel manufactured in India are not available. Mander's model (Mander et al. 1988) for concrete has been used with

'usable strain limits' prescribed in (ASCE-41 2007) as 0.02 for confined concrete in compression and 0.05 for longitudinal tension reinforcement. The yield moment capacity for columns is expressed in terms of a P-M2-M3 interaction surface corresponding to 0.4% strain in the extreme concrete fiber.

Figure 2.1 also shows the three performance levels of members, namely Immediate Occupancy (IO), Life Safety (LS) and Collapse Prevention (CP). The acceptance criteria for plastic rotations corresponding to the three performance levels have been considered as per ASCE/SEI-41 Supplement-1 (2007), based on design axial and shear forces at the critical section, longitudinal reinforcement ratio, and spacing of transverse (confining) reinforcement.

In the present study, lumped plasticity models of buildings have been developed in which flexural (M) hinges are assigned at both ends of beams, whereas axial force-bi-axial moment interaction hinges (P-M-M) are assigned to columns. Non-conforming, 'NC' and conforming, 'C' type of transverse reinforcement has been considered for gravity designed and SMRF infilled frames, respectively, to assign the plastic rotations for beams and columns as per ASCE/SEI-41 Supplement-1.

2.3.2 Modeling of Shear Failure of Columns

The seismic performance of reinforced concrete frame buildings in past earthquakes (Bertero and Collins 1973; EERI 1994; Saatcioglu et al. 2001; GSI 2003; Özcebe et al. 2003; Paul et al. 2004) demonstrates that loss of axial load carrying capacity due to shear failure in columns, is one of the most common causes of the building damage and failure. In a well designed column subjected to seismic actions, the contribution of shear deformation to the total deformation of column may be even less than 10% (Lehman and Moehle 2000), however, shear deformation becomes as significant as 40% of the total deformation (Sezen 2002) when the columns are designed only for gravity loads without considering seismic detailing requirements. The shear failure in columns is a brittle mode of failure (Fig. 2.2), which is considered as a 'force controlled' mode. It implies that the member cannot undergo any plastic deformation (points B and C coincide in Fig. 2.2) and for satisfactory performance of the structure, the shear force should be controlled within the expected capacity of the member. Therefore, estimation of shear capacity of columns is an important issue in simulation of seismic behaviour of RC frames.

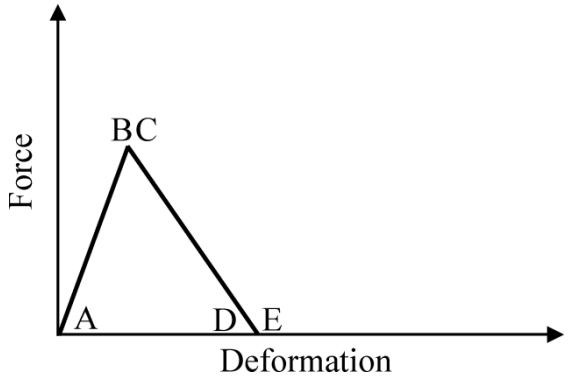

Fig. 2.2 Generalized force-deformation behavior of a typical RC member to define performance limit states under shear.

Extensive research on this front over the past decades has revealed that the shear strength (V_n) of a column can be considered to have distinct contributions from concrete (V_c) and transverse reinforcement (V_s). Contribution of concrete in shear strength is rather complex and is influenced by several factors including axial compressive force, column aspect ratio and deformation ductility demand (Priestley et al. 1994; Sezen and Moehle 2004; Erduran and Yakut 2007). A number of models are available for evaluation of shear strength of RC columns. Table 2.2 summarizes a few of the available models, which are simple to use and are applicable for the range of building parameters considered in the present study.

2.3.3 Modeling of Beam-Column Joints

Seismic response of reinforced concrete beam-column joints is a complex phenomenon. A number of design parameters affect the strength, stiffness and deformation capacity, and eventually the damage of the joint (Pagni and Lowes 2004). Several approaches, including lumped plasticity models (Otani 1974), multi-spring models (Biddah and Ghobarah 1999), and finite element simulations (Lowes and Altoontash 2003) have been proposed for modeling of joints in RC frames. In this section a review of the available beam-column joint models is presented with the objective of identifying a suitable model which can be easily implemented in simulating the response of the buildings considered for parametric study.

Table 2.2

Overview of shear strength models of RC columns considered in the present study

Model reference	V_c	V_s
FEMA-356 (2000)	$V_c = k\left(\frac{6\sqrt{f_c'}}{M/V_d}\sqrt{1+\frac{0.74P}{\sqrt{f_c'}A_g}}\right)0.8A_g$ $2<M/V_d<3$ k = 1.0 for low ductility region and 0.7 for high ductility region	$V_s = \frac{A_v f_{yv} d}{s}$
ACI 352R-02 (2002)	$V_c = k\left(\frac{0.5\sqrt{f_c'}}{S_s/d}\sqrt{1+\frac{P}{0.5\sqrt{f_c'}A_g}}\right)0.8A_g$	$V_s = k\frac{A_v f_{yv} d}{s}$
ACI 318 (2005)	$V_c = 0.17\left(1+\frac{P}{14A_g}\right)\sqrt{f_c'}A_g; \quad if \quad P \geq 0$ $V_c = 0.17\left(1+\frac{0.29P}{A_g}\right)\sqrt{f_c'}A_g > 0; \quad if \quad P < 0$	$V_s = \frac{A_v f_{yv} d}{s} \leq 0.66\sqrt{f_c'}A_g$
Sezen and Moehle (2004)	$V_c = \left(1+\frac{3P}{A_g f_c'}\right)(0.07+10\rho_w)\sqrt{f_c'}A_g$ $0.08\sqrt{f_c'} < (0.07+10\rho_w)\sqrt{f_c'} < 0.2\sqrt{f_c'}$	$V_s = \frac{A_v f_{yv} d}{s}$

where, M/V is the largest ratio of moment to shear under design loadings for the column, P is axial load on column, S_s is shear span, d is depth of column, ρ_w is area of flexural tension reinforcement, and A_v, S, and f_{yv} are area, spacing, and yield strength, respectively, of the transverse reinforcement.

The first attempt to model seismic behavior of RC beam-column joints was reported by Giberson (1969). Later, Townsend and Hanson (1973), Otani (1974) and Anderson and Townsend (1977) represented the inelastic behavior of the joint and the flexural response of the frame members by two inelastic lumped rotational spring elements. The model is computationally efficient and therefore suitable for parametric study, but calibration of the rotational springs is difficult.

Fillipou et al. (1983) proposed a model consisting of two rotational springs, for interior joints, which can be extended to exterior joints also. The moment rotation relationship for the rotational springs is derived with due consideration to the geometry, material properties, and reinforcement layout in the joint. Although, the model is easy to implement and is in good agreement with experimental results, the

model did not give due consideration to the joint shear and diagonal cracking in the hysteretic behaviour of beam–column joints.

El-Metwally and Chen (1988) modified the lumped plasticity model by introducing a zero length rotational spring between the beams and columns to separate the joint behaviour from that of beams and columns. Later, Alath and Kunnath (1995) and Deng et al. (2000) introduced rigid zones along with the single zero length rotational spring to define the joint area in the plane of the frame. The model is calibrated using joint moment-rotation data from 34 cruciform sub-assemblage tests. This modeling approach proves to be accurate and computationally efficient but it also fails to distinguish between the responses of the joint mechanisms.

To model the joint region more accurately Biddah and Ghobarah (1999) introduced two rotational springs to model failure of joint core due to shear, and bond-slip due to anchorage failure of beam or column reinforcing steel, separately. The joint shear spring was modelled using tri-linear idealization considering the softened truss theory by Hsu (1988) and the bond-slip spring had a bilinear hysteretic model based on analytical and experimental data for the bond slip. Youssef and Ghobarah (2001) proposed a more refined analytical model by implementing 12 springs to simulate concrete crushing, 12 steel springs to simulate bond slip of reinforcing bars, and two diagonal axial springs to simulate the joint shear deformation. The model was validated using experimental test results of ductile and non-ductile exterior beam-column joints. The main limitation of these models is that the calibration of the springs is quite cumbersome and therefore not suitable to study the seismic behaviour of the frame as a whole.

Pampanin et al. (2003) proposed a simple analytical model applicable to all type of joints, designed for gravity loads only. The model consists of a nonlinear rotational spring to simulate the relative rotation between beams and columns at the joint and to describe the post cracking shear deformation of the joint panel. The relationship between shear deformation and the principal tensile stress in the joint is transformed into moment–rotation relation to be assigned to the rotational spring. The model is calibrated using experimental test results and is suitable for use in parametric study of RC buildings designed for gravity load.

Lowes and Altoontash (2003) proposed a model for interior RC beam column joints. The model consists of one shear panel, eight bar slip springs, and four interface-shear spring elements. The behaviour of the joint core was defined based on the modified compression field theory (MCFT) and experimental data was used for defining the response under cyclic loading. Similar model for interior joints based on MCFT theory was also proposed by Shin and LaFave (2004); LaFave and Shin (2005). However, Celik and Ellingwood (2008) have explained unsuitability of MCFT for modeling the RC joints designed for gravity loads "which have little or no joint transverse shear reinforcement".

Mitra and Lowes (2007) modified the model proposed by Lowes and Altoontash (2003) to accurately predict the response of a wide range of joints by involving more than 30 parameters. In order to evaluate, calibrate, and verify the new model, they used an experimental data set of 57 interior joint sub-assemblages that did not include joints with plain round reinforcing steel bars therefore restricts its application to the older RC frames designed for gravity load only.

Anderson et al. (2008) proposed a cyclic shear stress–strain model and envelop curve for RC beam-column joints without transverse reinforcement. The model has been calibrated using measured data from tests (Walker 2001; Alire 2002) on joints without transverse reinforcement that were subjected to a range of displacement histories and joint shear stress demands. The model has a general form, and the model parameters are expressed as functions of the joint geometry and material properties. This model is suitable for study of seismic behaviour of RC frames having joints with no transverse reinforcement.

Sharma et al. (2011a) proposed a new model for reinforced concrete exterior joints. The model uses limiting principal tensile stress in the joint as the failure criteria so that due consideration is given to the axial load on the column. The spring characteristics are based on the actual deformations taking place in the sub-assemblage due to joint shear distortion.

Based on the ratio of flexural strength of beam(s) and column(s) framing into the joint (Leon 1990; Beres et al. 1992), ASCE/SEI-41 Supplement-1 (2007) provides a simple centre line model of beam-column joints with semi-rigid joint offsets, (Fig. 2.3) which accounts for joint shear flexibility and can be very easily implemented in

available commercial structural analysis software. Therefore, in the present study, the guidelines of ASCE/SEI-41 Supplement-1 (2007) for effective stiffness of RC beams, columns and beam-column joints have been considered for their simplicity and reasonable accuracy.

The model by Pampanin et al. (2003) is easy to implement and suitable for use in parametric study of RC buildings designed for gravity load and has been used in the present study to model the beam-column joints of RC buildings designed for gravity loads only as per relevant Indian Standards, whereas for all other design levels, the beam-column joint model of ASCE/SEI-41 Supplement-1 (2007) has been considered.

Beam–column joints, particularly in frames not designed for earthquake actions, have been damaged in past earthquakes. Behavior of beam-column joints in frames subjected to lateral loading is a complex phenomenon, as a number of parameters affect the strength of the joints. Further, there is significant difference in the mechanism of shear resistance in case of exterior and interior beam-column joints. Shear strength of beam-column joints is mainly influenced by compressive strength of concrete, joint aspect ratio (Vollum and Newman 1999; Bakir and Boduroglu 2002; Kim and LaFave 2007), amount of longitudinal reinforcement in beams connected to the joint (Bakir and Boduroglu 2002; Anderson et al. 2011), and axial force in column (Kitayama et al. 1991; Hegger et al. 2003; Park and Mosalam 2009; Muhsen and Umemura 2011; Unal and Burak 2012). Numerous studies have been carried out in the last decade to evaluate shear strength of the RC beam-column joints and several models of exterior and interior joints have been proposed. Table 2.3 provides the overview of the shear strength models of RC beam-column joints considered in the present study. Considering uncertainties regarding role of transverse reinforcement in failure mechanism of joints, the joint shear strength models prescribed in some of the codes/documents, viz., FEMA-356 (2000); (ACI-352R-02 2002); Eurocode-8 (2004), assume that the internal forces in the joint are to be transferred by diagonal compression strut of concrete core alone. The model proposed by Hegger et al. (2003) considers the maximum number of parameters influencing the shear strength of joints, including the role of transverse reinforcement, and is applicable for all types of joints considered in the present study.

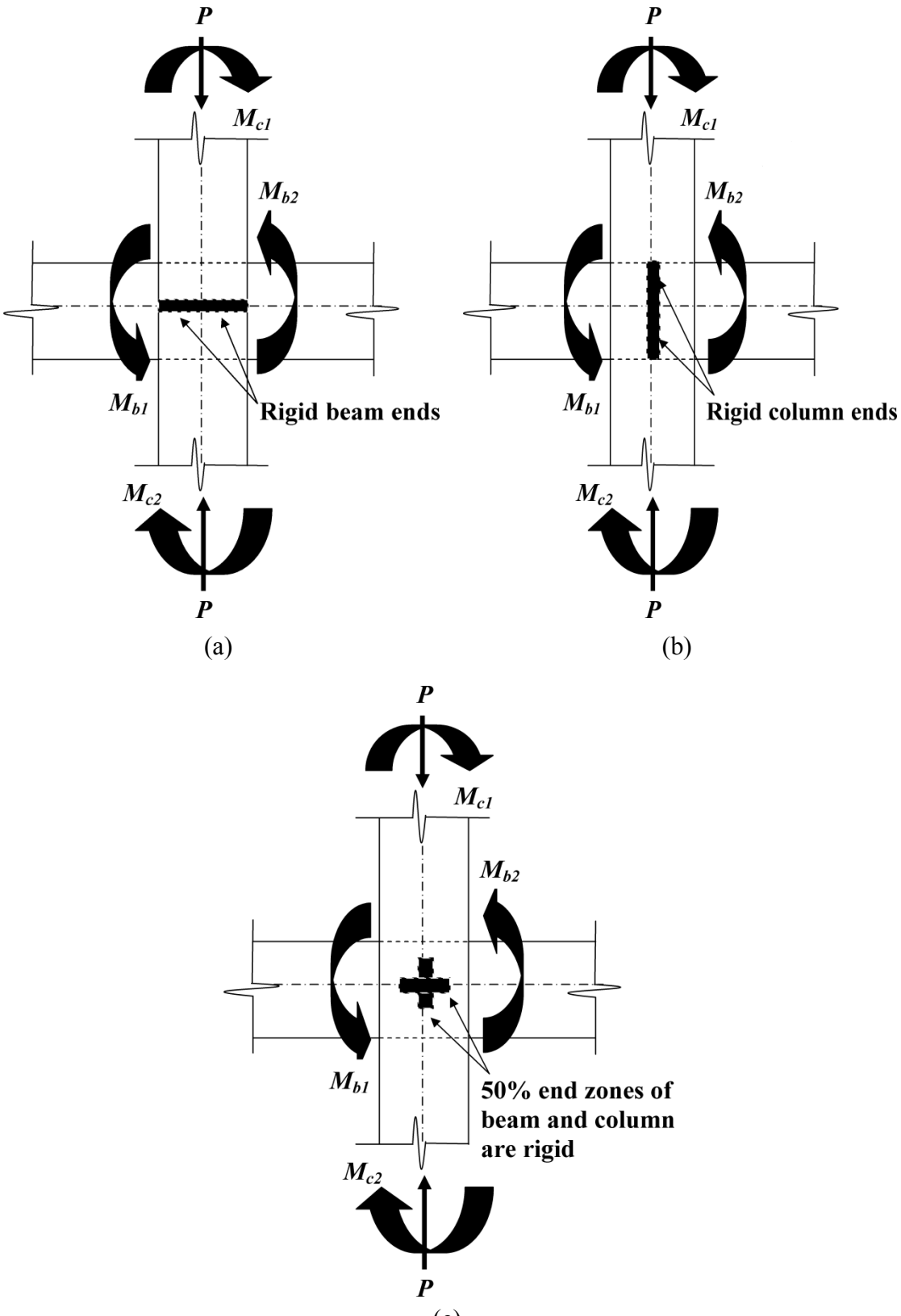

Fig. 2.3 Beam-column joint model as per ASCE/SEI-41 Supplement-1 (2007) for effective stiffness considered in the present study, when ratio of flexural strength of columns and beams framing into joint is: (a) 0.8, (b) in between 0.8 and 1.2, and (c) greater than 1.2.

Unlike, the joint strength models of Eurocode-8 (2004), ACI-352R-02 (2002) and FEMA-356 (2000), the model in NZS-3101:Part1 (2006) requires considerable amount of transverse reinforcement in the joint to transfer the tensile forces and therefore not applicable to the non-ductile gravity designed buildings, where no transverse reinforcement is provided in the joint region. Indian Standard (BIS 1993) provides some detailing guidelines for beam-column joints, but does not provide any model for estimation of joint shear strength.

Table 2.3

Overview of shear strength models of RC beam-column joints

Model reference	Interior Joint	Exterior Joint
FEMA-356 (2000)	$V_{nj} = \gamma\sqrt{f_c'}\, b_j h_c$	
Park and Mosalam (2012)	$V_{nj} = 0.083\gamma\sqrt{f_c'}\, b_j h_c$	
Hegger et al. (2003)	$V_{nj} = 0.25 f_c' b_j h_c$	$V_{nj} = \gamma_1\gamma_2\gamma_3\, 0.25 f_c' b_j h_c$
Eurocode-8 (2004)	$V_{nj} = 0.4 f_c'\left(1-\frac{f_c'}{250}\right)\sqrt{1-\frac{P/A_g f_c'}{0.6\left(1-\frac{f_c'}{250}\right)}}\; b_j h_c$	80% of interior strength

where, γ is nominal strength coefficient based on joint geometry and amount of transverse reinforcement; γ_1, γ_2, γ_3, are coefficients to account for anchorage efficiency in beam reinforcement, axial force in column, and slenderness of joint, respectively; b_j is effective width and h_c is depth of joint.

2.4 MODELING OF URM INFILLS

Modeling of infills is an important step in assessment of seismic safety of URM infilled RC frame buildings. The fact has been recognized for long, and extensive research on analytical modeling of masonry infills has been carried out since early 1960's. As simulation of the actual behavior of infilled frame is a complex task, because of infill-frame interaction, many different modeling techniques for the simulation of the infilled frames are available in literature. The available models can be broadly classified into two categories – 'Micro' models and 'Macro' models. Micro-models are based on finite element representation of each infill panel and thus are able to account for the local infill-frame interaction and to capture the behavior in a much detailed manner. However, these are computationally very expensive, whereas

macro-models are based on physical understanding of the behavior of the infill panel as a whole and therefore are able to simulate the gross behavior of infill efficiently, though approximately.

2.4.1 Micro-Models

The finite element method of modeling infill panels has been widely used after Mallick and Severn (1967) first suggested the finite element approach to analyze infilled frames. The infill panels were represented by linear elastic rectangular finite elements with two degrees of freedom at each of the four corner nodes. The boundary conditions at the interface between frame and infill were modeled by introducing different translational degrees of freedom in adjacent elements, where separation between infill panel and frame may occur and thus contact length was estimated. The slip between frame and infill was taken into account by considering frictional shear forces in the contact region.

Different approaches have been used to simulate the interface conditions between infill and frame. In order to represent the interaction between rocks, Goodman et al. (1968) modified a four-nodded plane strain rectangular element of predefined length and zero width such that it has resistance to compressive force and has no resistance to tensile force perpendicular to its length. This concept has been used by many researchers (King and Pandey 1978; Page 1978; Lofti and Shing 1994; Mehrabi and Shing 1994) to simulate infill-frame interaction with refinements over the years.

Axley and Bertero (1979) suggested two finite element approaches, exact scheme and constraint scheme, to find the stiffness contribution of infill panel to infill-frame system. In constraint scheme, the infill-frame system is sub-structured and 12 degrees of freedom system elements, which can be easily plugged into any conventional frame analysis programs, were used for modeling of infill panels. To validate the results, exact scheme with a refined assemblage of the beam and plane stress elements, was adopted.

The advancement of nonlinear finite element analysis and experimental studies have provided much deeper insight into the complex collapse behavior of infilled frames. Based on this understanding, Liauw and Kwan (1984) proposed a plastic theory of infilled frame in which the infill-frame system was idealized as either integral, or

semi-integral, or non-integral frame, depending on the interface conditions. Behavior of infilled frame ranging from elastic to collapse mode was studied by nonlinear finite element analysis and three different plastic collapse loads corresponding to different failure modes relative to strengths of columns, beams and infills were identified.

Rivero and Walker (1984) developed a nonlinear model with reduced degrees of freedom, suitable for dynamic analysis of infilled frames. The model was divided into three parts representing un-cracked elastic behavior of infill panel, infill-frame interface, and cracking in the infill panel. Un-cracked behavior of infill panel was represented by an assemblage of elastic triangular elements. Nonlinearities were considered through the inelastic behavior of the frame, the interaction between the frame and the infill, and the cracking of the infill. For simulation of the interface between frame and infill, a 'gap' element and a 'joint' element were developed. The gap element was used to represent the space between frame and infill for no-contact conditions, while the joint element was used to represent continuity between infill and frame up-to a certain stress level and then allowed to behave like gap element.

Rots (1991) implemented three basic approaches, proposed by researchers at different times, to model the mechanical properties of masonry infills numerically, using finite element code DIANA (Coenraads 1991). The first approach (one-phase material model) is the least refined, where infills are assumed to be homogeneous material and joints are represented by continuum elements. The one-phase material model was adopted by many researchers (Dhanasekar 1985; Gambarotta and Lagomarsino 1997b; Zhuge et al. 1998) to reduce the problem for dynamic analysis. However, local failure of masonry at weak joints cannot be simulated by continuum joint model and therefore, applicability of one-phase material model is limited to the large structures, not requiring detailed stress analysis. In the second approach, based on two-phase material model, masonry units were represented by continuum elements, but joints were represented by discontinuum elements and separate mechanical properties were assigned for brick and mortar. This refined two-phase material model was first implemented by Page (1978) and followed by many researchers (Ali and Page 1987; Lofti and Shing 1994; Lourenco 1996; Gambarotta and Lagomarsino 1997a) over the years. This model was successfully implemented in commercial software ABAQUS (HKS: Hibbitt et al. 1997). In the finest third approach, masonry

was assumed as an anisotropic composite where masonry units were represented by continuum elements and mortar joints were modeled with interface elements (Lofti and Shing 1994; Mehrabi and Shing 1994). This model was further developed to consider an important feature of unreinforced masonry infills, i.e. cracking. The smeared crack model was used by Mosalam et al. (1993) to model overall cracking within an area rather than tracing individual crack. However, Schnobrich (1985) brought out the high sensitivity of this approach to mesh refinement and later Shing et al. (1992) concluded about its incapability in capturing brittle shear failure of infill panel and suggested use of interface elements in the discrete crack approach.

2.4.2 Macro-Models

The very high degree of non-homogeneity and widely varied non-linear brittle behavior of masonry units and mortar, resulting in time intensive and computationally complex Finite Element problem, deter its applicability to the practical problems of real structure. Therefore, the need of simplified models of infills, requiring lesser computational effort with sufficient accuracy lead to formulation of macro-modeling based analysis procedure of masonry infills.

Based on the diagonal compression action of an infill within a frame system, the idea of a strut model was first introduced by Polyakov (1960). In this concept, the global effect of an infill panel is represented by a single or multiple compressive diagonal strut(s) within the frame, having an equivalent width with same thickness same as that of the infill panel. This revolutionary concept of diagonal struts was further investigated by many researchers (Smith 1962; Liauw and Kwan 1984; Paulay and Priestley 1992) and a variety of macro-models based on different empirical formulations of diagonal width, strength, and stiffness properties of the strut, were developed over the decades. The first approximation of the width of the diagonal strut as one third of its diagonal length was proposed by Holmes (1961). Smith (1966) proposed the width of the equivalent diagonal strut as a function of relative stiffness of infill and frame and considered the width approximately as one fourth of diagonal length of infill panel. This approximation of the equivalent width of diagonal strut is still recommended by NZS-4230 (2004) for modeling of infills. Paulay and Priestley (1992) pointed out that the stiffer structure resulting due to larger diagonal width of the strut attracts higher seismic force, and recommended conservative value of

diagonal strut applicable up to a lateral force level of 50% of the ultimate capacity. More recently, Angel (1994) investigated the behavior of RC frames with masonry infills and concluded that the in-plane stiffness can be better approximated using equivalent diagonal strut with a width equal to one eighth of its length. Smith and Carter (1969) observed that the contact length between infills and frame has significant influence on the behavior of the infilled frame and based on the relative stiffness of infills and frame they proposed a formulation for contact length. Similar formulations based on the finite contact length of infills were also proposed by Mainstone (1971) and Kadir (1974). Liauw and Lee (1977) proposed a modified equivalent strut model with shear connectors at the infill-frame interaction to simulate the effective stiffness and the ultimate strength of infilled frames with openings. An elastic-perfectly plastic behavior of masonry under monotonic static loading was considered. Thiruvengadam (1985) proposed multiple strut model of infill panel by considering the reciprocal stiffening effect. The model consists of a moment resisting frame with a number of pin-jointed struts in both the diagonal directions. FEMA-356 (2000) has recommended the diagonal strut model of infill with deformation controlled action and specified strength and deformation properties. This model can capture the frame infill interaction globally. Bed joint sliding shear is considered as the controlling action and drift of the infill as corresponding deformation parameter.

In order to study the non-linear dynamic response of infilled frames, Klinger and Bertero (1978) first proposed a diagonal strut model of infills with hysteretic behavior to simulate the stiffness degradation due to cyclic loading. Two diagonal struts were used to model infill panels for alternate directions of cyclic loading and the width of the diagonal struts was kept same as proposed by Smith (1966). The model was calibrated with the experimental results of Klinger and Bertero (1978) and was found unsuitable for simulation of infilled frames, particularly for the cycles with large displacement. Doudoumis and Mitsopoulou (1986) considered the initial lack of fit between infill and surrounding frame due to shrinkage and proposed a new hysteretic model for equivalent diagonal strut, where the stiffness decreases gradually due to cracking along the compressed diagonal till corner crushing of infills. The model was implemented in ANSR-I (Mondkar and Powell 1975). Later, hysteretic behavior of infills was widely studied and several hysteretic models were proposed (Doudoumis and Mitsopoulou 1986; Chrysostomou 1991; Chrysotomou et al. 1992; Flores and

Alcocer 1996; Moroni et al. 1996; Panagiotakos and Fardis 1996; Madan et al. 1997) with further refinement. Madan et al. (1997) have proposed an analytical macro-model that takes into account the strength and stiffness degradation with slip pinching effect. The model was incorporated in a nonlinear program IDARC2D (Valles et al. 1996) for dynamic analysis of infilled frames. Another analytical formulation considering hysteretic axial behavior of the diagonal struts has been proposed by Crisafulli (1997), which is implemented in computer program RUAUMOKO (Carr 1998).

2.5 EFFECTIVE STIFFNESS OF URM INFILLS

In the present study, the diagonal strut model of ASCE-41 (2007) has been used for modeling the infills. According to this model, the thickness and modulus of elasticity of the equivalent strut are considered to be the same as those of the infill, whereas the equivalent width, *a* of the infill panel prior to cracking is defined as

$$a = 0.175\left(\lambda_1 h_{col}\right)^{-0.4} r_{\text{inf}} \tag{2.1}$$

where,

$$\lambda_1 = \left[\frac{E_{me} t_{\text{inf}} \sin 2\theta}{4 E_{fe} I_{col} h_{\text{inf}}}\right]^{\frac{1}{4}}$$

h_{col} = column height between centerlines of beams
h_{inf} = height of infill panel
E_{fe} = expected modulus of elasticity of frame material (concrete)
E_{me} = expected modulus of elasticity of infill material
I_{col} = moment of inertia of column
L_{inf} = length of infill panel
r_{inf} = diagonal length of infill panel
t_{inf} = thickness of infill panel and equivalent strut

2.6 STRENGTH OF INFILLS IN DIFFERENT FAILURE MODES

The diagonal strut action of infills was recognized as early as in 1950's (Polyakov 1956) and since then it has been the main feature of all the studies on infilled frames using discrete modeling approach. Based on the extensive investigations in the last

five decades (Smith 1967; Smith and Carter 1969; Mainstone 1971; Smith and Coull 1991; Paulay and Priestley 1992; Saneinejad and Hobbs 1995; Crisafulli 1997; Flanagan and Bennett 2001; Al-Chaar 2002), four distinct failure modes of the infill panels viz., bed-joint sliding shear failure, cracking due to diagonal tension, failure due to diagonal compression, and corner crushing of infills, have been identified and several models have been proposed for evaluating strength of the equivalent diagonal strut in these failure modes. Table 2.4 gives a chronological overview of the various failure modes and models for evaluation of strength of infills, reported in literature. It can be seen from the Table that a consensus on the observed failure modes of infills has been lacking; and bed-joint sliding and compression/crushing are the most commonly identified failure modes.

Table 2.4
Overview of identified failure modes of infills

Sl. no.	Reference	Identified failure modes of infill panels			
		Sliding shear failure	Diagonal tension	Diagonal compression	Corner crushing
1	Smith (1967)	○	●	●	○
2	Smith and Carter (1969)	●	●	●	○
3	Mainstone (1971)	○	●	○	●
4	Wood (1978)	●	●	○	●
5	Liauw and Kwan (1985b)	○	○	●	●
6	Smith and Coull (1991)	○	○	○	●
7	Priestley and Calvi (1991)	●	●	●	○
8	Paulay and Priestley (1992)	●	○	●	○
9	Saneinejad and Hobbs (1995)	●	●	●	●
10	Flanagan and Bennett (1999)	○	○	○	●
11	Al-Chaar (2002)	●	○	●	○
12	ACI 530 (2005)	●	○	●	●
13	ASCE-41 (2007)	●	○	○	○

○ – Failure mode not considered; ● – Failure mode considered

2.6.1 Shear Strength of Infills

Sliding shear failure along bed-joints has been recognized as one of the most commonly observed failure modes of infills in infilled frames during earthquakes (EERI 2002; Özcebe et al. 2003; Paul et al. 2004; Johansson et al. 2007; Sharma et al. 2011b) as wells as in laboratory experiments (Mehrabi et al. 1996; Kaushik and Manchanda 2010). Smith and Carter (1969) developed a model for shear strength of URM infills in terms of bond shear strength (f'_{bs}) between the masonry and mortar, coefficient of internal friction between the masonry and mortar (μ), horizontal shear stress (f_{st}), and corresponding vertical compressive stress (f_{nt}). A non-dimensional expression (Eq. (2.2)) for shear strength (R_s) was presented and the same was also plotted as a function of non dimensional parameter λh representing stiffness of the frame relative to infill, panel aspect ratio (l': h'), and μ varying from 0 to 0.6.

$$\frac{R_s}{f'_{bs} ht} = \frac{100}{8 f_{st}} \frac{1}{\left[1 - \left(\mu . f_{nt}\right) / f_{st}\right]} \tag{2.2}$$

and

$$\lambda h = h \sqrt[4]{\frac{E_f t \sin 2\theta}{4 E_c I h'}} \tag{2.3}$$

where,

E_c = Young's modulus of column material
E_f = Young's modulus of infill material
h = height of column between center line of beams
h' = height of infill panel
I = moment of inertia of column
t = thickness of infill panel
θ = slope of equivalent diagonal strut from horizontal

Wood (1978) identified possibility of shear failure in case of strong frame and weak wall systems and provided design charts similar to those by Smith and Carter (1969), for estimating racking loads based on relative strength and stiffness of frame members and infill. Priestley (1980) expressed bed-joint sliding shear strength as a function of the compressive strength of infill material (f'_m) and geometry of infill and frame; and the same was adopted by Priestley and Calvi (1991) and Paulay and Priestley (1992). According to this model, the diagonal force (R_s) to initiate bed-joint sliding in infill panel is expressed as

$$R_s = \frac{0.03 f_m^{'}}{1 - 0.3\left(h/l\right)} d_m t \tag{2.4}$$

where, d_m is the diagonal length of the infill, and h and l are height and length, respectively of the frame, as shown in Fig. 3.1.

Saneinejad and Hobbs (1995) obtained the shear strength (R_s) of the diagonal strut "corresponding to a complete horizontal crack through bed joints over the entire length of the infill" as

$$R_s = \frac{\gamma v t l^{'}}{\left(1 - 0.45 \tan\theta^{'}\right)\cos\theta} \leq \frac{0.83\gamma l}{\cos\theta} \tag{2.5}$$

where,

l' = length of infill panel
v = basic shear strength of bed joints of masonry
γ = load factor
θ' = sloping angle of masonry diagonal strut at shear failure, $\tan\theta' = (1-\alpha_c)\, h'/l'$
α_c = normalized contact length of column-infill (contact length/length of member)

Al-Chaar (2002) considered effect of opening and damage on the shear strength of infills and estimated the shear strength (R_s) of equivalent diagonal strut (Eq. (5)), as the combination of shear strength of masonry ($f_v^{'}$) and net grouted area of infill panel (A_n) along its length, with two reduction factors R_1 and R_2 for presence of opening and for any existing infill damage, respectively.

$$R_s = A_n f_v^{'} R_1 R_2 \sec\theta \tag{2.6}$$

ACI 530 (2005) provides the in-plane shear strength of infill as

$$R_S = 0.375 A_n \sqrt{f_m^{'}}\, sec\theta \tag{2.7}$$

with an upper bound of $0.83A_n$ (A_n is in mm^2 and $f_m^{'}$ is in MPa) on the value of $\sqrt{f_m^{'}}$.

ASCE-41 (2007) also provides a similar expression to estimate the in-plane shear strength of infill,

$$R_s = A_n f_v^{'} \sec\theta \tag{2.8}$$

where $f_v^{'}$ can be obtained experimentally using in-situ tests, or can be read from the table provided in ASCE 41 for varying quality of masonry.

It can be observed that all the models described above, except the Smith and Carter model, are similar in form, providing shear strength as product of bond (sliding along bed joint) shear strength and the net grouted sectional area of the infill. The differences arise only in specification of the value of the sliding shear strength. In absence of openings and initial damage, the model by Al-Chaar is identical to the ASCE 41 model. The models of ASCE-41 (2007), ACI 530 (2005) and Paulay and Priestley (1992) are the most recent and simple to use and the same have been considered in the present study for the purpose of comparison of strength with other modes of failure.

2.6.2 Strength of Infills in Diagonal Tension

Under lateral loading, infills are subjected to very high compressive force along the loaded diagonal. As the tensile strength of masonry is much lower than the compressive strength, chances of failure in compression are remote, except in case of very slender infills, and in most of the cases, the infills are observed to fail due to diagonal cracking. Due to Poisson's effect, infills develop tension cracks along the loaded diagonal, which widen up with increasing lateral displacement, resulting in diagonal failure of the infill panels. The diagonal cracking strength of infill panels is related to the shape and tensile strength ($f_t^{'}$) of infills, and for infills with low aspect ratio ($h^{'}/l^{'}$), the diagonal cracking strength can be greater than the corner crushing strength (Flanagan and Bennett 2001).

Smith (1967) considered that the tensile strength of masonry infills is equal to the tensile strength $f_t^{'}$ of mortar ($f_t^{'}$ considered as 10% of compressive strength of masonry $f_m^{'}$), as the mortar is generally much weaker in tension than an individual brick. He proposed expressions for computation of the diagonal cracking strength (R_t) as

$$R_t = f_t^{'} ht \tag{2.9}$$

The above model for diagonal tensile strength of infills was also adapted by Smith and Carter (1969). Mainstone (1971) experimentally correlated the nominal diagonal

cracking strength (R_t) of URM infills with the stiffness (λh) of infills relative to frame, and provided the following expressions and also presented them in form of charts:

$$R_t = 0.56(\lambda h)^{-0.875} f_m' d_m t \sin 2\theta, \quad \text{for} \quad 4 \le \lambda h \le 5 \tag{2.10}$$

$$R_t = 0.52(\lambda h)^{-0.8} f_m' d_m t \sin 2\theta, \quad \text{for} \quad \lambda h > 5 \tag{2.11}$$

Similar charts were also provided by Wood (1978) to estimate the diagonal cracking strength based on aspect ratio and relative stiffness of infill. Priestley and Calvi (1991) estimated the load required to induce diagonal cracking, as

$$R_t = \frac{\Pi}{2} d_m t f_t' \tag{2.12}$$

Saneinejad and Hobbs (1995) recommended the diagonal tensile strength of infill strut (R_t) at infill cracking as

$$R_t = 2\sqrt{2}\ th' f_t' \cos\theta \tag{2.13}$$

Although the diagonal tension cracking initiates diagonal compression failure, most of the researchers (Smith and Carter 1969; Paulay and Priestley 1992; Saneinejad and Hobbs 1995; Flanagan and Bennett 2001) consider this as a serviceability limit state rather than a strength limit state. However, in opinion of Priestley and Calvi (1991), even if diagonal cracking does not produce collapse of infills, it has to be considered in estimating capacity of infills due to the "possibility of out-of-plane expulsion of the panel when diagonal cracks are present on both diagonals". In the present study, the models proposed by Smith (1967), Priestley and Calvi (1991) and Saneinejad and Hobbs (1995) have been considered for evaluation of strength of infills against diagonal tension failure, as these models are based on the properties of infill alone and do not require additional information about the surrounding frame.

2.6.3 Strength of Infills in Diagonal Compression

Compressive failure of masonry infill panels along the loaded diagonal has also been observed in some past earthquakes (Özcebe et al. 2003; Durrani et al. 2005; Johansson et al. 2007) as well as in the experiments (Al-Chaar 1998). Smith (1967) proposed expressions for computation of the diagonal compressive strength (R_c) of the

equivalent strut, as given by Eq. 2.14. This model was also adapted by Smith and Carter (1969).

$$R_c = \alpha t f_m^{'} \sec\theta \tag{2.14}$$

where, $\alpha \left(= \frac{\pi}{2\lambda} \right)$ is contact length between frame and infill.

Liauw and Kwan (1985b) proposed two different models for evaluation of diagonal compressive strength of infills, based on assumption of failure at interface of infill with beam or column. The diagonal compressive strength of infills with "failure in infill-beam connections" (R_{cb}) was proposed as

$$R_{cb} = \frac{1}{cos\,\theta}\left(\frac{4M_{pj}}{h^{'}} + \frac{\sigma_c t h^{'}}{6} \right) \tag{2.15}$$

Whereas, the diagonal compressive strength of infills with "failure in infill-column connections" (R_{cc}) was estimated as

$$R_{cc} = \frac{1}{cos\,\theta}\left(\frac{4M_{pj}}{h^{'}} + \frac{\sigma_c t h^{'}}{6 tan^2\,\theta} \right) \tag{2.16}$$

where, σ_c is crushing strength of infill panel, and M_{pj} is the minimum of the plastic moment capacity of beam (M_{pb}) and column (M_{pc}).

The strength of the equivalent strut in diagonal compression failure mode (R_c), derived by Paulay and Priestley (1992) is function of vertical contact length (z) between infill panel and surrounding column, and is expressed as

$$R_c = \frac{2}{3}\alpha t f_m^{'} \sec\theta \tag{2.17}$$

Saneinejad and Hobbs (1995) recommended the diagonal compression strength (R_c) of the slender infill as

$$R_c = 0.5 h^{'} t f_a \sec\theta \tag{2.18}$$

where, f_a is the compressive strength of infill in its central region, considering out-of-plane buckling.

Al-Chaar (1998) considered the effect of openings and existing damage on crushing strength (R_c), using two multiplication factors (R_1) and (R_2), respectively.

$$R_c = aR_1R_2tf'_m \tag{2.19}$$

where, a is the width of equivalent diagonal strut.

ACI 530 (2005) has adapted the model proposed by Saneinejad and Hobbs (1995) for estimating diagonal compressive strength of infills. The following values of f_a recommended for masonry piers, can also be used for infill panels:

$$f_a = f'_m\left(1-\left(\frac{d_m}{140r}\right)^2\right), \qquad \text{if } \frac{d_m}{r} \le 99 \tag{2.20}$$

$$f_a = f'_m\left(\frac{70r}{d_m}\right)^2, \qquad \text{if } \frac{d_m}{r} > 99 \tag{2.21}$$

where, d_m is the diagonal length, and r is radius of gyration of the equivalent strut.

Among various models described above for estimating diagonal compressive strength of infills, the model by Liauw and Kwan (1985b) is complex, as it requires computation of plastic moment capacity of frame members, whereas the models by Smith (1967), Paulay and Priestley (1992) and ACI 530 (2005) do not require strength of frame members and are easier to use, and the same have been used for further comparative study of different modes of failure.

2.6.4 Strength of Infills in Corner Crushing

This mode of failure occurs at one of the loaded corners of the infills, where the concentrated compressive force caused by lateral loading exceeds compressive strength of infill. Mainstone (1971) correlated the nominal diagonal crushing strength (R_{cr}) of URM infills with the relative stiffness parameter (λh), as

$$R_{cr} = 0.17(\lambda h)^{-0.4}\ f'_m d_m t \sin 2\theta, \qquad \text{for } 4 \le \lambda h \le 5 \tag{2.22}$$

$$R_{cr} = 0.15(\lambda h)^{-0.3}\ f'_m d_m t \sin 2\theta, \qquad \text{for } \lambda h > 5 \tag{2.23}$$

Based on the experimental results of steel frames with URM infills, Wood (1978) also observed that the crushing strength of infills is dependent on the relative stiffness of infills and frame members and aspect ratio of infills; and developed design charts for determination of crushing strength of infills.

On the other hand, Liauw and Kwan (1985b) performed non-linear finite element analysis of infilled frames and identified two different modes of corner crushing of infills considering plastic moments of the surrounding beams and columns. They estimated the corner crushing strength of infills (R_{crb}) with "failure in columns and infill-beam connections," as

$$R_{crb} = \frac{\sigma_c th'}{\cos\theta} \sqrt{\frac{2(M_{pj} + M_{pc})}{\sigma_c th'^2}} \tag{2.24}$$

Similarly, the corner crushing strength of infills (R_{crc}), with "failure in beams and infill-column connections," was estimated as

$$R_{crc} = \frac{1}{\sin\theta}\left[\sqrt{\frac{2(M_{pj} + M_{pb})}{\sigma_c th'^2}}\sigma_c th'\right] \tag{2.25}$$

According to Saneinejad and Hobbs (1995), the corner crushing strength (R_{cr}) of equivalent strut along the loaded diagonal can be represented as

$$R_{cr} = \frac{(1-\alpha_c)\alpha_c th'\sigma_c + \alpha_b tl\tau_b}{cos\theta} \tag{2.26}$$

where, α_c and α_b are normalized contact lengths of column and beam, respectively, σ_c is the normal contact stress along the column, and τ_b is the shear stress along the beam.

Based on a series of large-scale tests on URM infilled steel frames, Flanagan and Bennett (1999) have developed a simple method for determining the corner crushing strength (R_{cr}) of diagonal strut as a function of the infill thickness (t) and the infill compressive strength (f_m').

$$R_{cr} = \frac{K_{ult} t f_m'}{cos\theta} \tag{2.27}$$

The empirical constant, K_{ult} was determined from the experimental results.

Corner crushing is a relatively rare phenomenon reported in case of strong infills with strong surrounding frame. Masonry infills are more likely to fail under other modes of failure, viz. sliding shear, diagonal tension, and diagonal compression due to buckling of infills. A comparative study of capacity of infills in different modes of failures has been presented in the next Chapter, to identify the most likely mode of failure.

2.7 INELASTIC MODELING OF URM INFILLS

The shear behavior of masonry infill panels is considered (ASCE-41 2007) as a deformation controlled action and nonlinearity of infills is considered through a generalized force-deformation relationship and acceptance criteria. Fig. 2.4 represents the generalized force deformation curve according to ASCE-41 (2007), where points B and C represent the yield point, and the point of significant strength degradation, respectively. The various limit states (IO, LS, and CP) are specified by ASCE- 41 in terms of the drift ratio (Δ_{eff} / h_{eff}). In the present study, lumped plasticity models of the infills are used, in which axial plastic hinges with strength capacity as described earlier, has been assigned at mid-length of the equivalent diagonal struts.

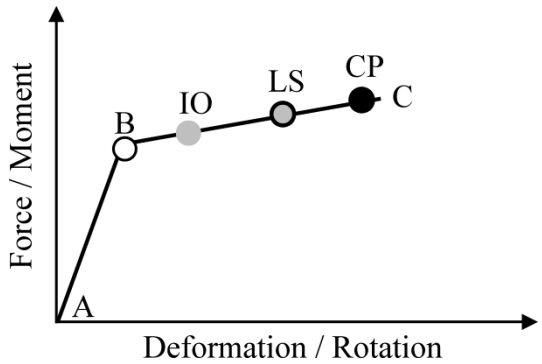

Fig. 2.4 Generalized force-deformation behavior of a typical URM infill, with performance limit states as per ASCE-41 (2007).

2.8 CONSTRUCTION SEQUENCE OF INFILLED FRAMES AND ITS EFFECT ON SEISMIC BEHAVIOR

Traditionally, infill panels in framed buildings are provided after construction of the frame is completed, at least for a few storeys. The construction sequence of infill

panels relative to RC frame followed in India is shown in Fig. 1. 1. Figs. 1.1 (a) and 1.1 (c) show intermediate stages of construction of infill panels in RC frames, whereas Figs. 1.1 (b) show the final stage. The construction sequence of infilled frames leads to a gap between the infill panel and the beam above (Fig. 1.1 (c)). This gap spares the infill panels from resisting any gravity load coming to the frame. Even relatively small initial gap can have significant effect on the structural behavior of infilled frames (Riddington 1984; Saneinejad and Hobbs 1995). According to Moghaddam and Dowling (1987), parameters like initial lack of fit between infill and frame, and workmanship may have even higher impact on the strength of infilled frame than the parameters like strength and stiffness of infills, though these are difficult to be quantified and generalized.

Contrary to the actual sequence of construction, in the conventional 'simultaneous' analysis procedure, the infills and the frame are considered to come to existence instantaneously, and the infills are also subjected to vertical as well as lateral loads, along with the frame members. The application of this fictitious vertical load in the infills may significantly affect their behavior, simulated in a simultaneous analysis. In order to predict realistic behavior of infilled frames, an attempt has been made in the present study to simulate the effect of construction sequence of infilled frames, in non-linear static pushover analysis, where no vertical load is transferred to infills under gravity loading.

To study the effect of the construction sequence on the predicted behavior of the infilled frames, two sets of four and ten storey uniformly infilled RC frame buildings have been considered. The buildings considered in the study have generic plan geometry as shown in Fig. 2.5 with two heights - four and ten storeys.

The first set of the four and ten storey buildings are designed for gravity loads only considering relevant Indian Standards (BIS 1987 (Part 1), 1987 (Part 2), 2000) whereas the second set of buildings are designed for earthquake loading also (BIS 2002) and reinforcement has been detailed as per the requirement for 'Special Moment Resisting Frame (SMRF)' (BIS 1993). Both the sets of buildings have been assumed to be situated on hard soil in Seismic Zone IV (Effective Peak Ground Acceleration, EPGA = 0.24*g* for the Maximum Considered Earthquake). India being seismically active region, all the buildings should be designed for earthquake loads,

however, due to poor enforcement and lack of awareness, buildings are still being constructed without any consideration for seismic actions, and there exists a huge stock of such buildings, even in the high seismicity zones (Ghosh 2008; DEQ 2009). It has been observed in past earthquakes that the frame-infill interaction plays an even important role in such buildings. Therefore, buildings designed for gravity loads alone, have also been considered in the present study.

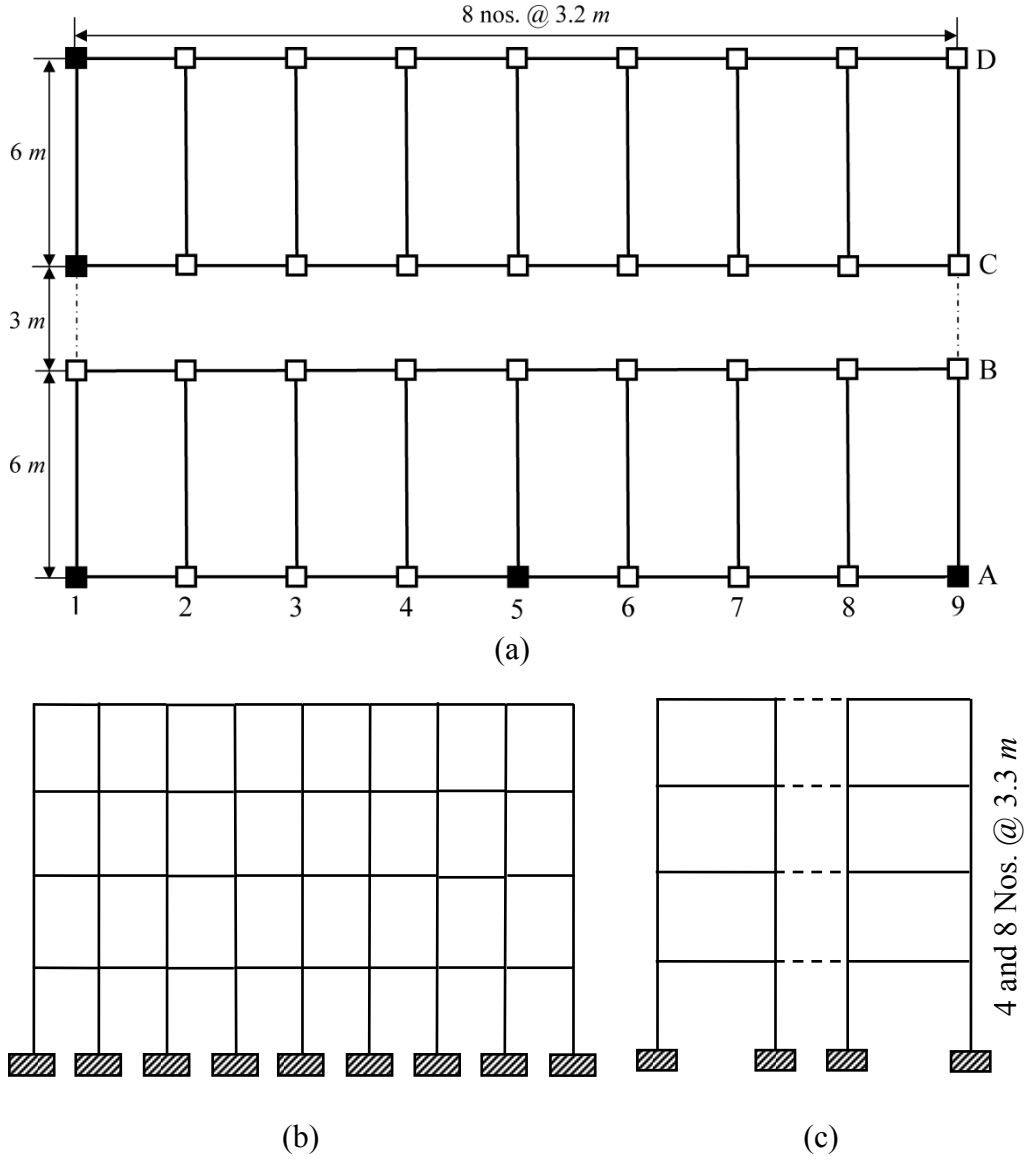

Fig. 2.5 (a) Plan of the considered buildings (columns with black shade are the representative columns chosen for detailed investigation); (b) front and (c) side elevation of the considered buildings (the dotted lines represent the floor slabs rigid in plane).

Infill panels are modelled as concentric equivalent diagonal struts. Both the sets of the buildings have been analyzed for lateral loads due to earthquake with and without considering the construction sequence of infills. To simulate the construction sequence, the analysis has been done in two stages. In the first stage, the bare frame has been subjected to gravity load; and in the second stage, the infills are added and lateral load is applied along with the existing gravity load. The buildings have also been analyzed neglecting the stiffness and strength of infills (i.e. considering the buildings as bare frames), as is the case in normal course of design. Nonlinear static (pushover) analysis has been carried out using nonlinear analysis software SAP2000 (2010) to estimate the capacity curves of the buildings in different cases. Non-conforming, 'NC' and conforming, 'C' type of transverse reinforcement has been considered for gravity designed and SMRF frames, respectively, to assign the plastic rotations for beams and columns as per ASCE-41 (2007).

Figures 2.6 and 2.7 show the hinge pattern of the infill panels in the four and ten storey gravity load designed buildings, respectively, subjected to gravity load alone, when the initial gap between infill and frame is not considered in the modeling. It can be observed from the Figs. that some of the infill panels in the longitudinal direction, in bottom storey of the four storey building have yielded under the gravity load itself. In case of the ten storey building, the effect is even more pronounced, where all the infill panels in the bottom three storeys in longitudinal direction, and the bottom two storeys in transverse direction, have crossed "Immediate Occupancy" (IO) performance level (ASCE-41 2007). Similarly, Figs. 2.8 and 2.9 show the yield pattern of the infill panels in the four and ten storey buildings, respectively, designed for earthquake loads. The buildings are subjected to gravity load alone without considering the construction sequence. Similar behavior is observed in this case also, except that the number of panels yielding under gravity load reduces due to relative increase in the size of frame members in case of buildings designed for earthquake forces. This behavior is contradictory to the common observation and understanding that the infills do not share gravity loads. Therefore, there is need to simulate the construction sequence in the analysis of infilled frames to get realistic results. Figures 2.10 and 2.11 compare the capacity curves of the four storey and ten storey gravity load designed bare and uniformly infilled frames with and without considering the construction sequence.

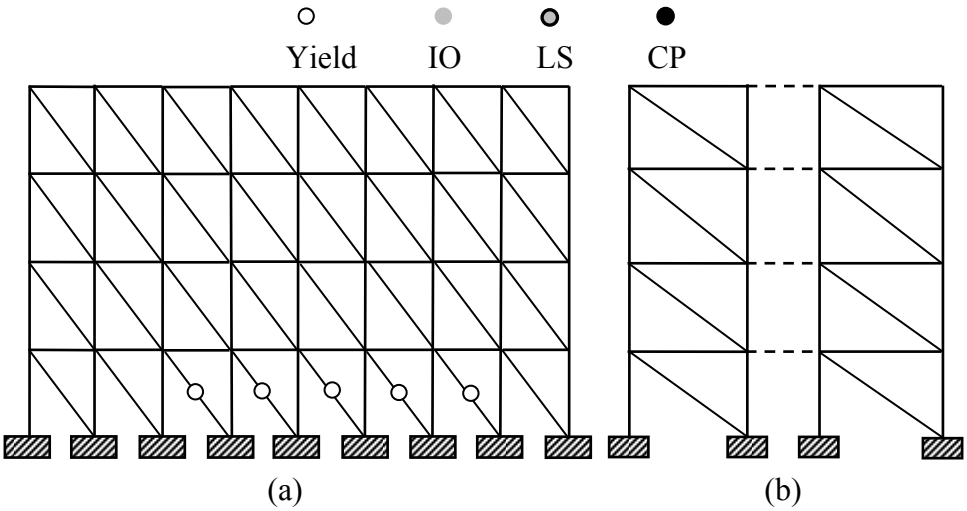

Fig. 2.6 Hinge pattern under gravity load for the four storey uniformly infilled frame building, designed for gravity loads only, when construction sequence is not considered in analysis: (a) typical longitudinal frame; (b) typical transverse frame.

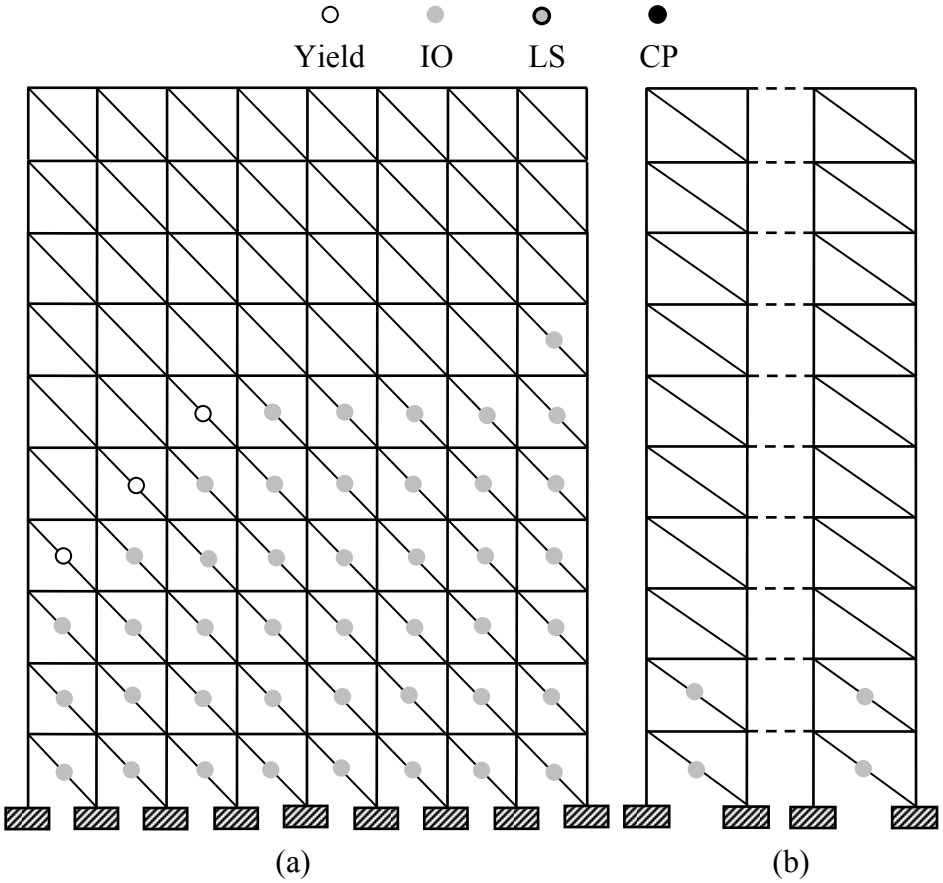

Fig. 2.7 Hinge pattern under gravity load, for the ten storey uniformly infilled frame building, designed for gravity loads only, when construction sequence is not considered in analysis: (a) typical longitudinal frame; (b) typical transverse frame.

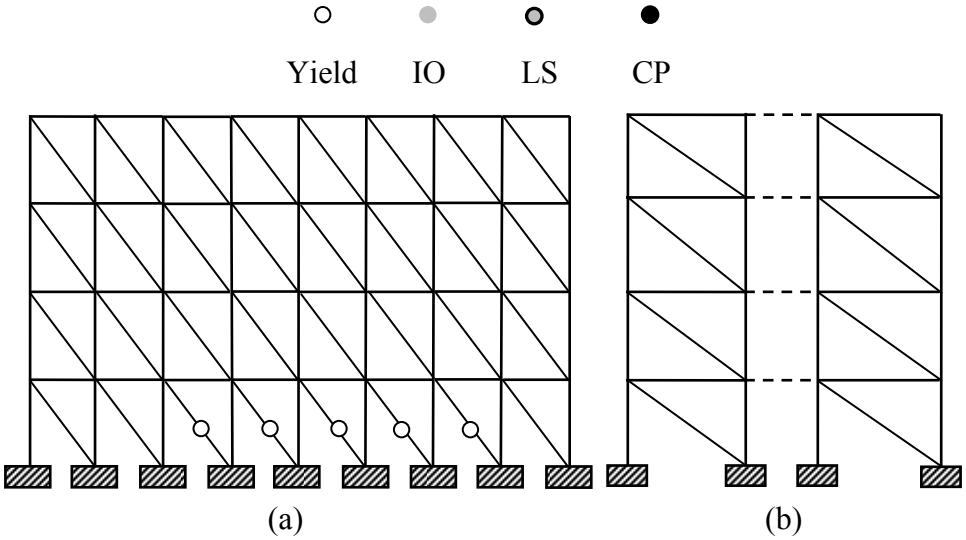

Fig. 2.8 Hinge pattern under gravity load for the four storey uniformly infilled SMRF building, when construction sequence is not considered in analysis: (a) typical longitudinal frame; (b) typical transverse frame.

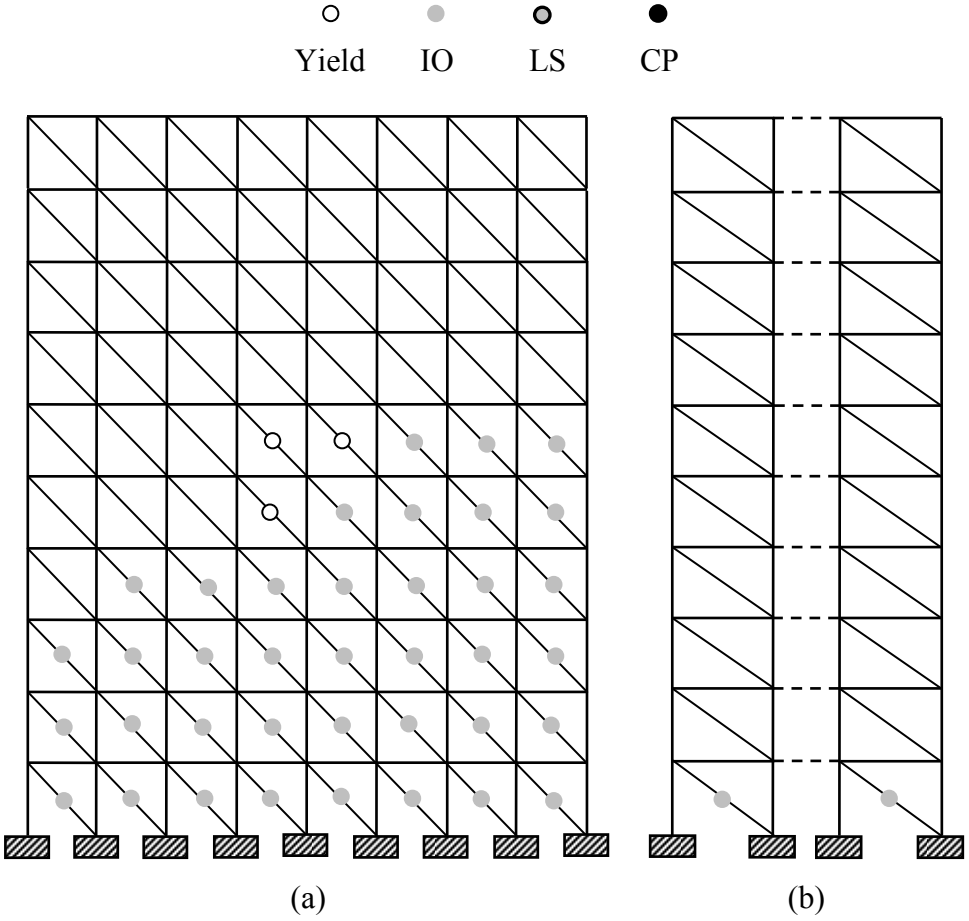

Fig. 2.9 Hinge pattern under gravity load for the ten storey uniformly infilled SMRF building, when construction sequence is not considered in analysis: (a) typical longitudinal frame; (b) typical transverse frame.

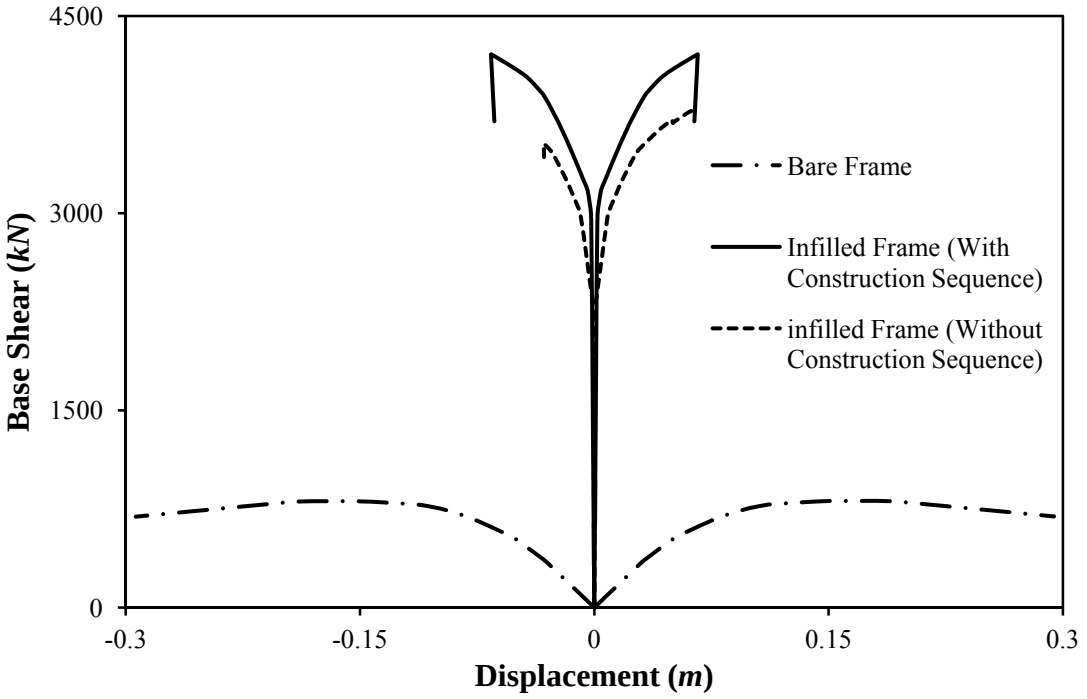

(a)

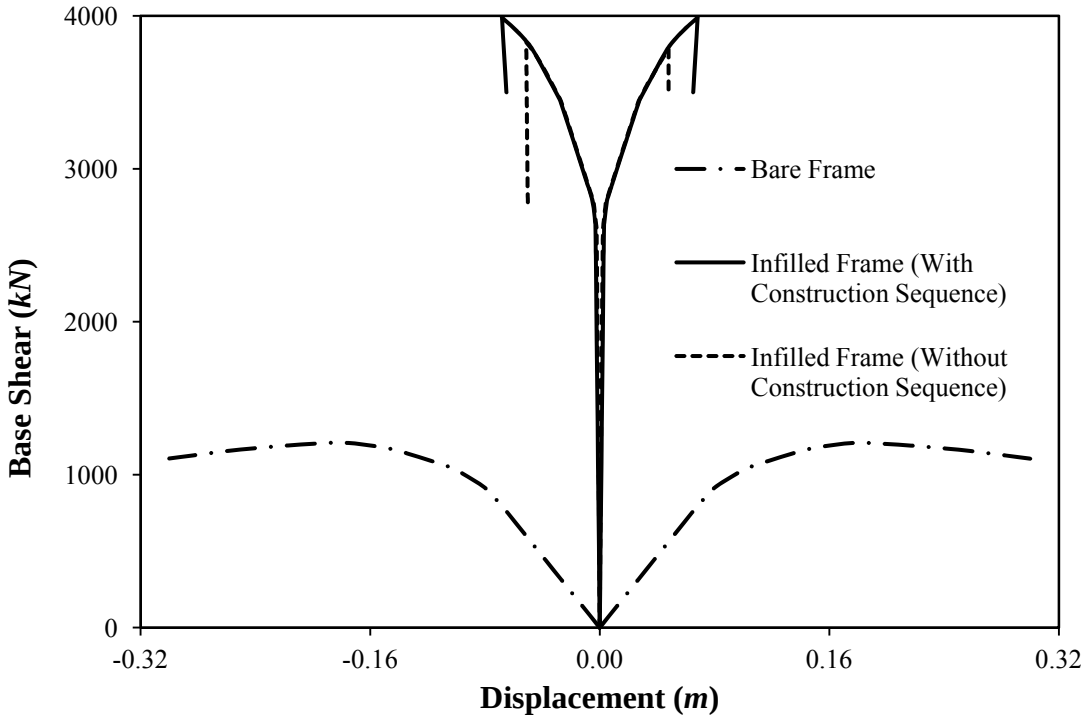

(b)

Fig. 2.10 Comparison of capacity curves for the four storey bare and uniformly infilled RC frame building designed for gravity load only: (a) longitudinal direction; (b) transverse direction.

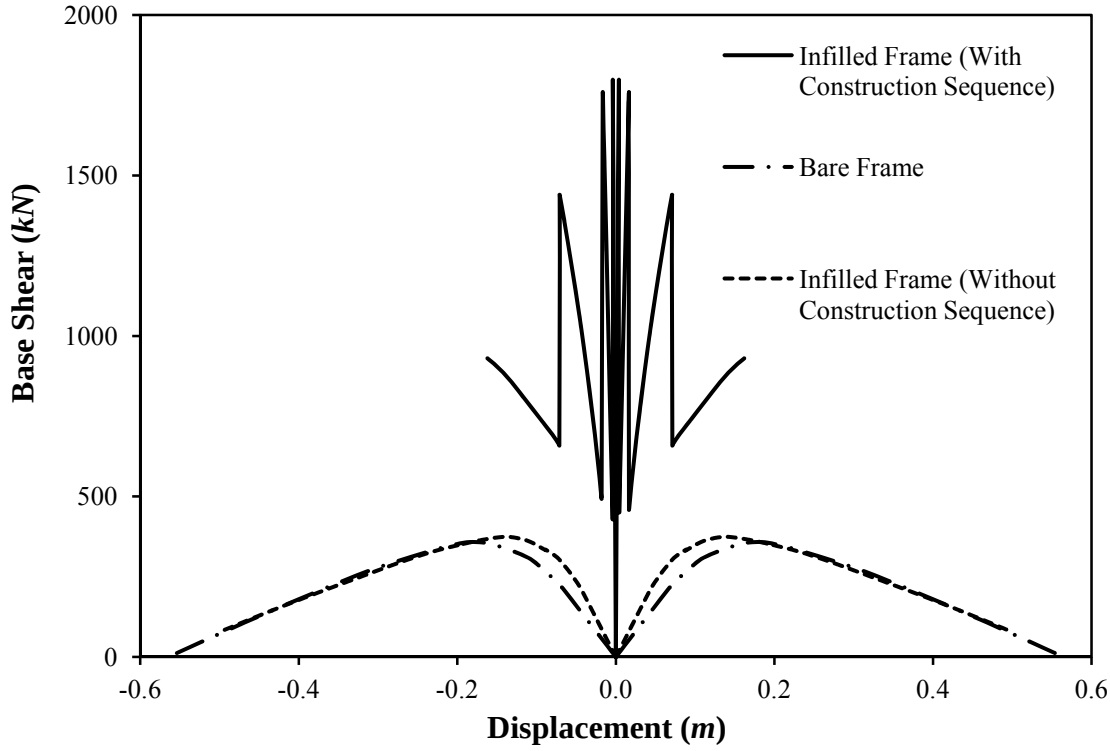

(a)

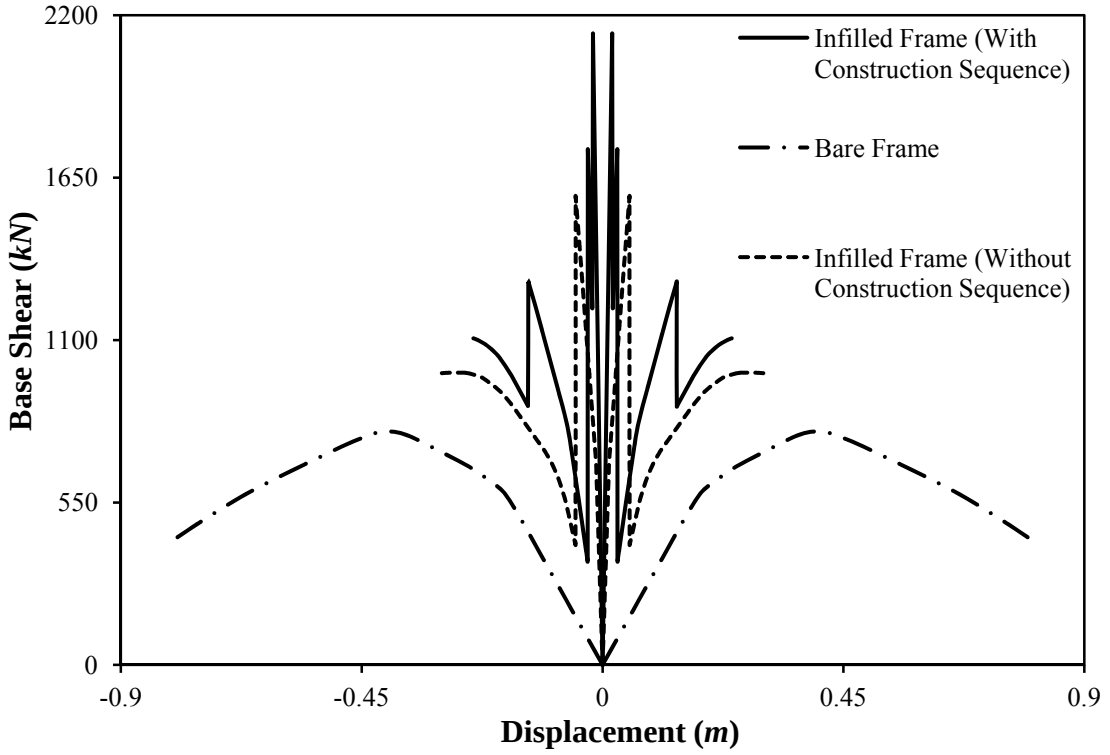

(b)

Fig. 2.11 Comparison of capacity curves for the ten storey bare and uniformly infilled RC frame building designed for gravity load only: (a) longitudinal direction; (b) transverse direction.

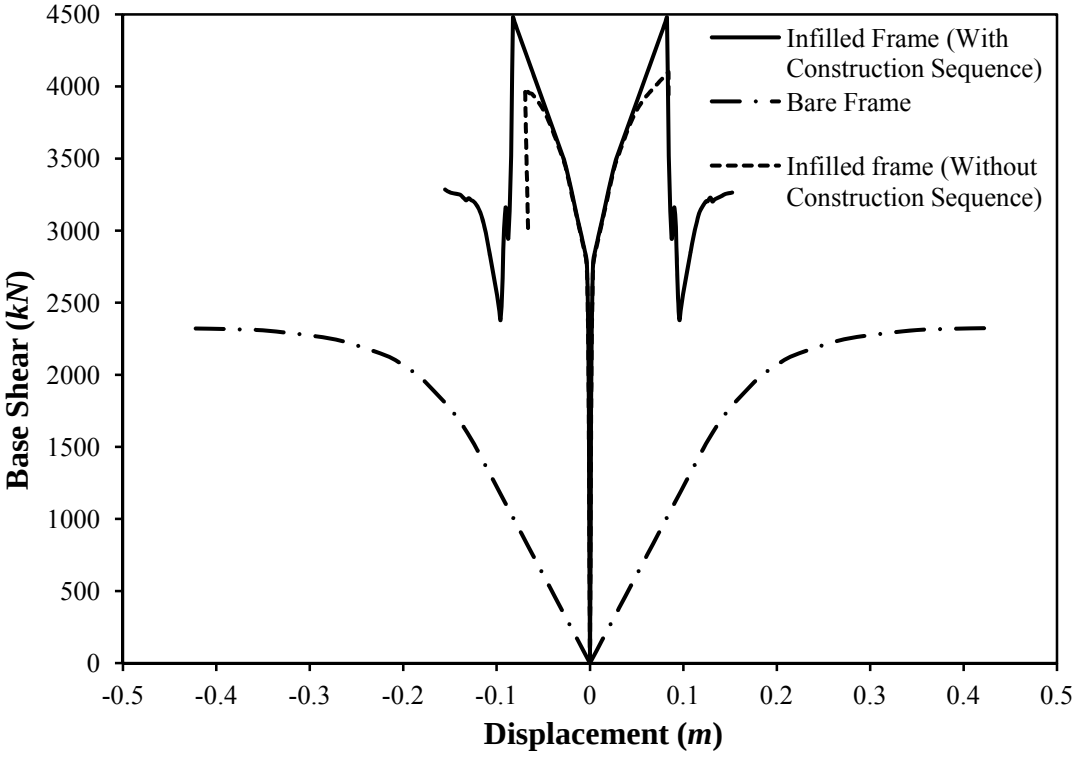

(a)

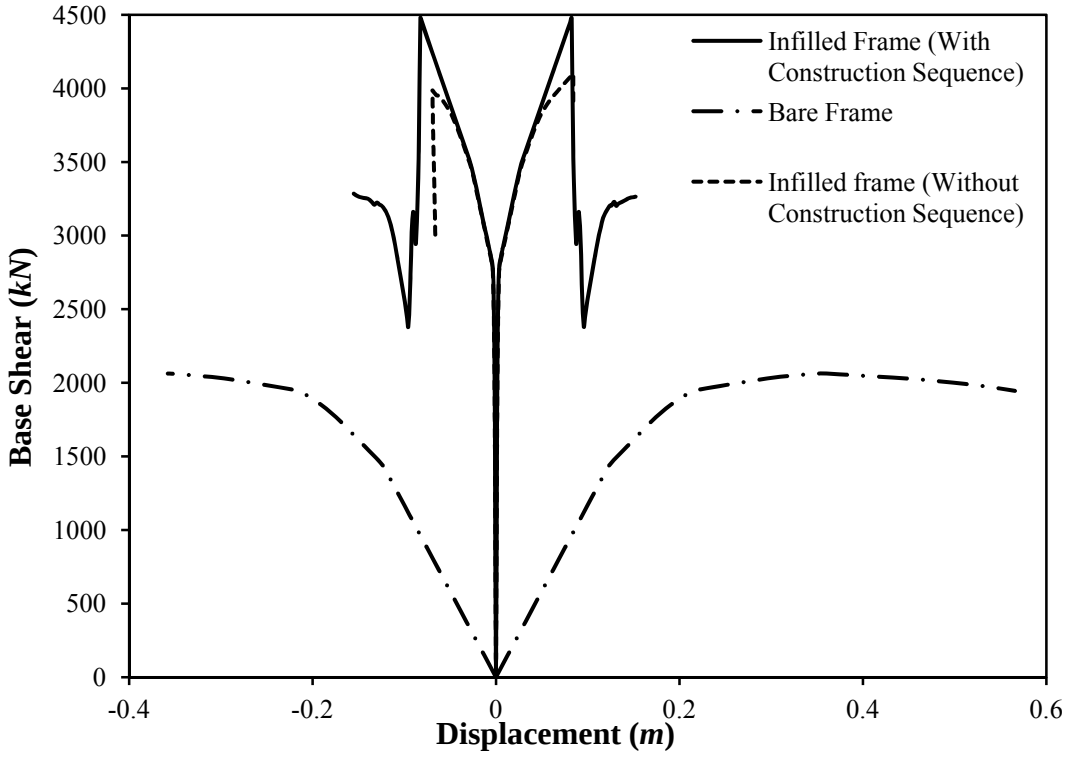

(b)

Fig. 2.12 Comparison of capacity curves for the four storey bare and uniformly infilled SMRF building: (a) longitudinal direction; (b) transverse direction.

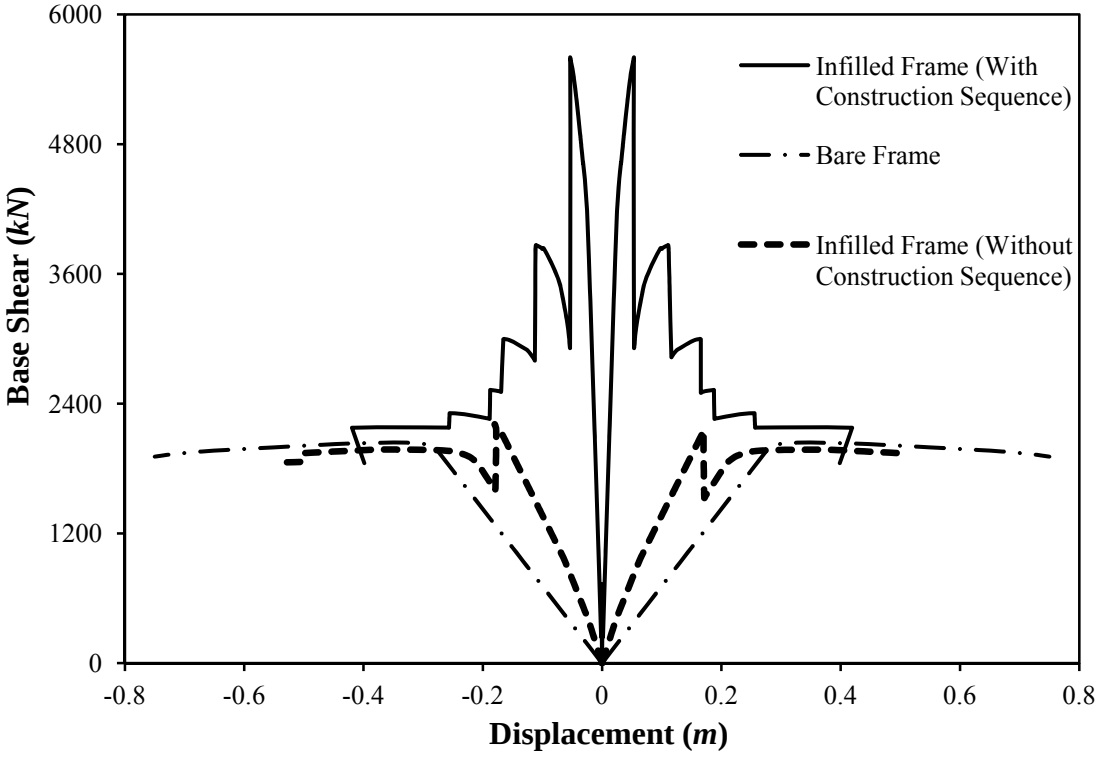

(a)

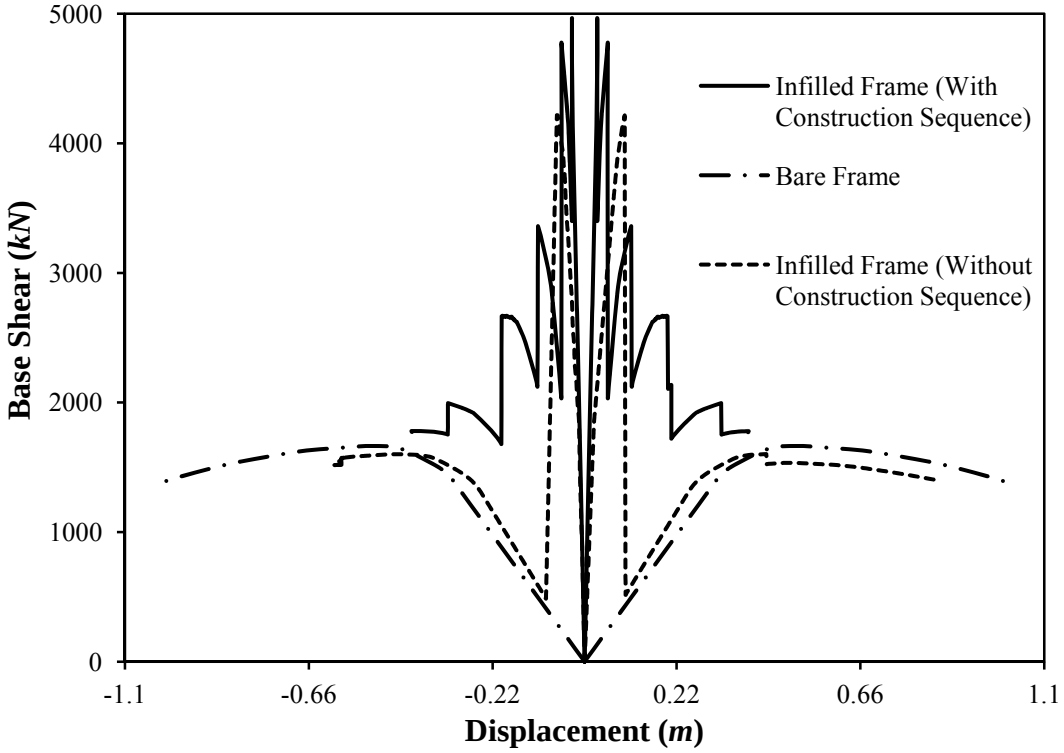

(b)

Fig. 2.13 Comparison of capacity curves for the ten storey bare and uniformly infilled SMRF building: (a) longitudinal direction; (b) transverse direction.

It can be observed from the Figs. that in case of the four storey gravity load designed building, the effect of construction sequence is relatively small and the capacity curve is close to the case when construction sequence is ignored, whereas in case of the ten storey building the effect of construction sequence is so dramatic that the capacity curve in the longitudinal direction is close to that of the bare frame. This is because in case of four storey building, no infill panel in transverse direction and a very few infill panels in longitudinal direction (Fig. 2.6), yielded under gravity load, whereas in case of the ten storey buildings, a large number of infill panels (particularly in the longitudinal direction) yielded under gravity load itself (Fig. 2.7). The comparison of capacity curves of the four and ten storey SMRF buildings is presented in Figs. 2.12 and 2.13, respectively. As these buildings are designed for earthquake forces also, the strength and ductility increases as compared to the gravity load designed buildings. Further, as the stiffness and strength of the frame members increase, relative to the infills, the effect of infills on capacity curve reduces. The effect of construction sequence of infill panels on the capacity curves of the four and ten storey SMRF buildings is similar as in case of the corresponding gravity load designed buildings, i.e. dramatic effect of construction sequence is observed in case of 10 storey SMRF building, as well.

2.9 SELECTION AND VALIDATION OF STRUT MODEL FOR INFILLS

This section aims to select and validate the most reliable strut model for simulating the failure modes in URM infilled frames observed during past earthquakes and experimental studies. Figure 2.14 summarizes the 1-, 2- and 3-strut models considered in the present study to estimate shear force demand on columns adjacent to URM infill. Saneinejad and Hobbs (1995) and some other researchers have suggested that single-strut model may not be able to represent the interaction between the infill and the bounding frame, and the force distribution in frame elements, accurately.

However, most of the available models consider infills to be in full contact with the adjacent frame members, whereas, in practice, the construction sequence does not allow a full contact between infill and soffit of the beam above (Fig. 1.1 (c)). The gap between infills and beams has a significant effect on the seismic behavior of infilled frames (Riddington 1984; Moghaddam and Dowling 1987).

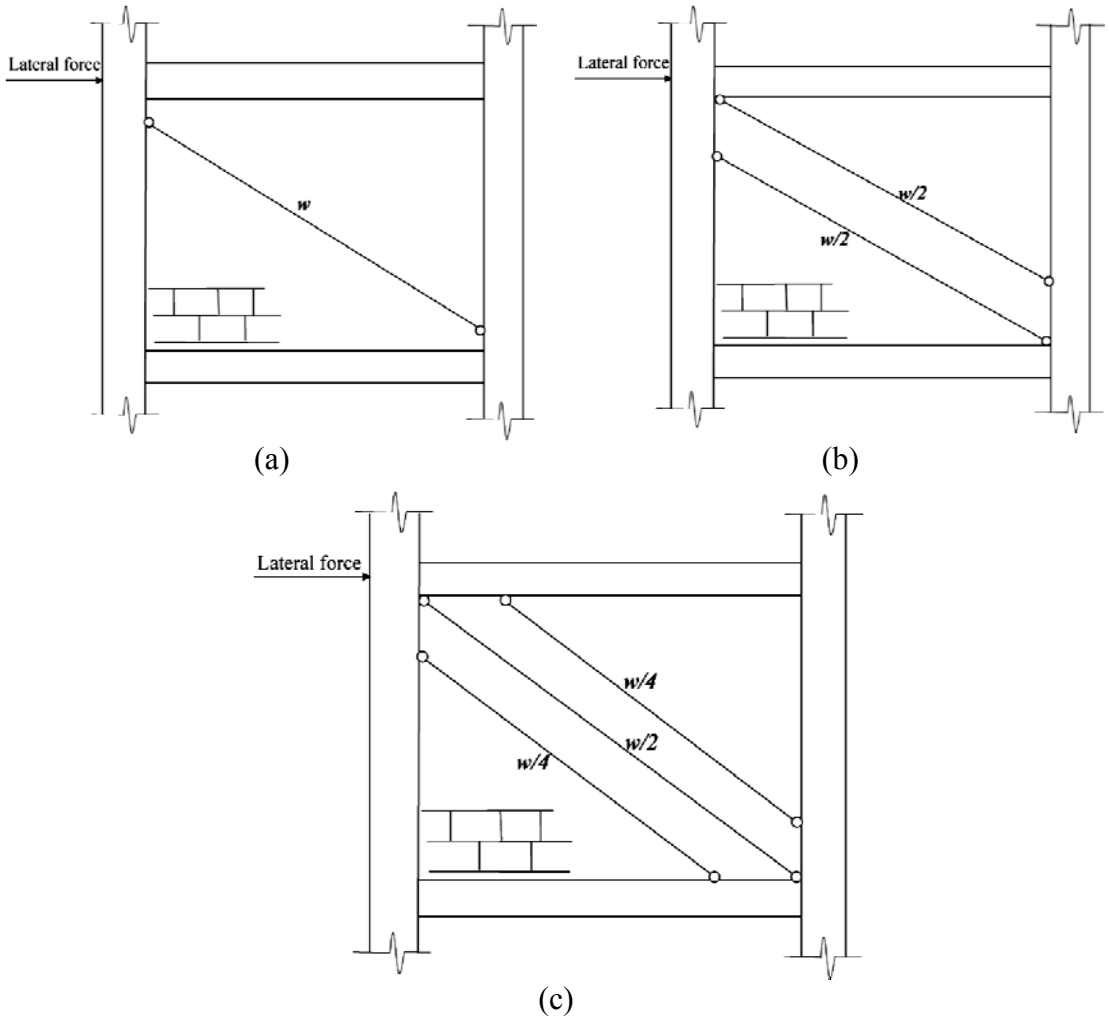

Fig. 2.14 Different strut models considered in the study.

Based on a comparative study, Crisafulli (1997) concluded that the single-strut model gives reasonably accurate estimation of stiffness of the infilled frame and the axial forces induced in the frame members under lateral loading; and is adequate for prediction of the overall response of the infilled frame. In the present study, efficacy of 1-, 2-, and 3-strut models to predict the failure modes of adjacent columns has been evaluated against the experimental results of Mehrabi et al. (1996), Al-Chaar (2002), and Kaushik and Manchanda (2010), shown in Table 2.5.

Shear force applied to columns in different models has been considered as horizontal component of the capacity (minimum of the strength estimated in different failure modes of infills) of the strut connected to the column. In case of single strut model, the horizontal component of the full strut force is applied to the column, whereas in case of 2- and 3-strut models, the strut capacity is distributed in proportion to the cross-sectional area of struts, and the shear force applied on the column is half and

one fourth, respectively of that in case of single strut. It can be observed from the Table that shear force demand predicted using the single strut model exceeds the column capacity in case of Mehrabi et al. (1996) and Kaushik and Manchanda (2010) whereas in case of Al-Chaar (2002), shear force demand predicted by all the three models exceeds the capacity, indicating shear failure. The Table shows that the single strut model predicts the shear failure of columns in all the cases, which is in agreement with the experimental observations, whereas, the 2- and 3- strut models are not able to predict the experimentally observed behavior in three of the five considered cases. This is due to the gap between the infill and the soffit of the beam (Fig. 1.1 (c)), as evident from the failure modes shown in Fig. 3.2 (b), where the top one or two courses of masonry become loose and slide, negating the possibility of formation of struts in contact with the beam. Therefore, a single eccentric strut in contact with columns (Fig. 2.14 (a)) simulates the behavior of infilled frame, most realistically, and has been used for further study.

Table 2.5
Evaluation of efficacy of 1-, 2-, and 3-strut models to predict the failure modes observed during experimental studies on infilled frames

Reference of experimental study	Column shear strength (*kN*)	Shear force applied to column (*kN*)			Experimental observation
		1-strut model	2-strut model	3-strut model	
RC frame with unreinforced solid concrete block masonry infill (Mehrabi et al. 1996)	92.95	130.98	65.49	32.74	Shear failure of columns
RC frame with burnt clay brick infill (Al-Chaar 1998)	29.06	124.41	62.20	31.1	Shear cracks in column
RC frame with concrete masonry infill (Al-Chaar 1998)	29.06	345.55	172.77	86.39	Shear cracks in column
Non ductile RC frame with burnt clay brick infill (Kaushik and Manchanda 2010)	51.14	57.75	28.88	14.44	Shear cracks in columns
Ductile RC frame with URM infill (Kaushik and Manchanda 2010)	60.31	66.00	33.00	16.50	Columns suffer shear damage

2.10 PROPOSED MODELING OF URM INFILLS

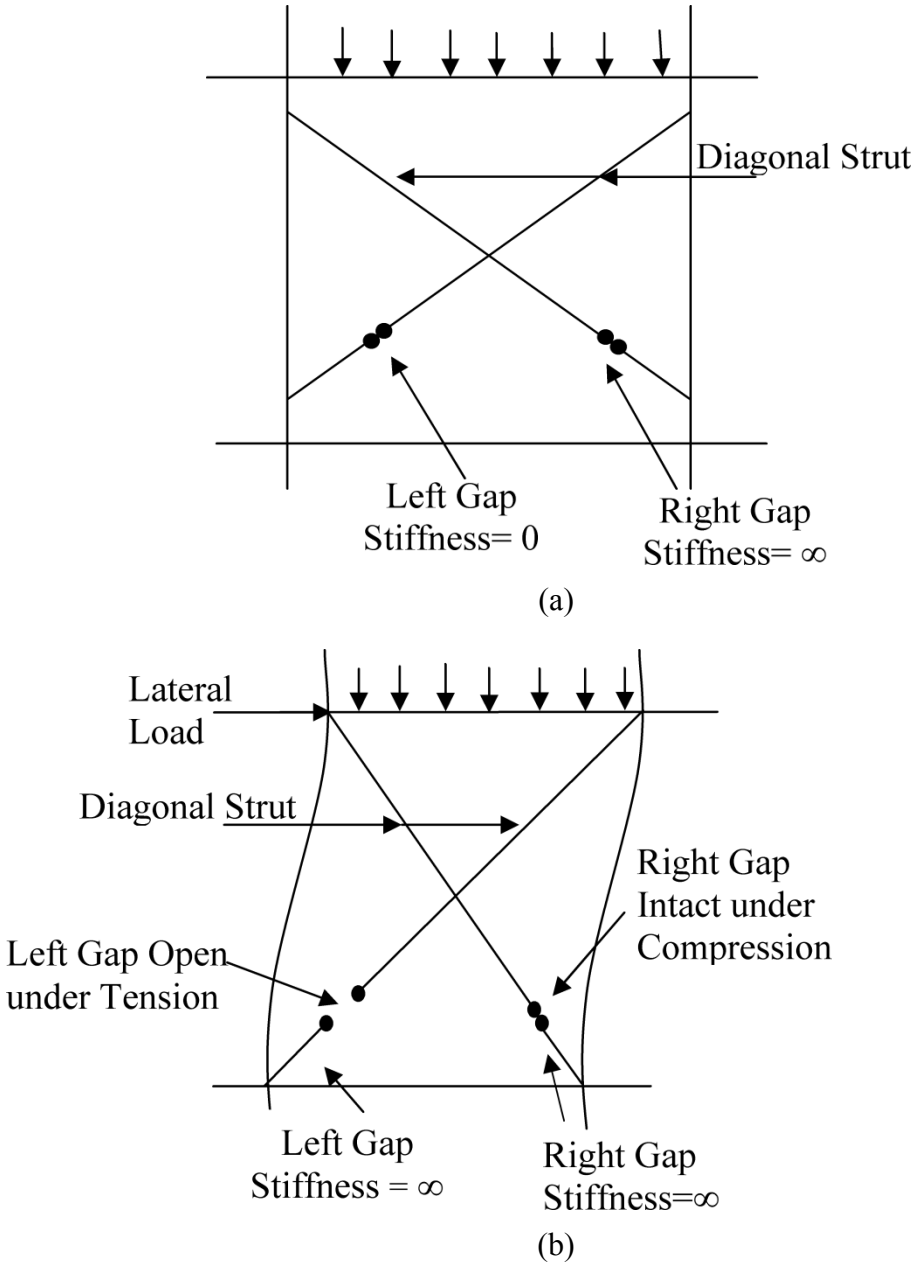

Fig. 2.15 Proposed model for infill panel for: (a) linear analysis; (b) non-linear analysis.

As described earlier, the observations made in the past studies (Smith 1962; Madan et al. 1997; Asteris 2003; ASCE-41 2007) and as shown in that a single equivalent eccentric diagonal compressive strut element can simulate the behavior of an infill panel, quite realistically. To simulate the effect of initial lack of fit between infilled panel and beam, in the present study, 'gap' elements have been used. In presence of gap elements, the struts are active in compression only. Since the 'gap' element is

active in nonlinear analysis only, the stiffness of the gap elements has been assigned in such a way that it will result in identical initial stiffness in the linear as well as nonlinear analysis of the infilled frame. In linear analysis, the action of strut with gap element is shown in Fig. 2.15 (a), where one brace is inactive due to zero stiffness of gap element. Similarly, the action of struts with gap elements in nonlinear analysis is shown in Fig. 2.15 (b), where the gap element makes the strut ineffective in tension.

2.11 SUMMARY

A review of available techniques for elastic and inelastic modeling of RC frame members and their strength in various failure modes has been presented. For simulation of URM infills in infilled frames, a stock of techniques available in literature and different design codes is taken. The effect of construction sequence on seismic performance of URM infilled RC frame buildings has been studied with the help of an analytical study carried out on four and ten storey buildings with different design levels. It has been observed that simulation of construction sequence of infills relative to frame has a drastic impact on the estimated capacity curve of the infilled frames and this effect increases with the height of the building. The conventional simultaneous analysis ignoring the construction sequence may be highly erroneous in some cases, and it has been found to almost nullify the effect of infills in longitudinal direction of the ten storey building considered in the present study. To identify the most realistic macro-model of URM infills, a comparative study has been carried out using the selected equivalent diagonal strut models of infills and validated with the field and laboratory observations reported in literature. The comparison of numerical study with the experimetal observations suggests that simulation of infills using single equivalent strut, eccentrically connected to columns, can realistically predict the failure modes in infilled frames. Thereafter, a macro-model for simulation of the URM infill panels with lack of fit has been presented, which can be easily implemented on available software for nonlinear analysis.

Chapter 3

IDENTIFICATION OF FAILURE MODES OF URM INFILLED RC FRAME BUILDINGS

3.1 INTRODUCTION

Despite research efforts of several decades, assessing seismic performance of masonry-infilled RC frame buildings remains a challenging task. Under lateral load, infills act as diagonal struts (Fig. 3.1) and interact with frame, leading to complex failure mechanisms (Shing et al. 1992; Mehrabi et al. 1996). Considering the complexity of infill-frame interaction, most of the design codes are silent about design of infilled frames. However, popularity of URM infilled RC frame buildings and devastating consequences of their poor performance, even in moderate earthquakes, highlight the need for further understanding of their inelastic behavior considering various failure mechanisms of infills and frame members.

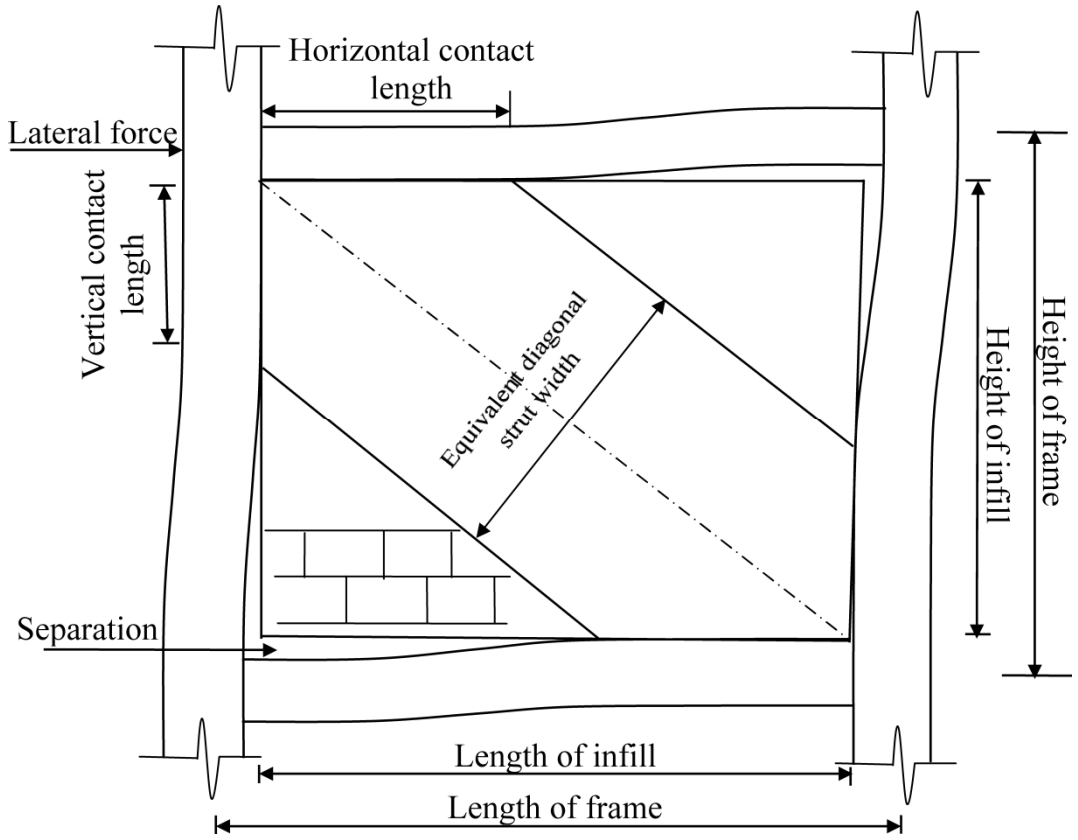

Fig. 3.1 Behavior of infilled frame under lateral load.

As URM infilled RC frame buildings constitute the majority of the existing building stock in many countries, reliable estimation of seismic fragility of such buildings is an important task in order to plan effective mitigation measures. With this objective, an attempt has been made in the present study to identify the various probable/observed modes of failure in infilled frames of different design levels under combined action of gravity and lateral loading. The literature including available earthquake damage survey reports (GSI 1995; DEQ 1999; EERI 2002; GSI 2003; Özcebe et al. 2003), experimental studies (Mehrabi et al. 1996; Al-Chaar 1998; Yuksel et al. 2006; Kaushik and Manchanda 2010), analytical models (Smith 1967; Mainstone 1971; Liauw and Kwan 1985b; Paulay and Priestley 1992; Saneinejad and Hobbs 1995; Al-Chaar 2002; El-Dakhakhni et al. 2003; Hegger et al. 2003; Sezen and Moehle 2004) and design codes (FEMA-356 2000; ACI 352R-02 2002; Eurocode-8 2004; ACI 318 2005; ACI 530 2005 ; NZS-3101:Part1 2006; ASCE-41 2007), generated from the scrupulous research on infilled frames, which started in early 1950s, has been reviewed. Based on the review, an analytical study has been carried out to identify the governing failure modes in URM infilled RC frame buildings designed with and without considering seismic actions as per Indian codes.

3.2 FAILURE MODES OF INFILLED FRAMES

The damage surveys during past earthquakes (GSI 1995; DEQ 1999; EERI 2002; GSI 2003; Özcebe et al. 2003) have shown that the infill-frame interaction alters the behavior of infilled frames, significantly, as compared to bare RC frames, and mostly leads to poor structural performance due to unintended failure mechanisms either at member level (e.g. shear failure in columns, damage to beam-column joints, short-column failure, or flexural failure of columns) or of the structure as a whole (e.g. soft storey mechanism, torsional failure, etc).

Figure 3.2 shows some observations of shear failure of columns due to strut action of infills. Figs. 3.2 (a) and 3.2 (b) show the observations from a post-earthquake damage survey (Özcebe et al. 2003), whereas Figs. 3.2 (c) and 3.2 (d) show the results of experimental studies (Mehrabi et al. 1996; Kaushik and Manchanda 2010). The field observations as well as experimental studies show shear failure of columns near the beam-column joints due to high shear force resulting from the horizontal component

of eccentric diagonal strut action of the masonry infills. The figures also show an important observation about the construction sequence of the infilled frames. Usually, the frames are constructed first, and then masonry is infilled within the frame panels. This results in a gap or lack of fit of masonry with soffit of the beam. This lack of fit of masonry at top of infill panel causes sliding along the infill-beam interface or along bed-joints, and explains the relatively lesser (or mostly no) damage to beams.

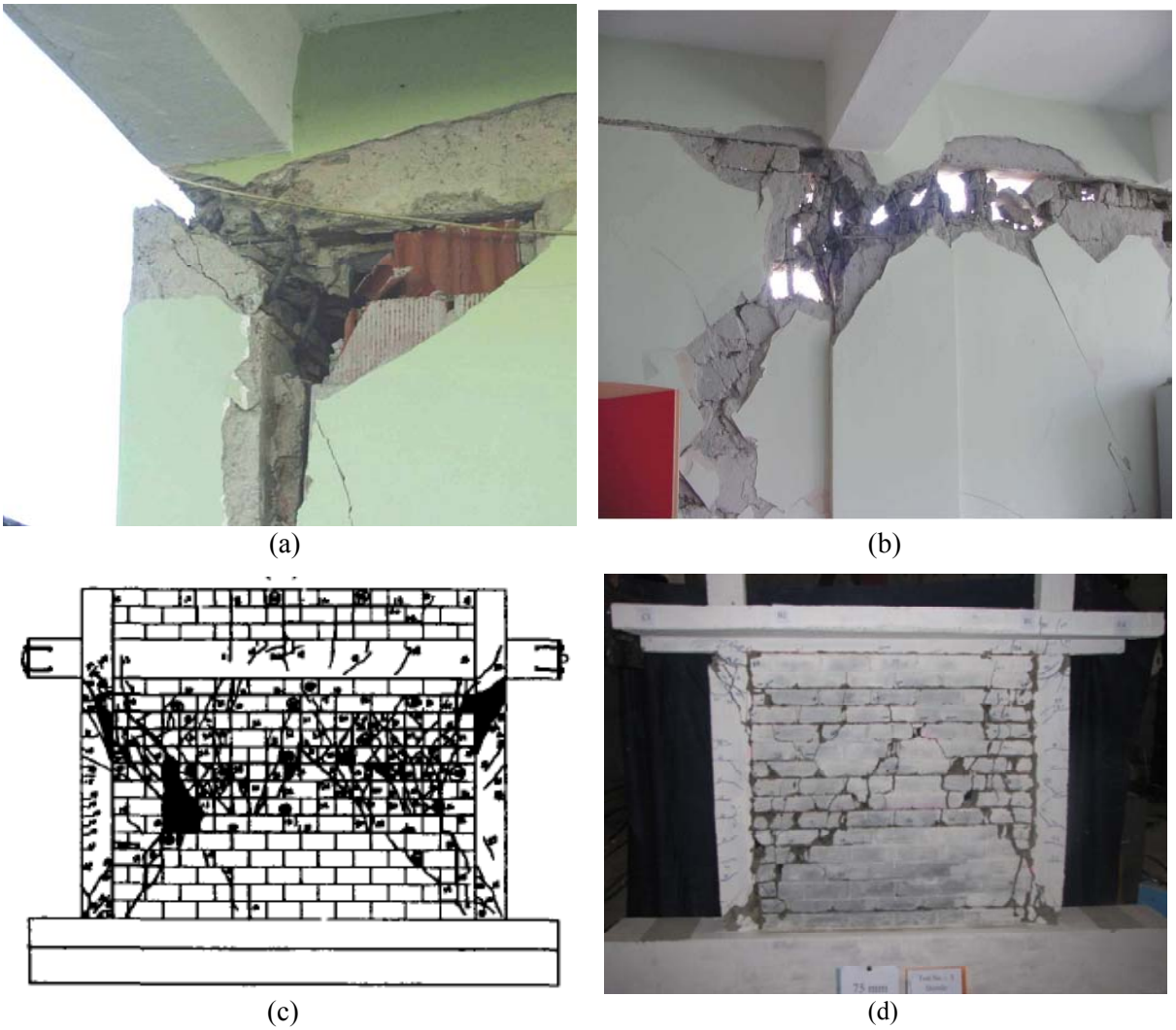

(a) (b) (c) (d)

Fig. 3.2 Shear failure of RC columns caused due to strut action of masonry infill: (a) failure of exterior column, and (b) failure of interior column observed in 2003 Bingöl earthquake (Özcebe et al. 2003); (c) column shear failure in experimental study (Mehrabi et al. 1996); (d) column shear failure due to strut action combined with bed-joint sliding of masonry infill (Kaushik and Manchanda 2010).

A few cases of damage to beam-column joints in infilled frames have also been reported in literature (Saatcioglu et al. 2001; Johansson et al. 2007). However, as it

will be shown later in this Chapter, the strut action of infill tends to reduce the shear stress in beam-column joint, and failure of joints in infilled frames appears to be less probable. The photographs taken during post-earthquake damage surveys also do not conclusively establish whether the beam-column joint failures occurred due to strut action of masonry or after failure (out-of-plane collapse) of infill panels when the frame essentially acts as a bare frame. Actually, the columns develop very high shear at the face of the beams and the shear cracks in columns may extend to some depth into the joint, particularly due to bond failure of bottom face reinforcement of beams (Fig. 3.2 (a)), which may not be properly anchored into columns in traditional constructions.

Short column effect due to partial infills is a frequently observed phenomenon in Indian buildings. Often, the top portion of the frame bay is kept open for sunlight and ventilation in the basement/ground (or an upper) storey of multistory-buildings. These partial infills have eccentric strut action resulting in excessive shear in columns. Due to the short bending length, the columns typically fail in shear (Fig. 3.3). Short column effect may also develop due to bed-joint sliding of the infill near mid-height (Paulay and Priestley 1992). Depending on the relative strength in the two modes, the columns may fail in shear (Fig. 3.3) or flexure-shear (Fig. 3.4).

(a) (b)

Fig. 3.3 Shear failure due to short column effect observed in Port-Blair, India, during 2004 Sumatra earthquake (Paul et al. 2004).

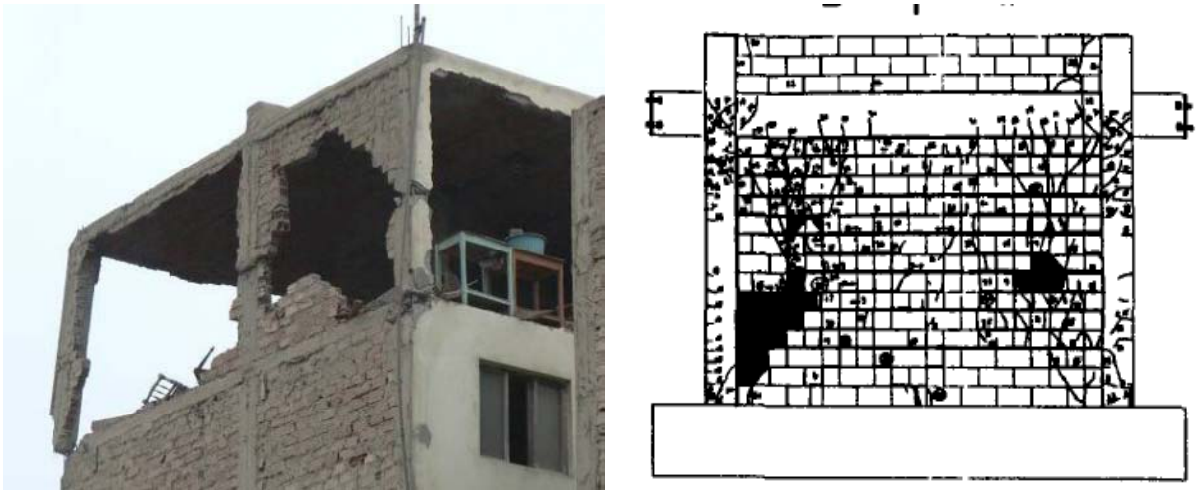

(a) (b)

Fig. 3.4 Flexure-shear yielding of columns due to bed-joint sliding of infill observed during: (a) 2007 Peru Earthquake (Johansson et al. 2007); and (b) experimental study by Mehrabi et al. (1996).

Irregular placement of infills in plan or elevation has been observed to cause drastic effect on seismic performance of infilled frame buildings. It is a prevalent practice in India as well as in many other countries to keep the ground storey open (without partitions) for parking or for commercial purposes. The lack of infills in such 'open' storeys, results in extreme soft and weak ground storeys, which are highly susceptible to damage during earthquakes. Failure of open ground storey buildings has been observed extensively during 2001 Bhuj earthquake (EERI 2002) in India, and also in many other earthquakes (Özcebe et al. 2003; Durrani et al. 2005; Johansson et al. 2007; Sharma et al. 2011) in different parts of the world. Complete collapse of an open ground storey building in 2001 Bhuj earthquake is shown in Chapter 1 (Fig. 1.2 (b)). The soft storey phenomenon can also occur in case of uniformly infilled frame buildings, where the infills in the ground storey may collapse first (Fig. 3.5) due to larger storey shear as compared to upper storeys.

Another common practice resulting in devastating consequences is keeping the front or side(s) of buildings open for commercial or other reasons. Such buildings develop excessive torsion resulting in collapse of flexible side columns. Fig. 3.6 shows failure of open front buildings observed during 2007 Peru earthquake (Johansson et al. 2007) and 2011 Sikkim earthquake.

Fig. 3.5 Soft storey phenomenon due to out of plane failure of infills in bottom storeys, during 2001 Bhuj earthquake.

(a) (b)

Fig. 3.6 Ground story failure due to torsional effect caused by irregular (asymmetric) ploacing of infills, during: (a) 2007 Peru earthquake (Johansson et al. 2007), and (b) 2011 Sikkim earthquake.

Table 3.1 presents an overview of different failure modes of RC members in URM infilled frames, as identified by various researchers. Brittle shear failure of beams and columns occurs due to strut action of infills (Smith 1967; Smith and Carter 1969; Fiorato et al. 1970; Paulay and Priestley 1992; Mehrabi et al. 1996) in case of weak frames with strong infills (Paulay and Priestley 1992) and frames with infills of partial height, whereas flexural yielding of columns is observed in case of frames with weak infills (Paulay and Priestley 1992; Mehrabi et al. 1996). Failure of the tension side

columns due to excessive overturning forces in infilled frames has been observed (Smith 1967; Smith and Carter 1969; Fiorato et al. 1970; Paulay and Priestley 1992) in case of infill panels with large aspect ratio (Paulay and Priestley 1992). Failure of compression side columns due to crushing of concrete has also been reported (Fiorato et al. 1970) in the frames with very high gravity loads.

Table 3.1
Identified failure modes of infilled frame members

Reference	Tension failure of columns	Compression failure of columns	Short-column effect	shear failure of beam/column	Flexural failure of columns	Failure of beam-column joints
Smith (1967)	●	○	○	●	○	○
Smith and Carter (1969)	●	○	○	●	○	○
Paulay and Priestley (1992)	●	○	●	●	●	○
Mehrabi et al. (1996)	○	○	○	●	●	○
Fiorato et al. (1970)	●	●	○	●	○	○
El-Dakhakhni et al. (2003)	○	○	○	○	●	●

● – Failure mode considered; ○ – Failure mode not considered

For reliable analytical investigation of infilled frames, identification of all possible failure modes and estimation of strength in those modes are essential. However, in spite of significant experimental research on the behavior of un-reinforced masonry infilled frames under in-plane loading (Ockleston 1955; Smith 1968; Paulay and Priestley 1992; Mehrabi et al. 1996; Crisafulli 1997; Hashemi and Mosalam 2007), no consensus method for modeling of infilled frames is available. A review of available literature on in-plane failure modes and different models for estimating the strength of URM infills and frame members in the identified modes of failure have been presented in Chapter 2. In this Chapter, a parametric study has been presented, where the estimated capacity and demand in different modes are investigated to identify the most likely modes of failure in typical URM infilled RC frame buildings, so that the same can be simulated in the analytical models for further study on seismic behaviour and vulnerability assessment of such buildings.

3.3 PARAMETRIC STUDY

From the review of the literature on in-plane behavior of the URM infilled frames, it can be concluded that the composite behavior of infilled frames is dependent not only on the properties of the frame and infill, individually, but also on their relative strength and stiffness. Depending on the relative capacity and demand, the failure of infilled frames may be governed either by the frame members or by infills and is highly dependent on the degree of infill-frame interaction. To examine the influence of individual parameters and to identify the most probable modes of failure in frames of different design levels infilled with URM of varying quality, a parametric study has been carried out on two generic sets of URM infilled multi-storey RC frame buildings, selected from a pilot survey (DEQ 2009), representing the wide stock of existing buildings in India.

3.3.1 Selection of Representative Buildings

To encompass the wide spectrum of infilled RC frame buildings in India, the representative building configurations have been selected from the pilot survey in the New Okhla Industrial Development Authority (NOIDA), a model township in the National Capital Region (NCR) (DEQ 2009). The selection has been based on the statistical evaluation of structural parameters such as range of building dimensions (Fig. 3.7 (a)), number of frames in each direction (Fig. 3.7 (b)), height of building (Fig. 3.7 (c)), period of vibration (Fig. 3.7 (d)), range of beam spans, redundancy in two directions, etc., which are expected to affect the seismic response.

Due to lack of enforcement, buildings are still being constructed in India without following any seismic safety provisions, even in high seismicity zones. To evaluate the seismic safety of the surveyed buildings, average shear stress and axial force due to overturning, in the ground storey columns was investigated using the FEMA-310 (1998) procedure. Buildings are designated as safe, unsafe and highly unsafe depending on the average shear stress value less than $0.15\sqrt{f_{ck}}$, in between $0.15\sqrt{f_{ck}}$ and $0.225\sqrt{f_{ck}}$, and higher than $0.225\sqrt{f_{ck}}$, respectively. Similarly, buildings having column axial stress caused by overturning moment, less than $0.24f_{ck}$, in between $0.24f_{ck}$ and $0.36f_{ck}$, and higher than $0.36f_{ck}$ are designated as safe, unsafe, and

highly unsafe, respectively. (The stress limits for 'highly unsafe' category were arbitrarily fixed in the study as 1.5 times of the safe limits provided in FEMA-310). Surprisingly, only a small fraction (21%) of surveyed buildings are found to be safe against earthquake forces (Fig 3.7 (e)) and a large proportion of buildings existing in seismic zone IV (Effective Peak Ground Acceleration for the Maximum Considered Earthquake, equal to 0.24*g*) are found to be unsafe either in shear or against overturning. Among these, 22% surveyed buildings are unsafe in both in shear and overturning and 17% buildings are found to be highly unsafe both in shear as well as in overturning.

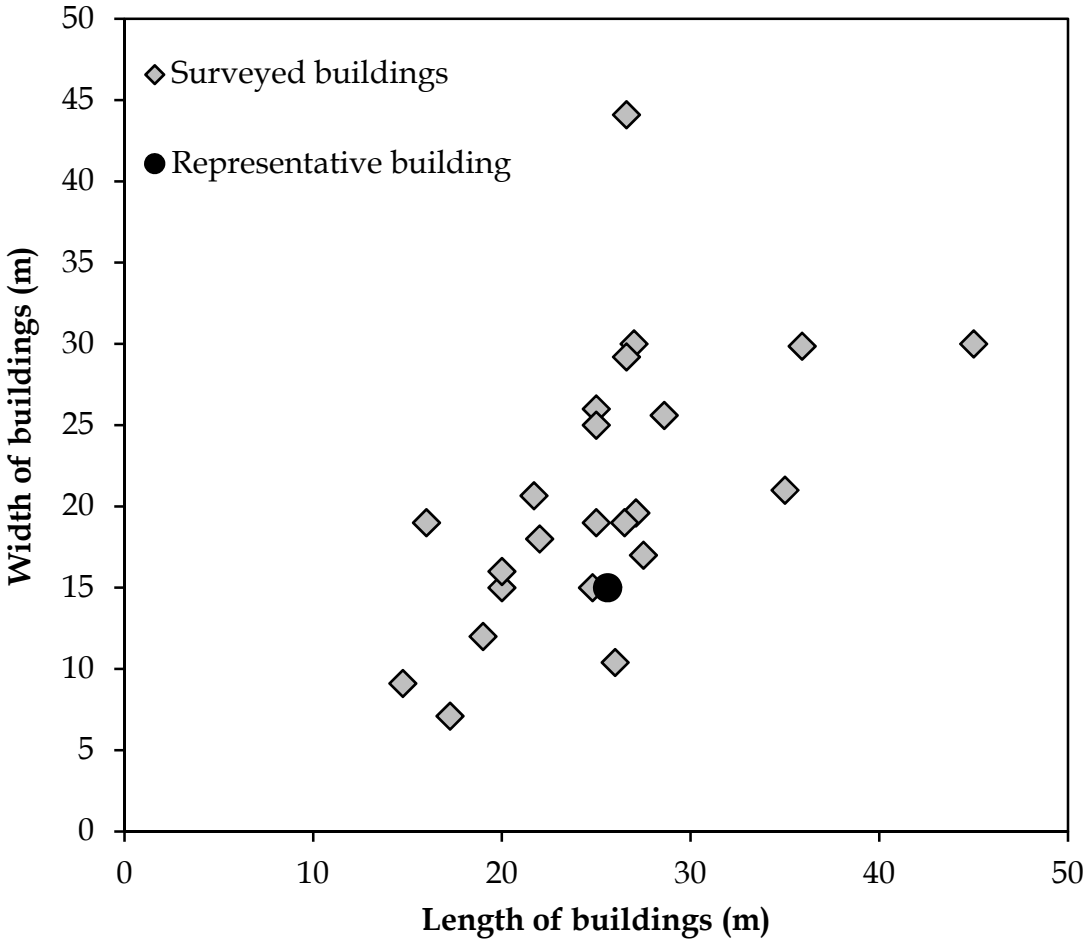

(a)

Fig. 3.7 (contd.)

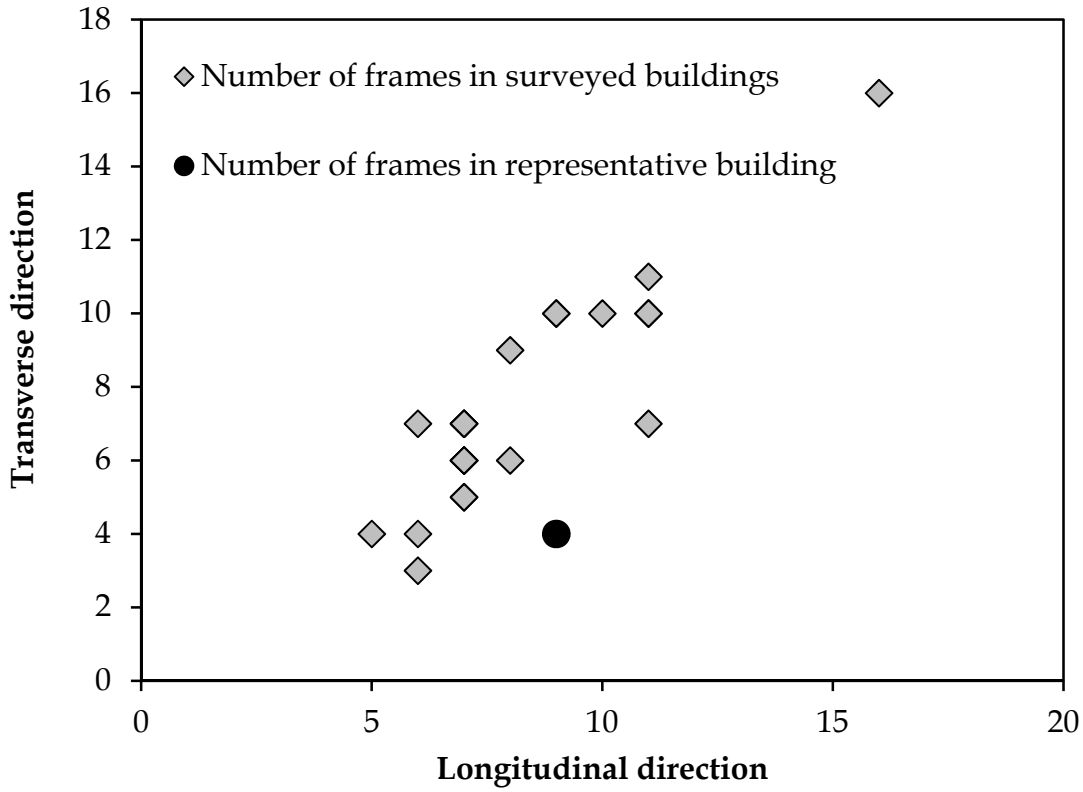

(b)

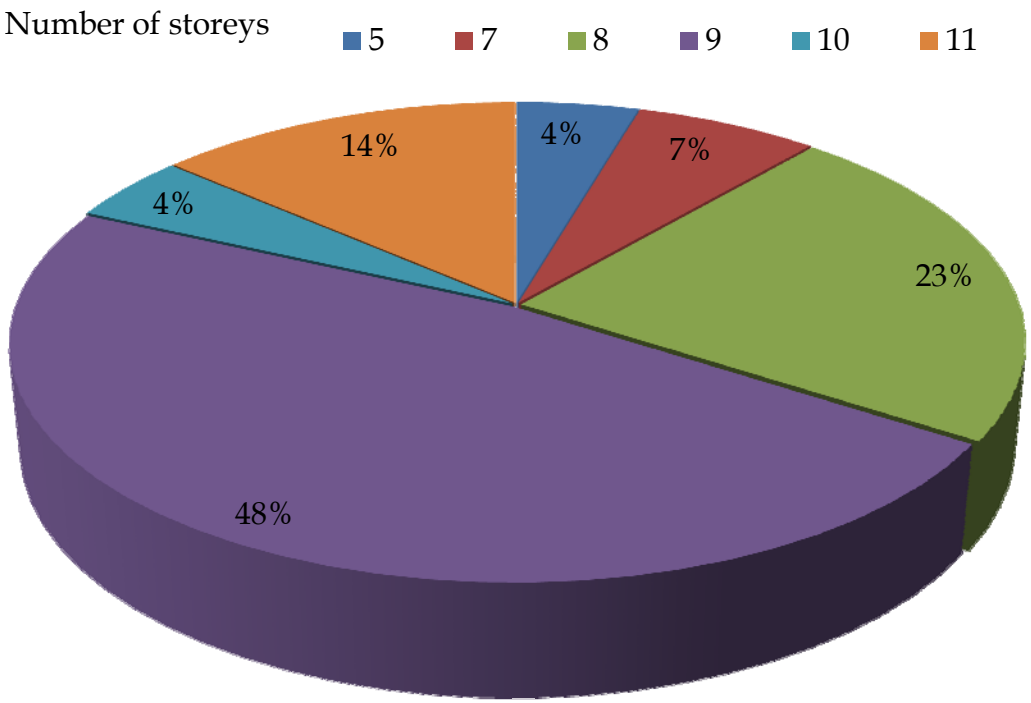

(c)

Fig. 3.7 (contd.)

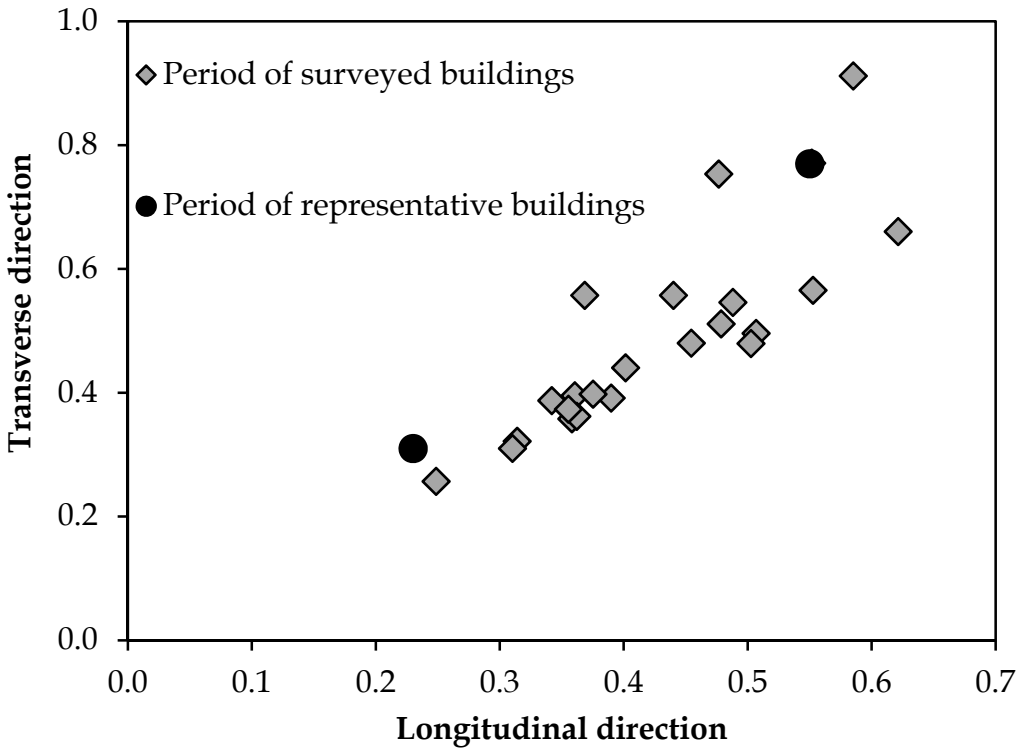

(d)

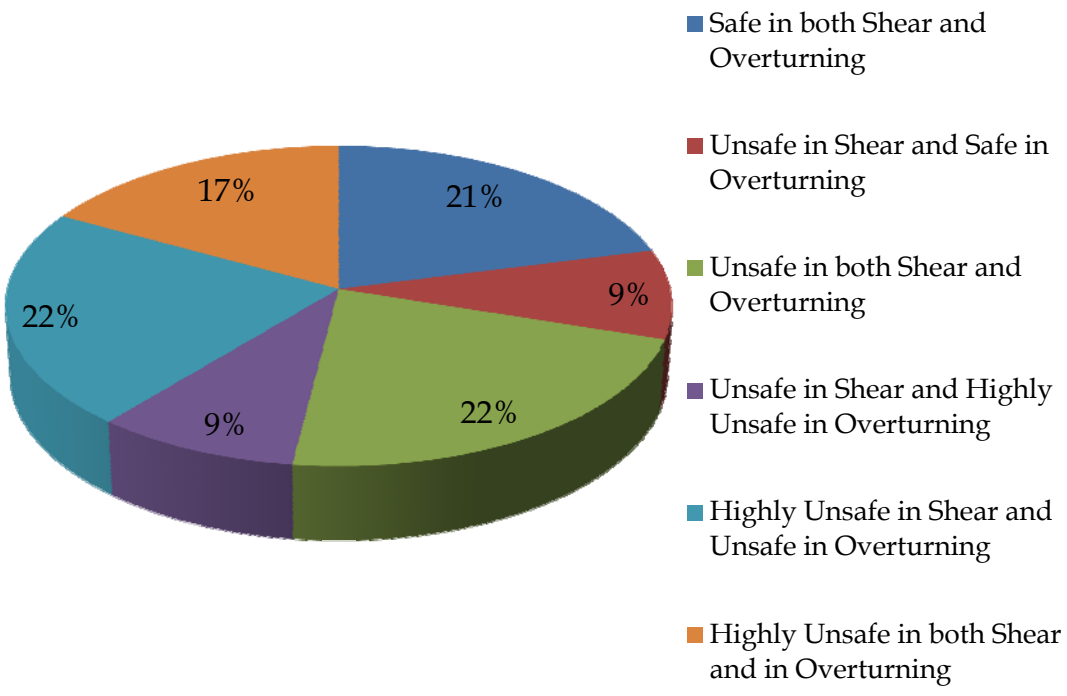

(e)

Fig. 3.7 Parameters of surveyed and representative buildings: (a) Plan dimensions; (b) number of column lines (frames); (c) percentage of buildings having different number of storeys; (d) periods of vibration; and (e) safety of the surveyed buildings against earthquake forces (DEQ 2009).

The representative buildings selected for parametric study in this Thesis have identical plan as shown in Fig. 2.5 (a) and two different heights - four and ten storeys, representing the wide range of medium rise buildings in India. The front and side elevations of the buildings have been shown in Fig. 2.5 (b) and 2.5 (c), respectively. The considered plan is symmetric in both directions but has significantly different redundancy and beam spans in the two directions. Further, the corridor of the considered buildings is free from beams and the two frames in the transverse direction are connected by rigid slab, as observed (DEQ 2009) in a wide range of buildings in India. It can be observed from the survey statistics that majority of the existing buildings have plan dimensions varying from 15 to 30 *m*. Accordingly the plan dimensions of the representative buildings have been chosen equal to 15 *m* and 25.6 *m* in the two directions (Fig. 2.5) to represent the range of observed dimensions. Most of the existing buildings have column lines (frames) varying from 4 to 12. The plan selected in the present study has 4 column lines along the longitudinal direction and 9 column lines in the transverse direction. As period of vibration is the most important parameter governing seismic response of buildings, two heights of the buildings (4 storey and 10 storey) are selected to represent the full range of the periods observed in the pilot survey (Fig. 3.7 (d)). Further, the different beam spans in the two directions of the representative buildings are also selected to represent the observed range of spans in the existing buildings. The existing buildings generally have torsional irregularity of varying degree, however, the building plans selected in the present study are symmetric in the two directions, and the torsional irregularity has been considered only due to irregular placement of infills.

A uniform height of 3.3 *m* has been considered for all the storeys of the representative buildings. The slab thickness has been assumed as 150 *mm* and a uniform weight of 0.5 kN/m^2 has been considered for flooring. The Dead Load (DL) and Live load (LL) have been estimated using Indian Standard BIS (1987 (Part 1)) and BIS (1987 (Part 2)) respectively**.** Seismic design has been performed as per Indian Standard BIS (2002). For design, M20 concrete and Fe415 steel have been used and member sections have been proportioned to have about 2-4% steel in columns and about 1% steel (on each face) in beams, wherever permitted by other code requirements.

The thickness of solid infill panels is considered as 115 *mm* and 230 *mm* for interior and exterior partitions, respectively, as per the prevailing practice in India. The same

buildings have also been analyzed neglecting the stiffness and strength of infills (i.e. considering the buildings as bare frames), as is the case in normal course of design. All the buildings have been assumed to be situated on hard soil in seismic zone IV (Effective Peak Ground Acceleration, EPGA = 0.24*g* for Maximum Considered Earthquake, MCE).

Considering the fact that buildings are still being constructed in India without following any seismic safety provisions, even in high seismicity zones, the first set of buildings is designed for gravity loads (GLD) alone, considering relevant Indian Standards (BIS 1987 (Part 1), 1987 (Part 2), 2000). Whereas, the second set of buildings is designed for earthquake loading along with gravity loads, with ductile detailing for 'Special Moment Resistant Frames (SMRF)' of Indian Code (BIS (1993)). The Indian code does not ensure the strong column-weak beam design, even in the case of Special Moment Resisting Frame. Since it is a widely recognized capacity design criterion, the present study has been conducted ensuring the strong column-weak beam design for SMRF.

3.3.2 Modeling and Analysis

Three dimensional space frame models of the selected representative buildings have been developed using nonlinear structural analysis software SAP2000 (2010). Beams and columns have been modeled as 3D frame elements and infill panels as equivalent diagonal struts. The floor/roof slabs are modelled as rigid diaphragms and the rigidity of beam-column joints is simulated using the guidelines of ASCE/SEI-41 Supplement-1 (2007). Realistic idealization of infill panels is the most crucial issue in simulating the behavior of URM infilled RC frame buildings. Equivalent strut modeling is the most commonly used approach for simulating the action of infills, and a number of models with one (Polyakov 1960; Smith 1962; Smith and Carter 1969), two (Saneinejad and Hobbs 1995; Crisafulli 1997), three (Chrysostomou 1991), five (Syrmakezis and Vratsanou 1986), and multiple (Thiruvengadam 1985) struts are available for this purpose. Two issues related to simulation of infill panels are examined in this study: (i) the most likely failure modes of infills of different geometry, thickness, and quality of masonry, and (ii) the most realistic model of infills to simulate the failure modes of infilled RC frames observed during past earthquakes and experimental studies. The latter has already been discussed in the

previous Chapter and the former is being studied here. Fig. 3.8 compares the strength of 230 *mm* and 115 *mm* thick infill panels in different failure modes discussed earlier in Chapter 2, for the two different aspect ratios of 0.52 and 1.05, in the considered buildings. The quality of bricks and masonry varies significantly in different regions of India. Prasad (2009) and Kaushik et al. (2007) have compiled the results for burnt clay brick masonry tested in different parts of the country. The reported masonry strength in India varies from 4 *MPa* to 7 *MPa* which ranges from 'Fair' (4.1 *MPa*) to 'Good' (6.2 *MPa*) quality of masonry specified in ASCE-41 (2007). The results presented herein are for fair quality of masonry (4.1 *MPa*) infills in the considered buildings. (Similar studies were also performed for other combinations of masonry quality and RC frame designs, but no significant difference was observed and hence the results are not produced here.)

It is observed from Fig. 3.8 that significant differences exist in the three models of diagonal compression strength of the infill, whereas in case of sliding shear, the three considered models result in close estimates of strength. Diagonal compression model of ACI 530 (2005) predicts the highest strength in case of 230 *mm* thick infills (Figs. 7(a) and (c)); but the lowest strength in case of 110 *mm* thick infills (Fig. 3.8 (b) and (d)), as this is the only model which takes into account the slenderness ratio of the infill. It is interesting to note that the diagonal tension strength (Smith 1967) of 110 *mm* thick squat infills (aspect ratio= 0.52) is higher than diagonal compressive strength (ACI 530 2005) which is in agreement with Flanagan and Bennett (2001). However, sliding shear governs the strength of infills in all the cases. This is in agreement with ASCE-41 (2007), where sliding shear has been considered as the sole failure mode for infills. Therefore, the ASCE-41 model for estimating strength of infills, has been considered for further study in this Thesis.

3.3.3 Axial Force in Columns

The strut action of infills is expected to alter the axial force, and hence the failure mode of columns, significantly. The effect of infills on axial force in columns has been studied by plotting the axial force ratio (ratio of axial force, P, at any step of pushover analysis under combined gravity and lateral loading, to the axial force, P0, under gravity loading alone) with the lateral displacement ratio (ratio of roof

displacement at each step of pushover to the yield displacement obtained from idealized bi-linear pushover curve of the building) for the considered buildings.

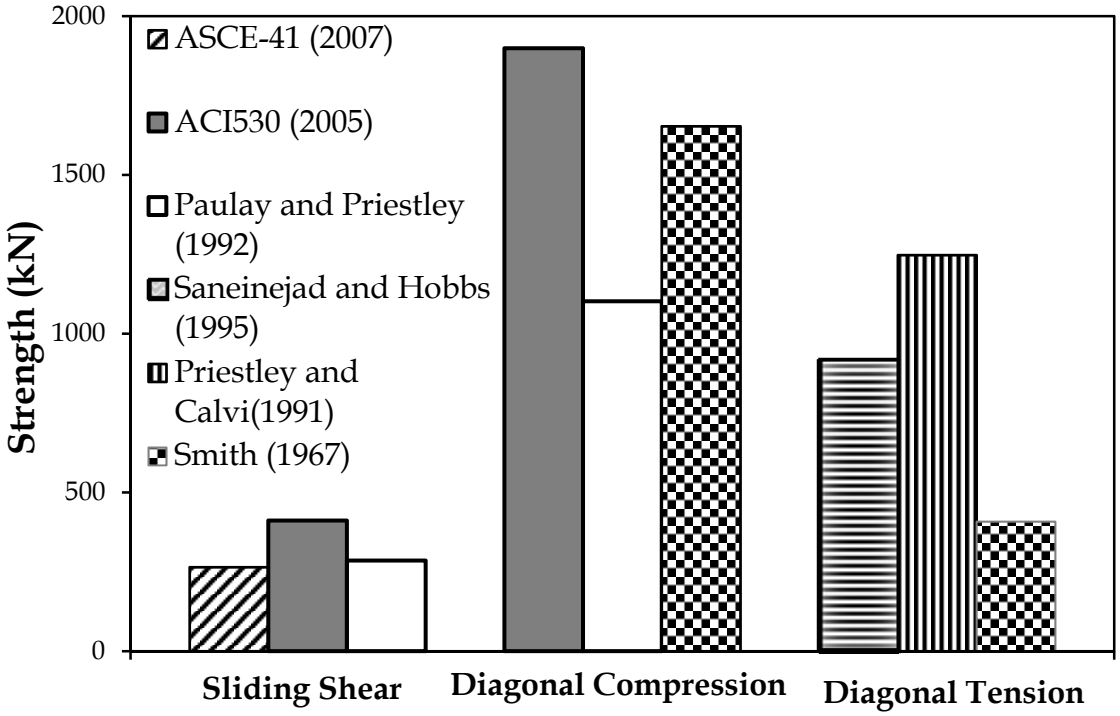

(a)

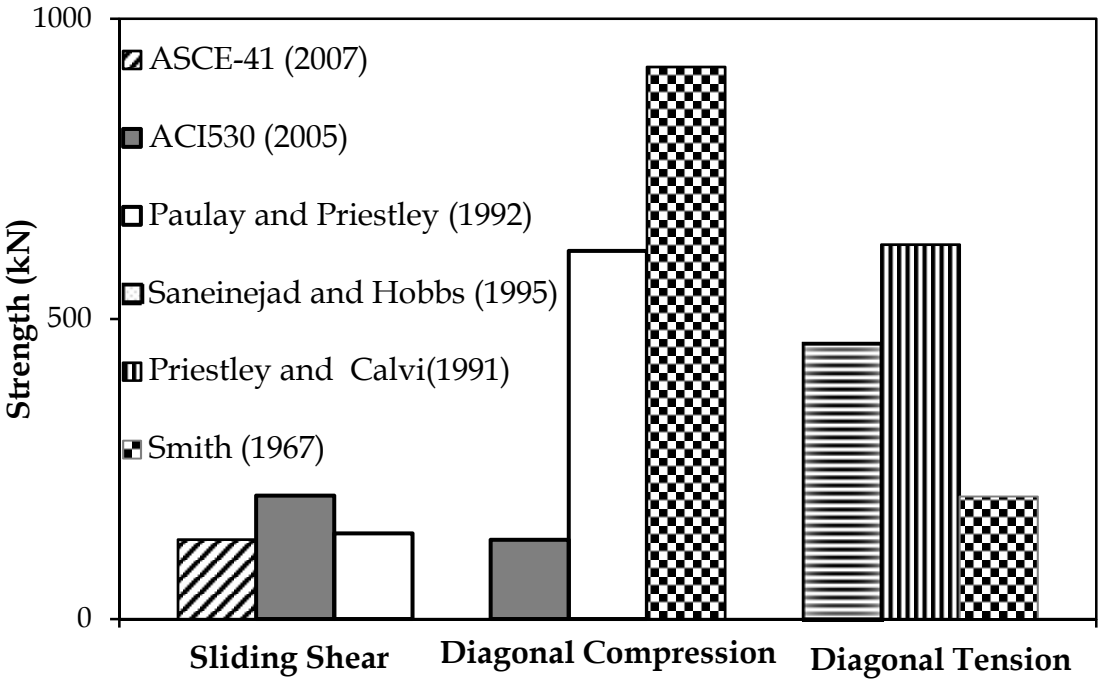

(b)

Fig. 3.8 (contd.)

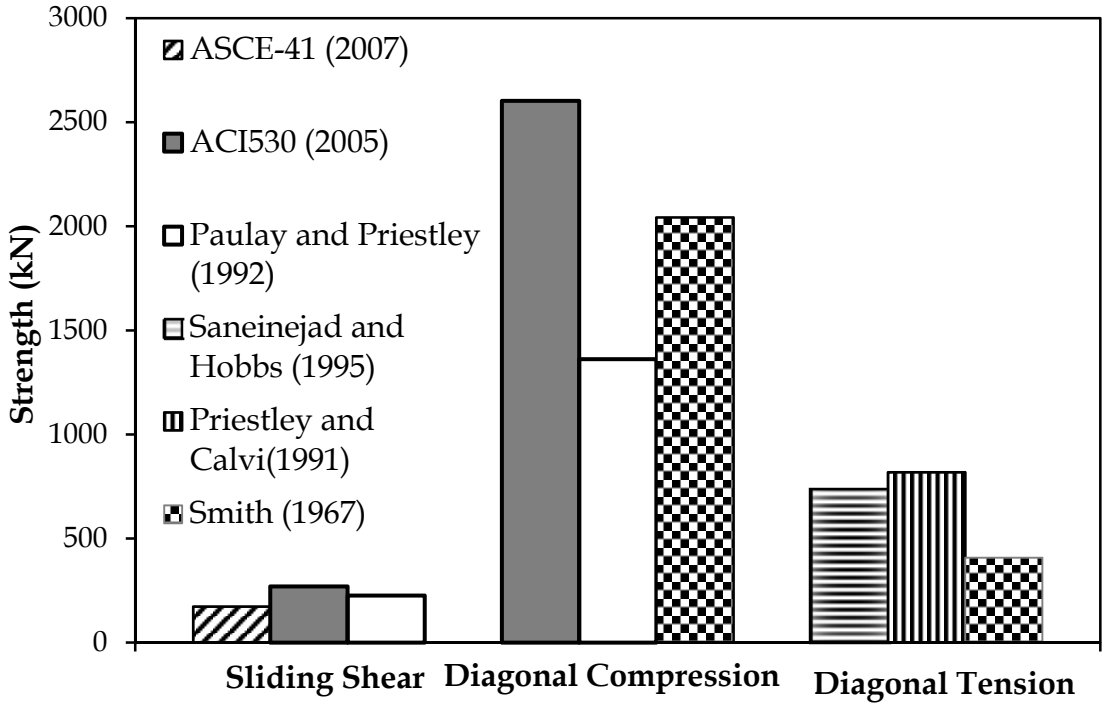

(c)

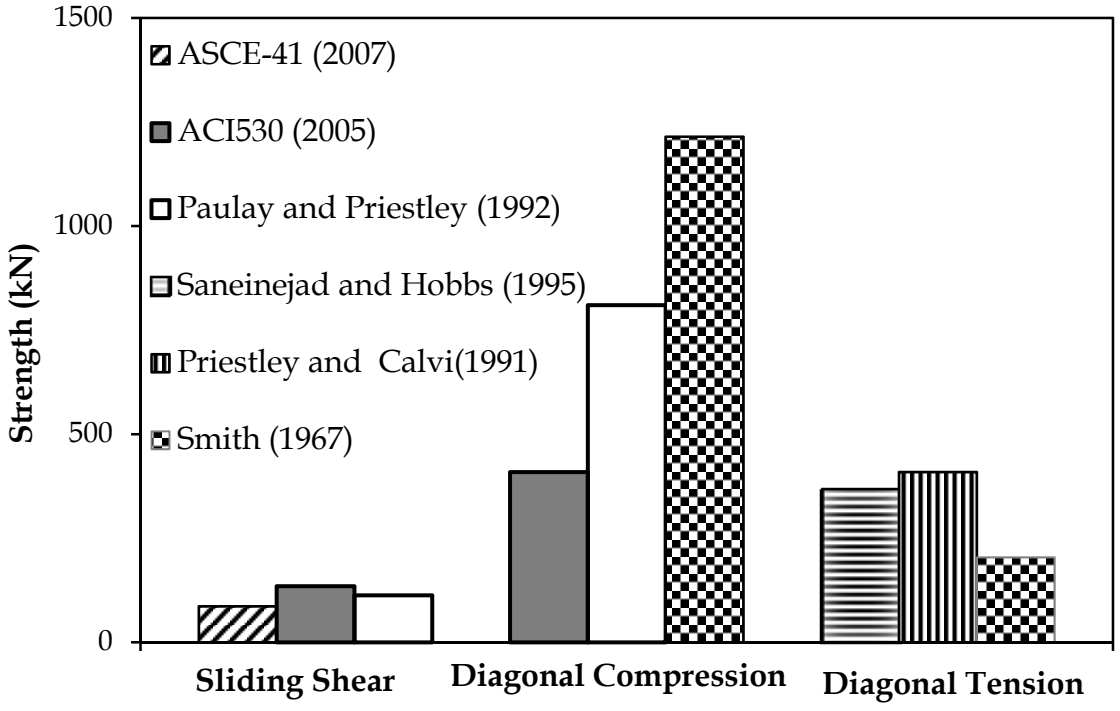

(d)

Fig. 3.8 Strength of infills of varying thickness and aspect ratio in different failure modes: (a) 230 *mm* thick panel with 0.52 aspect ratio; (b) 115 *mm* thick panel with 0.52 aspect ratio; (c) 230 *mm* thick panel with 1.05 aspect ratio; and

(d) 115 *mm* thick panel with 1.05 aspect ratio.

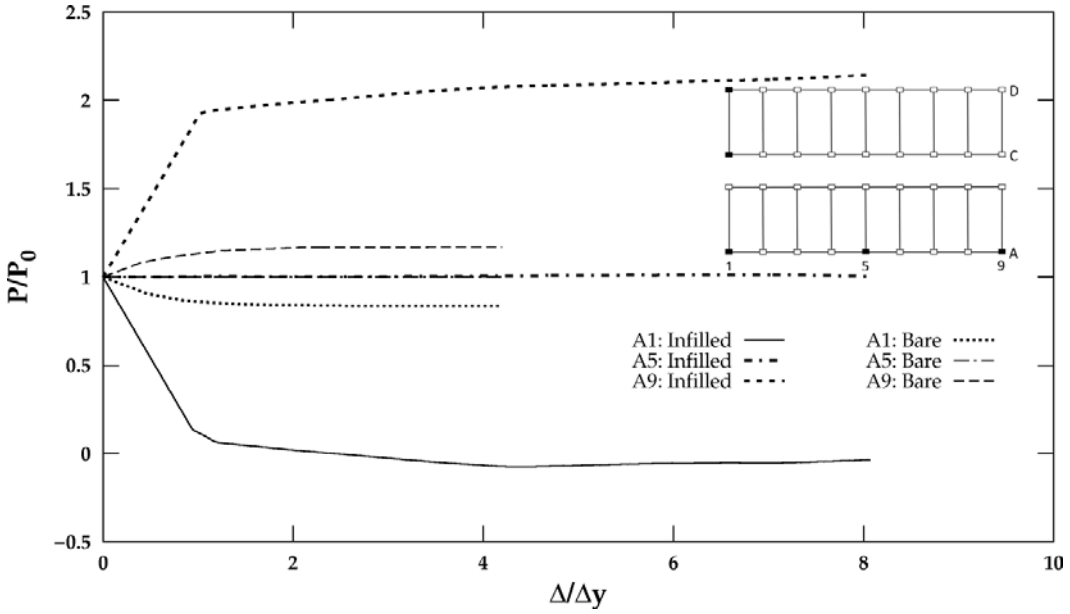

(a)

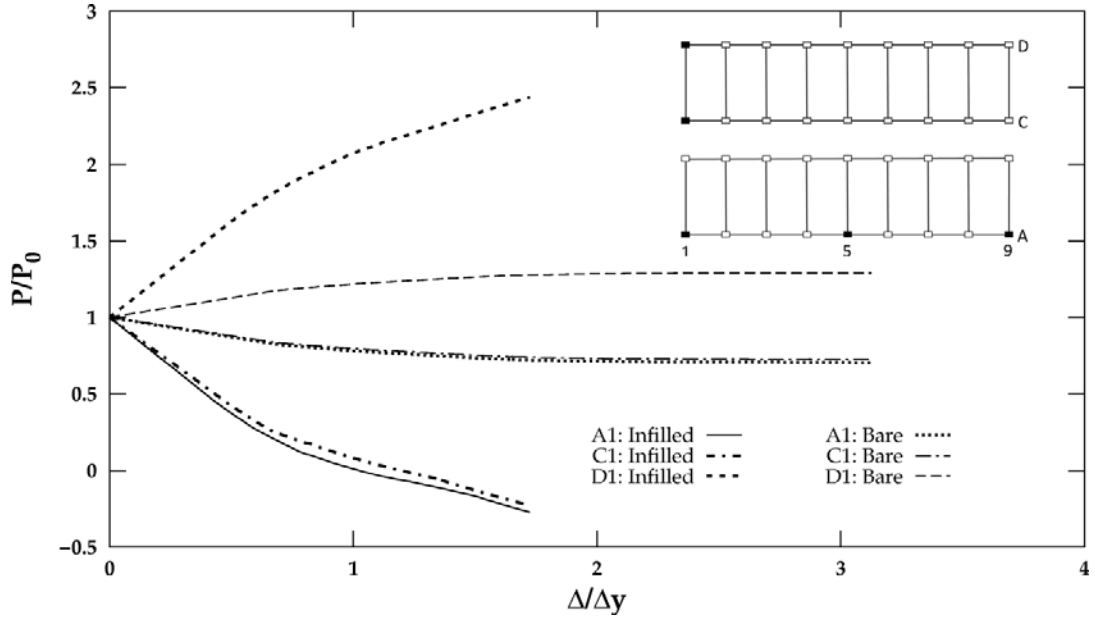

(b)

Fig. 3.9 Variation of axial force ratio in columns of four storey building designed for Gravity Load only (GLD) as per relevant Indian codes: (a) longitudinal direction; (b) transverse direction.

Figs. 3.9 and 3.10 show the variation of axial force ratio (P/P_0) with displacement ratio (Δ/Δ_y) for the four storey bare and infilled frame buildings, designed for gravity load only (GLD), and considering earthquake resistant design provisions of Indian Standards (BIS 1993, 2002) (SMRF). The same comparison for the ten storey buildings has been shown in Figs. 3.11 and 3.12. Variation of axial force ratio has

been studied for representative ground storey columns A1, A5, and A9 in longitudinal direction and A1, C1, and D1 in transverse direction. The selected columns are marked with black shade in Fig. 2.5 (a).

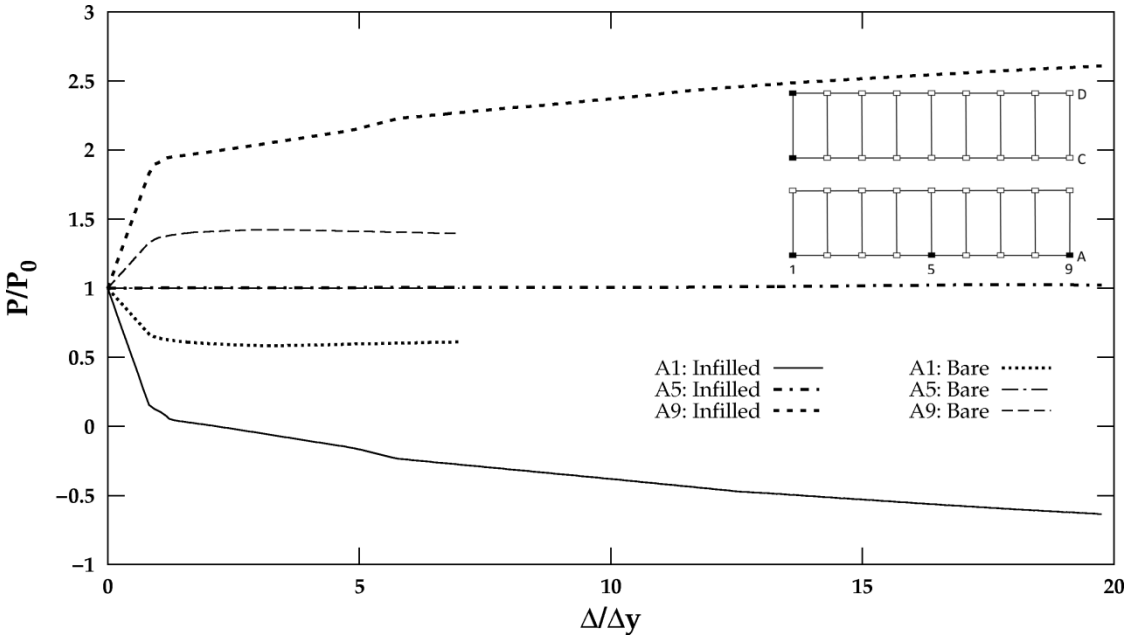

(a)

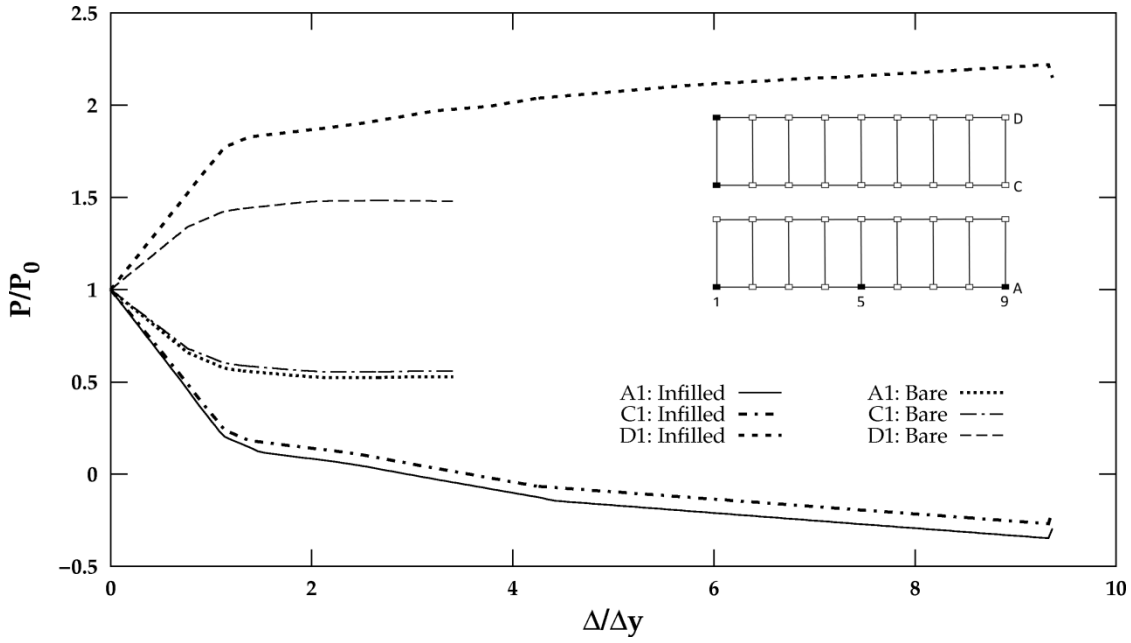

(b)

Fig. 3.10 Variation of axial force ratio in columns of four storey building designed as SMRF as per relevant Indian codes: (a) longitudinal direction; (b)

transverse direction.

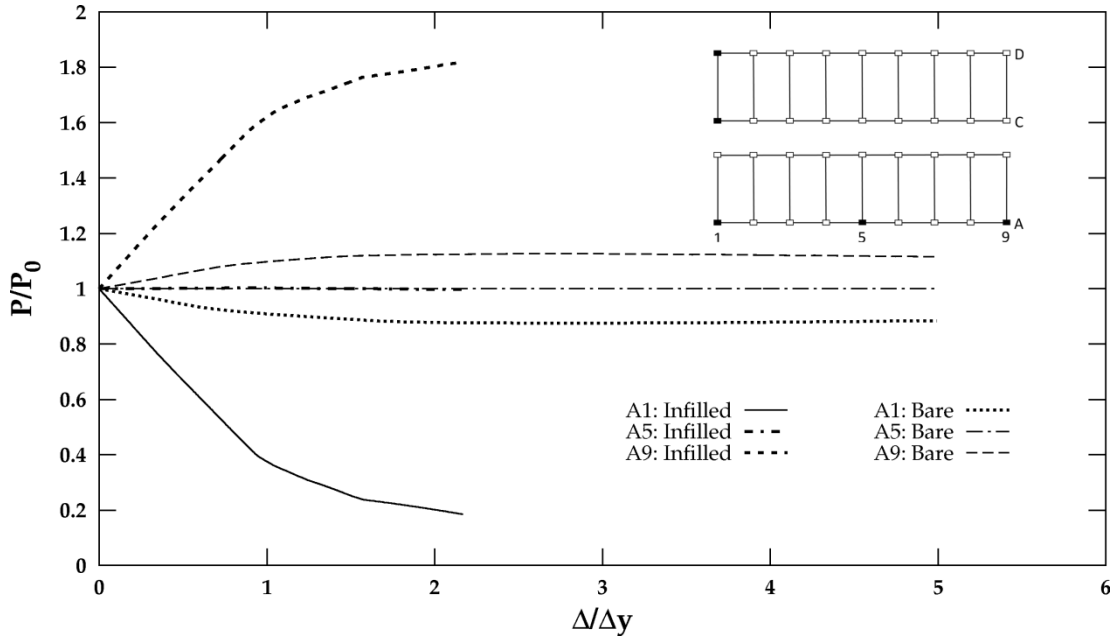

(a)

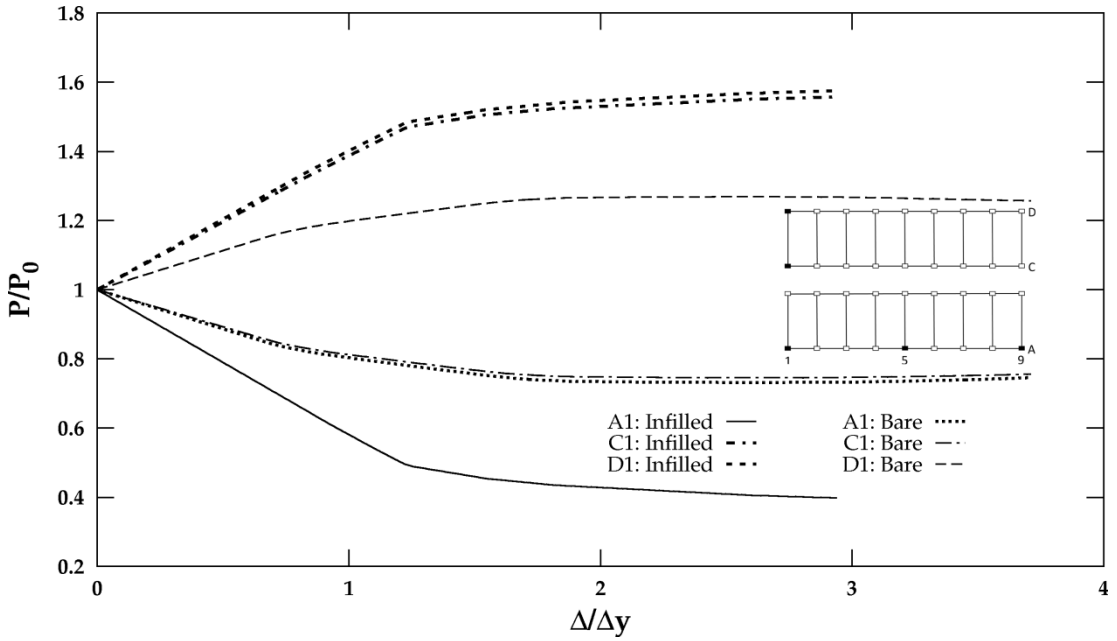

(b)

Fig. 3.11 Variation of axial force ratio in columns of ten storey building designed for Gravity Load only (GLD) as per relevant Indian codes: (a) for lateral force in longitudinal direction; (b) for lateral force in transverse direction.

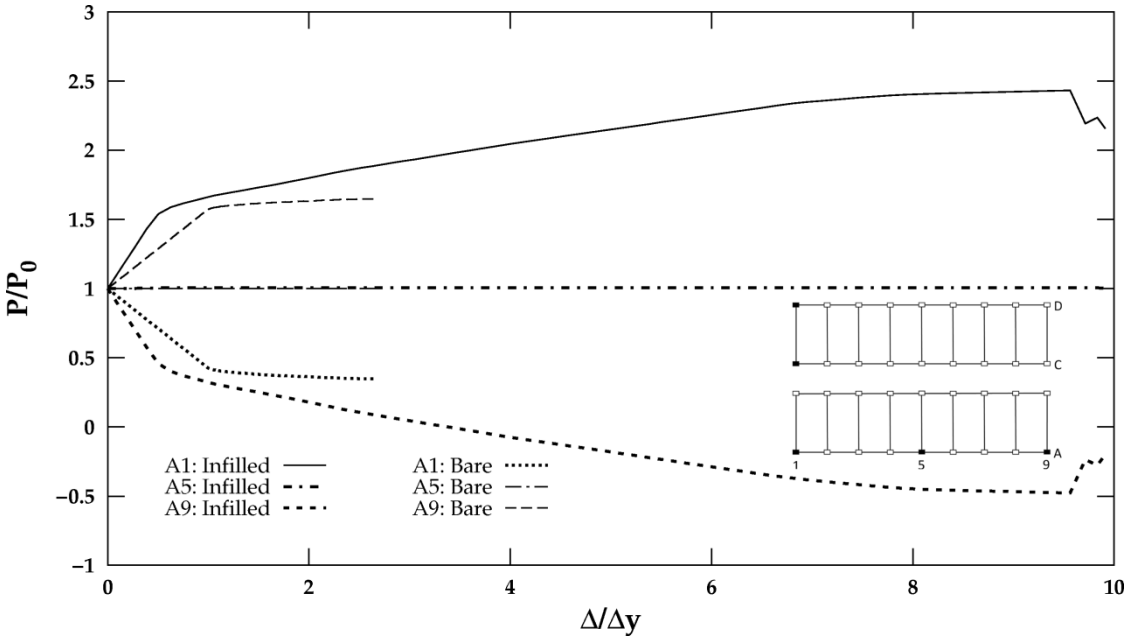

(a)

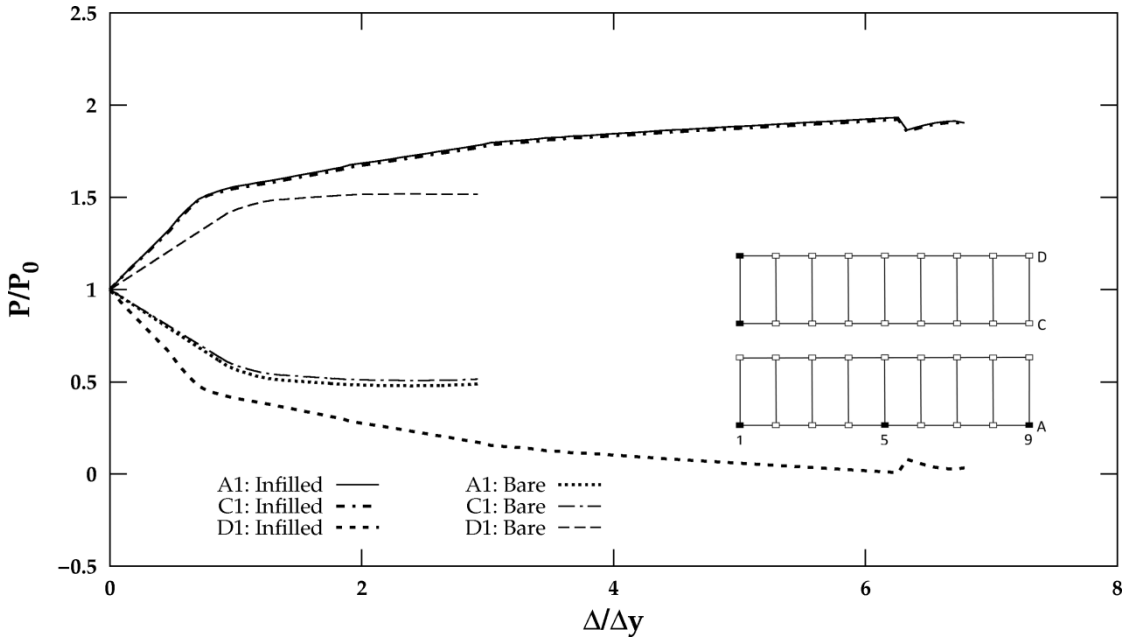

(b)

Fig. 3.12 Variation of axial force ratio in columns of ten storey building designed as SMRF as per relevant Indian codes: (a) for lateral force in longitudinal direction; (b) for lateral force in transverse direction.

It can be clearly observed from Figs. 3.9-3.12 that infills have a very strong influence on the column axial force. Inclusion of infills increases the peak axial force ratio by

45% and 36% in the four and ten storey buildings, respectively, when designed as SMRF and the relative increase is up to 47% and 20% in the four and ten storey buildings, respectively, designed for gravity loads alone. It can also be observed from Figs. 3.10 and 3.12 that as the lateral displacement increases the axial force decreases rapidly in the tension side columns of the infilled frame buildings, leading to net tension at higher displacement ratios. Another interesting observation from the Figures is that in some cases, the range of displacement ratio (representing the ductility ratio) is much higher in case of infilled frame, as compared to the corresponding bare frame. This may be somewhat misleading as the absolute values of displacement, and interstorey drift ratios are much reduced in case of infilled frames. The larger displacement ratios are due to much lower yield displacement in case of infilled frame, as infills increase the stiffness of the frame several times and yielding of infills in infilled frames occurs at much lower interstorey drift, as compared to the yielding of beams in case of bare frames. For example, in case of the four storey SMRF building (Fig. 3.10), with URM infills, the first member (infill panel) yields at an average drift ratio of 0.04% and failure of the building occurs at a drift ratio of 1.18%, whereas in case of bare frame the corresponding interstorey drifts are 0.92 % and 7.39%, respectively. The aim of the study presented in this Chapter is limited to identification of potential failure modes in infilled RC frames. The effect of infills on stiffness, strength, and ductility, and consequent seismic performance of the RC frame buildings, is discussed in Chapter 4.

3.3.4 Effect of Infills on Bending Moment in Columns

The strut action of infills transforms the behaviour of the infilled frame similar to that of a braced frame. This results in significant increase (or decrease) in column axial forces, as shown in previous Section, and at the same time, a significant reduction in the bending moment in frame members. Figs. 3.13 and 3.14 show variation of bending moment with displacement ratio (Δ/Δ_y) in selected ground storey columns of the four storey bare and infilled frame buildings designed for gravity load only, and considering earthquake resistant design provisions of Indian Standards (BIS 1993, 2002), respectively, under combined action of gravity and lateral load. The corresponding variations in case of ten storey buildings are shown in Figs. 3.15 and 3.16. The Figures show significant decrease in column moments in infilled frames as

compared to their bare frame counterparts. The variation of column moments in case of infilled frame is slightly irregular as it depends on the sequence of failure of infills.

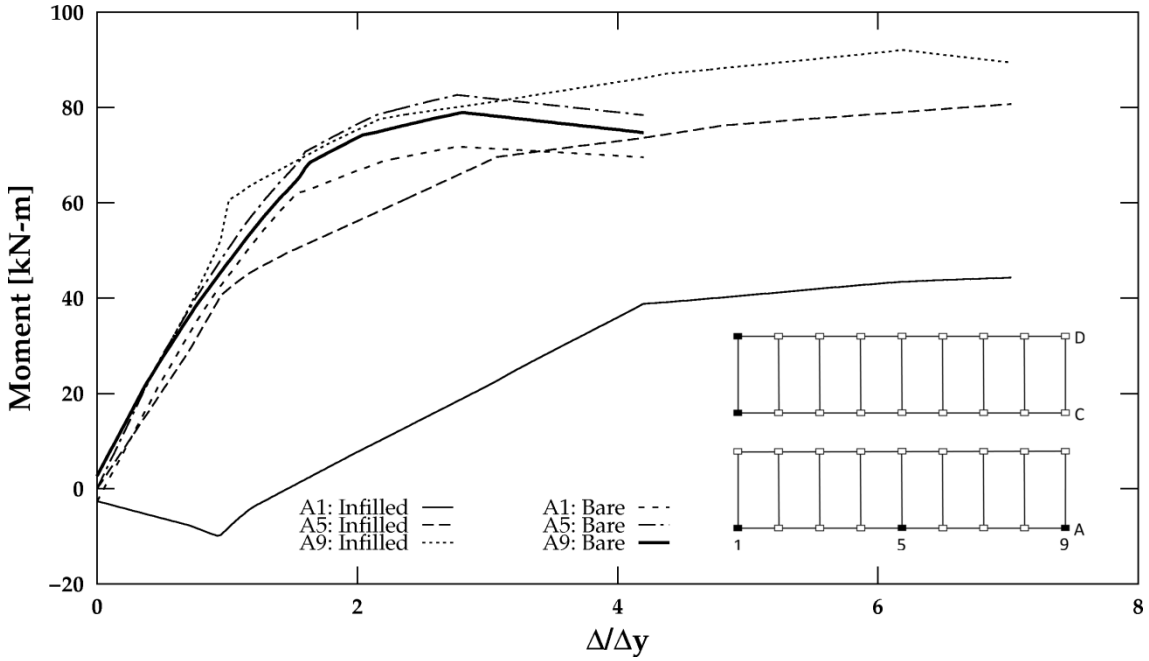

(a)

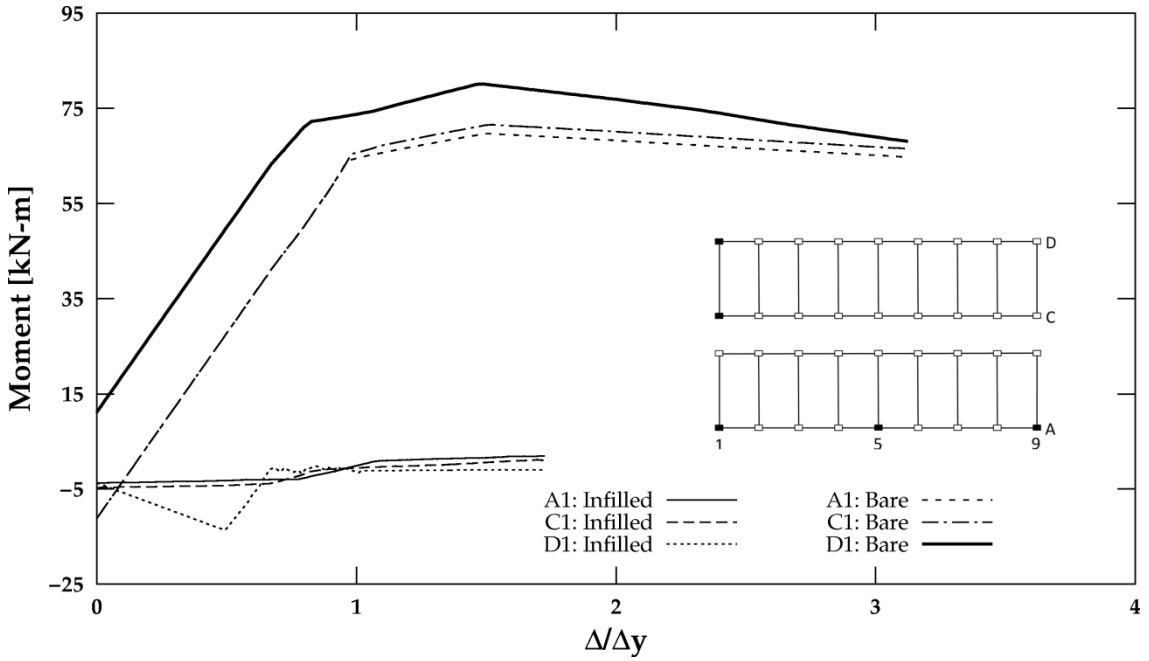

(b)

Fig. 3.13 Variation of bending moment in columns of the four storey buildings designed for Gravity Load only (GLD) as per relevant Indian codes: (a) lateral force in longitudinal direction; (b) lateral force in transverse direction.

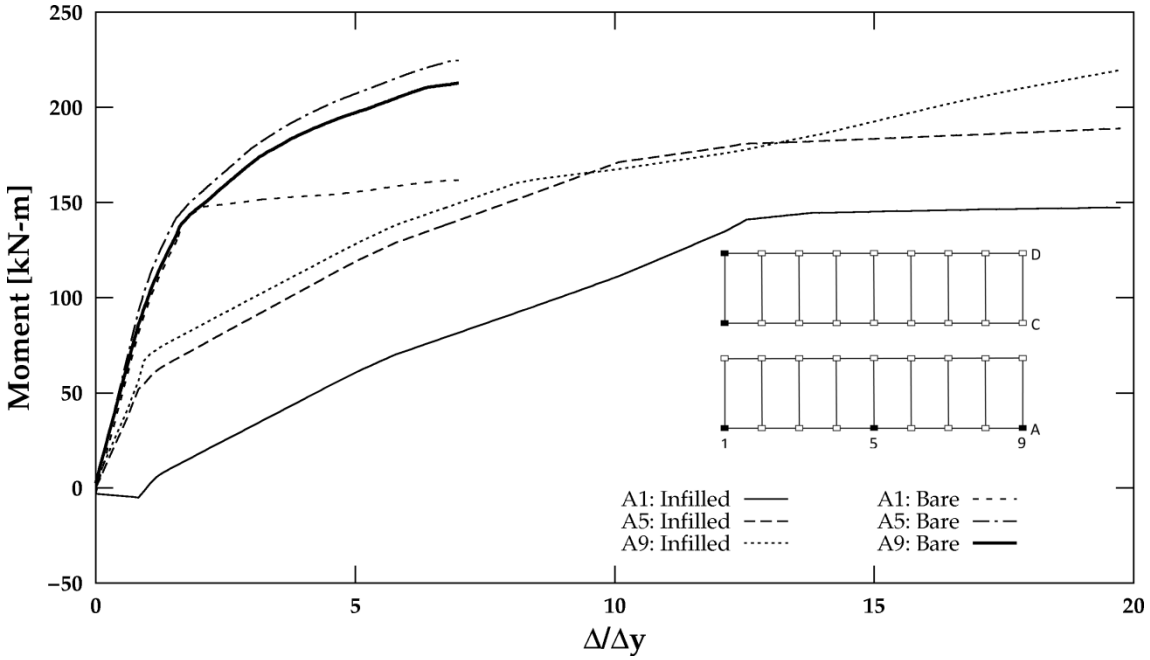

(a)

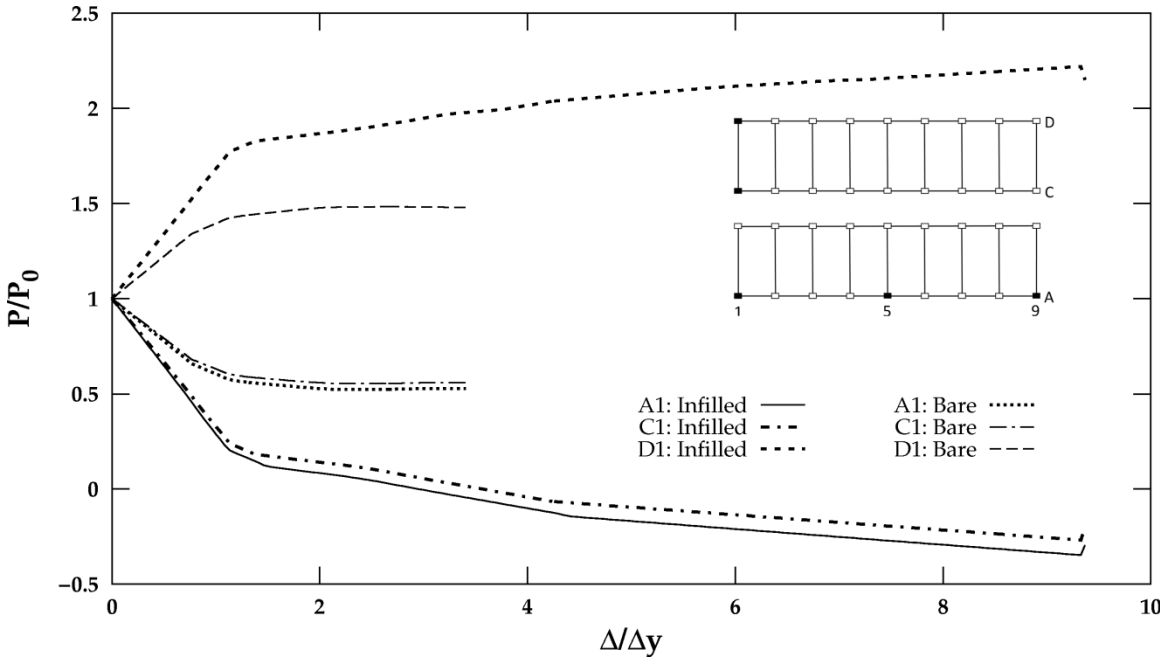

(b)

Fig. 3.14 Variation of bending moment in columns of the four storey buildings designed as SMRF as per relevant Indian codes: (a) lateral force in longitudinal direction; (b) lateral force in transverse direction.

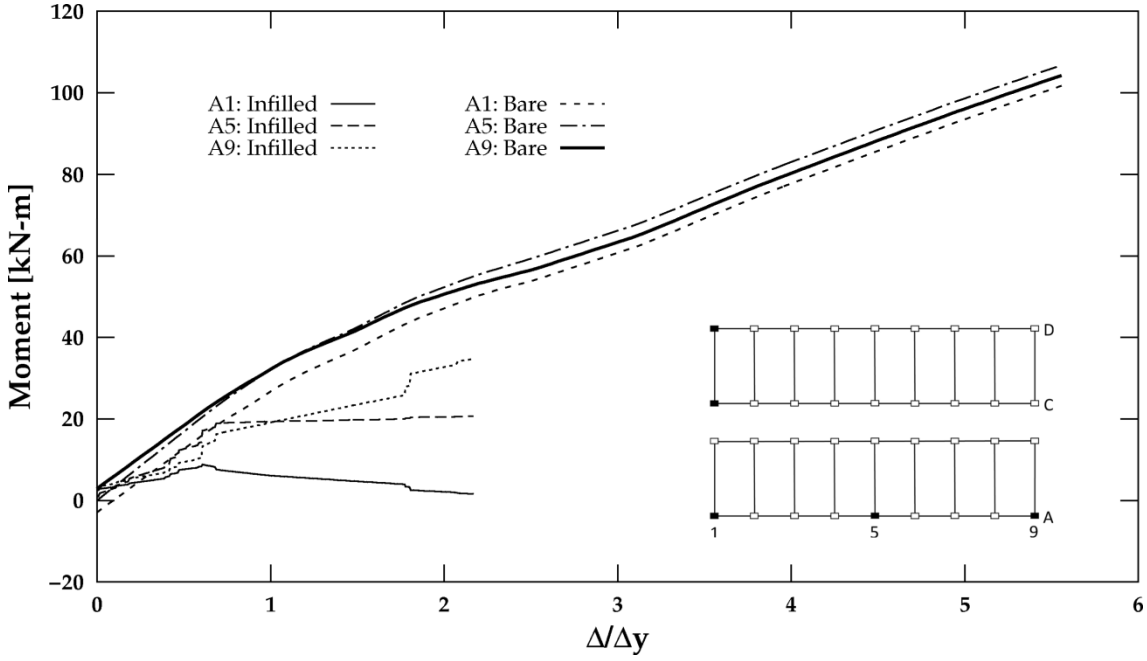

(a)

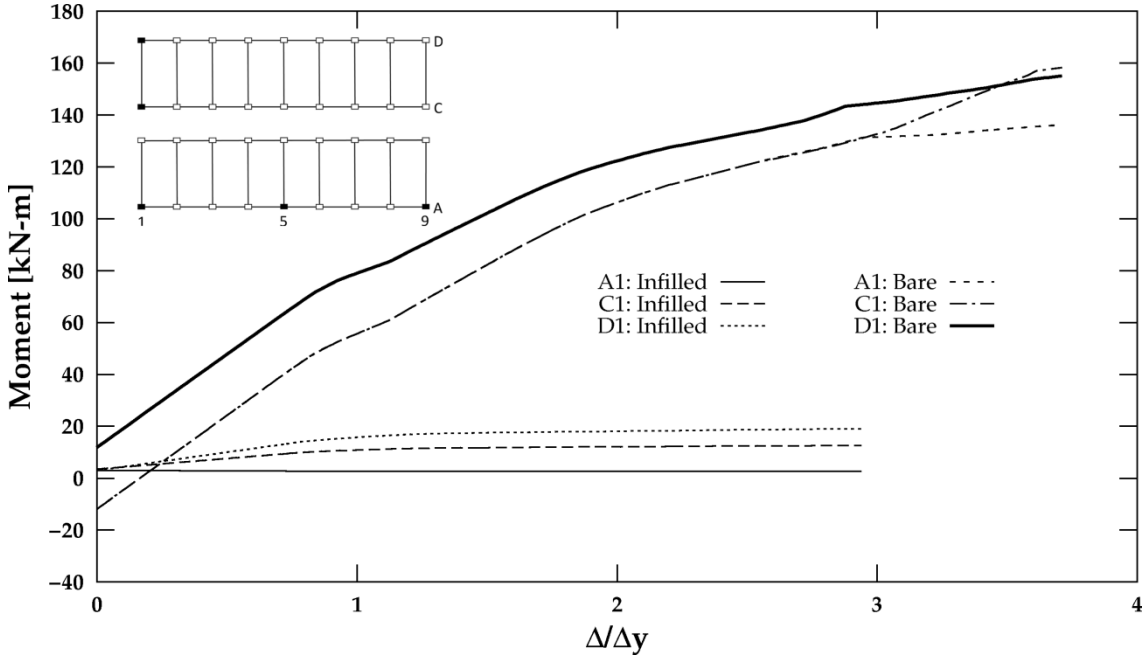

(b)

Fig. 3.15 Variation of bending moment in columns of the ten storey buildings designed for Gravity Load only (GLD) as per relevant Indian codes: (a) lateral force in longitudinal direction; (b) lateral force in transverse direction.

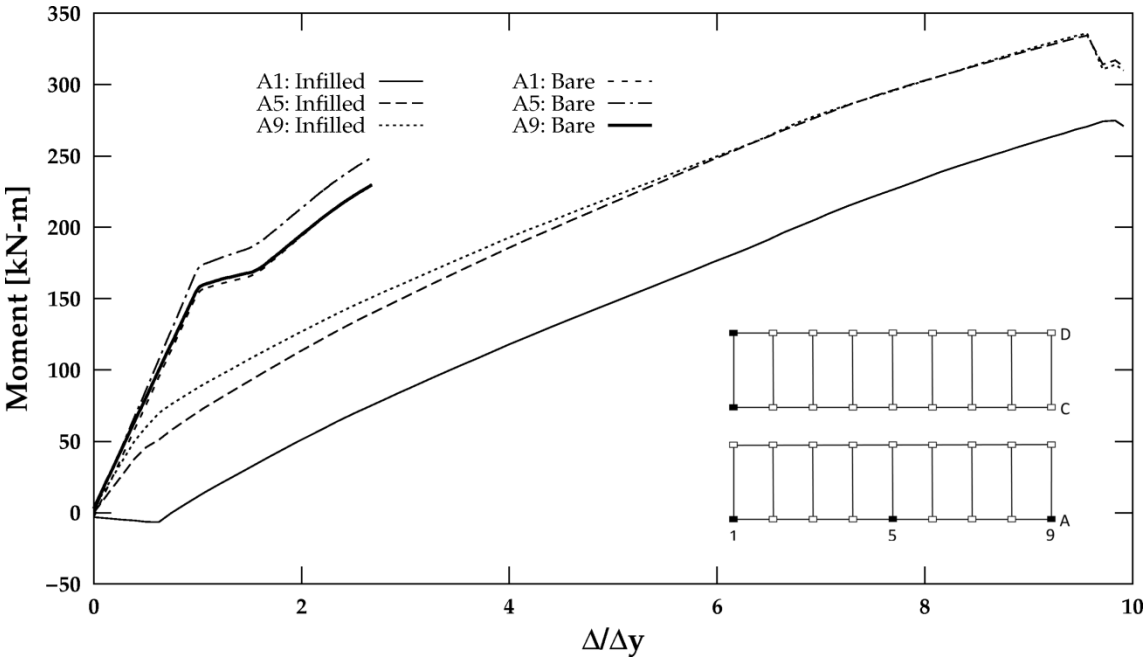

(a)

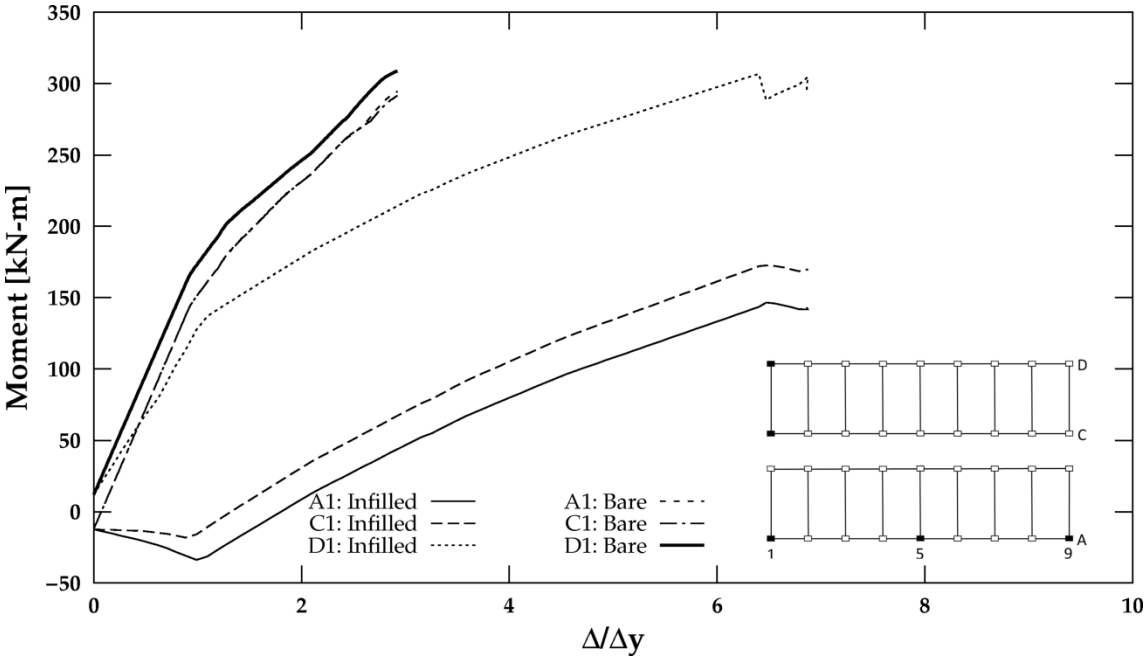

(b)

Fig. 3.16 Variation of bending moment in columns of the ten storey infilled frame building designed for Gravity Load only (GLD) and as SMRF as per relevant Indian codes: (a) lateral force in longitudinal direction; (b) lateral force in transverse direction.

3.3.5 Effect of Infills on Shear Force in Columns

To examine the possibility of shear failure of columns in infilled frames, the Demand Capacity Ratio (DCR) in representative frames, A1-D1, and A1-A9 infilled with 230 *mm* (one brick) thick, and A5-D5 infilled with 115 *mm* (half brick) thick panels of 'fair' quality URM (compressive strength, f_m' = 4.1 *MPa* as per ASCE-41 (2007)) have been examined in the four and ten storeyed buildings with and without earthquake resistant design. Figs. 3.17-3.18 show the DCR for shear in columns, obtained using three representative models (ACI 352R-02 2002; Sezen and Moehle 2004; ACI 318 2005), identified earlier in Chapter 2. It can be observed from the figures that the aspect ratio of infill panels plays an important role in shear failure of columns. In the transverse direction (having infill panel aspect ratio of 1.8), all the three models predict possibility of shear failure in columns adjacent to 230 *mm* thick panel in the four as well as ten storey GLD buildings, and even in columns adjacent to 115 *mm* thick panels in four storey building. The 115 *mm* thick panels are not able to cause shear failure in columns of 10 storey buildings (except in case of Sezen and Moehle (2004) model, as the shear capacity of columns is higher due to increased size. The DCR in columns adjacent to 230 *mm* thick URM infills is as high as 2.5 in some cases, suggesting high possibility of shear failure of columns in case of GLD buildings. On the other hand, in the longitudinal direction (having infill panel aspect ratio of 1.05) the columns are safe in shear in most of the cases. The Sezen and Moehle (2004) and NZS-3101:Part1 (2006) models predict shear failure of columns in some cases in longitudinal direction also, whereas ACI 318 (2005) model predicts that the columns are safe against shear failure. In case of SMRF buildings, due to special confining transverse reinforcement in the potential hinge region, and capacity design of columns in shear, all the columns are found to be safe against shear failure and the results are not produced here.

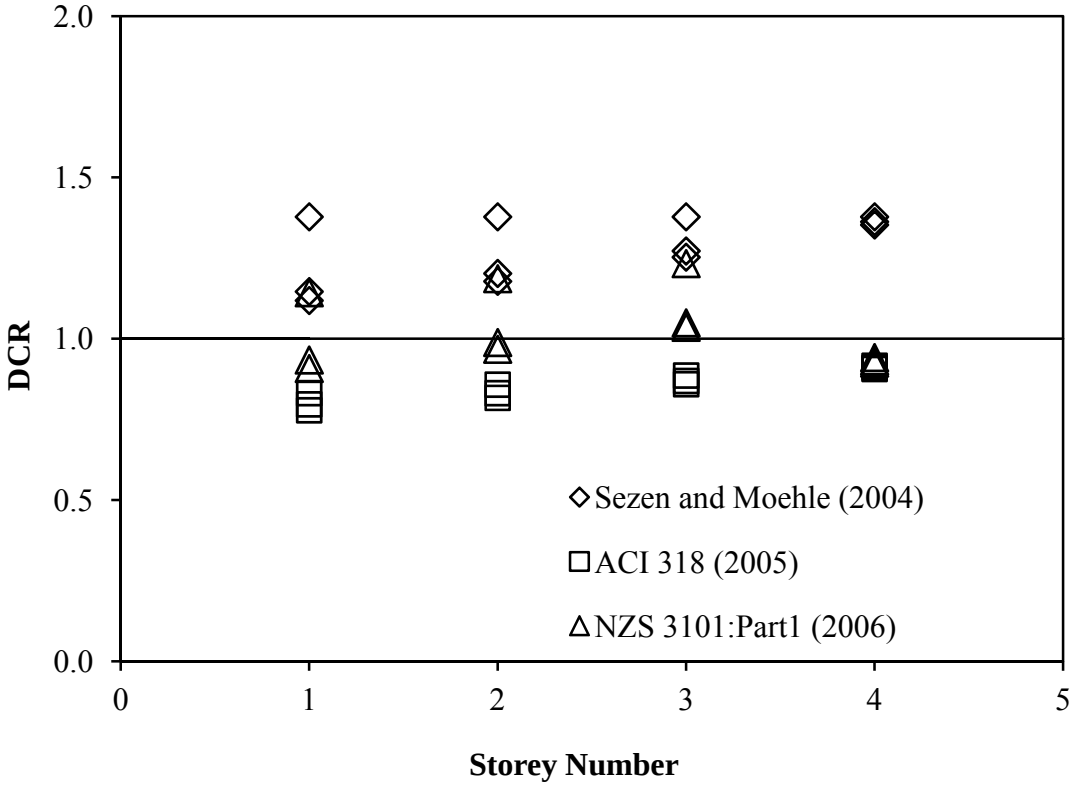

(a)

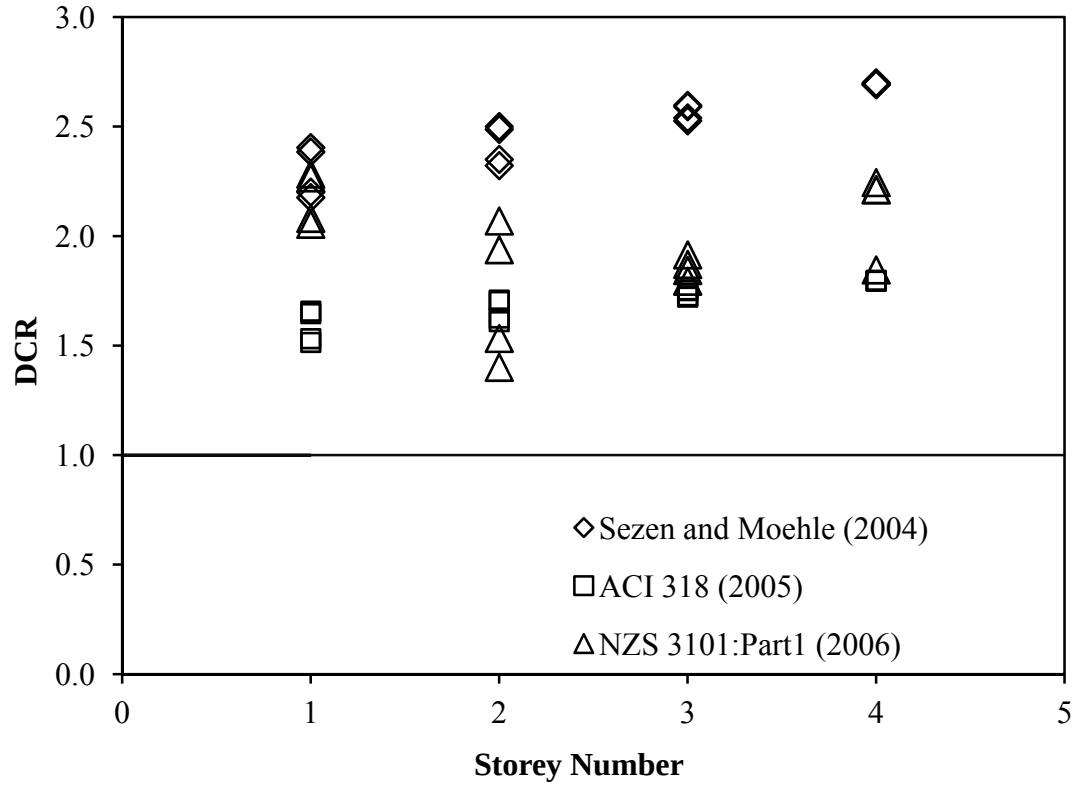

(b)

Fig. 3.17 (contd.)

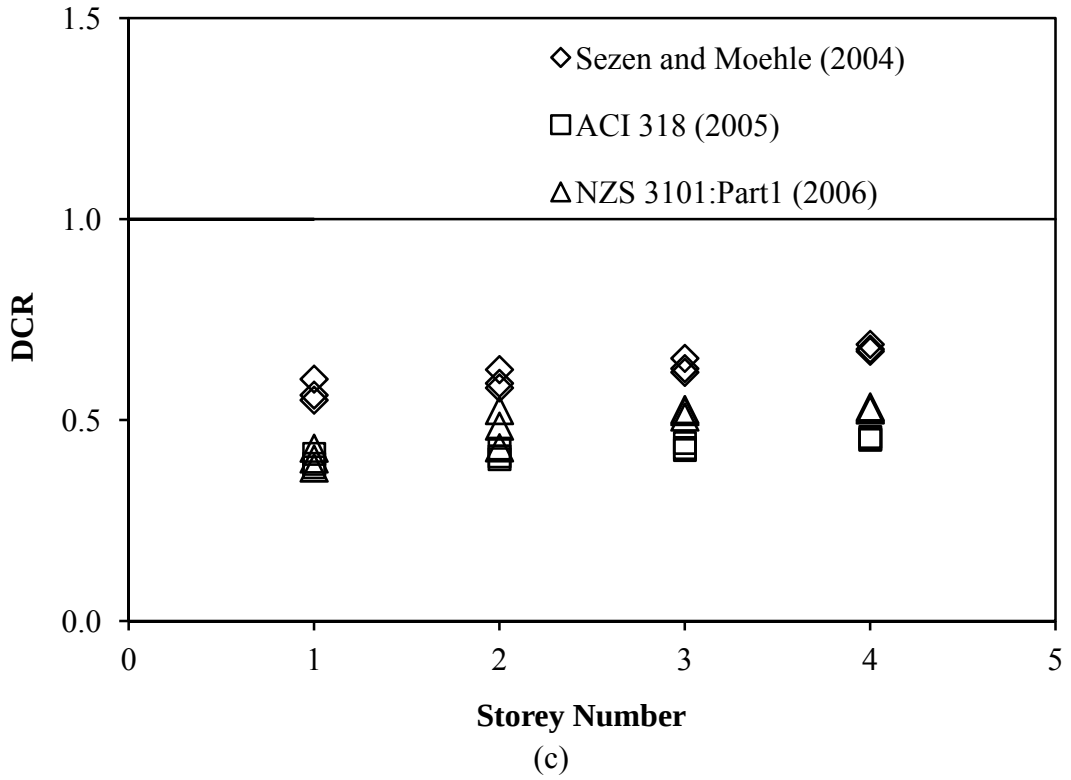

(c)

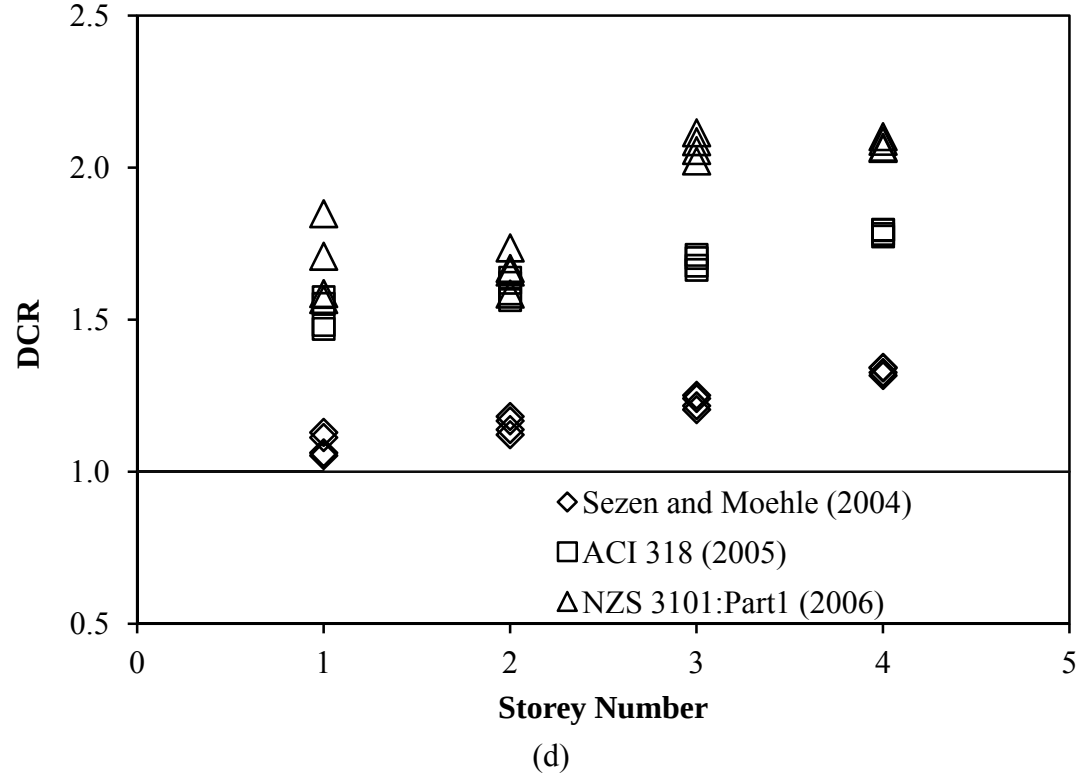

(d)

Fig. 3.17 Demand-Capacity Ratio for shear in columns of four storey Gravity Load Designed (GLD) frame building infilled with 'fair' quality (ASCE-41 2007) URM: (a) with 230 *mm* thick infills and lateral force in longitudinal direction; (b) with 230 *mm* thick infills and lateral force in transverse direction; (c) with 115 *mm* thick infills and lateral force in longitudinal direction; and (d) with 115 *mm* thick infills and lateral force in transverse direction.

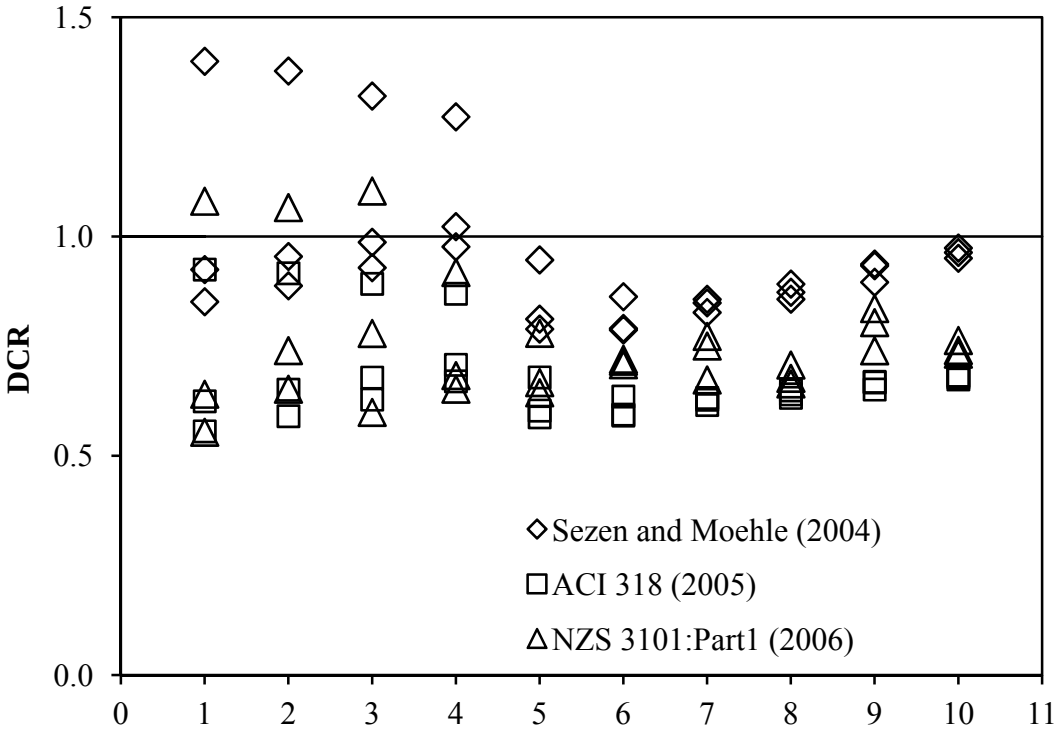

(a)

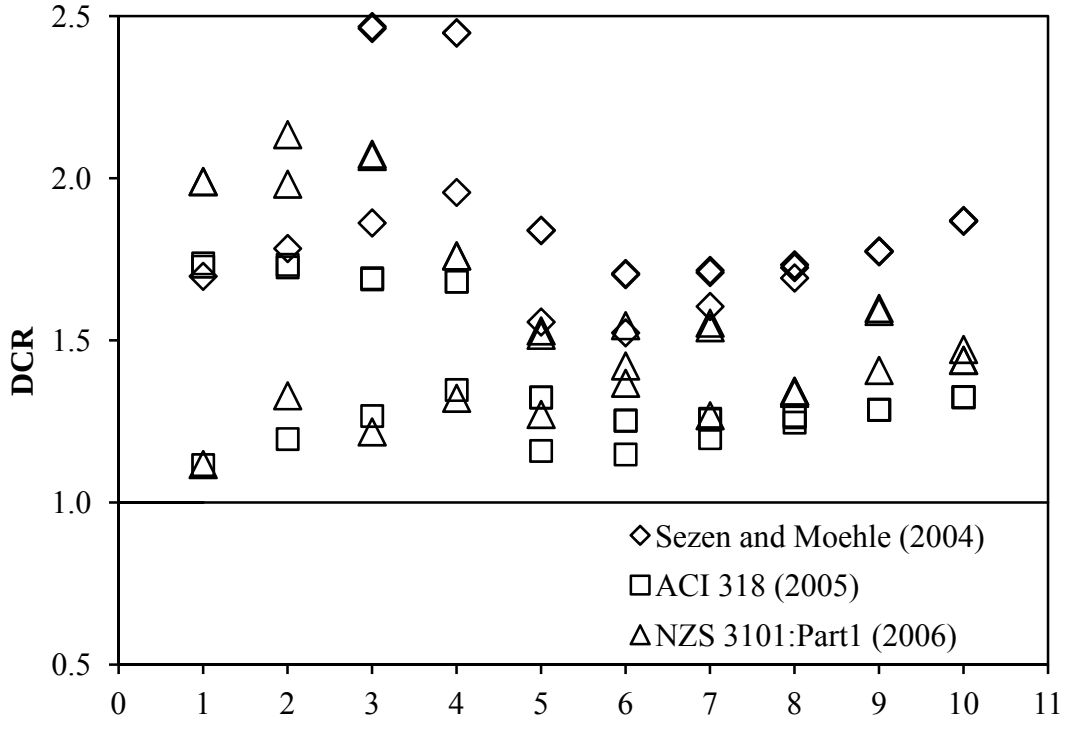

(b)

Fig. 3.18 (contd.)

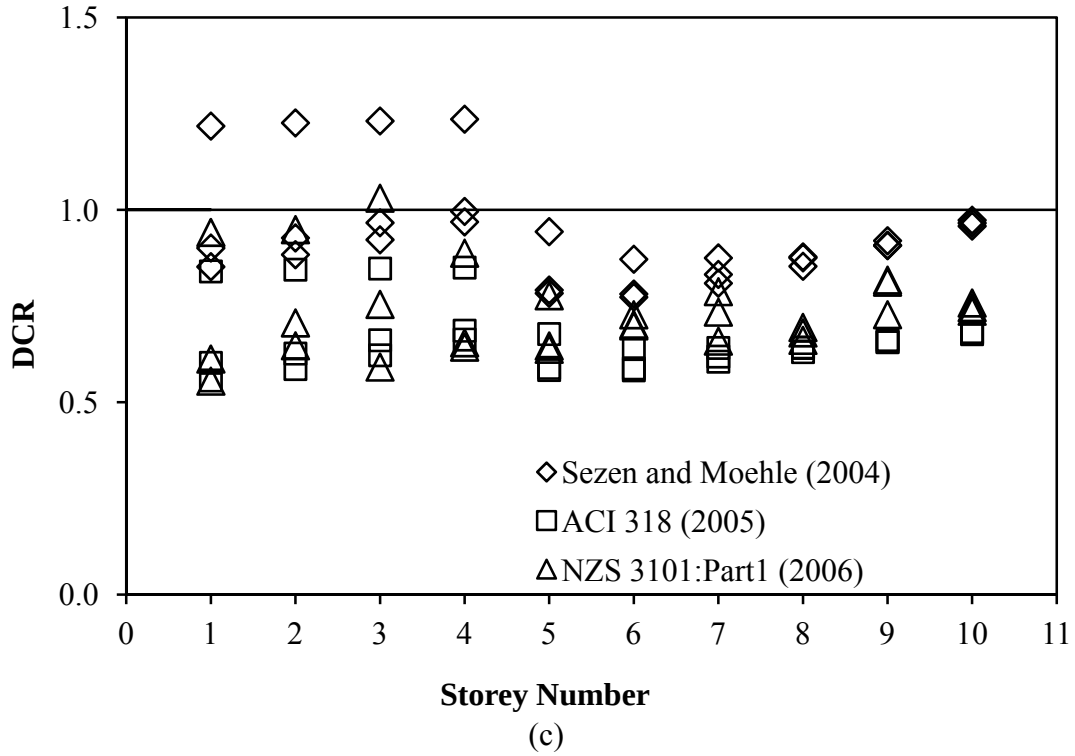

(c)

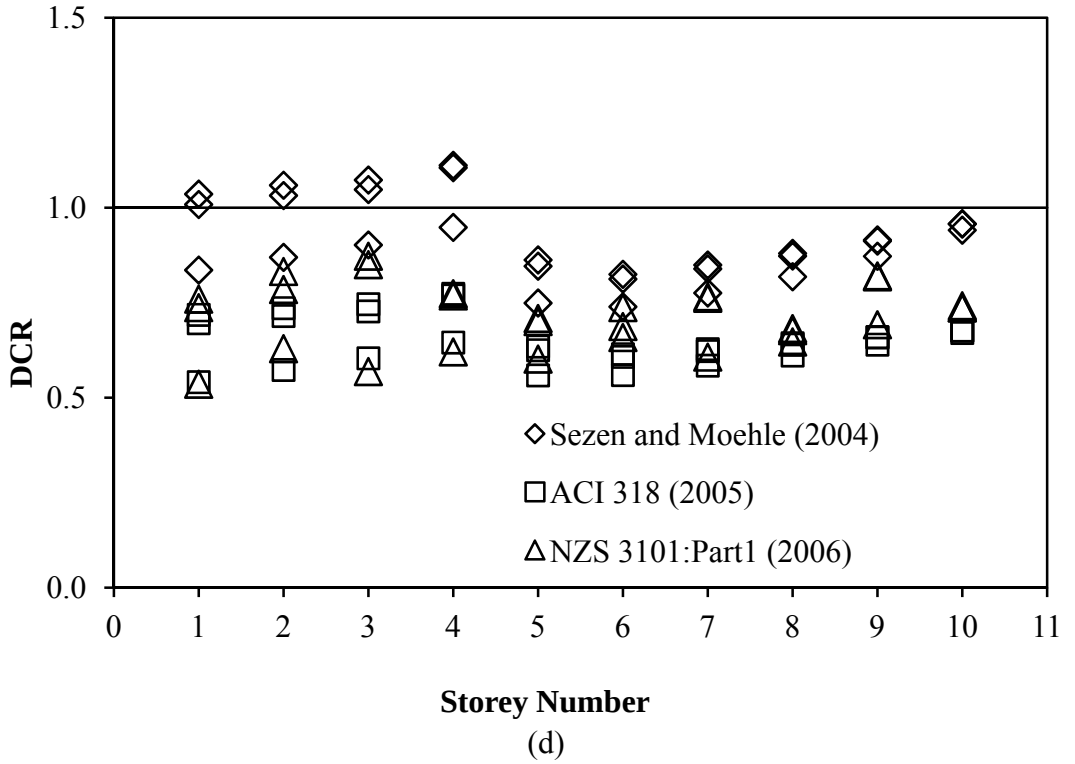

(d)

Fig. 3.18 Demand-Capacity Ratio for shear in columns of ten storey Gravity Load Designed (GLD) frame building infilled with 'fair' quality (ASCE-41 2007) URM: (a) with 230 *mm* thick infills and lateral force in longitudinal direction; (b) with 230 *mm* thick infills and lateral force in transverse direction; (c) with 115 *mm* thick infills and lateral force in longitudinal direction; and (d) with 115 *mm* thick infills and lateral force in transverse direction.

3.3.6 Effect of Infill on Shear in Beam-Column Joints

Figure 3.19 shows the shear resistance mechanism of a beam-column joint in bare and infilled RC frames. Assuming that the tension (T) in beam reinforcement is equal to the compressive force (C) in beam, the joint shear force (V_{jh}) of bare and infilled frame can be represented as in Eqs. (3.1) and (3.2), respectively.

$$V_{jh} = C + T - V_c \tag{3.1}$$

$$V_{jh} = C + T - V_c - R\cos\theta \tag{3.2}$$

where, V_c is the shear force in column, and $R\ cos\theta$ is the shear force exerted by the infill. It is evident from the figure that strut action of infill results in increased shear in column, which in-turn results in reduced shear force in the joint. To examine the effect of infills on shear failure of beam-column joints, the DCR in joints of four and ten storey GLD and SMRF buildings with and without infills were studied using four representative models (FEMA-356 2000; ACI 352R-02 2002; Hegger et al. 2003; Eurocode-8 2004), identified earlier in Chapter 2. Figure 3.20 shows the DCR for shear in beam-column joints of the four storey GLD building. It can be observed that most of the joints of the bare frame show DCRs higher than unity, indicating failure. The value of the DCR is up to 1.2 in case of Park and Mosalam (2012), Eurocode-8 (2004), and Hegger et al. (2003) models, but it is much higher (up to 1.8) in case of FEMA-356 (2000) model. On the other hand, in case of infilled frames, only FEMA-356 (2000) model predicts shear failure of the joints, which are safe according to Park and Mosalam (2012), Eurocode-8 (2004), and Hegger et al. (2003) models.

Similar observations were also made in case of the ten storey building (Fig. 3.21). In case of ten storey GLD bare frame building, all the considered models predict failure of joints above fifth floor, whereas FEMA-356 (2000) model predicts shear failure of joints at all the floors. Based on the experimental results, Firat Alemdar (2007) have concluded that FEMA-356 (2000) model greatly underestimate the shear strength capacity of joints. Therefore, the joints which are predicted to fail in shear only by the FEMA-356 (2000) model, and are safe according to the other models, can be considered to be safe. In case of ten storey infilled frame buildings, all the joints have much lower value (up to 0.8) of DCR and are safe against shear failure by all the models considered. In case of the SMRF buildings, shear reinforcement is provided in

the joints, and all joints in bare as well as in infilled frames were found to be safe in shear.

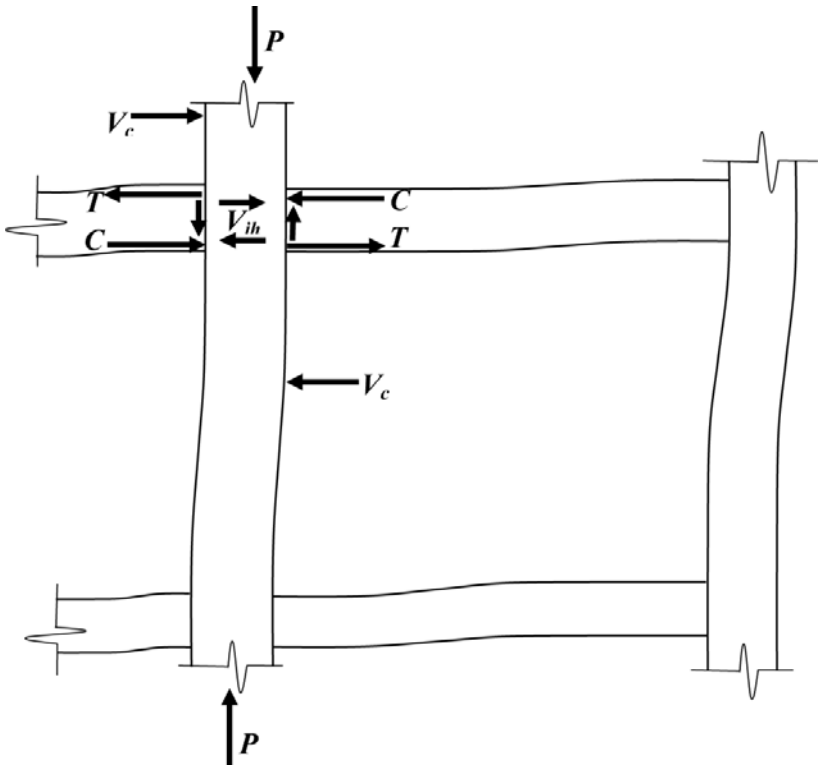

(a)

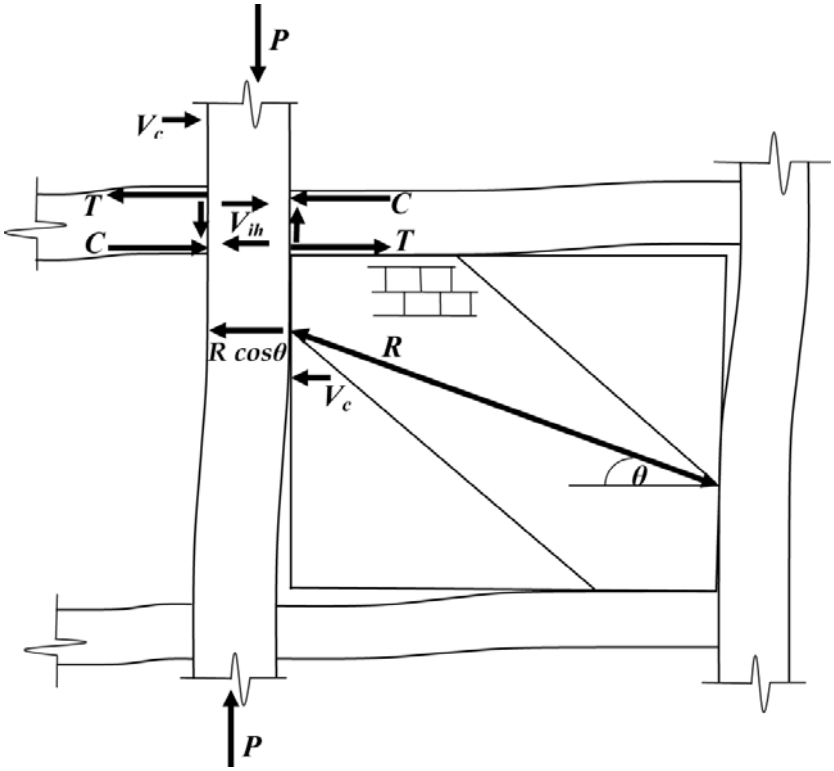

(b)

Fig. 3.19 Shear resistance mechanism of beam-column joint in: (a) bare and (b) infilled RC frame.

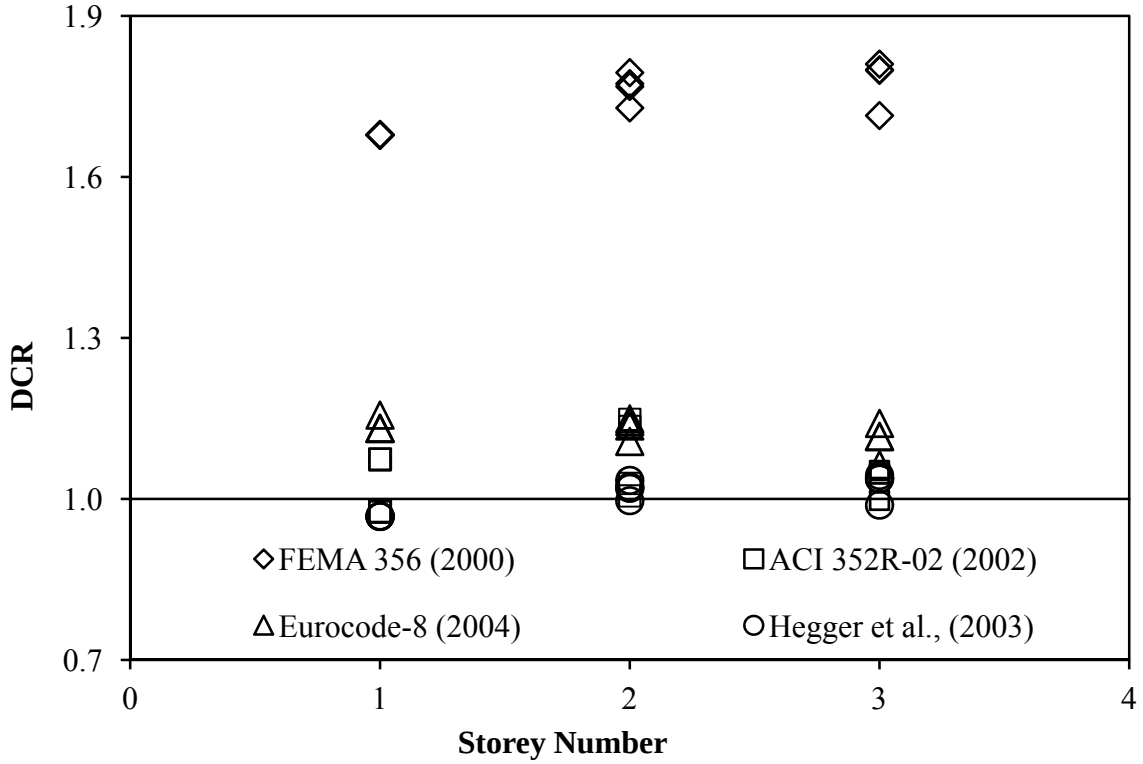

(a)

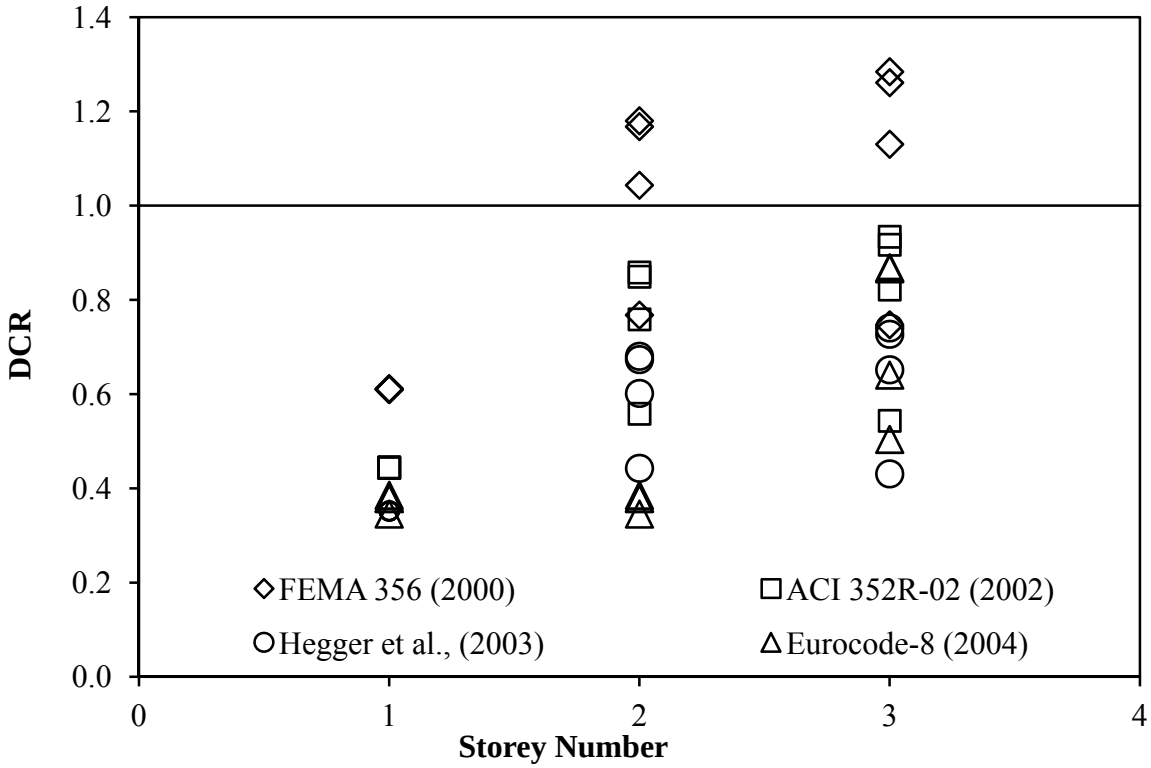

(b)

Fig. 3.20 Demand-Capacity Ratio for shear in beam column joints of four storey Gravity Load Designed (GLD) building: (a) bare frame; (b) infilled frame.

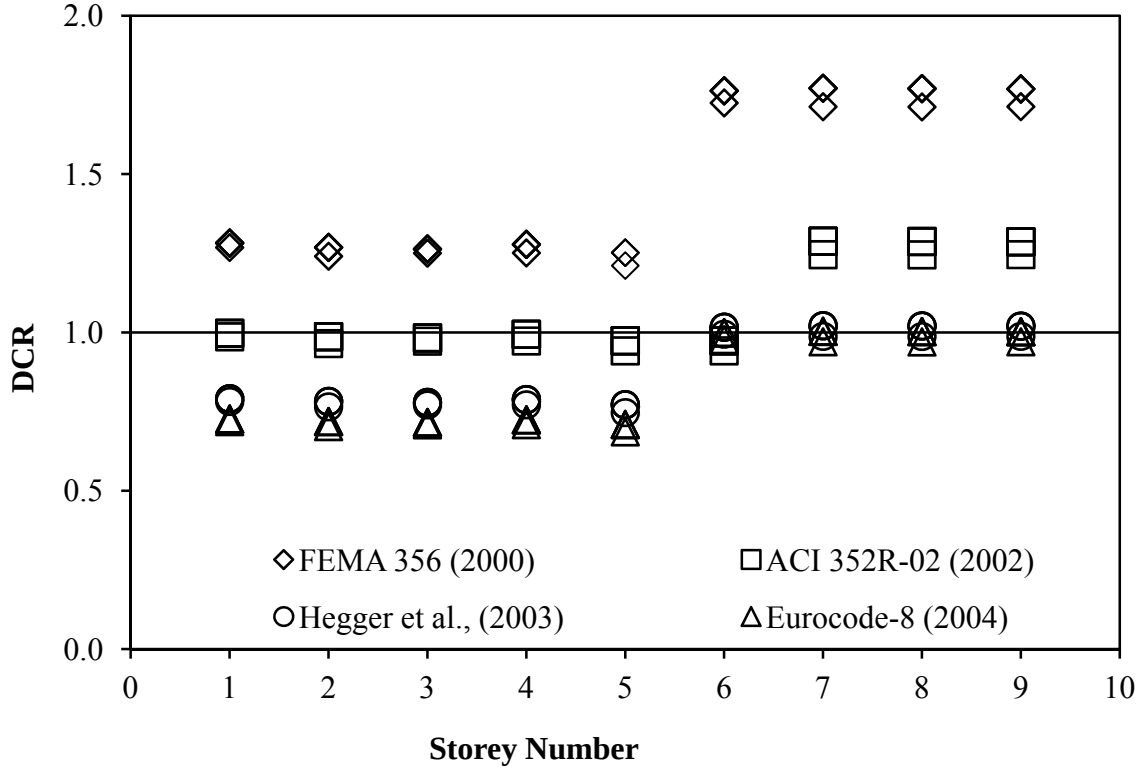

(a)

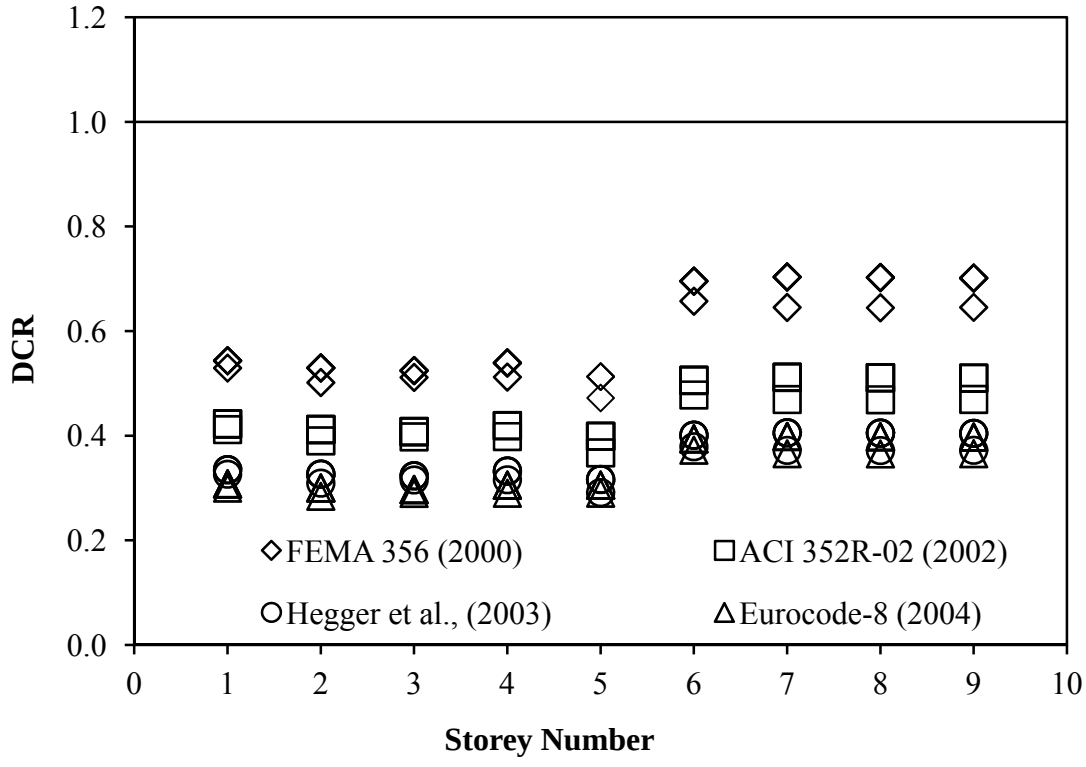

(b)

Fig. 3.21 Demand-Capacity Ratio for shear in beam column joints of ten storey Gravity Load Designed (GLD) building: (a) bare frame; (b) infilled frame.

The results presented above and in the previous Sections, correspond to the fair quality of masonry in infills. As mentioned earlier, similar studies were also conducted for good and poor quality of masonry. The cases of particular interest are, shear demand in columns due to good quality of masonry infills, and failure of joints in frames infilled with poor quality masonry. However, no deviation from the observations cited above was noticed and hence the results are not produced here. The DCR for shear in beam-column joints increases in case of poor quality masonry infills and reaches close to unity for ACI model, in case of the four storey GLD building. But, sufficient margin of safety was predicted by Eurocode-8 (2004) and Hegger et al. (2003) models.

3.4 SUMMARY

Various probable modes of failure in RC frame buildings, with and without URM infills, have been explored, from the view point of simulation of seismic behaviour of such buildings. For this purpose, representative buildings have been identified based on a field survey and a parametric study has been conducted on the representative buildings. Using the representative models identified in Chapter 2, the strength of infills in different modes has been compared and sliding shear has been observed as the most probable mode of failure in URM infills, which is in agreement with the provisions of ASCE-41 (2007).

The presence of infills significantly alters the combination of interacting axial force and moment in the columns. It increases (and reduces on tension side) axial force but reduces the bending moment in columns. This is expected to affect not only the strength, but also the ductility of columns, due to alteration of failure mode. The resulting net tension significantly reduces the shear strength of columns on tension side of the building.

The shear failure of columns due to high shear force resulting from the eccentric strut action of infills, has been predicted in case of non-ductile (without closely spaced stirrups in the potential plastic hinge regions) RC frame buildings. On the other hand, the chances of shear failure in beam-column joints are reduced in presence of infills due to reduction in shear force in the joints. The observed failures of beam-column joints in infilled frames during past earthquakes may be attributed to bond-slip failure and/or collapse of infills in out-of-plane action resulting in behavior similar to that of

bare frames. In case of ductile RC frame buildings having closely spaced stirrups in plastic hinge regions and joints, the shear failure of columns as well as joints, is avoided, even in presence of infills of 'good' quality of masonry.

Chapter 4

SEISMIC PERFORMANCE OF URM INFILLED RC FRAME BUILDINGS

4.1 INTRODUCTION

Earthquake resistant design of structures is a comparatively new concept which started in early 1900s. After Biot (1933) introduced the concept of Response Spectrum where the maximum response amplitude of single degree of freedom systems with varying periods has been plotted, it became an integral part of the subsequent building design codes. Till 1970s, various design philosophies like Working Stress Design, Ultimate Strength Design and Limit State Design were developed, in which individual members are proportioned for strength on the basis of internal forces computed from elastic analysis. However, in case of earthquake loading, the energy dissipation because of the ductility present in the structure enables us to design the structure for only a fraction of the forces corresponding to elastic response of the structure. It is expected that the structure will undergo large inelastic deformations without collapse. The collapse can be avoided by facilitating plastic deformations in desirable ductile modes only. This can be achieved by designing the brittle modes to have the higher strength. The concept of 'Capacity Design' paved the way for the development of a new design philosophy through which a desired strength hierarchy can be incorporated within the structural elements. Gradually, the Earthquake Resistant Design (ERD) methods have developed significantly in the form of Capacity Design, and Displacement Based Design (Qi and Moehle 1991; Browning 2001; Xue and Chen 2003; Priestley et al. 2007). The current seismic design practice, in India, is based on Force Based Design method, with partial incorporation of Capacity Design concepts. In the code design philosophy the exact assessment of seismic capacity of the structure, particularly of its ductility, is not made. The buildings designed using the current Indian Standards (BIS 1993, 2002) performed well in the recent earthquakes for Life Safety point of view, however, code based design philosophy does not provide insight into the expected seismic performance and possible damage of the structure.

This Chapter presents design philosophy of RC frame buildings with and without URM infills in different seismic design codes viz. BIS (2002); (Eurocode-8 2004); NZS-1170.5 (2004); NZS-4230 (2004); ACI 318 (2005); ASCE-7 (2006); ASCE-41 (2007) and deals with the effect of URM infills on the estimated performance of RC frames by comparing the seismic performance of RC frame buildings of different design levels, with and without URM infills. The model of infills developed in Chapter 2 has been used in the study. This Chapter also examines the adequacy of the provisions of the Indian seismic design code and relative importance of various code provisions by estimating the expected performance of a set of buildings designed for Indian code.

4.2 FORCE-BASED DESIGN METHOD

Code design practices, world-over, are traditionally based on Force-Based Design (FBD) concept, in which individual members of the structure are proportioned for strength, so that these can sustain shaking of moderate intensities without structural damage and shaking of heavy intensities without total collapse, on the basis of internal forces computed using an elastic analysis. The inelastic effects are indirectly accounted for using a Response Reduction Factor based on some form of Equal Displacement and Equal Energy Principles. In the code procedures, an explicit assessment of the anticipated performance of the structure is not made. To ensure the desired seismic performance, the design codes exercise three types of controls in the design:

1. Control of Ductility Demand, using the effective Response Reduction Factor $\frac{I}{R}$, where I represents the Importance Factor and R represents the reduction factor for ductility and overstrength. Overstrength arises due to use of material and load safety factors and characteristic strength (nominal) of material (usually defined as 95% confidence value).
2. Control of minimum design base shear through the use of capping on design natural period and/or flooring on the design base shear.
3. Control of flexibility through the limit on maximum permissible interstorey drift.

Another crucial issue in the code based design is enhancement of ductility by proper detailing and proportioning of members. Ductility can be enhanced by facilitating plastic deformations in desirable ductile modes only. This can be achieved by designing the brittle modes/members to have strength higher that in case of ductile modes. This concept of 'Capacity Design' introduced by Park and Paulay (1975) has become integral part of the national design codes.

Seismic performance of a building, designed according to the code, depends on the overall effect of the above controls, and several other provisions for design and detailing, and the role of an individual control parameter is not explicit in ensuring the desired performance. In the following Sections, a comparative study of present Indian Standards with some of the selected major seismic design codes, viz. Eurocode-8 (2004); NZS-1170.5 (2004); ACI 318 (2005); (ASCE-7 2006); ASCE-41 (2007) to ensure desired seismic performance of RC frame buildings with and without URM infills is presented.

4.3 KEY PROVISIONS IN SEISMIC DESIGN CODES

4.3.1 Specification of Seismic Hazard

The Indian code of practice for seismic design (BIS (2002), defines two levels of seismic hazard, namely Maximum Considered Earthquake (MCE) and Design Basis Earthquake (DBE). The Effective Peak Ground Acceleration (EPGA) in DBE is considered as half of the EPGA in MCE, and structures are designed for DBE with partial load and material safety factors. The building is designed for a base shear (V_B) calculated as

$$V_B = \frac{Z}{2}\frac{I}{R}\frac{S_a}{g}W \tag{4.1}$$

where, W is the seismic weight of the building, Zone Factor (Z) represents the EPGA for MCE, Importance Factor (I) and Response Reduction Factor (R) control the Ductility Demand, based on the anticipated Ductility Capacity and the post earthquake importance of the structure. Unlike BIS (2002), ASCE-7 (2010) recommends to reduce the MCE by a factor of 2/3 to obtain DBE. Contrary to ASCE-

7 (2010), NZS-1170.5 (2004) and Eurocode-8 (2004) provide different multiplication factors to specify different hazard levels.

4.3.2 Classification of Ductility Class and Response Reduction Factor

In Indian Standard, based on reinforcement detailing and capacity design, two ductility classes for RC buildings – Ordinary Moment Resisting Frame (OMRF) and Special Moment Resisting Frames (SMRF) are specified. In case of SMRF, the code provides specifications for reinforcement detailing and Capacity Design of members to avoid brittle shear failure. In general, the reinforcement detailing and capacity design provisions for OMRF and SMRF of Indian code correspond to the OMRF and IMRF (Intermediate Moment Resisting Frame), respectively, of ASCE-7 (2006)/ACI 318 (2005). There is no class of RC frames in the Indian code corresponding to the SMRF of ASCE-7 (2006)/ACI 318 (2005). Similarly, as compared to Eurocode-8 (2004), the OMRF and SMRF of Indian code correspond to ductility class 'Low' and 'Medium' and there is no class defined corresponding to ductility class 'High' of the Eurocode-8 (2004). The ductility class, "Ductile" and "Limited Ductility" of NZS-1170.5 (2004) corresponds to SMRF of ASCE-7. However, no class is defined in Indian Standard corresponding to any of the three ductility class of NZS-1170.5. This indicates the inadequacy of ductility provisions in Indian code as compared to ACI 318 (2005), Eurocode-8 (2004), and NZS-1170.5 (2004). The response reduction factors of 3 and 5, specified in the Indian code for OMRF and SMRF, respectively, are same as for OMRF and IMRF, respectively, in case of ASCE-7 and much higher than the corresponding values of behaviour factor specified in Eurocode-8 (2004) for the corresponding ductility classes. NZS-1170.5 (2004) considers the effect of period and provide different reduction factors for any ductility class corresponding to short and long period.

4.3.3 Design Period of Buildings

The natural period of vibration has a very important role in the seismic design of a structure since the design spectral acceleration and therefore the design base shear is strongly dependent on the natural period. As there is significant uncertainty about effective stiffness of RC members and stiffness of secondary components is ignored, in many cases the designers develop too flexible models of structures, which results in

much lower design base shear due to lengthened period of vibration. To safeguard against this error, ASCE-7 (2006), NZS-1170.5 (2004), and BIS (2002) provide a capping on the natural period of vibration obtained from the analytical model. Actually, the capping on the design period is exercised in form of a flooring (minimum value) to the design base shear. The empirical expression for design natural period of RC frame buildings, provided in BIS (2002) and Eurocode-8 (2004) is given as:

$$T_a = 0.075H^{0.75} \tag{4.2}$$

where, T_a (*sec*) is the design natural period of a building having height equal to H (*m*). Indian seismic code (BIS 2002) prescribes scaling of all the response quantities by a factor equal to $\frac{\overline{V_B}}{V_B}$, where $\overline{V_B}$ is the base shear calculated using the empirical design period (Eq. 4.2) and V_B is the base shear obtained analytically. On the other hand, Eurocode-8 (2004) prescribes the above expression, only for approximate estimation of period for preliminary design. ASCE-7 (2006) also prescribes a similar empirical expression for period of RC moment resisting frames,

$$T_a = 0.0466H^{0.9} \tag{4.3}$$

New Zealand code (NZS-1170.5 Supplement-1 (2004)) recommends different periods for serviceability and ultimate limit state. The period for serviceability limit state of RC moment resisting frames is identical to BIS (2002) and Eurocode-8 (2004) (Eq. 4.2), however, the design period used for ultimate limit state is lengthened 1.25 times as compared to the serviceability limit state period.

4.3.4 Control of Drift

Contrary to many other national codes, Indian Standard (BIS 2002) specifies a limit of 0.4% for allowable interstorey drifts at the design (elastic) force level, whereas in Eurocode-8 (2004), NZS-1170.5 (2004), and ASCE-7 (2006), limits are specified for the total interstorey drift (including elastic and inelastic components). As different Reduction Factors (and hence different Ductility Demands) have been specified for OMRF and SMRF (BIS 2002), it results in different limits on total drift for OMRF and SMRF. This is contrary to other codes, where equal drift limits irrespective of the

ductility class of structures are specified, and leads to some discrepancies in the design (Haldar and Singh 2009). Further, the Indian Standard does not specify any additional control over plastic deformations in structural and non-structural components, as in Eurocode-8 (2004).

4.4 PROVISIONS FOR URM INFILLED RC FRAMES IN SEISMIC DESIGN CODES

Despite scrupulous research on infilled frames, traditionally, infill panels in frame buildings are not considered as structural components, mostly because of the absence of adequate modeling guidelines in the design standards. Some of the national codes, viz. Eurocode-8 (2004), and NZS-4230 (2004) recognize the need of considering the effect of infills in the seismic response evaluation of infilled frames and prescribe some precautionary checks, whereas other codes (BIS 2002; ASCE-7 2006) are silent on this issue. BIS (2002) controls the minimum design base shear of infilled frames by providing capping on the design period, given as

$$T_a = \frac{0.09H}{\sqrt{D}} \tag{4.4}$$

where, T_a (*sec*) is the design natural period of a building having height equal to H (*m*) and base dimension D (*m*) along the direction of the vibration.

The Eurocode-8 (2004), without recommending any particular model, emphasizes on the use of a reliable model for simulating the effect of infills. It specifies that in absence of a precise model, the design period to be used to evaluate the seismic base shear should be taken as the average of that for the bare frame and for the elastic infilled frame. Seismic demand on frame members can then be determined by modeling the frame structure without the infills. The code provides the following expressions for approximate periods of infilled RC frames:

$$T_a = C_t H^{\left(\frac{3}{4}\right)} \tag{4.5}$$

where,

$$C_t = \frac{0.075}{\sqrt{A_c}} \tag{4.6}$$

and

$$A_c = \sum A_i \left(0.2 + \frac{l_{wi}}{h}\right)^2 ; \quad \frac{l_{wi}}{h} \leq 0.9 \tag{4.7}$$

H is the height of the building; A_c is the total effective area of the masonry infills in the first storey of the building; A_i is the effective cross-sectional area and l_{Wi} is the length of the i^{th} infill in the first storey, in the direction parallel to the applied forces.

The influence of the irregular distribution of infill panels, in plan or in elevation, is also addressed in Eurocode-8 (2004). It suggests increasing the effects of the accidental eccentricity by a factor of 2 when masonry infill panels are irregularly distributed but do not constitute a severe irregularity in the plan. In case of severe plan irregularities, sensitivity analysis regarding the position and properties of the infills is recommended, whereas, non-uniform distribution of infills in elevation can be catered by amplifying the effect of seismic action on columns through a magnification factor (η>1.1), given as

$$\eta = \left(1 + \frac{\Delta V_{RW}}{\sum V_{Ed}}\right) \leq q \tag{4.8}$$

where, ΔV_{RW} is the total reduction in the resistance of masonry walls in the concerned storey, compared to the more infilled storeys above it; $\sum V_{Ed}$ is the sum of the seismic shear forces acting on all vertical primary seismic members of the concerned storey; and q is the behavior factor.

The New Zealand code (NZS-4230 2004) deals with infilled frames in a more detailed manner. The code acknowledges that infill panels modify the structural behavior and have an adverse effect on the seismic performance of frame, unless complete separation from the surrounding frame is provided. The design provisions of this code are governed by the reduced period of vibration resulting in increased seismic load and ductility demand on the frame members. NZS-1170.5 Supplement-1 (2004) does

not provide any expression for estimation of design period for infilled RC frames, however, the empirical expression prescribed for RC frames with concrete shear walls is identical to that (Eqs. 4.5-4.7) prescribed in Eurocode-8 (2004) for URM infilled RC frame buildings. For the purpose of force distribution, the code recommends to idealize the infilled frame as an equivalent diagonally braced frame having the width of the masonry infill diagonal as one quarter of its length. Possible failure modes, i.e. shear failure of infill panels, crushing of the diagonal strut, tension failure of infill panels, flexural or shear failure of columns, soft storey mechanism after failure of infill panels, have been identified, though not quantified, as prediction of strength of infills with accuracy is difficult. To avoid shear failure of the supporting columns, NZS-4230 (2004) recommends designing infilled frames for higher structural type factors unless the infills are properly tied with the surrounding frames to act together in full composite action. To ensure satisfactory performance of infilled frame after shear failure of infills in a storey, NZS-4230 (2004) suggests that the ductility demand at any storey level should not be more than two. Accordingly, the maximum storey ductility demand μ_s, for a building of equal story height, is limited to

$$\mu_s = \frac{n+1}{n} \tag{4.9}$$

where, n is the number of storeys.

Unlike the design code for new buildings, the US American code for rehabilitation of existing buildings (ASCE-41 2007) and FEMA guidelines (FEMA-273 1997; FEMA-306 1998; FEMA-356 2000) clearly explain the procedure to assess the seismic response of infilled frames. According to these documents, the effect of masonry infill panels can be simulated by introducing one or more concentrically or eccentrically placed equivalent diagonal struts where the equivalent width is expressed by Eq. (2.1).

4.5 CONCEPT OF PERFORMANCE BASED DESIGN

Priestley (1993, 2000, 2003) has pointed out that force is a poor indicator of damage and there is no clear relationship between strength and damage. Hence, force cannot be a sole criterion for design. Further, assuming a flat Response Reduction Factor for a class of buildings is not realistic, because ductility depends on many factors, such

as, degree of redundancy, axial force, steel ratio, structural geometry, etc. Therefore, there is need for a design procedure, which is based on explicit estimates of the seismic performance.

To overcome these limitations of the Forced-Based Design, an alternative design philosophy named "Displacement-Based Design" (DBD) was first introduced by Qi and Moehle (1991), which includes translational displacement, rotation, strain, etc. in the basic design criteria. It is a very promising design tool, which enables designer to design a structure with predictable performance. Considerable research effort has been devoted to this topic in the past few decades and different variants of this method have been developed, in which, different deflection parameters are chosen as performance indicators and different techniques are used to proportion the members to achieve the desired performance. A detailed review of these procedures is beyond the scope of this Thesis, and only the two main approaches are being mentioned here. Priestley (2000) and his group (Priestley et al. 2007) have made significant contribution in developing a practical methodology for Displacement Based Design. In their approach, the interstorey drifts and ductility demand are considered as control parameters for ensuring the desired performance. They have specified engineering limit states for different Performance Levels and a draft code on Displacement Based Design has also been proposed (Priestley et al. 2007).

Another significant development has been in the form of development of Performance Based Design (PBD) methodology for performance evaluation and rehabilitation of existing buildings, documented by ATC-40 (1996); FEMA-273 (1997); FEMA-356 (2000); FEMA-440 (2006) and ASCE-41 (2007). In PBD, design criteria are expressed in terms of achieving a set of performance objectives. A performance objective represents a specific risk. This approach provides the building owners and policy makers a framework for informed judgment about acceptability of seismic risk. A seismic performance objective has two essential parts – an acceptable damage state, i.e., performance levels and a level of hazard. In PBD, a realistic estimate of strength and ductility of the structure is made and the Performance Level (acceptable damage state) is controlled in terms of inelastic deformations in different members, as inelastic deformations are the best indicators of damage. A nonlinear analysis is imperative. For this purpose, the advent of pushover analysis (ATC-40 1996) has been the most significant development, to make it affordable by common designer.

4.6 NONLINEAR ANALYSIS

The most sophisticated nonlinear analysis procedure is nonlinear time history analysis or the Nonlinear Dynamic Procedure (NDP) for predicting forces and displacements under seismic input. However, this method has difficulty in selection of design time history. The calculated response can be very sensitive to the characteristics of the individual ground motion used as seismic input; therefore several time-history analyses are required using different ground motion records. To overcome the uncertainty in ground motion, a relatively new concept of Incremental Dynamic Analysis (IDA) is introduced by Vamvatsikos and Cornell (2002). In this method of dynamic analysis, the analytical model of a structure is subjected to a ground motion record, and the nonlinear dynamic analysis is repeated, each time increasing the scale factor on the ground motion's intensity, until that record causes structural collapse under lateral load. This process is then repeated for an entire suite of ground motion records, thus the record to record uncertainty in the response is captured. Further details of IDA are provided in Chapter 5.

Since the Nonlinear Dynamic Procedure (NDP) is complex and computationally very expensive, this method seems impractical for general use in design offices. To overcome this limitation of NDP, FEMA-273 (1997); FEMA-356 (2000); FEMA-440 (2006) and ATC-40 (1996) presented a simplified nonlinear analysis method, which can be used easily and provide valuable insight into the behaviour of the structure under lateral loading. This method is known as Nonlinear Static Procedure (NSP), or pushover analysis method. Pushover or capacity curve of a building is the plot between the base shear and roof displacement, under an assumed distribution of lateral load. The magnitude of the lateral load is increased monotonically, identifying the weak links and failure modes. Accuracy of pushover analysis depends on a number of factors including the distribution of lateral load, consideration of higher mode effects (Chopra and Goel 2002), and the procedure used to obtain the performance point. In the present study, a load pattern proportional to fundamental mode in the direction considered for pushover analysis, has been applied, according to the recommendations of ASCE-41 (2007).

4.6.1 Estimation of Inelastic Response

An important step in evaluation of seismic performance of structures using pushover analysis is estimation of inelastic response of the structure from the capacity curve. A large number of methods are available to estimate inelastic response of the structure using elastic demand response spectrum, viz. Inelastic Spectrum Estimation (ISE) approach (Veletsos and Newmark 1960; Newmark and Hall 1982; Riddell et al. 1989; Krawinkler and Nassar 1992; Miranda 1993; Vidic et al. 1994; Ordaz and Pérez-Rocha 1998; Miranda 2000; Riddell et al. 2002; Cuesta et al. 2003; Chopra and Chintanapakdee 2004; Ruiz-García and Miranda 2004), Equivalent Linearization (EL) approach (Rosenbleath and Herrera 1964; Gulkan and Sozen 1974; Iwan 1980; Kowalsky 1994; Grant et al. 2005; Priestley et al. 2007; Pennucci et al. 2011), Displacement Modification approach (FEMA-356 2000; FEMA-440 2006; ASCE 41-06 2007), and using Ground Motion Prediction Equations (GMPEs) for inelastic spectrum (Akkar and Bommer 2007; Rupakhety and Sigbjörnsson 2009; Bozorgnia et al. 2010a; Bozorgnia et al. 2010b).

Inelastic Spectrum approach provides relationships for estimating a 'Ductility Factor', $R_{\mu d}$ by which the elastic acceleration response spectrum is divided to get the yield acceleration spectrum and the yield displacement spectrum for given ductility, μ_d. Eventually the inelastic displacement is estimated by multiplying the 'Ductility Factor', $R_{\mu d}$ with the obtained yield displacement. The factor $R_{\mu d}$ depends on factors like ductility, period of vibration (Veletsos and Newmark 1960; Newmark and Hall 1982; Riddell et al. 1989), and site class (Miranda 1993; Chopra and Chintanapakdee 2004; Ruiz-García and Miranda 2004). In Equivalent Linearization approach, inelastic behavior of the structure is represented by an equivalent linear system having an equivalent damping, and equivalent period of vibration. In this approach, the estimated equivalent damping is sensitive to ductility (Rosenbleath and Herrera 1964; Gulkan and Sozen 1974; Iwan 1980; Kowalsky 1994), choice of hysteresis model, and effective period (Kwan and Billington 2003; Grant et al. 2005; Dwairi et al. 2007). FEMA-440 (2006) has presented a comprehensive study on different methods of estimating performance point and has recommended improvements over the original procedures of ATC-40 (1996) and FEMA-273 (1997) known as 'Capacity Spectrum Method' and 'Displacement Modification Method' (DMM), respectively. In

the 'Displacement Modification Method' the inelastic spectral displacement can be obtained directly from the elastic spectral displacement by multiplying with some factors prescribed in FEMA-440 (2006). The conversion of elastic acceleration spectrum to inelastic displacement spectrum is prone to the uncertainties of the elastic spectrum itself in addition to the uncertainties involved in the process of conversion (Akkar and Bommer 2007). Further, the acceleration response spectra prescribed in seismic design codes are unrealistic (Bommer and Elnashai 1999). Due to these reasons, recently there is a trend to obtain the inelastic spectrum directly using the Ground Motion Prediction Equations (GMPEs) (Akkar and Bommer 2007; Rupakhety and Sigbjörnsson 2009; Bozorgnia et al. 2010a; Bozorgnia et al. 2010b).

FEMA-440 (2006) provides a brief commentary in section A.3.2.3 on the choice between the methods to estimate inelastic response of the structure and concludes, "The choice between the two procedures is largely a matter of personal preference as opposed to relative accuracy". However, a comparative study of the available methods to estimate inelastic response of structures by Khose and Singh (2012) shows that different methods may yield largely varied results. The study indicates that the DMM is in good agreement with analytically obtained inelastic response of the structure. Accordingly, in the present study the Displacement Modification Method of ASCE-41 (2007) has been preferred. DMM has another advantage over other methods of inelastic response estimation, that it does not require iterations and therefore is more suitable for parametric study. According to DMM the target displacement Δ_{roof} at roof level can be obtained as:

$$\Delta_{roof} = C_0 C_1 C_2 S_a \frac{T_e^{\,2}}{4\pi^2} g \tag{4.10}$$

where, C_0 is modification factor to relate spectral displacement of an equivalent single degree of freedom (SDOF) system to the roof displacement of the building. C_1 is modification factor to relate expected maximum inelastic displacements to displacements calculated for linear elastic response. C_1 is given as:

$$C_1 = 1 + \frac{R-1}{a_s T_e^{\,2}} \tag{4.11}$$

For effective period greater than 1.0 *sec* the value of C_1 is taken as 1 and for effective period less than 0.2 *sec* the value of C_1 is considered equal to the value of C_1 at period 0.2 *sec*. T_e is effective fundamental period of the building, the constant a_s is equal to 130, 90, and 60 for site Classes B, C, and D, respectively, and R is the ratio of elastic strength demand to calculated strength capacity, given as:

$$R=\frac{S_a}{V_y/w} \tag{4.12}$$

V_y is the lateral yield strength of the building, w is the seismic weight of the building, S_a is the demand spectral acceleration, at the effective fundamental period and damping ratio of the building.

C_2 is the modification factor to represent the effect of pinched hysteretic shape, stiffness degradation, and strength deterioration on the maximum displacement response. ASCE-41 (2007) provides the following relationship for estimating C_2:

$$C_2 = 1+\frac{1}{800}\left(\frac{R-1}{T_e}\right)^2 \tag{4.13}$$

4.7 SEISMIC PERFORMANCE OF CODE DESIGNED BUILDINGS

Effect of infills on the seismic performance of RC frame buildings is studied using Nonlinear Static Pushover analysis of the two sets of representative buildings, described in Section 3.3.1. The plan and elevation of the buildings has been presented in Fig. 2.5. The design and modeling parameters for the considered buildings, as per relevant Indian codes, are summarized in Table 4.1. Figures 4.1 and 4.2; show the collapse mechanisms of four and ten storey Gravity Load Designed (GLD) bare RC frame buildings, respectively. Similar hinge patterns for the four and ten storey uniformly infilled GLD buildings are presented in Figs. 4.3 and 4.4, respectively. It is observed from the Figures that in case of the bare frame buildings, the failure occurred when all the columns (Fig. 4.1) or all the beams (Fig. 4.2) in ground storey crossed “Collapse Prevention” (CP) performance level (ASCE-41 2007), whereas in case of infilled frame buildings, failure occurred due to shear failure of the first storey columns in longitudinal direction and shear failure of some of the second storey columns in transverse direction.

Table 4.1
Design and modeling parameters for the considered buildings

General	Design Levels	• Bare Frame designed for Gravity Loads • Infilled Frame designed for Gravity Loads • Bare Special Moment Resisting Frame (BIS 2002) • Infilled Special Moment Resisting Frame (BIS 2002)
	No. of Storeys	4 and 10
Seismic Hazard	Soil Type	Soil Type I (BIS 2002)
	Seismic Zone	All the buildings are situated on Seismic Zone IV (BIS 2002) (EPGA=0.24*g*)
Material	Concrete	Nominal cube strength = 20 *MPa*
	Steel	Nominal yield strength = 415 *MPa*
	Compressive strength of infill, f_c'	4.1 *MPa*
	Modulus of elasticity of infill	550 f_c' (as per ASCE 41)
Loading	Dead load	• Self weight of members • Weight of infills • Weight of slabs and floor finish • Weight of 1*m* high and 115 *mm* thick masonry parapet wall
	Live load	• 4 kN/m^2 on corridor • 3 kN/m^2 on other floor area
	Design load combination for gravity designed buildings	1.5 (Dead load + Live load)
	Design load combinations for SMRF buildings	• 1.5 (Dead load + Live load) • 1.2 (Dead load + Live load ± Earthquake load) • 1.2 (Dead load ± Earthquake load) • 0.9 Dead load ± 1.5 Earthquake load
Structural modeling	Software used	SAP2000 Nonlinear (SAP2000 2010)
	Structure Model	Space frame model
	Element models	• 3D frame elements for beams and columns • Slabs as rigid diaphragm • Strut element for infill
	Plasticity model	Lumped plasticity model based on chord rotation (ASCE-41)
	P-delta effect	Considered in pushover analysis

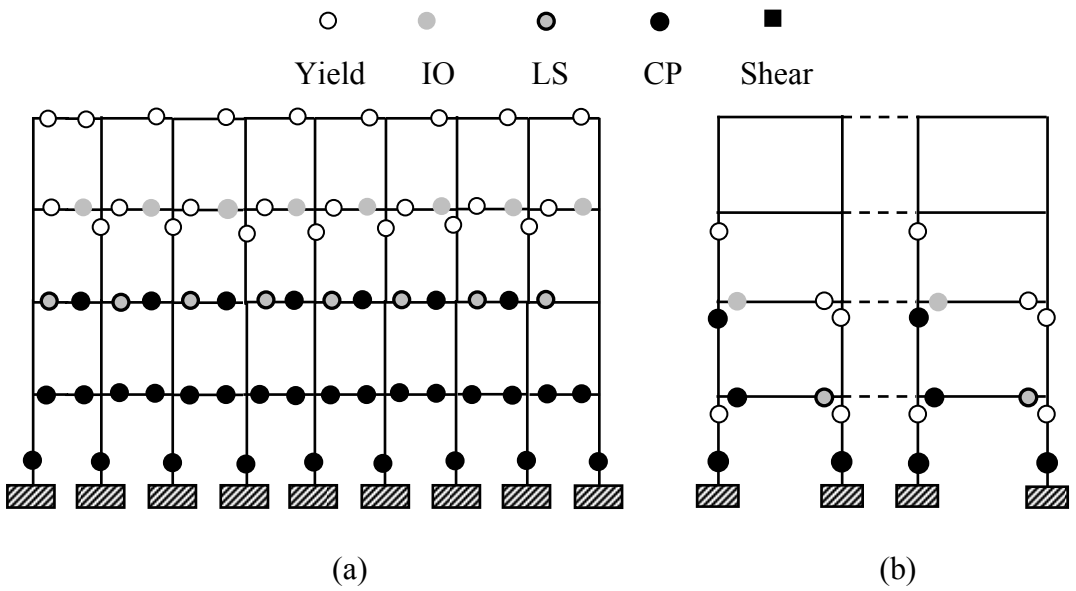

Fig. 4.1 Collapse mechanism of four storey RC bare frame building, designed for gravity loads only as per relevant Indian Standards: (a) typical longitudinal frame; (b) typical transverse frame.

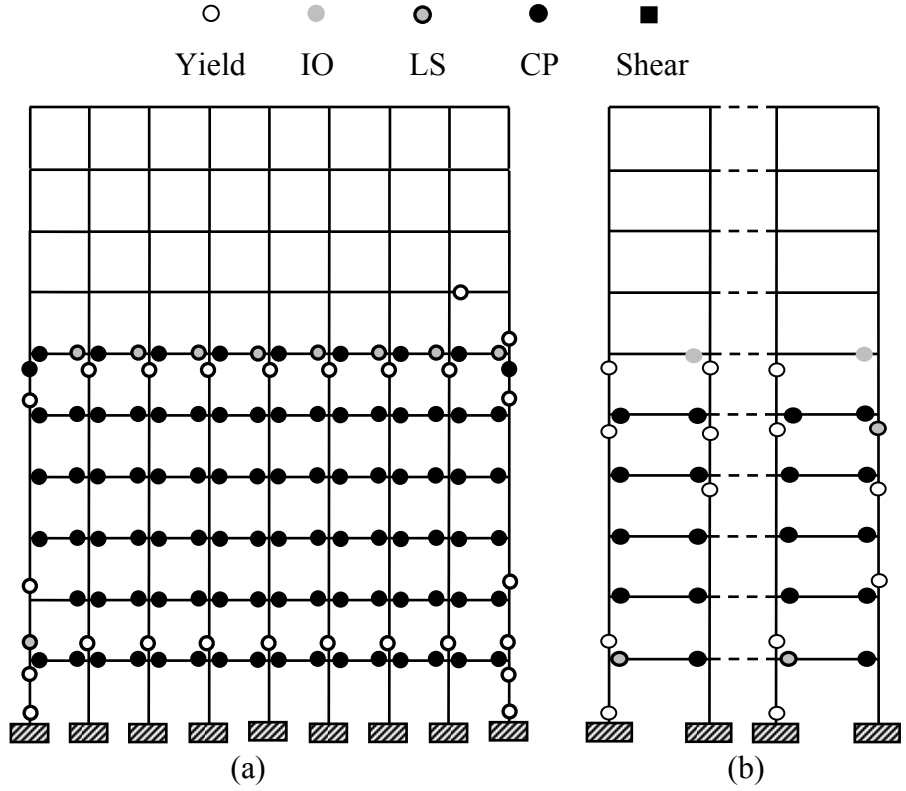

Fig. 4.2 Collapse mechanism of ten storey RC bare frame building, designed for gravity loads only as per relevant Indian Standards: (a) typical longitudinal frame; (b) typical transverse frame.

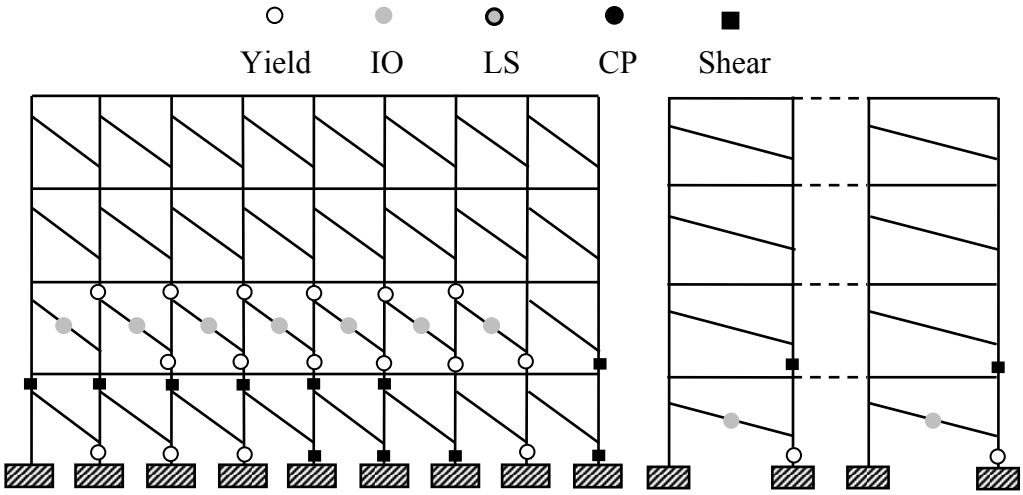

Fig. 4.3 Collapse mechanism of four storey RC frame buildings with uniform infills designed for gravity loads only as per relevant Indian Standards: (a) typical longitudinal frame; (b) typical transverse frame.

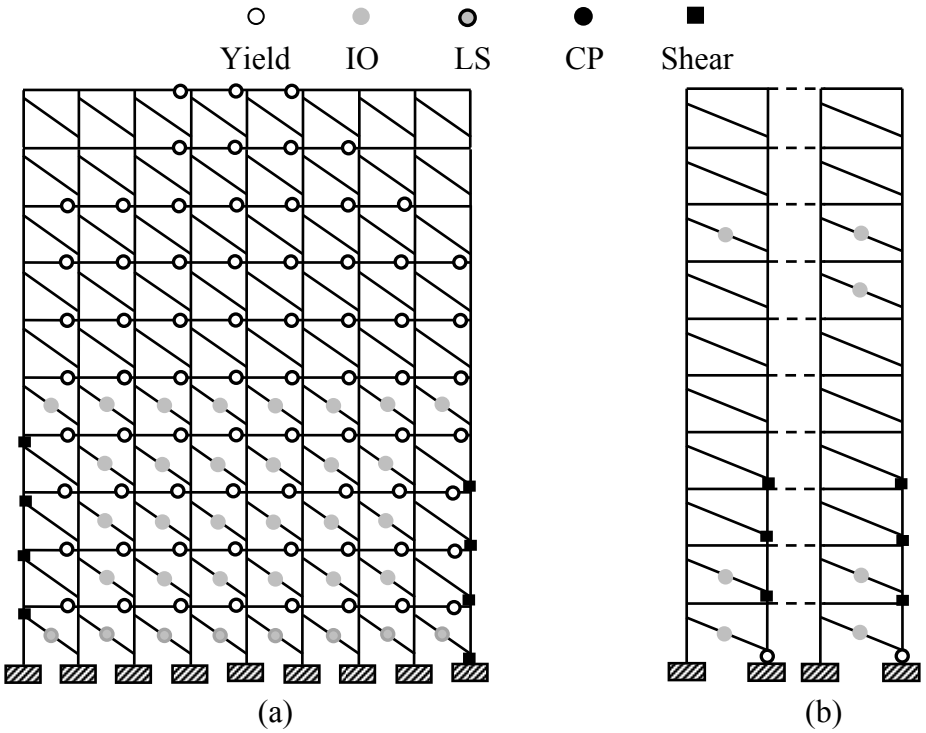

Fig. 4.4 Collapse mechanism of ten storey RC frame building with URM infills, designed for gravity loads only as per relevant Indian Standards: (a) typical longitudinal frame; (b) typical transverse frame.

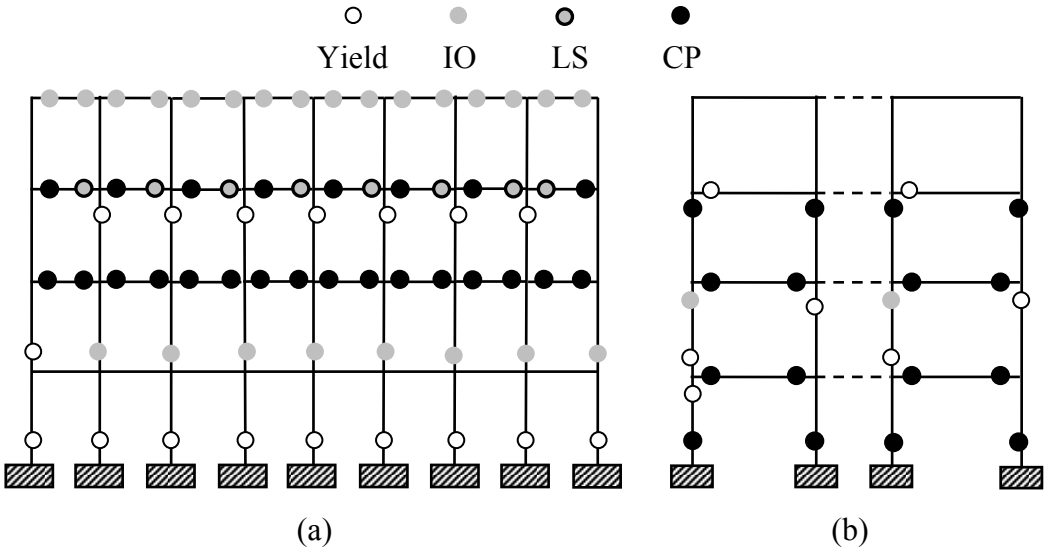

Fig. 4.5 Collapse mechanism of four storey RC bare frame building, designed as SMRF as per relevant Indian Standards: (a) typical longitudinal frame; (b) typical transverse frame.

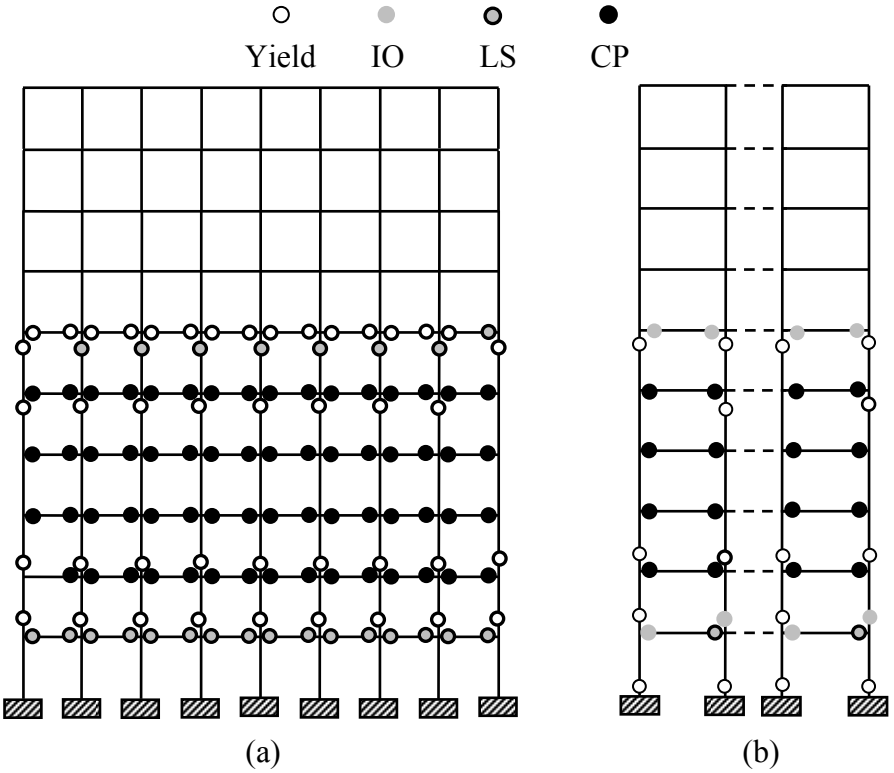

Fig. 4.6 Collapse mechanism of ten storey RC frame building with URM infills, designed as SMRF as per relevant Indian Standards: (a) typical longitudinal frame; (b) typical transverse frame.

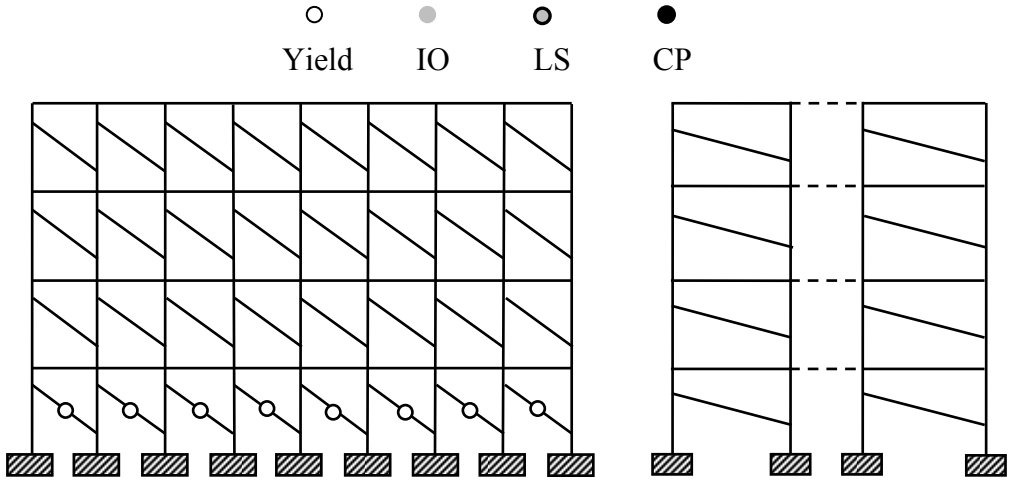

Fig. 4.7 Hinge pattern of four storey RC frame building with URM infills at performance point for DBE, designed as SMRF as per relevant Indian Standards: (a) typical longitudinal frame; (b) typical transverse frame.

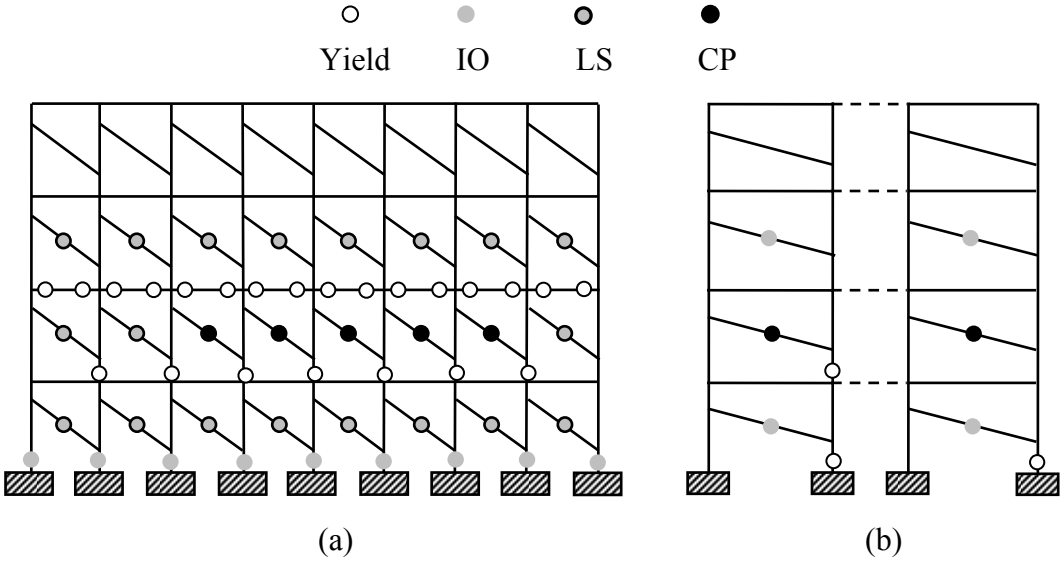

Fig. 4.8 Collapse mechanism of four storey RC frame building with URM infills, designed as SMRF as per relevant Indian Standards: (a) typical longitudinal frame; (b) typical transverse frame.

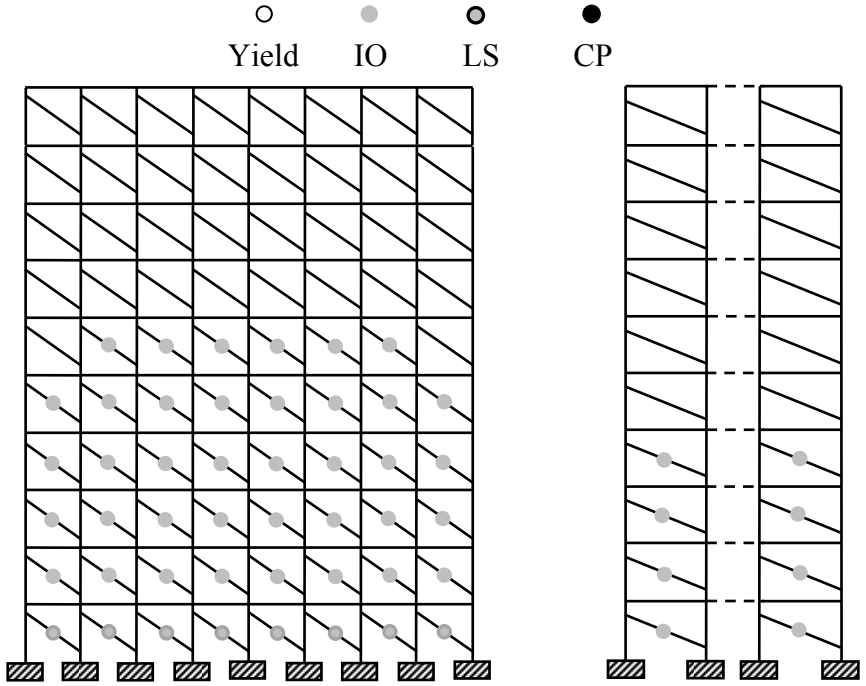

Fig. 4.9 Hinge pattern at performance point under DBE of ten storey RC frame building with URM infills, designed as SMRF as per relevant Indian Standards: (a) typical longitudinal frame; (b) typical transverse frame.

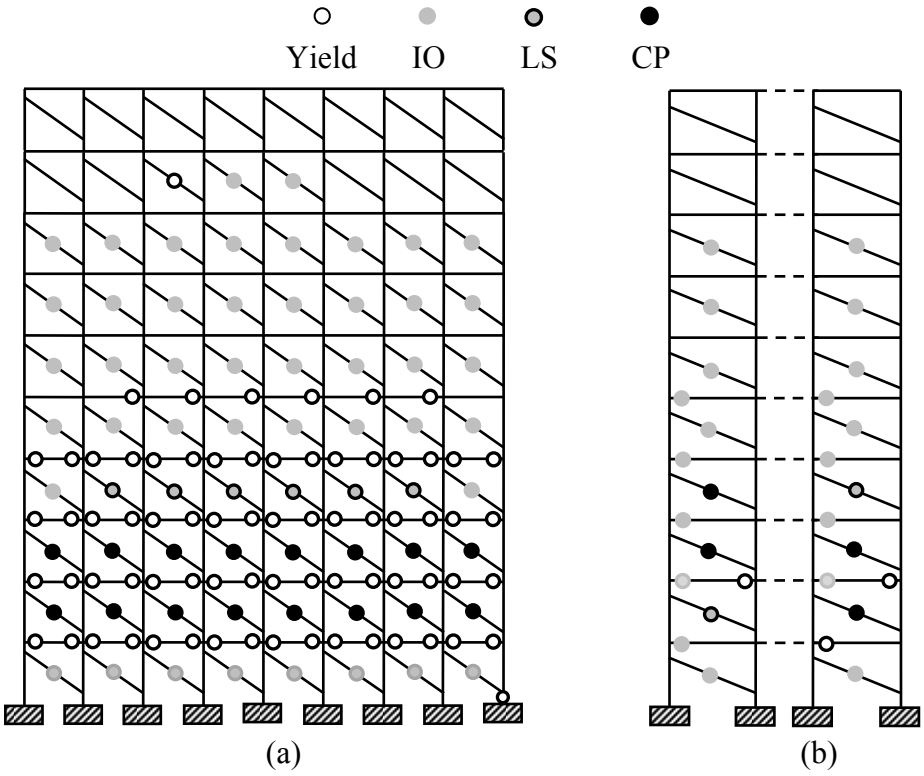

Fig. 4.10 Collapse mechanism of ten storey RC frame building with URM infills, designed as SMRF as per relevant Indian Standards: (a) typical longitudinal frame; (b) typical transverse frame.

Figures 4.5 and 4.6 show the collapse mechanisms of four and ten storey RC bare frame buildings, respectively, designed as SMRF (BIS 1987 (Part 1), 1987 (Part 2), 1993, 2000, 2002). Figs. 4.7 and 4.8 show the hinge patterns at performance point under DBE of Seismic Zone IV (0.12*g* EPGA) and at failure, respectively, of four storey uniformly infilled RC frame buildings designed as SMRF, under the combined action of gravity and lateral loads. Similarly, hinge pattern at performance point under DBE (0.12g PGA) and at failure of ten storey SMRF RC frame buildings with URM infills are presented in Figs. 4.9 and 4.10, respectively.

In case of ten storey SMRF infilled frame building, many of the infill panels in longitudinal direction and all the panels of the bottom four storeys in transverse direction have yielded at 0.12*g* PGA. At failure of four storey building, some of the infill panels in first floor crossed 'CP' performance levels and all (longitudinal direction) or some of the bottom storey columns (transverse direction) have yielded. It has been observed that in case of infilled frames, hinges first occur in infills as these are attracting large forces due to much higher stiffness in comparison to columns. Whereas in case of bare frames, hinges first occur in beams and at further pushing, flexure hinges form in all the first and second floor columns in longitudinal direction and ground storey columns in transverse direction, after formation of hinges in almost all the beams. However, no shear failure of members has been observed because of the ductile detailing of SMRF buildings as per BIS (1993).

Figures 4.11 and 4.12 compare the capacity curves/pushover curves of four and ten storey RC frame buildings, respectively, designed for gravity loads only, as per relevant Indian Standards (BIS 1987 (Part 1), 1987 (Part 2), 2000), with and without infills. Similarly, Figs. 4.13 and 4.14 compare the seismic performance of four and ten storey RC frame buildings designed as SMRF. It is observed from Figs. 4.11-4.14 that infills have very significant effect on capacity curves of both the gravity load designed as well as SMRF buildings. A sharp increase in stiffness and strength accompanied by a drastic reduction in ultimate displacement capacity is observed due to infills, in both longitudinal and transverse directions. It can be noted that there is only a small difference in yield strength of the four storey infilled frame buildings of two design levels (GLD and SMRF) because a major part of the lateral strength is contributed by the infills. It is important to note that in case of gravity load designed infilled frame buildings, the failure is caused by brittle shear failure of columns in

ground storey (Figs. 4.3 and 4.4), hence no (or very little) plastic deformation of the buildings is achieved. The ductility of SMRF buildings is much higher than gravity load designed buildings, due to ductile detailing of reinforcement. However, the inelastic deformation capacity of the SMRF buildings also decreases drastically, due to presence of infills, as compared to its bare frame counterpart. This is because of failure of significant number of infills at very small drift. However, in case of SMRF buildings with uniform infills, the undesired brittle shear failure mode of columns is avoided (Figs. 4.8 and 4.10) due to closely spaced stirrups in ductile detailing of reinforcement. The saw-tooth curve in case of ten storey infilled frame building (Fig. 4.14 (b)) shows the sudden drop in the lateral force due to failure of a set of infills, and quick re-gains in lateral force with displacement, due to high stiffness of the infills.

The Figures also illustrate the effect of seismic design and detailing on the capacity of buildings. The strength capacity of bare SMRF buildings is 2.6 and 8.9 times of the corresponding 4 and 10 storey GLD buildings, respectively. The higher effect in case of taller buildings is expected as earthquake forces become more crucial in design with increasing height. In case of infilled frames, the enhancement in strength is relatively less and equal (2 times) for both 4 and 10 storey buildings, as infills provide the major share in lateral resistance, and the infills are identical in all the buildings. The ductile detailing of reinforcement in case of SMRF buildings results in significant increase in plastic deformation capacity. The plastic deformation in case of bare SMRF buildings is 1.5 and 2.9 times of 4 and 10 storey GLD bare frame buildings, respectively. On the other hand in case of infilled frame buildings, the corresponding increase is up to 12 and 8 times, respectively, as brittle shear failure of columns in infilled frames is avoided due to increased shear strength in case of SMRF buildings.

The Figures also show the performance levels and performance points of the corresponding buildings. The black triangle (▲) represents the performance point for DBE and black dot (●) represents the performance point for MCE corresponding to Seismic Zone IV (BIS 2002); the three crosses (×) represent ‘IO’, ‘LS’ and ‘CP’ performance levels, consecutively. The black square (■) as shown in the capacity curves of GLD RC frames with uniform infills (Figs. 4.11 and 4.12) represents the pushover step at which the column(s) suffer shear failure. The performance levels have been shown according to the acceptance criteria of ASCE-41 (2007) and

performance points have been obtained using the Displacement Modification Method (DMM) of ASCE-41 (2007) described in Section 4.7. It is to be noted that ASCE-41 (2007) specifies performance limits in terms of plastic rotations in individual members. The different performance levels on building pushover curve have been marked by identifying the pushover step, at which first member in the building undergoes the corresponding plastic rotation, specified in ASCE-41 (2007) for the respective performance limit, and noting the roof displacement corresponding to that step. With sufficiently large number of analysis steps, the performance levels can be marked with reasonable accuracy. It is interesting to note that in Seismic Zone IV, the RC bare frame building designed without any consideration for earthquake force can sustain MCE. This means that even if the building is designed and constructed properly for the gravity loads alone, as per the relevant Indian Standards, it has sufficient overstrength and ductility to survive, without collapse, even the MCE level of ground shaking specified by BIS (2002) for Seismic Zone IV. Of course, in case of the buildings designed for seismic effects, the performance is much better and it is observed from the Figs. 4.13 and 4.14 that both the four and ten storey bare SMRF buildings designed for DBE of Zone IV have 'IO' performance for MCE of Zone IV. In case of infilled frame buildings, the performance is deteriorated as compared to the corresponding bare frame buildings. Performance point could not be achieved for the Zone IV, in case of both the GLD buildings with infills, indicating collapse. In case of the 4 storey infilled SMRF building, the estimated performance is 'IO' and 'LS' for DBE and MCE of Zone IV, whereas in case of the 10 storey infilled SMRF building it is 'LS' for DBE as well as MCE.

Table 4.2 summarizes the effect of infills on stiffness and strength of RC frame buildings of different design levels and heights. It is observed that in case of the four storey gravity load designed building, the stiffness of the building increases 29 times and 16 times in the longitudinal and transverse directions, respectively. The strength increases 2.7 times in the longitudinal direction, but no increase in strength is observed in transverse direction, due to brittle shear failure of columns, as shown in Fig. 4.3. Similarly, in case of the ten storey GLD building, the increase in stiffness is 27 times and 13 times, in the longitudinal and transverse directions, respectively, and the increase in strength is 7.3 times in longitudinal directions whereas the strength in transverse direction increases marginally (1.2 times) because of the shear failure of the first second and third floor columns, as shown in Fig. 4.4 (b), at early stage of

lateral loading. In SMRF RC frames, the stiffness and strength of the infilled frame is 35 times and 2.2 times, respectively of the bare frame in the longitudinal direction, and 19 times and 1.6 times, respectively, in the transverse direction, for the four storey building. In case of the ten storey building, these values are 13.4 times and 1.6 times, respectively in longitudinal direction and 9 times and 1.3 times, respectively in the transverse direction.

Table 4.3 summarizes the capacity curve parameters of RC frame buildings with different design levels and heights. The Table also presents the performance points for DBE and MCE of Indian Seismic Zone IV and V. It can be observed from the Table that both four and ten storey RC bare frames as well as uniformly infilled frame buildings designed as SMRF for DBE of Indian Seismic Zone IV survive even MCE of Seismic Zone V excitation. It is also observed that the RC bare frame buildings designed without any consideration for earthquake forces, sustained MCE excitation of Seismic Zone V. However, inclusion of infills deteriorated the performance of RC frames.

4.8 SUMMARY

Using the macro model for simulation of the URM infill panels with initial lack of fit developed in Chapter 2, an analytical study has been carried out on four and ten storey buildings with two design levels to study the effect of infills on the seismic performance of RC frame buildings. It has been observed that infills have drastic effect on capacity curves of the infilled frames and their stiffness and strength has been found to increase up to 35 times and 7.3 times, respectively as compared to the bare frames for the studied buildings and this effect increases with the height of the building. In most of the cases, considered in this study, the RC bare frame buildings designed and constructed properly for the gravity loads alone, have survived the earthquake effects up to those specified for Seismic Zone V. This shows the significant overstregth available in case of code designed buildings. Consideration of earthquake effects in the design, as per BIS (2002), increases the strength and ductility capacities of the buildings significantly and this effect increases with increase of building height. Buildings designed in accordance with the present seismic code requirements for DBE, show ‘LS’ and ‘IO’ level seismic performance for MCE, in case of SMRF RC frame with and without URM infills, respectively. Collapse

mechanism of RC frames changes significantly due to inclusion of infills and the collapse of the gravity load designed infilled frame buildings is caused by brittle shear failure of columns in ground storey, whereas the collapse mechanism of the SMRF infilled frames is governed by flexural yielding of a sizeable number of RC members.

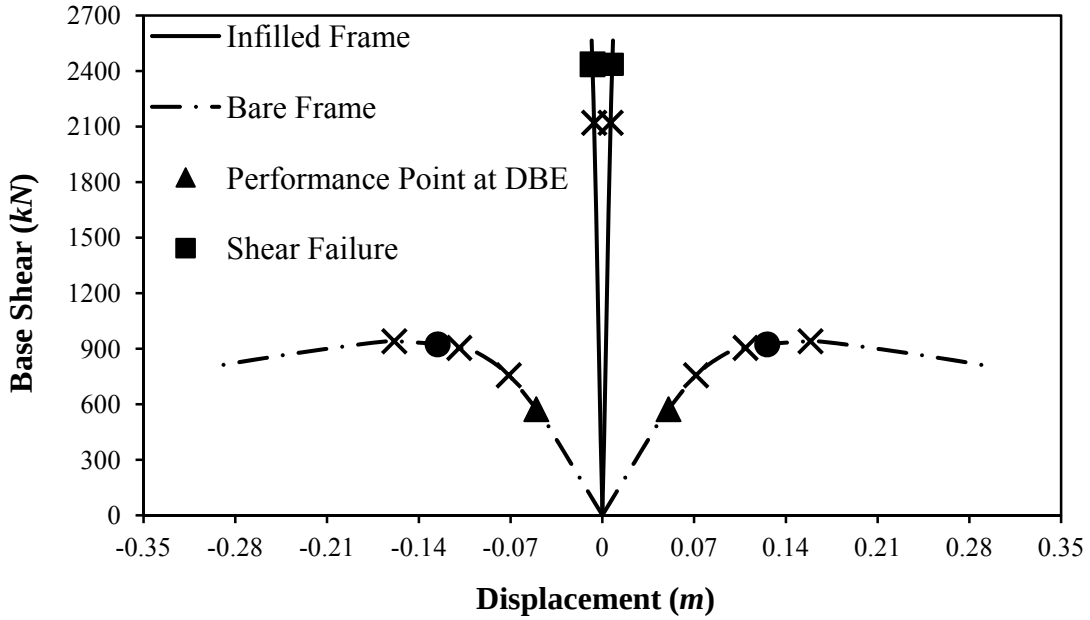

(a)

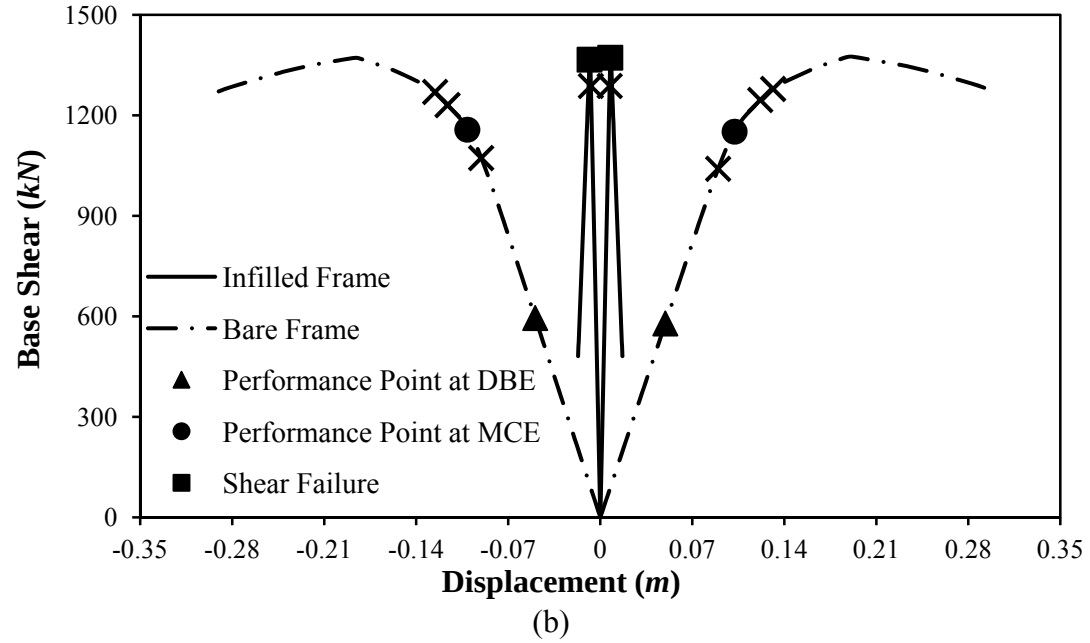

(b)

Fig. 4.11 Comparison of capacity curves and performance points of the four storey RC frame building with and without URM infills, designed for gravity loads only, as per relevant Indian Standards, in: (a) longitudinal direction; (b) transverse direction. The three crosses (×) represent IO, LS, and CP performance levels, consecutively.

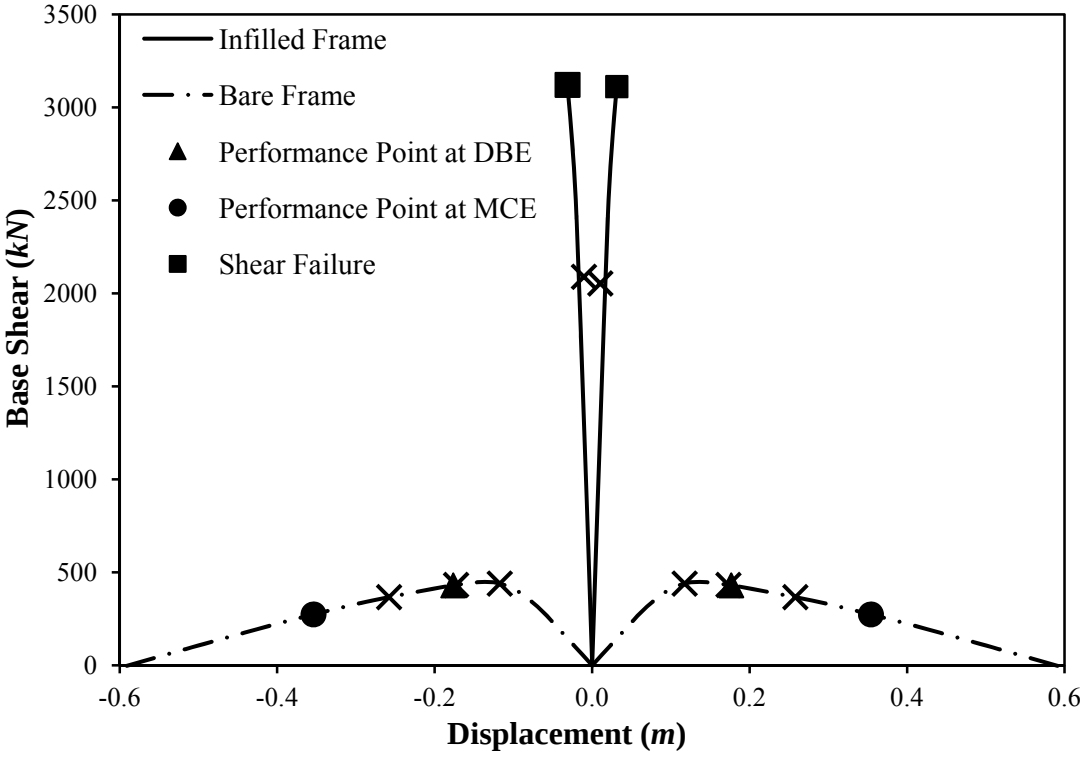

(a)

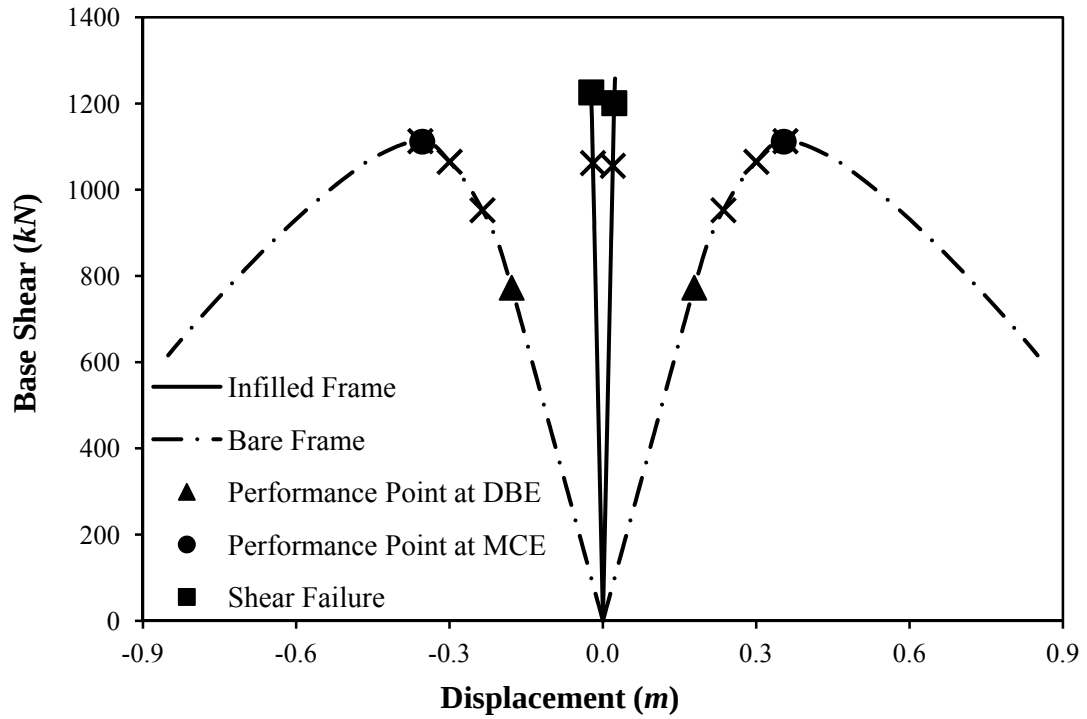

(b)

Fig. 4.12 Comparison of capacity curves and performance points of the ten storey RC frame building with and without URM infills, designed for gravity loads only, as per relevant Indian Standards, in: (a) longitudinal direction; (b) transverse direction. The three crosses (×) represent IO, LS, and CP performance levels, consecutively.

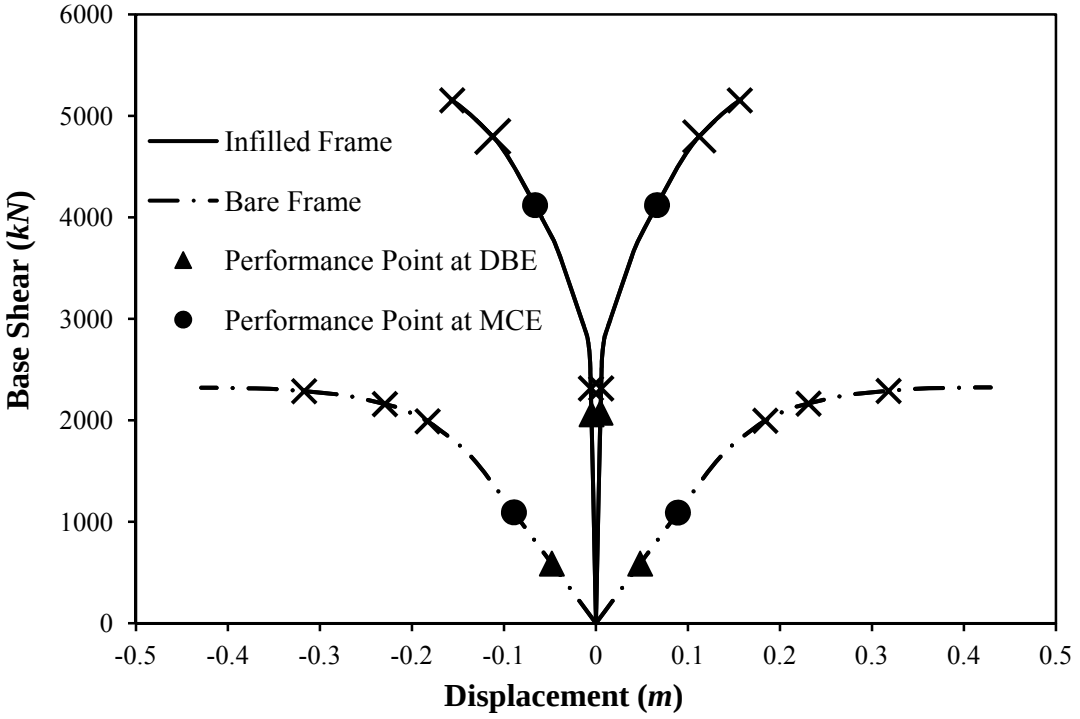

(a)

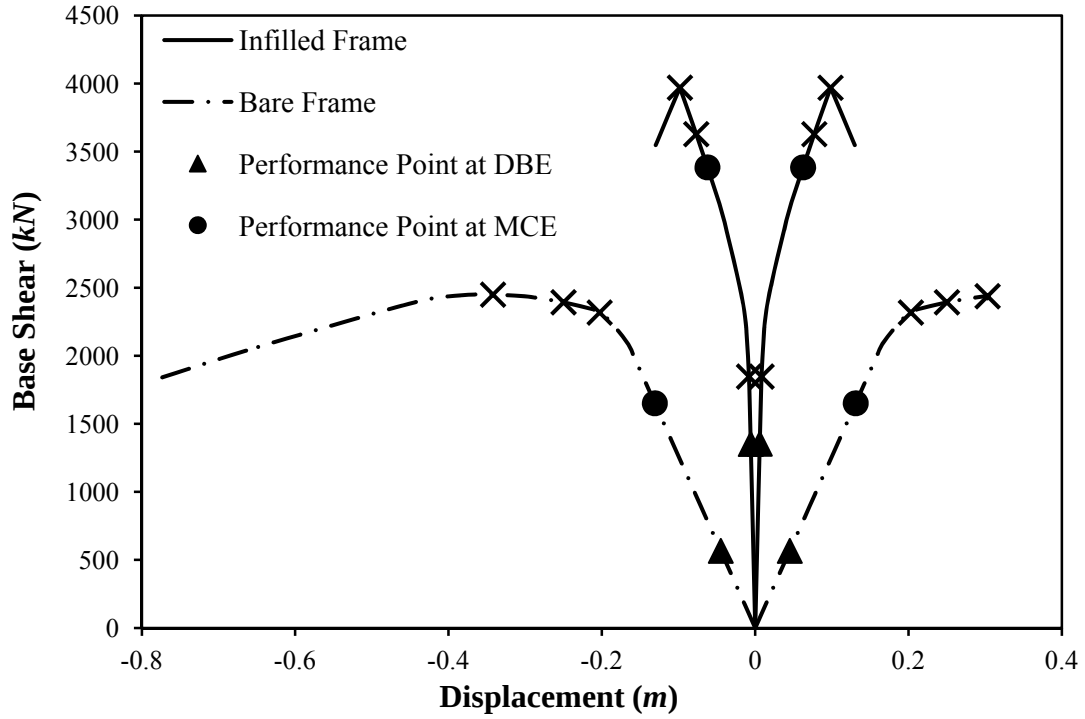

(b)

Fig. 4.13 Comparison of capacity curves and performance points of the four storey RC frame building with and without URM infills, designed as SMRF, as per relevant Indian Standards, in: (a) longitudinal direction; (b) transverse direction. The three crosses (×) represent IO, LS, and CP performance levels, consecutively.

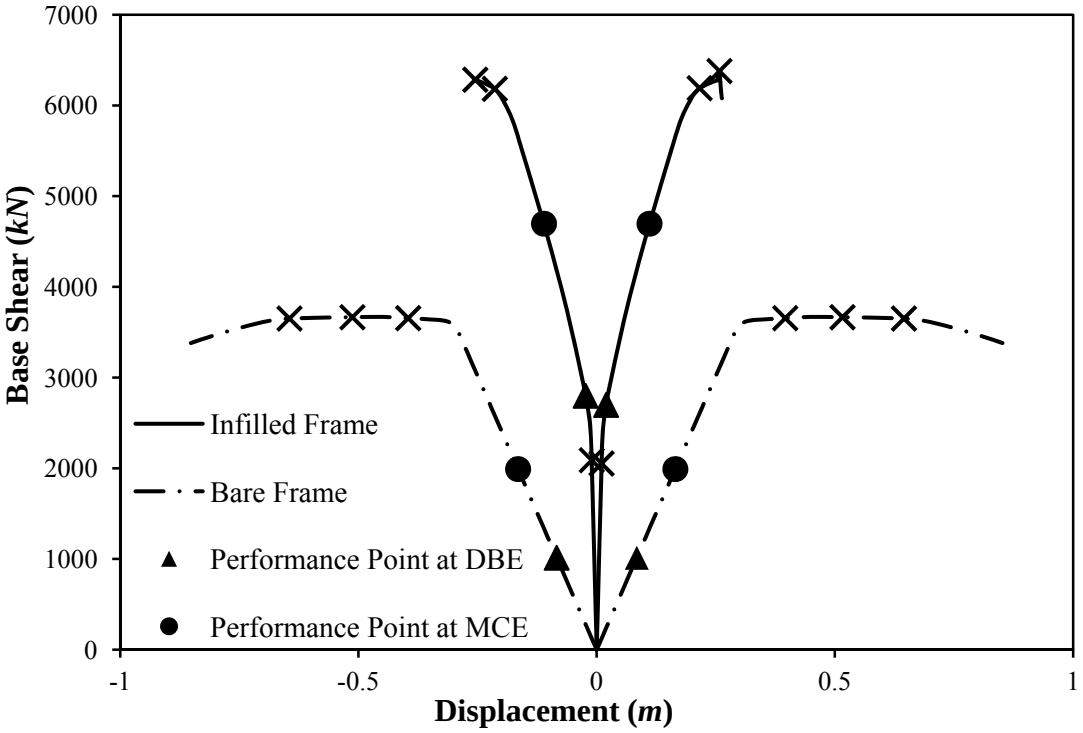

(a)

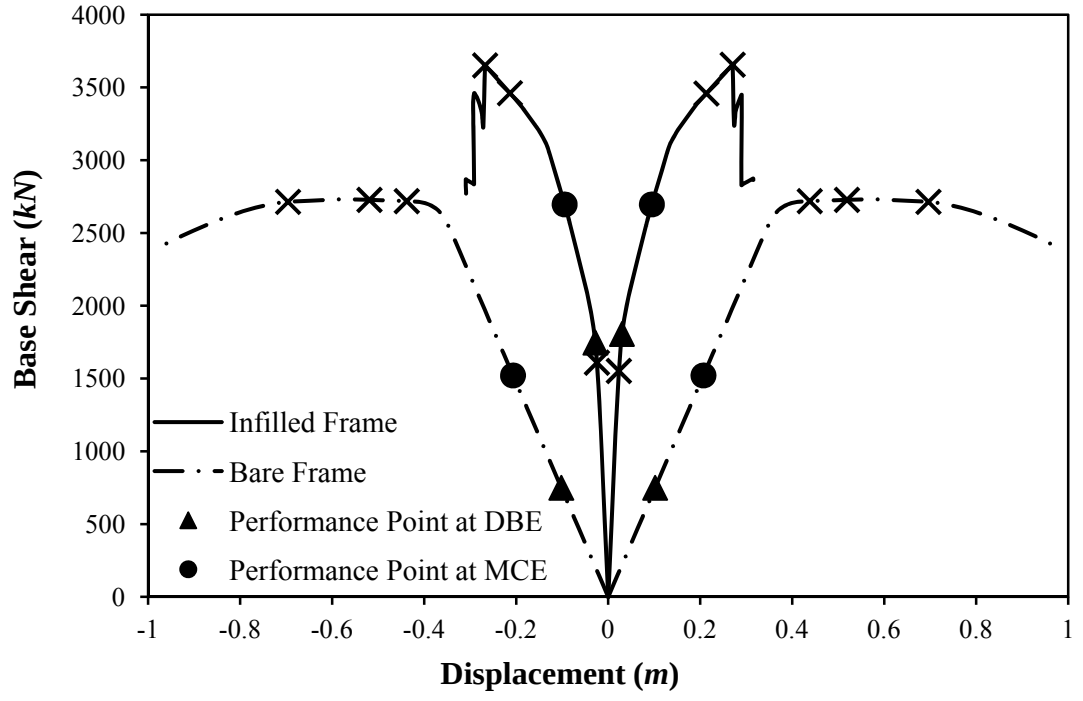

(b)

Fig. 4.14 Comparison of capacity curves and performance points of the ten storey RC frame building with and without URM infills, designed as SMRF, as per relevant Indian Standards, in: (a) longitudinal direction; (b) transverse direction. The three crosses (×) represent IO, LS, and CP performance levels, consecutively.

Table 4.2

Effect of URM infills on strength and stiffness of RC frames

Design Level	Frame Configuration	No. of Storeys	Strength (*kN*)		Stiffness (*kN/m*)	
			Longitudinal	**Transverse**	**Longitudinal**	**Transverse**
Gravity Designed (BIS 1987 (Part 1), 1987 (Part 2), 2000)	Bare	4	895.33	1340.29	11619.46	11696.29
	Infilled		2445.50	1350.86	336908.72	180280.59
Gravity Designed (BIS 1987 (Part 1), 1987 (Part 2), 2000)	Bare	10	404.72	1012.20	4629.30	4338.76
	Infilled		2938.10	1235.20	124321.14	54594.26
SMRF (BIS 1987 (Part 1), 1987 (Part 2), 1993, 2000, 2002)	Bare	4	2323.27	2438.28	12255.48	12605.09
	Infilled		5152.85	3969.80	423153.43	229896.93
SMRF (BIS 1987 (Part 1), 1987 (Part 2), 1993, 2000, 2002)	Bare	10	3611.40	2661.74	12069.58	7352.33
	Infilled		5801.55	3393.06	161296.53	64924.56

Table 4.3

Capacity curve parameters and performance point of RC frame buildings with and without URM infills

Direction	Design Level	No. of Storey	Capacity Curve Parameters				Estimated Spectral Displacement at Performance Point (m)			
			Yield Capacity Point		Ultimate Capacity Point		Zone IV (BIS 2002)		Zone V (BIS 2002)	
							DBE	MCE	DBE	MCE
			D_y/H	V_y/W	D_u/H	V_u/W	0.12 (g)	0.24 (g)	0.18 (g)	0.36 (g)
Longitudinal	Gravity designed RC frame buildings without infills	4	0.006	0.061	0.022	0.063	0.050	0.126	0.075	0.150
		10	0.003	0.010	0.009	0.010	0.160	0.319	0.239	0.479
	Gravity designed RC frame buildings with uniformly placed URM infills	4	0.001	0.163	0.001	0.166	0.008	0.020	0.011	0.021
		10	0.001	0.070	0.001	0.073	0.035	0.069	0.052	0.104
	RC frame buildings designed as SMRF without infills	4	0.013	0.147	0.033	0.162	0.048	0.097	0.072	0.145
		10	0.009	0.084	0.026	0.084	0.083	0.166	0.124	0.249
	RC frame buildings designed as SMRF with uniformly placed URM infills	4	0.001	0.233	0.012	0.359	0.005	0.064	0.008	0.096
		10	0.001	0.100	0.008	0.135	0.020	0.107	0.080	0.161
Transverse	Gravity designed RC frame buildings without infills	4	0.008	0.091	0.023	0.094	0.049	0.099	0.074	0.148
		10	0.007	0.026	0.021	0.026	0.167	0.335	0.251	0.502
	Gravity designed RC frame buildings with uniformly placed URM infills	4	0.001	0.084	0.001	0.084	0.012	0.024	0.018	0.035
		10	0.008	0.091	0.023	0.094	0.053	0.101	0.080	0.160
	RC frame buildings designed as SMRF without infills	4	0.014	0.159	0.023	0.170	0.045	0.121	0.067	0.182
		10	0.011	0.062	0.029	0.062	0.103	0.206	0.154	0.309
	RC frame buildings designed as SMRF with uniformly placed URM infills	4	0.001	0.169	0.007	0.277	0.006	0.062	0.009	0.093
		10	0.001	0.064	0.010	0.079	0.028	0.093	0.070	0.140

Shaded cells show that performance point could not be achieved, i.e. building is expected to collapse.

where, D_y, D_u are yield and ultimate displacement, respectively; V_y and V_u are base shear corresponding to yield and ultimate displacement and H is height of the building

Chapter 5

SEISMIC PERFORMANCE OF BUILDINGS WITH IRREGULARLY PLACED INFILLS

5.1 INTRODUCTION

As discussed in the previous Chapter, URM infills are capable of drastically changing the behavior and performance of RC frame buildings. The behavior is further affected by the irregular placement of infills for creating space for parking or commercial purposes. The field study in the National Capital Region (DEQ 2009), presented in Chapter 3, revealed that 95% of URM infilled RC frame buildings have open ground storey (without partitions) and as many as 62% buildings have torsion irregularity. In the study presented in this Chapter, behavior and seismic performance of buildings having irregular infill placement in plan and elevation is studied. For this purpose, the selected representative buildings shown in Fig. 2.5 are considered with different infill configurations. Three most common configurations of RC frames with irregular placement of infills, viz. open ground storey, front bay open in the ground storey and three bays open in the ground storey, as identified in Chapter 3, have been considered.

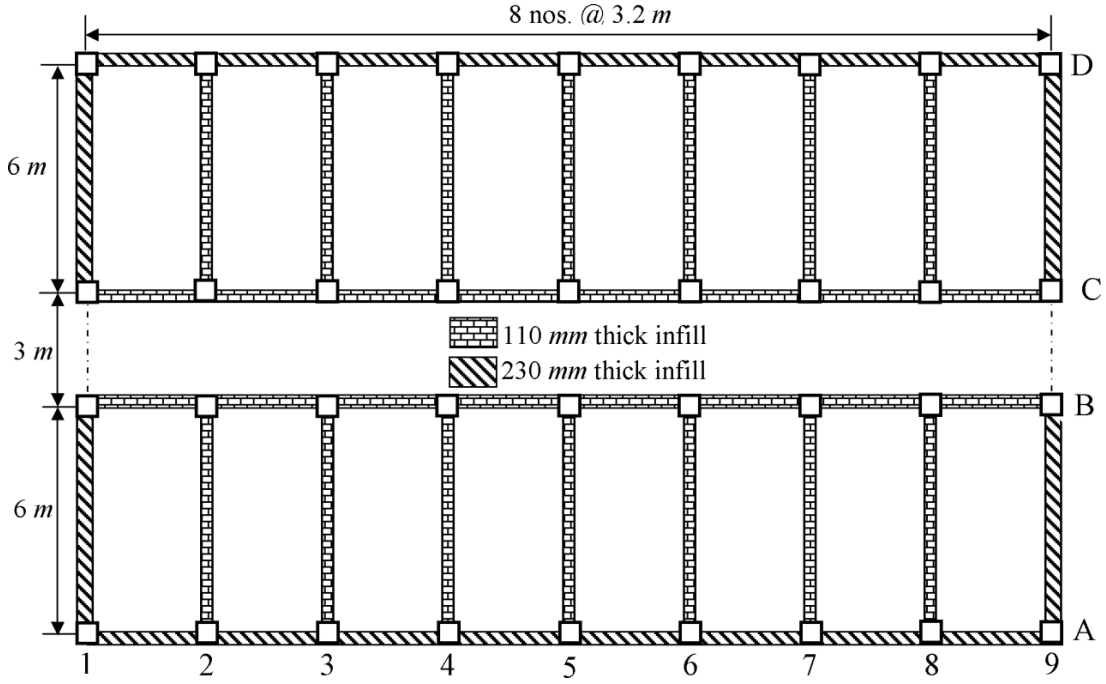

(a)

Fig. 5.1 (contd.)

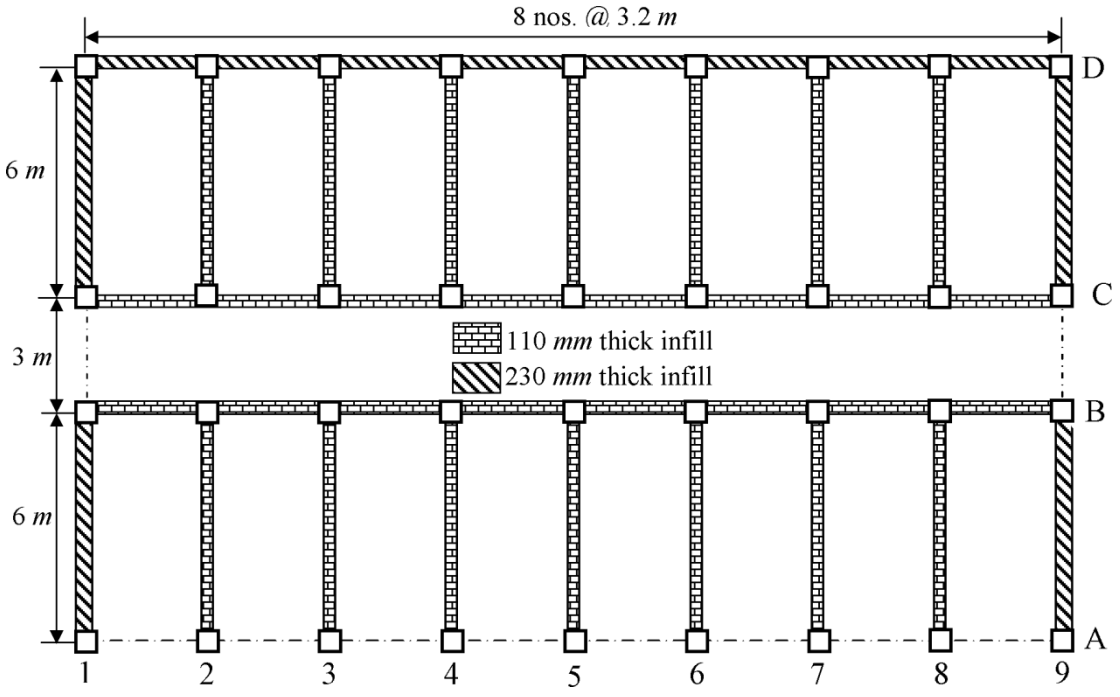

(b)

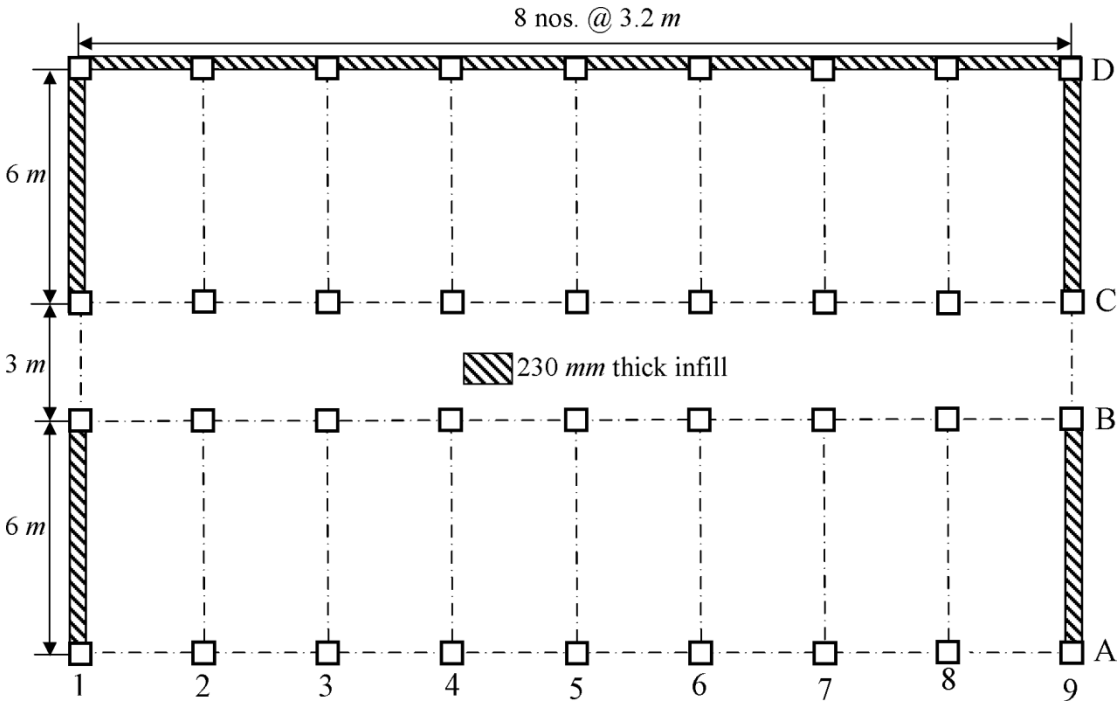

(c)

Fig. 5.1 Ground floor plan of the RC frame buildings with: (a) uniform infills; (b) front bay open in the ground storey; (c) three bays open in the ground storey.

All possible failure modes of infill panels and surrounding frame members identified in Chapter 3 have been considered for this purpose. Figure 5.1 shows the ground level plan of the uniformly infilled RC frame buildings and two other configurations,

considered for detailed study in this Thesis. The plan of the considered open ground storey is also similar to that shown in the Fig. 5.1, but without any infills in the ground storey.

5.2 DYNAMIC CHARACTERISTICS

A comparison of the dynamic characteristics of the buildings without infills, with uniform infills, and with irregularly placed infill panels has been presented in Tables 5.1 - 5.5. Table 5.1 shows the effect of infills and its placement on the period of vibration of RC frames. It has been observed that period get reduced tremendously due to inclusion of infills in the frame buildings. Table 5.1 also compares the periods obtained from analysis and from code provisions for approximate (empirical) design periods of bare and uniformly infilled frame buildings. However, the code does not provide empirical relationships for estimation of periods in case of buildings with irregularly placed infills, and therefore the expression for uniformly infilled frames has been considered for design. It shows that code (BIS 2002) expressions result in even smaller periods than those obtained from the analysis, duly considering the effect of infills. Further, the code specifies that the design base shear should not be smaller than that obtained from the empirical expressions. This, results in increased base shear for the building and consequently larger cross-sectional areas of frame elements are required. Modal mass participation factors for four and ten storey gravity load designed buildings are presented in Tables 5.2 and 5.3, respectively. Similarly, Tables 5.4 and 5.5 present modal mass participation factors for the four and ten storey SMRF buildings, respectively. It has been observed from Tables 5.2-5.5 that mass participation in fundamental mode is highest in case of open ground storey buildings, which has most of the deformation concentrated in the flexible ground storey, whereas the upper storeys move more or less like a rigid body. Further, the fundamental modal mass participation is more that 75% for all design levels and heights of buildings. According to FEMA-273 (1997), FEMA-356 (2000), FEMA-440 (2006), and ATC-40 (1996), the static analysis is considered to be adequate if the contribution of the first mode is more than 75%; whereas a dynamic analysis is necessary when the contribution of higher modes is more significant or the structure has torsional irregularities. Several different criteria exist in different seismic building codes to designate a building as torsonally irregular.

Table 5.1

Effect of infills and their placement on the period of vibration of RC frame buildings

Design Level	No. of Storey	Fundamental Period (*sec*) (From Analysis)		Design Period (*sec*) (From BIS (2002))	
		Longitudinal	Transverse	Longitudinal	Transverse
Gravity designed RC frame buildings without infills	4	1.68	1.66	0.52	
	10	4.04	4.14	1.03	
RC frame buildings without infills, designed as SMRF	4	1.62	1.50	0.52	
	10	2.78	3.45	1.03	
Gravity designed RC frame buildings with uniform URM infills	4	0.31	0.34	0.24	0.31
	10	0.80	1.03	0.59	0.77
RC frame buildings designed as SMRF with uniform URM infills	4	0.27	0.29	0.24	0.31
	10	0.65	0.93	0.59	0.77
Gravity designed RC frame buildings with open ground storey	4	0.89	0.90	0.24	0.31
	10	1.23	1.43	0.59	0.77
RC frame buildings designed as SMRF with open ground storey without any consideration of relevant provisions of Indian Standard (BIS 2002)	4	0.81	0.72	0.24	0.31
	10	0.99	1.20	0.59	0.77
RC frame buildings designed as SMRF with open ground storey designed and detailed as per Indian Standard (BIS 2002)	4	0.47	0.48	0.24	0.31
	10	0.62	0.87	0.59	0.77
Gravity designed RC frame buildings with front bay open in ground storey	4	0.33	0.34	0.24	0.31
	10	0.83	1.04	0.59	0.77
RC frame buildings designed as SMRF with front bay open in ground storey	4	0.29	0.30	0.24	0.31
	10	0.65	0.93	0.59	0.77
Gravity designed RC frame buildings with three bays open in ground storey	4	0.45	0.43	0.24	0.31
	10	0.93	1.11	0.59	0.77
RC frame buildings designed as SMRF with three bays open in ground storey	4	0.39	0.38	0.24	0.31
	10	0.75	0.99	0.59	0.77

Table 5.2

Modal mass participation factors (%) for four storey gravity load designed bare frame and frame with uniform and irregularly placed infills

Mode	Bare Frame		Uniform Infills		Open Ground Storey		Open Front Bay		Open Three Bays	
	Longitudinal	Transverse	Longitudinal	Transverse	Longitudinal	Transverse	Longitudinal	Transverse	Longitudinal	Transverse
1	83.2	0.0	0.0	82.7	0.0	99.5	0.0	82.7	74.5	0.0
2	0.0	83.3	84.2	0.0	99.6	0.0	68.9	0.0	0.0	93.8
3	0.0	0.0	0.0	0.0	0.0	0.0	18.6	0.0	19.6	0.0
4	11.3	0.0	0.0	11.6	0.0	0.4	0.0	11.6	0.0	5.1
5	0.0	11.3	10.0	0.0	0.3	0.0	6.4	0.0	2.4	0.0
6	0.0	0.0	0.0	0.0	0.0	0.0	2.2	0.0	2.0	0.0
7	4.2	0.0	0.0	0.9	0.0	0.1	0.0	0.1	0.0	0.5
8	0.0	4.2	0.0	0.0	0.1	0.0	0.0	0.2	0.0	0.0
9	0.0	0.0	0.2	0.0	0.0	0.0	0.1	0.0	0.0	0.1
10	1.3	0.0	0.0	0.0	0.0	0.0	0.0	0.0	0.1	0.0
11	0.0	1.3	0.0	2.2	0.0	0.0	0.0	2.5	0.0	0.0
12	0.0	0.0	0.0	0.0	0.0	0.0	1.4	0.0	0.3	0.0

Table 5.3

Modal mass participation factors (%) for ten storey gravity load designed bare frame and frame with uniform and irregularly placed infills

Mode	Bare Frame		Uniform Infilled		Open Ground Storey		Open Front Bay		Open Three Bays	
	Longitudinal	Transverse	Longitudinal	Transverse	Longitudinal	Transverse	Longitudinal	Transverse	Longitudinal	Transverse
1	0.0	81.9	0.0	79.6	0.0	93.5	0.0	79.7	0.0	80.2
2	83.2	0.0	80.1	0.0	97.2	0.0	63.8	0.0	69.0	0.0
3	0.0	0.0	0.0	0.0	0.0	0.0	17.1	0.0	17.9	0.0
4	0.0	10.6	0.0	16.7	0.0	6.0	0.0	16.7	0.0	15.8
5	10.4	0.0	11.8	0.0	2.4	0.0	9.5	0.0	6.8	0.0
6	0.0	0.0	0.0	0.0	0.0	0.0	2.1	0.0	2.6	0.0
7	0.0	4.0	0.0	4.0	0.0	0.4	0.0	4.0	0.0	2.4
8	3.9	0.0	3.4	0.0	0.2	0.0	2.9	0.0	1.4	0.0
9	0.0	0.0	0.0	0.0	0.0	0.0	0.4	0.0	0.6	0.0
10	0.0	2.3	0.0	0.0	0.0	0.0	0.0	0.0	0.0	0.0
11	2.3	0.0	0.0	0.0	0.0	0.0	0.0	0.0	0.0	0.0
12	0.0	0.0	0.4	0.0	0.0	0.1	0.2	0.0	0.1	0.0

Table 5.4

Modal mass participation factors (%) for four storey bare frame and frame with uniform and irregularly placed infills, designed as SMRF as per relevant Indian Standards

Mode	Bare Frame		Uniform Infilled		Open Ground Storey		Open Ground Storey as per BIS (2002)		Open Front Bay		Open Three Bays	
	Longitudinal	Transverse	Longitudinal	Transverse	Longitudinal	Transverse	Longitudinal	Transverse	Longitudinal	Transverse	Longitudinal	Transverse
1	81.3	0.0	81.8	0.0	99.4	0.0	0.0	99.8	0.0	80.7	73.6	0.0
2	0.0	81.4	0.0	69.2	0.0	99.9	98.4	0.0	65.4	0.0	0.0	92.4
3	0.0	0.0	0.0	0.0	0.0	0.0	0.0	0.0	19.9	0.0	19.3	0.0
4	11.6	0.0	10.0	0.0	0.4	0.0	1.4	0.0	0.0	11.8	0.0	6.1
5	0.0	11.6	0.0	4.5	0.0	0.0	0.0	0.1	6.9	0.0	2.9	0.0
6	0.0	0.0	0.0	0.0	0.0	0.0	0.0	0.0	2.2	0.0	2.1	0.0
7	4.9	0.0	0.0	0.0	0.1	0.0	0.1	0.0	0.0	0.1	0.0	0.9
8	0.0	4.8	0.2	0.0	0.0	0.0	0.0	0.0	0.0	0.2	0.0	0.0
9	0.0	0.0	0.0	15.4	0.0	0.0	0.0	0.0	0.2	0.0	0.4	0.0
10	2.2	0.0	0.0	0.0	0.0	0.0	0.0	0.0	0.0	0.0	0.0	0.1
11	0.0	2.1	0.0	4.6	0.0	0.0	0.0	0.0	0.0	3.4	0.0	0.0
12	0.0	0.0	0.0	0.0	0.0	0.0	0.0	0.0	0.0	0.1	0.4	0.0

Table 5.5

Modal mass participation factors (%) for ten storey bare frame and frame with uniform and irregularly placed infills, designed as SMRF as per relevant Indian Standards

Mode	Bare Frame		Uniform Infilled		Open Ground Storey		Open Ground Storey as per BIS (2002)		Open Front Bay		Open Three Bays	
	Longitudinal	Transverse	Longitudinal	Transverse	Longitudinal	Transverse	Longitudinal	Transverse	Longitudinal	Transverse	Longitudinal	Transverse
1	0.0	80.1	0.0	80.5	0.0	91.0	0.0	81.0	0.0	80.5	0.0	78.7
2	0.0	0.0	0.0	0.0	96.4	0.0	0.0	0.0	38.9	0.0	57.1	0.0
3	78.8	0.0	77.9	0.0	0.0	0.0	75.9	0.0	41.3	0.0	28.4	0.0
4	0.0	11.0	0.0	17.5	0.0	8.2	0.0	18.8	0.0	17.5	0.0	16.8
5	0.0	0.0	0.0	0.0	0.0	0.0	0.0	0.0	5.9	0.0	5.7	0.0
6	11.2	0.0	12.9	0.0	3.1	0.0	14.1	0.0	6.6	0.0	4.7	0.0
7	0.0	3.9	0.0	2.0	0.0	0.5	0.0	5.3	0.0	4.0	0.0	2.6
8	0.0	0.0	0.0	0.0	0.0	0.0	0.0	0.0	1.5	0.0	0.9	0.0
9	3.6	0.0	0.0	0.0	0.3	0.0	4.7	0.0	0.0	0.0	0.0	0.0
10	0.0	2.4	0.0	0.0	0.0	0.0	0.0	0.0	0.0	0.0	0.0	0.0
11	0.0	0.0	2.9	0.0	0.0	0.0	0.0	0.0	1.3	0.0	1.1	0.0
12	2.4	0.0	0.0	0.0	0.0	0.1	0.0	2.5	0.1	0.0	0.1	0.0

An overview of criteria for torsion irregularity laid down in some of the seismic building codes viz. BIS (2002), Eurocode-8 (2004), ASCE-7 (2006) and NZS-1170.5 (2004), is presented in Table 5.6

Table 5.6

Criteria for torsion irregularity in buildings, according to different seismic building codes

Reference	Criteria for torsion irregularity
BIS (2002)	$\delta_{\max} > 1.2\delta_{avg}$
Eurocode-8 (2004)	$e > 0.3r$ and $r < L_s$
NZS-1170.5 (2004)	$\delta_{\max} > 1.4\delta_{avg}$
ASCE-7 (2006)	$\delta_{\max} > 1.2\delta_{avg}$ when building is torsionally irregular $\delta_{\max} > 1.4\delta_{avg}$ when building is extreme torsionally irregular

where, e is static eccentricity, r is torsional radius, L_s is radius of gyration of the floor in plan, δ_{max} and δ_{avg} are the maximum storey drift and the average of the storey drifts, respectively, at the extreme points of the structure at any floor level.

Due to torsion, the displacement and member forces in some components of building increase over those caused by the translational deformation alone. To take into account the torsional effects arising due to irregular placement of infills/partitions, different seismic building codes specify different provisions. BIS (2002), Eurocode-8 (2004), NZS-1170.5 (2004), and ASCE-7 (2006) consider the effect of torsion by introducing a design eccentricity (e_d) which consists of the the static eccentricity (e_s) due to non coincidence of centre of mass and centre of stiffness, and an accidental eccentricity (e_a). Table 5.7 summerizes the design eccentricity (e_d) requirements of different seismic building codes. It can be observed from Table 5.7 that the accidental eccentricity (e_a) is considered as 5% of the plan dimension (b) of the building perpendicular to the direction of ground motion in all the considered seismic building codes, except NZS-1170.5 (2004), which requires to design for higher accidental eccentricity ($0.1b$). BIS (2002) recommends for dynamic analysis of torsionally irregular buildings situated in Seismic Zone IV and V with height $12m$ and more.

Table 5.7

Consideration of torsional effect in different seismic building codes

Reference	Design eccentricity
BIS (2002), Eurocode-8 (2004), and ASCE-7 (2006)	$e_d = 1.5e + 0.05b$ or $e_d = e - 0.05b$
NZS-1170.5 (2004)	$e_d = 1.5e + 0.1b$ or $e_d = e - 0.1b$

It can be observed from Table 5.6 that the controlling criterion for torsion irregularity in various codes is governed by ratio of maximum to average storey drift ($\delta_{max}/\ \delta_{avg}$) or the ratio of static eccentricity to torsional radius (e/r). The study by Kumar (2010) shows that the ratio $\delta_{max}/\ \delta_{avg}$ can be related to the ratio e/r and he provided a simple formulation for relationship between the two parameters and showed that the criteria of different codes are comparable. Due to simplicity in estimation of e/r, in the present study, the torsion irregularity criteria of Eurocode-8 (2004) is considered. Static eccentricity e is described as the distance between the centre of stiffness and centre of mass. The coordinates of center of stiffness and center of mass can be obtained as

$$X_r = \frac{\sum_i K_{yi} x_i}{\sum_i K_{yi}} \tag{5.1}$$

$$Y_r = \frac{\sum_i K_{xi} y_i}{\sum_i K_{xi}} \tag{5.2}$$

$$X_m = \frac{\sum_i W_i x_i}{\sum_i W_i} \tag{5.3}$$

$$Y_m = \frac{\sum_i W_i y_i}{\sum_i W_i} \tag{5.4}$$

where, K_{xi} and K_{yi} are stiffness of i^{th} lateral load resisting frame/element, along longitudinal and transverse directions, respectively, and W_i is weight lumped at i^{th}

element, and x_i and y_i are the coordinates of the centre of the i^{th} load resisting frame/element along longitudinal and transverse directions, respectively.

Torsional radius along longitudinal direction (r_x) and transverse direction (r_y) at each floor level has been obtained as follows:

$$r_x = \frac{\sqrt{\sum(K_{xi}\bar{y}^2) + \sum(K_{yi}\bar{x}^2)}}{\sqrt{\sum(K_{yi})}} \tag{5.5}$$

$$r_y = \frac{\sqrt{\sum(K_{xi}\bar{y}^2) + \sum(K_{yi}\bar{x}^2)}}{\sqrt{\sum(K_{xi})}} \tag{5.6}$$

where, $\bar{x}_i$ and $\bar{y}_i$ are distances of the i^{th} load resisting element from the centre of stiffness, in each storey along longitudinal and transverse directions, respectively.

In order to estimate the stiffness of the individual lateral load resisting elements, pushover analysis of the individual frames in each direction of the buildings with irregular infills has been carried out using a uniform load distribution along the height, in case of frames with open ground storey, and a linear distribution in case of uniformly infilled frames. Typical capacity curves of individual frames for four and ten storey RC frames with uniform and irregular infills in ground storey are shown in Figs. 5.2 and 5.3. The pushover curves are idealized as bilinear curves as per FEMA-356 (2000) for assessment of stiffness and yield strength for estimating torsional irregularity.

Table 5.8 provides the eccentricities, estimated using Eqs. 5.1- 5.6, in the three configurations of the RC frame buildings with irregular infills. The shaded values in Table 5.8 show that the eccentricity ratio (*e/r*) is higher than 0.3 and the building has been considered as torsionally irregular (Eurocode-8 2004).

5.3 SEISMIC PERFORMANCE OF RC FRAME BUILDINGS WITH IRREGULARLY PLACED INFILLS

Nonlinear Static Pushover analysis has been performed to study the effect of irregular placement of infills on the seismic performance of infilled RC frame buildings. In case of the buildings with three bays open in the ground storey, resulting in torsional

irregularity (Table 5.8), Incremental Dynamic Analysis (IDA) has also been performed, as discussed in the next section (Section 5.4).

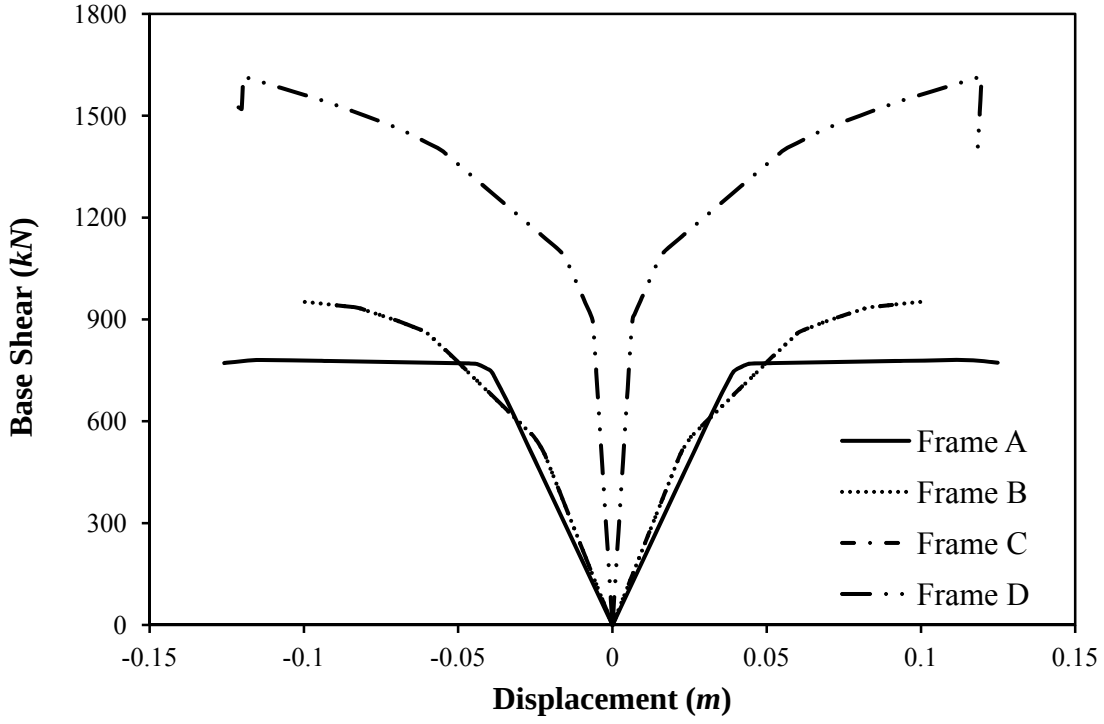

(a)

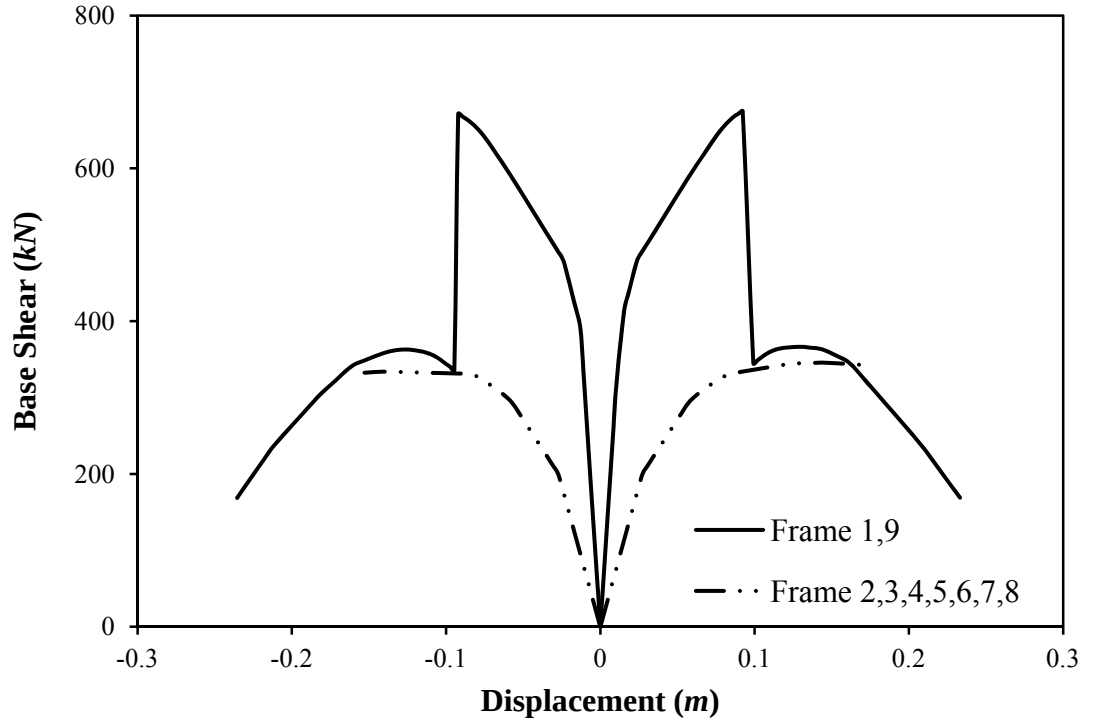

(b)

Fig. 5.2 Capacity curves of individual frames in the four storey RC frame building: (a) longitudinal direction; (b) transverse direction.

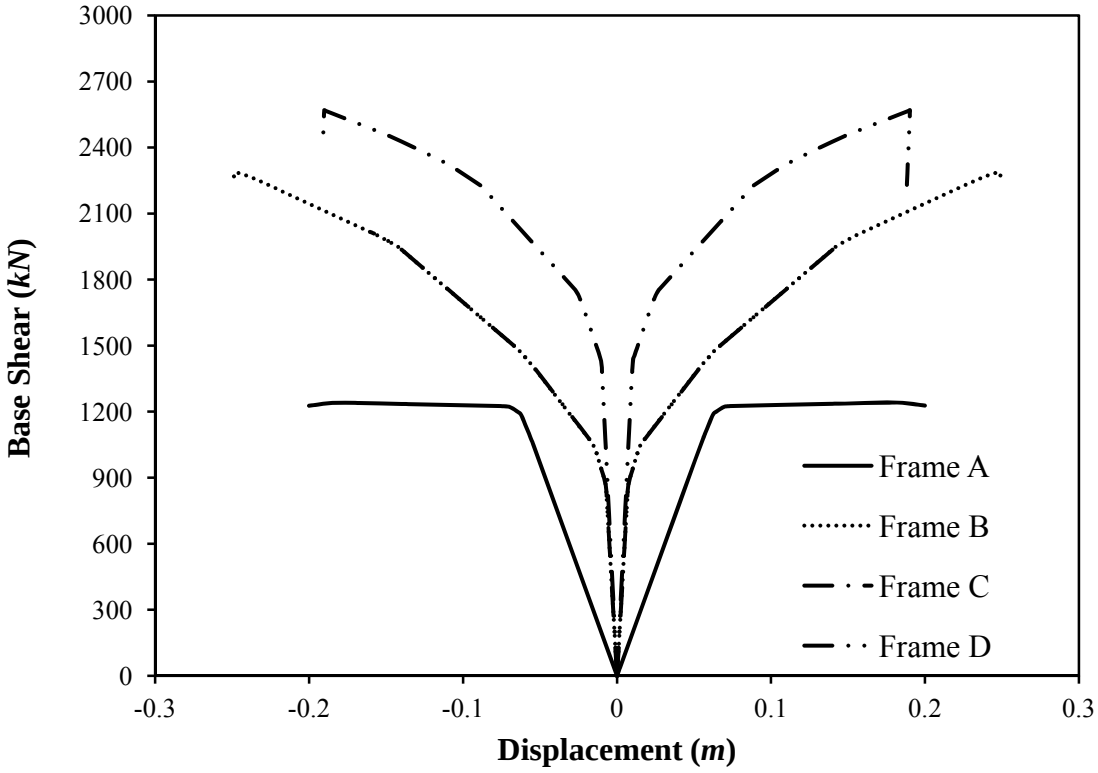

(a)

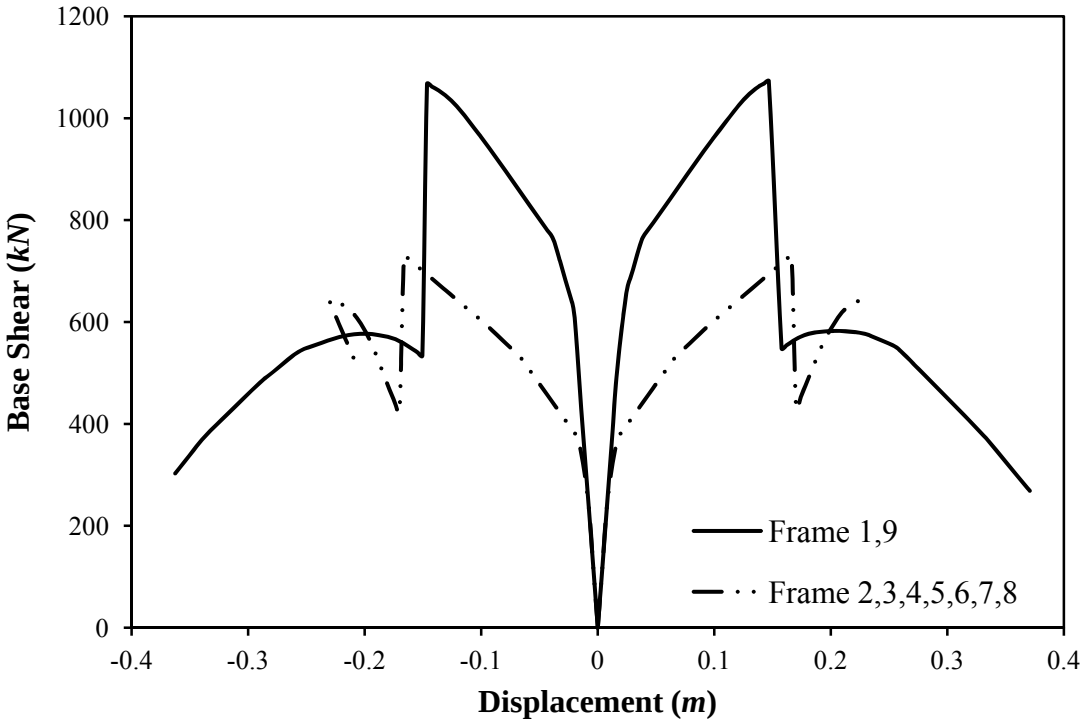

(b)

Fig. 5.3 Capacity curves of individual frames in the ten storey RC frame building: (a) longitudinal direction; (b) transverse direction.

Table 5.8

Torsional irregularity parameters of buildings with irregularly placed infills

Configuration	No. of Storey	X_r	Y_r	X_m	Y_m	r_x	r_y	e/r_x	e/r_y
URM infilled RC frame buildings with open ground storey	4	11.05	12.8	7.5	12.8	18.09	12.42	0	0.20
	10	8.29	12.8	7.5	12.8	8.14	17.27	0	0.10
URM infilled RC frame buildings with front bay open in ground storey	4	9.78	12.8	7.5	12.8	8.07	20.01	0	0.28
	10	9.32	12.8	7.5	12.8	7.93	16.1	0	0.23
URM infilled RC frame buildings with three bays open in ground storey	4	11.94	12.8	7.5	12.8	9.12	12.36	0	0.49
	10	14.21	12.8	7.5	12.8	12.47	12.74	0	0.54

Shaded cells represent torsionally irregular buildings (Eurocode-8 2004)

Figures 5.4 and 5.5 compare the capacity/pushover curves of the four and ten storey RC frame buildings, respectively, with uniform infills (UI), and infilled frame buildings with open ground storey (OG), designed for gravity loads only as per relevant Indian Standards (BIS 1987 (Part 1), 1987 (Part 2), 2000). The figures indicate that OG buildings are flexible and have some ductility as the columns of the ground storey govern the failure mode, whereas in case of uniformly infilled frames, the columns fail in shear resulting in brittle failure. In some cases, the OG buildings also suffer shear failure of upper storey columns, particularly in transverse direction, as shown in Figs. 5.6 and 5.7, due to larger shear force exerted by the infill panels of higher aspect ratio (*l*/*h*).

Taking a note of the widespread failure of open ground storey buildings during Bhuj earthquake, Indian standard revised in 2002 (BIS 2002) and included an amendment requiring the beams and columns of the open ground storey to be designed for 2.5 times the design base shear for the corresponding uniformly infilled frame buildings. Efficacy of this provision is examined in this study by comparing the capacity curves (Figs. 5.8 and 5.9) and hinge pattern (Figs. 5.10 - 5.17) of four and ten storey RC frame building with uniform infills, and infilled frame building with open ground storey, designed as SMRF with (designated as conforming ‘C’) and without

(designated as non-conforming 'NC') considering provisions of BIS (2002) for open ground storey buildings. Effect of irregular placement of infills on the strength and stiffness of RC frame buildings for the two design levels is shown in Table 5.9 (gravity load designed buildings) and Table 5.10 (buildings designed as SMRF). Figs. 5.8 and 5.9 show that both UI and OG (C) buildings have similar initial stiffness until yielding but the lateral strength of OG (C) buildings are found to increase significantly due to increase in the size and reinforcement of members of the open ground storey, however, the plastic displacement (D_u–D_y) reduces. The increase in strength of the four storey OG (C) building is 1.38 times, and 1.14 times and the decrease in plastic deformation is 23.4% and 36.2%, in longitudinal and transverse directions, respectively, whereas in case of the ten storey OG (C) building, the increase in strength is 1.1 times in both the directions; and 4.1% and 14.8% decrease in plastic deformation in longitudinal and transverse directions, respectively, as compare to the UI buildings. Four storey OG (C) building has shown 2.21 times higher strength and 1.4 times higher plastic deformation capacity in longitudinal direction, and 1.53 times higher strength and 1.25 times higher plastic deformation capacity in transverse direction as compared to the four storey OG (NC) building. For the ten storey building, there is 1.1 times higher strength and 1.14 times higher plastic deformation in both longitudinal as well as transverse directions. It can be concluded that both the four and ten storey open ground storey (OG) buildings designed for code (i.e. ground storey columns and beams designed for 2.5 times the normal base shear) are able to attain the stiffness and strength close to those of the corresponding uniformly infilled frame building. In fact, the estimated performance of such buildings is slightly better than the uniformly infilled frame buildings, indicating the adequacy of the code provisions for open ground storey buildings. As expected, the OG (NC) buildings (both four and ten storey) have shown the lowest strength and plastic deformation capacities among the three cases, considered.

Collapse mechanism of OG (NC) and OG (C) designed as SMRF is governed by ductile flexural mode of the members, whereas shear failure of columns governs the collapse mechanism of gravity load designed buildings (Figs. 5.6 (b) and 5.7(b)). The hinge pattern of OG (NC) differs from OG (C) buildings at DBE of Zone IV for which the buildings are designed. Plastic hinges are observed to be concentrated only in infill panels of OG (C) buildings (Figs. 5.12 and 5.16) whereas OG (NC) buildings

undergo yielding of some columns in ground storey also (Fig. 5.10). The collapse mechanisms of the two design levels (C and NC) of SMRF OG buildings also differ significantly. Due to strengthening of the ground storey beams and columns of OG (C) buildings, collapse mechanism is formed due to plastic hinges in upper storey beams and columns (Figs. 5.13 and 5.17), whereas, in case of OG (NC) buildings (Figs. 5.11 and 5.15) the ground storey columns fail, first. It is important to note that all the ground storey columns of four storey OG building designed for gravity loads alone and as SMRF (NC) yielded before yielding of any beam (Figs. 5.6 and 5.11) because of high seismic demand concentrated in the weaker and flexible ground storey due to irregularly placed infills in elevation. On the other hand, yielding of ground storey columns is avoided when the same buildings are designed as SMRF (C) considering provisions of BIS (2002) for open ground storey. It can also be observed from the Figs. 5.5 and 5.6 that in case of gravity load designed open ground storey buildings, no performance point is achieved under DBE excitation of Seismic Zone IV (BIS 2002) and the buildings are expected to collapse, while the SMRF OG (C) as well as OG (NC) buildings, designed for DBE, show 'LS' performance level even under MCE of Seismic Zone IV.

Figures 5.18 and 5.19 compare the static capacity (pushover) curves of four and ten storey RC frame buildings, respectively, designed for gravity loads only (BIS 1987 (Part 1), 1987 (Part 2), 2000), with uniformly placed infills and having front bay open in the ground storey (designated as O1B), while Figs. 5.20 and 5.21 present the collapse mechanism of the same buildings. Similar comparison of seismic performance of four and ten storey RC frame buildings with UI and O1B, designed as SMRF (BIS 1987 (Part 1), 1987 (Part 2), 1993, 2000, 2002) for Seismic Zone IV (BIS 2002) is made in Figs. 5.22 and 5.23. It is observed that the capacity curve of O1B building, in longitudinal direction (Fig. 5.18 (a)) is close to the capacity curve of uniformly infilled building initially, but it shows reduced strength due to absence of the front bay infill panels. On the other hand, in transverse direction, as expected, the capacity curve follows the capacity curve of uniformly infilled building for the entire range and the failure occurred at the same base shear due to shear failure of ground storey columns (Fig. 5.20 (b)). The effect of irregularity is more pronounced in case of the ten storey building, where the O1B building suffers premature failure at very early stage of lateral loading due to shear failure of exterior columns (Fig. 5.21) in the

direction of irregularity. Similar observation is made in case of SMRF O1B buildings; however, the strength and ductility of SMRF O1B buildings are much higher than their GLD counterparts. Under DBE of Seismic Zone IV, the four storey SMRF O1B building shows 'LS' performance in both longitudinal as well as transverse direction, where only the first storey infill panels undergo damage (shown in Fig. 5.24 (a)). The collapse mechanism is formed when some of the ground storey columns undergo 'CP' state (Fig. 5.25 (a)). In case of the ten storey SMRF O1B building, failure occurs due to collapse of infills (Fig. 5.27) and consequent yielding of a large number of beams.

The effect of irregular placement of infills on the strength and stiffness of RC frame buildings with different design levels and heights has been shown in Tables 5.9 and 5.10. The Tables also present the strength and stiffness parameters obtained from the capacity curves of buildings having three longitudinal bays open (designated as O3B). The capacity curves of O3B buildings are presented in Section 5.4 along with the dynamic analysis results. It is observed form the Tables that the strength and stiffness of infilled frame buildings are reduced significantly because of irregular placement of infills, except for SMRF buildings designed as per code provisions for open ground storey buildings. In case of the four storey gravity load designed buildings with open ground storey, with front bay open, and with open three bays, the strength decreases to 34.3%, 32% and 64.1%, respectively in the direction of asymmetry, whereas the strength remains almost the same in the other direction. In case of the ten storey GLD buildings, the decrease in strength is up to 12%, 46% and 84%, respectively. The reduction in stiffness is highest in case of the open ground storey buildings. The stiffness of the four storey GLD OG building reduces 81% and 69% in the longitudinal and transverse directions, respectively (Table 5.9) whereas in case of four storey SMRF OG (NC) building, the reduction is up to 82% and 70.5% in longitudinal and transverse directions, respectively (Table 5.10). For both the design levels and heights O3B buildings have minimum strength among all the considered configurations of irregularly placed infills. However, the strength of SMRF OG (C) buildings increases due to BIS (2002) design provisions for open ground storey buildings, which resulted in higher member sizes in ground storey beams and columns.

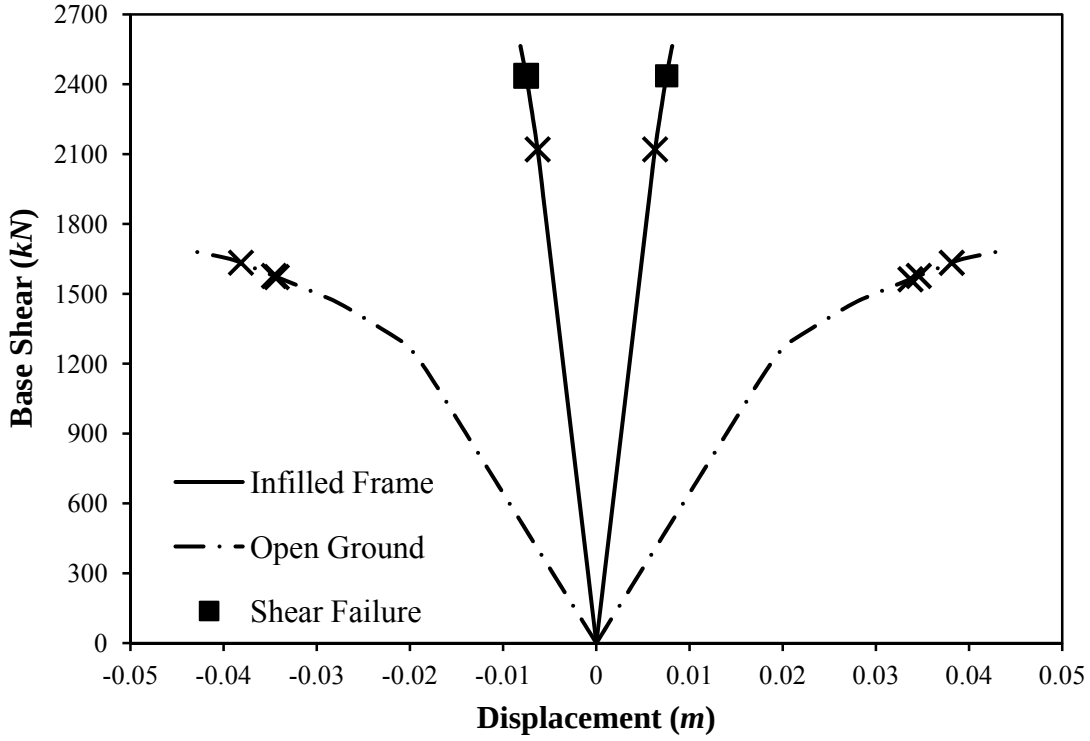

(a)

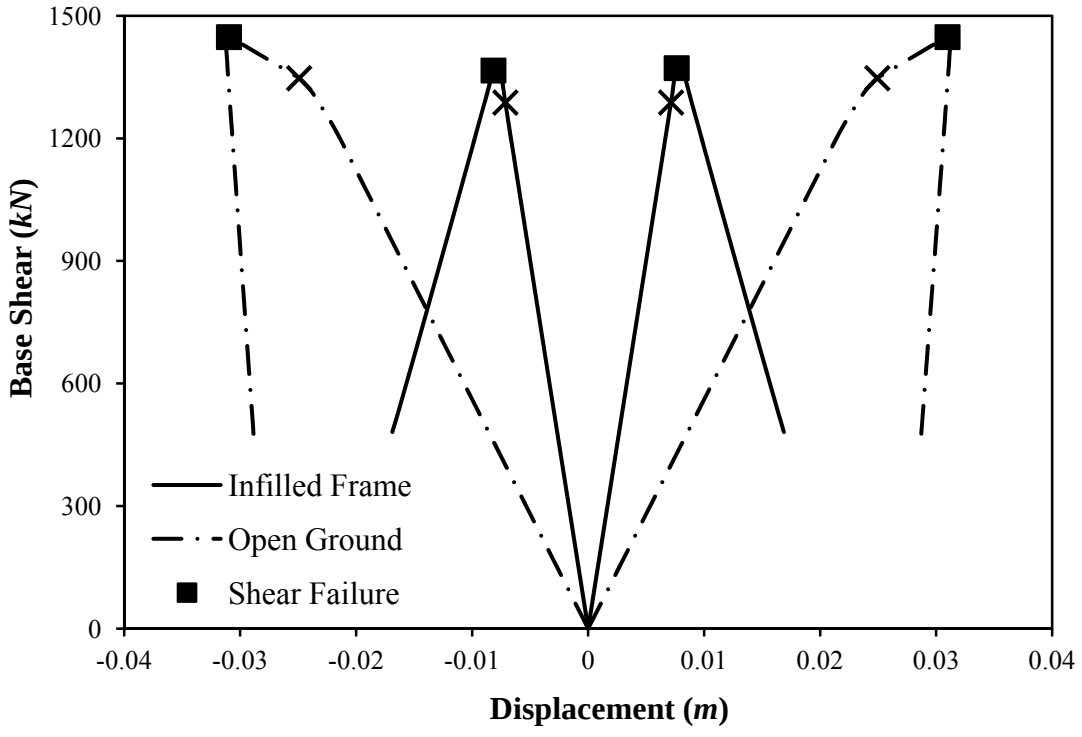

(b)

Fig. 5.4 Comparison of capacity curves for the four storey RC frame building with uniform infills and infilled frame building with open ground storey, designed for gravity loads only as per relevant Indian Standards; the crosses (×) represent IO, LS, and CP performance levels, consecutively: (a) longitudinal direction; (b) transverse direction.

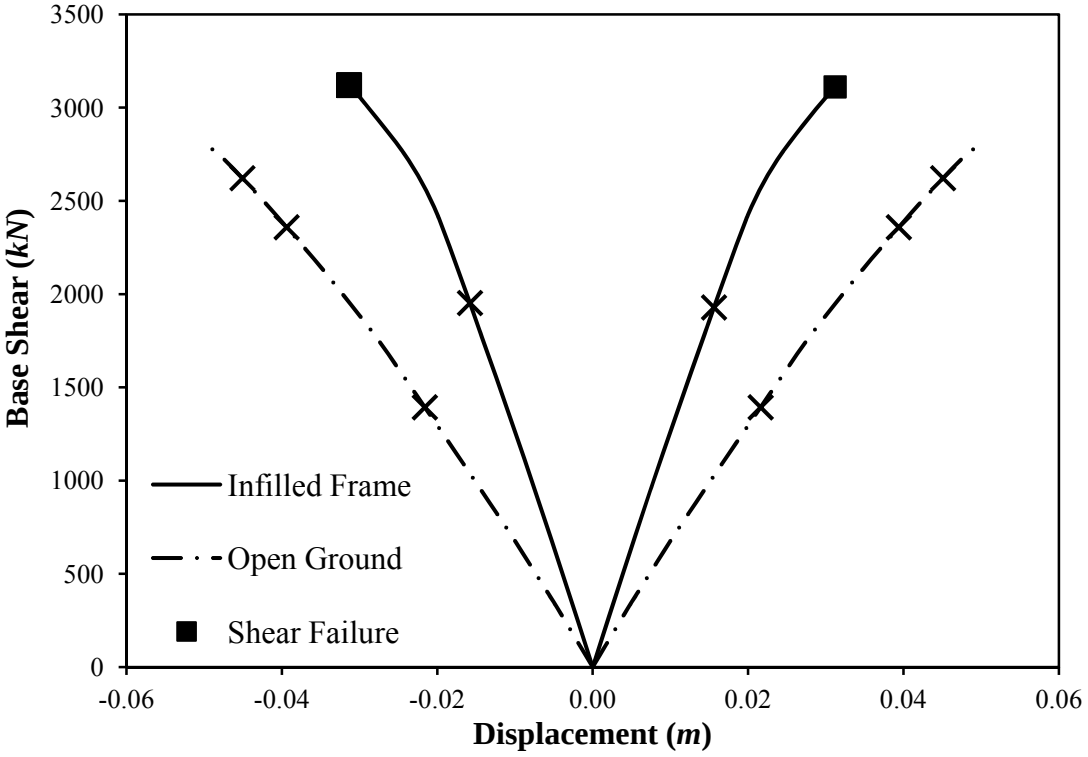

(a)

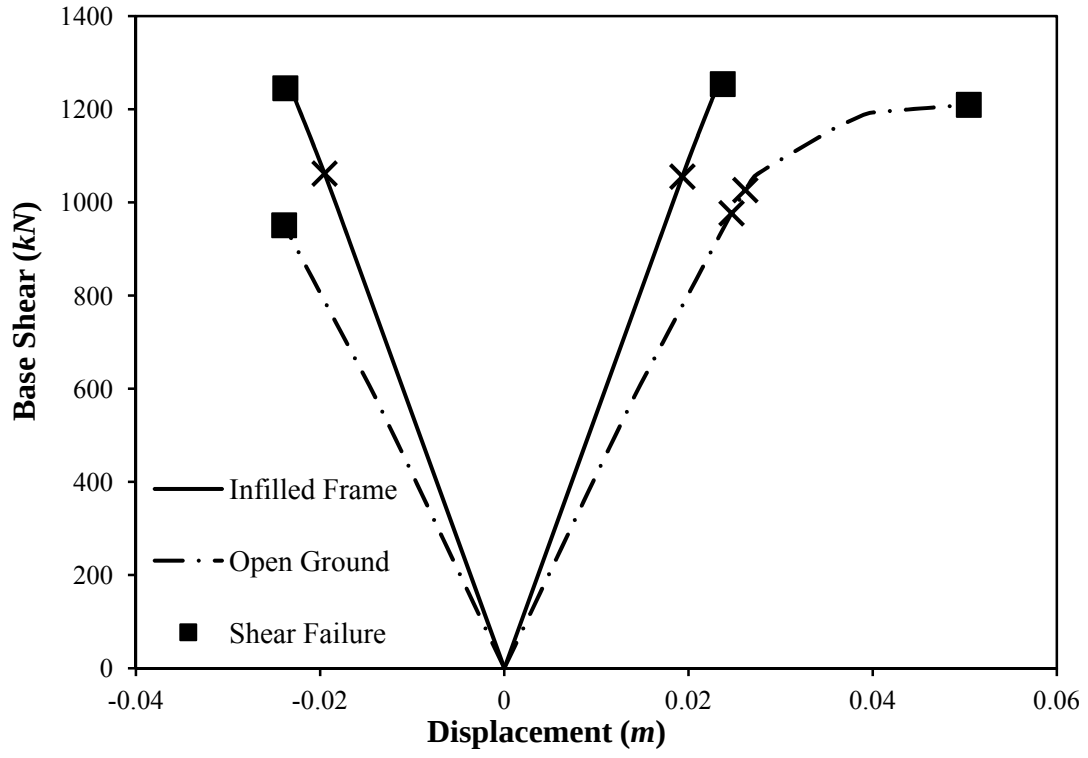

(b)

Fig. 5.5 Comparison of capacity curves for the ten storey RC frame building with uniform infills and infilled frame building with open ground storey, designed for gravity loads only as per relevant Indian Standards; the crosses (×) represent IO, LS, and CP performance levels, consecutively: (a) longitudinal direction; (b) transverse direction.

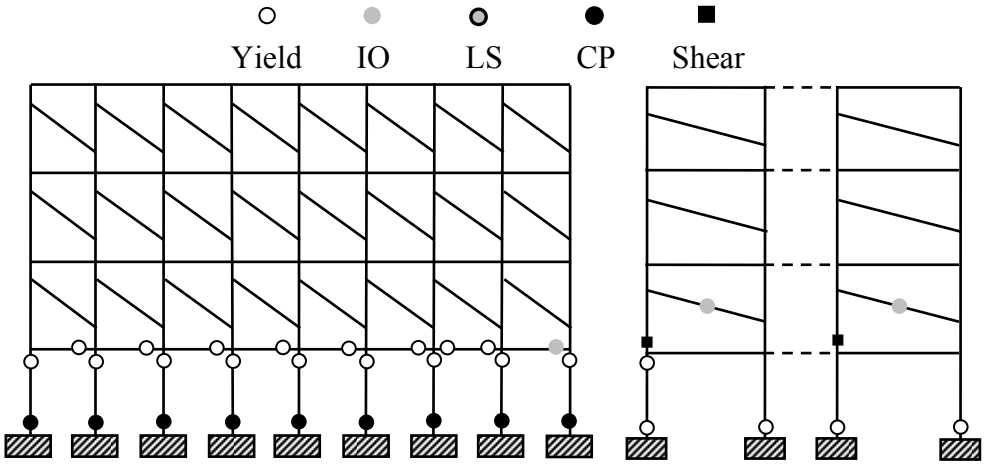

Fig. 5.6 Collapse mechanism of four storey infilled RC frame building with open ground storey, designed for gravity loads alone as per relevant Indian Standards: (a) typical longitudinal frame; (b) typical transverse frame.

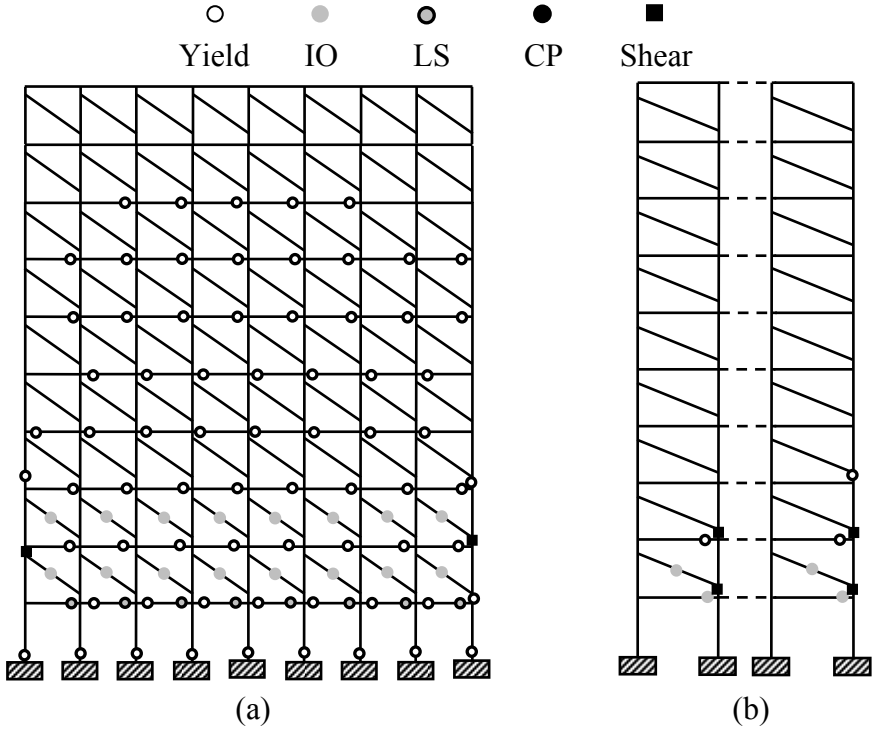

Fig. 5.7 Collapse mechanism of ten storey infilled RC frame building with open ground storey, designed for gravity loads alone as per relevant Indian Standards: (a) typical longitudinal frame; (b) typical transverse frame.

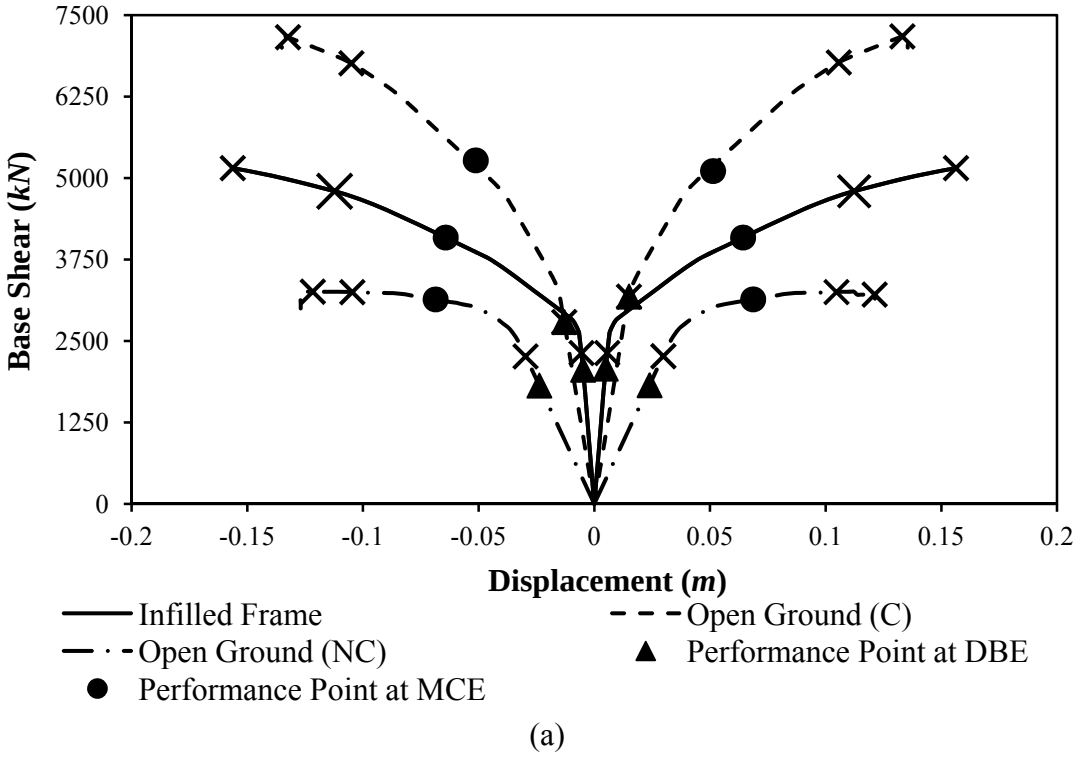

(a)

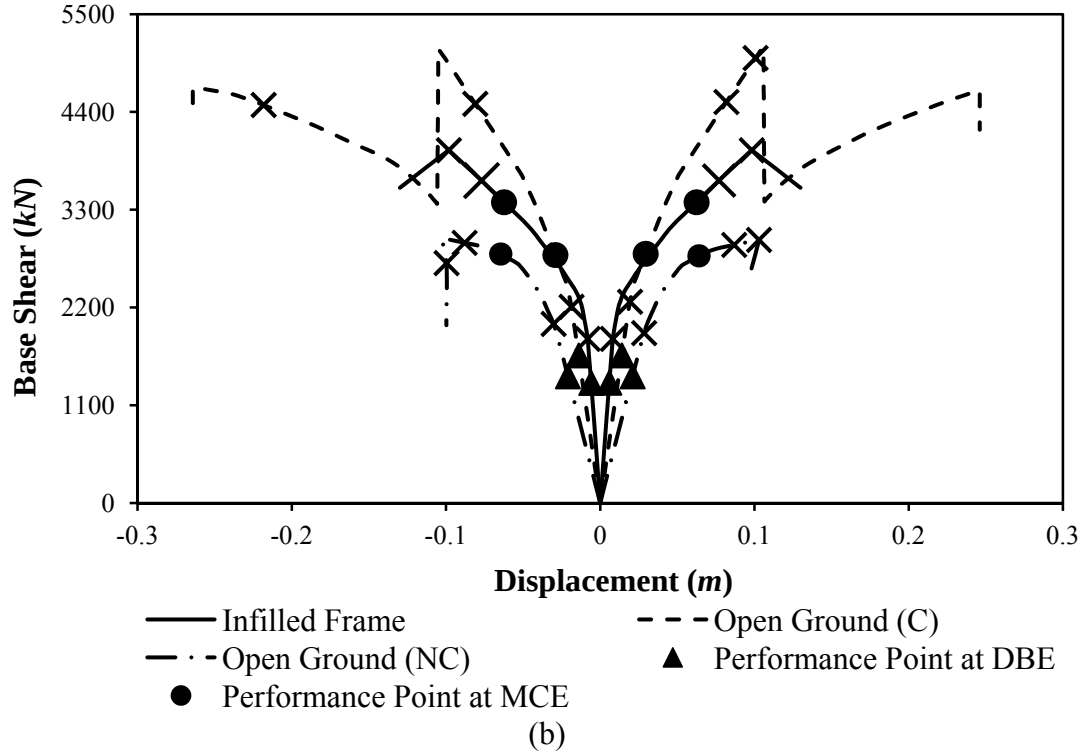

(b)

Fig. 5.8 Comparison of capacity curves and performance points for the four storey RC frame building with uniform infills, and infilled frame building with open ground storey, designed as SMRF, with and without considering provisions of BIS (2002) for open ground storey (denoted by C and NC respectively): (a) in longitudinal direction; (b) in transverse direction. The three crosses (×) represent IO, LS, and CP performance levels, consecutively.

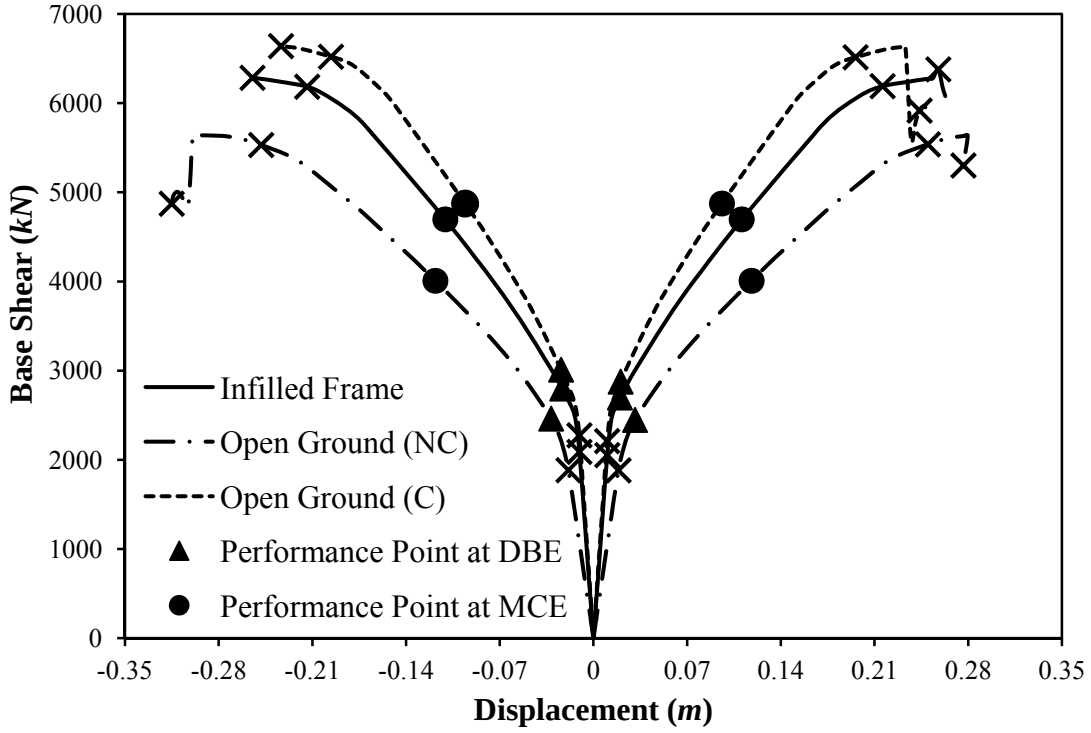

(a)

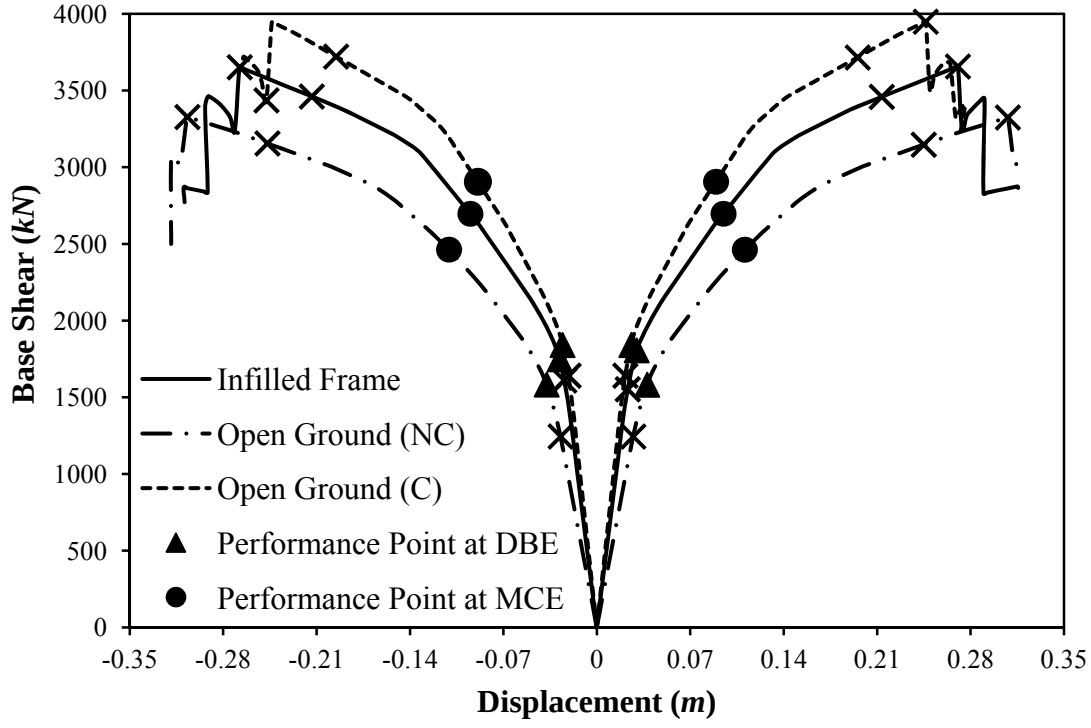

(b)

Fig. 5.9 Comparison of capacity curves and performance point for the ten storey RC frame building with uniform infills, and infilled frame building with open ground storey, designed as SMRF, with and without considering provisions of BIS (2002) for open ground storey (denoted by C and NC respectively): (a) in longitudinal direction; (b) in transverse direction. The three crosses (×) represent IO, LS, and CP performance levels, consecutively.

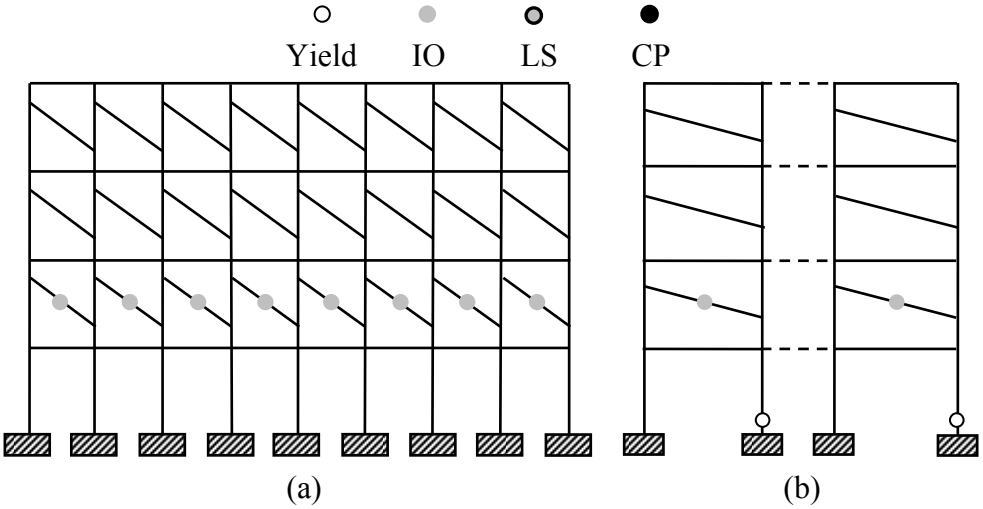

Fig. 5.10 Hinge pattern at performance point for DBE of four storey RC infilled frame buildings with open ground storey, designed as SMRF without considering provisions of BIS (2002) for open ground storey: (a) typical longitudinal frame; (b) typical transverse frame.

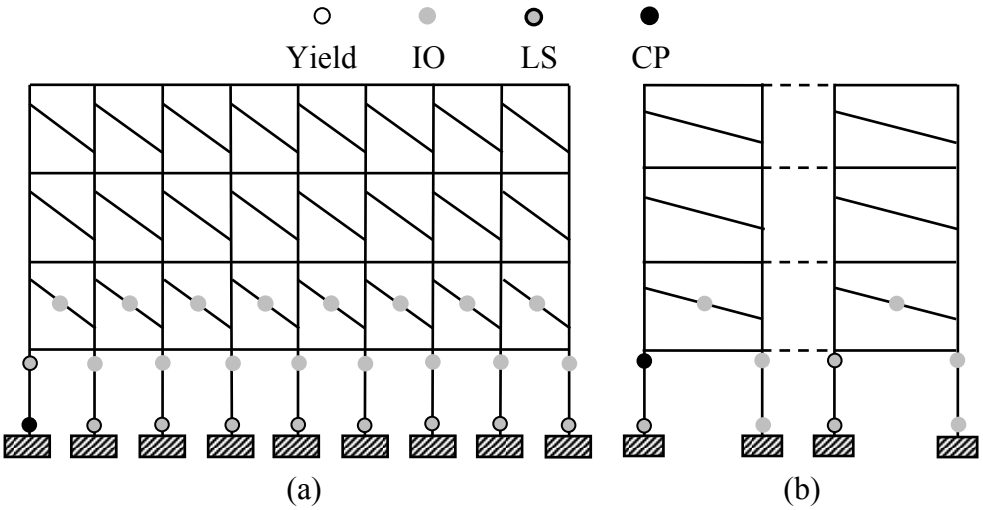

Fig. 5.11 Collapse mechanism of four storey RC infilled frame buildings with open ground storey, designed as SMRF without considering provisions of BIS (2002) for open ground storey: (a) typical longitudinal frame; (b) typical transverse frame.

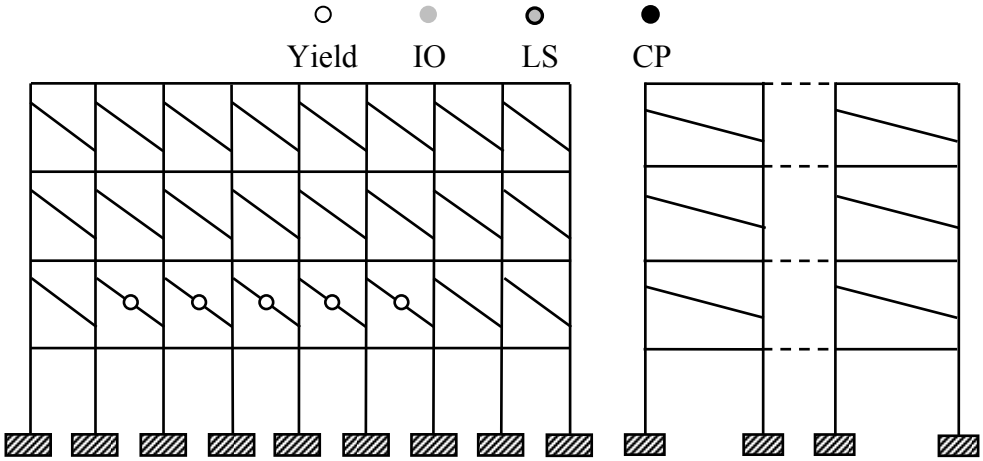

Fig. 5.12 Hinge pattern at performance point for DBE of four storey RC infilled frame buildings with open ground storey, designed as SMRF considering provisions of BIS (2002) for open ground storey: (a) typical longitudinal frame; (b) typical transverse frame.

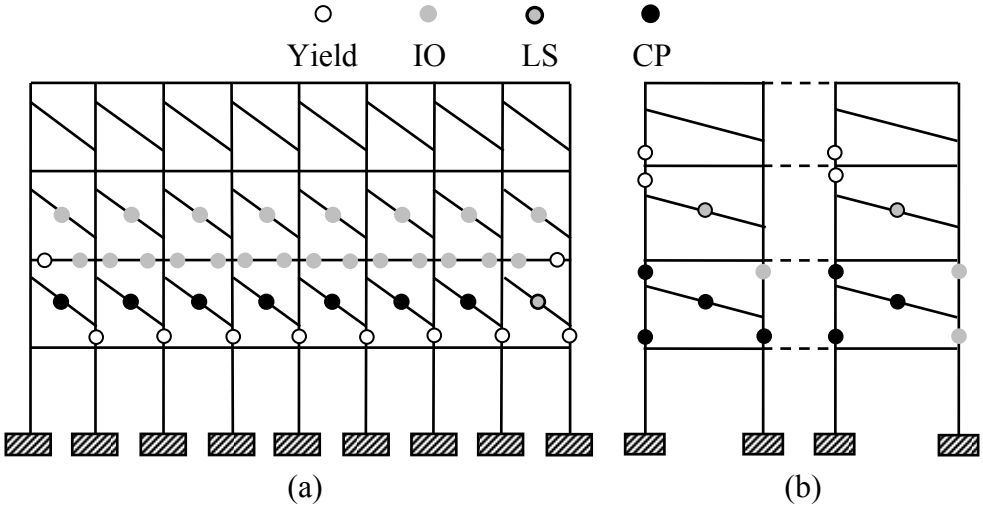

Fig. 5.13 Collapse mechanism of four storey RC infilled frame buildings with open ground storey, designed as SMRF considering provisions of BIS (2002) for open ground storey: (a) typical longitudinal frame; (b) typical transverse frame.

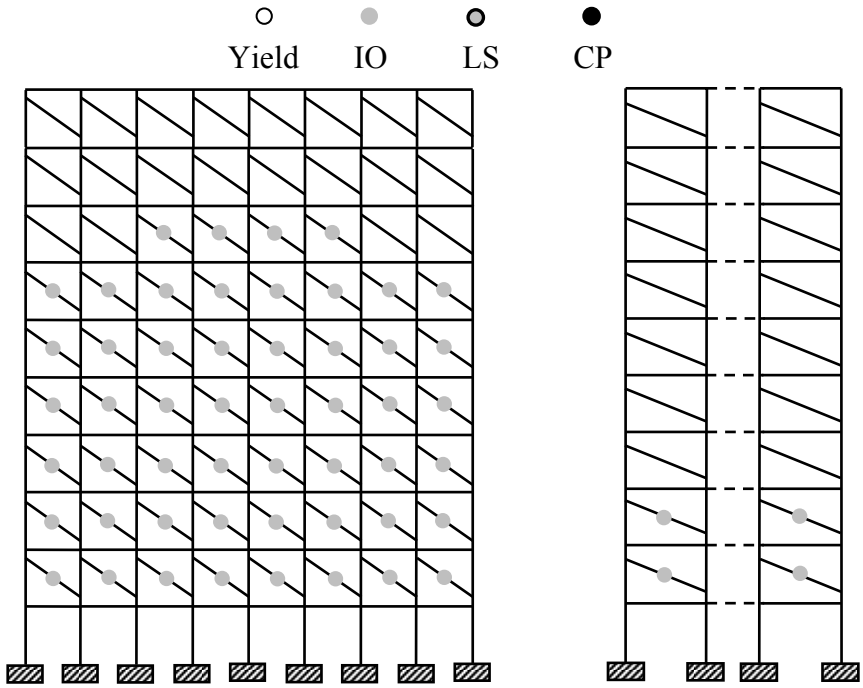

Fig. 5.14 Hinge pattern at performance point under DBE of ten storey RC infilled frame buildings with open ground storey, designed as SMRF without considering provisions of BIS (2002) for open ground storey: (a) typical longitudinal frame; (b) typical transverse frame.

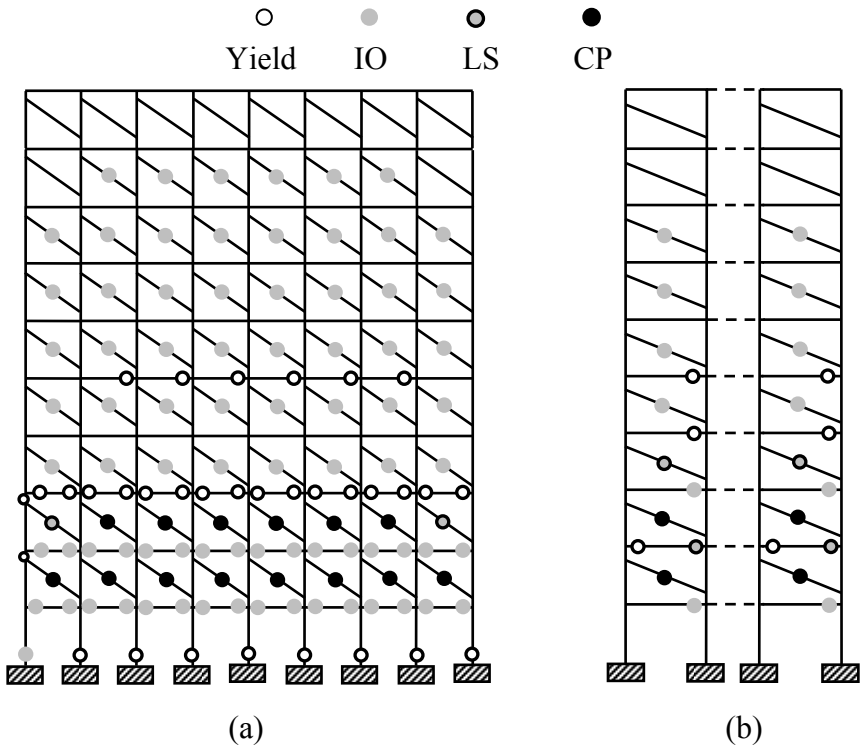

Fig. 5.15 Collapse mechanism of ten storey RC infilled frame buildings with open ground storey, designed as SMRF without considering provisions of BIS (2002) for open ground storey: (a) typical longitudinal frame; (b) typical transverse frame.

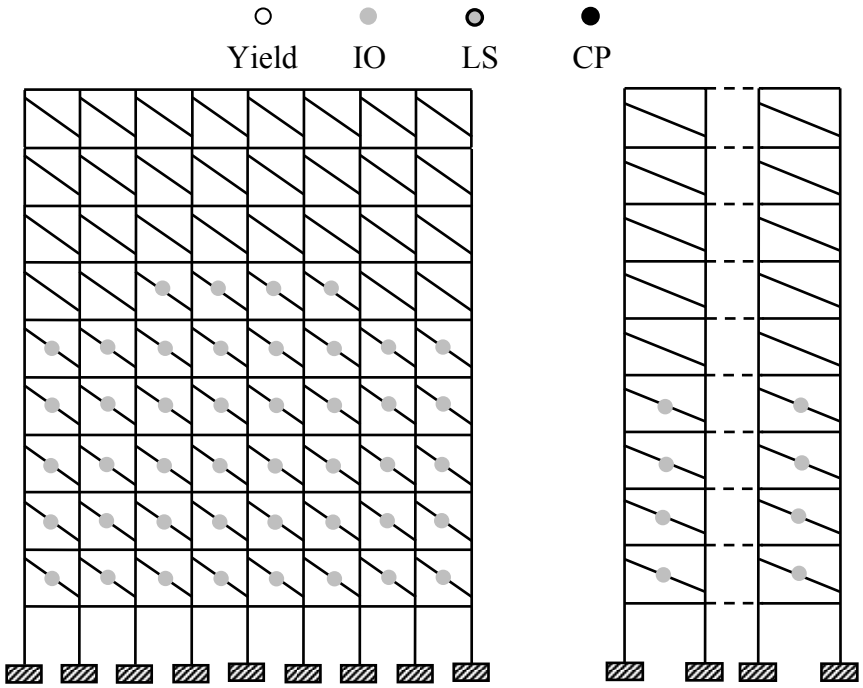

Fig. 5.16 Hinge pattern at performance point under DBE of ten storey RC infilled frame buildings with open ground storey, designed as SMRF considering provisions of BIS (2002) for open ground storey: (a) typical longitudinal frame; (b) typical transverse frame.

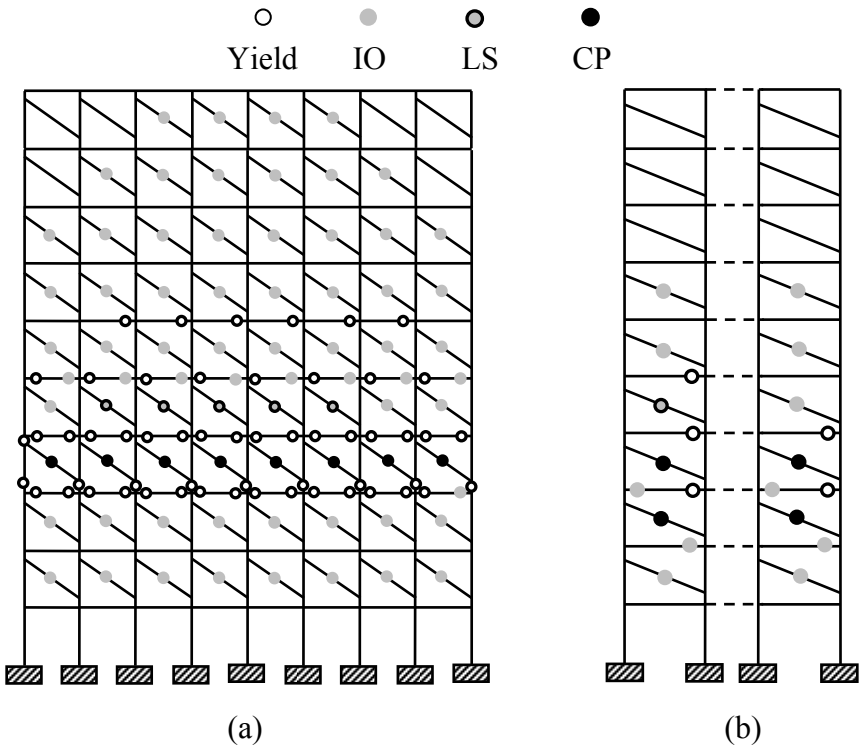

Fig. 5.17 Collapse mechanism of ten storey RC infilled frame buildings with open ground storey, designed as SMRF considering provisions of BIS (2002) for open ground storey: (a) typical longitudinal frame; (b) typical transverse frame.

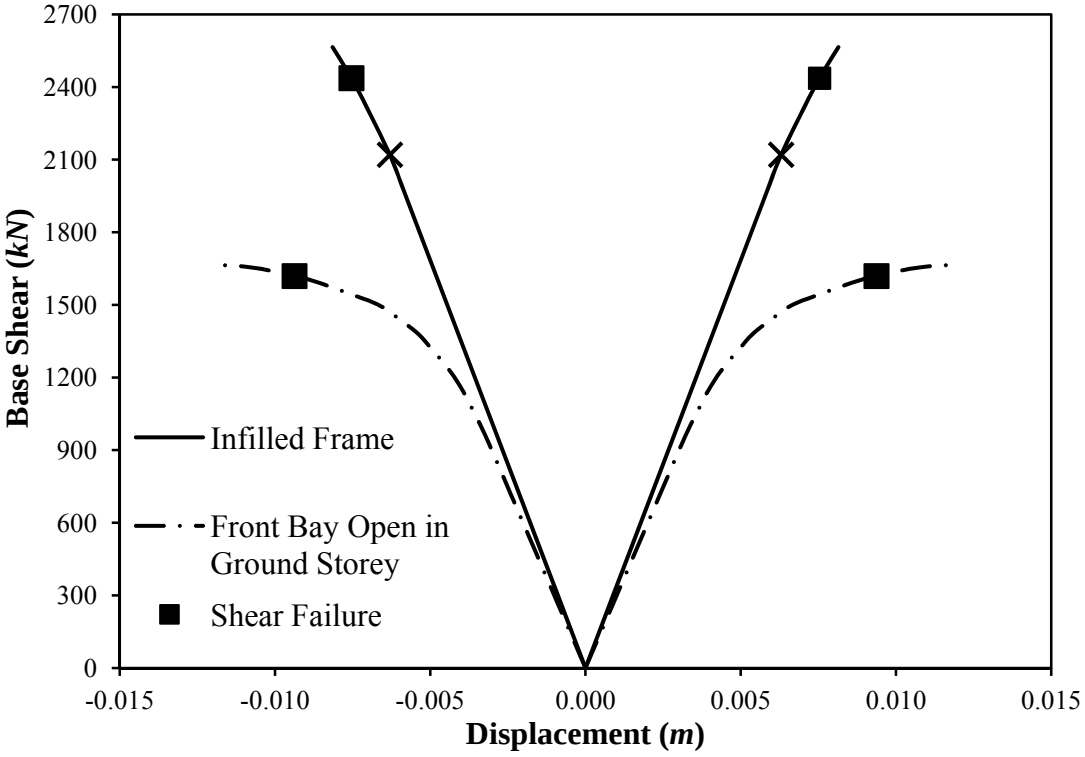

(a)

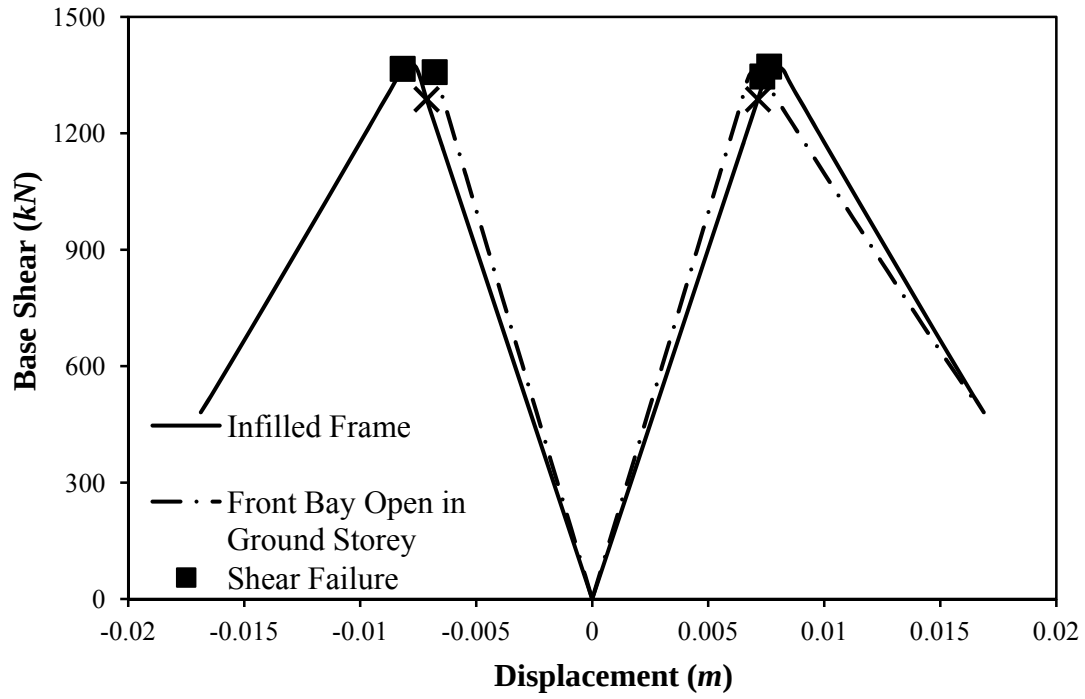

(b)

Fig. 5.18 Comparison of capacity curves for the four storey RC frame building with uniform infills and infilled frame building with front bay open in ground storey, designed for gravity loads only as per relevant Indian Standards: (a) longitudinal direction; (b) transverse direction. The three crosses (×) represent IO, LS, and CP performance levels, consecutively.

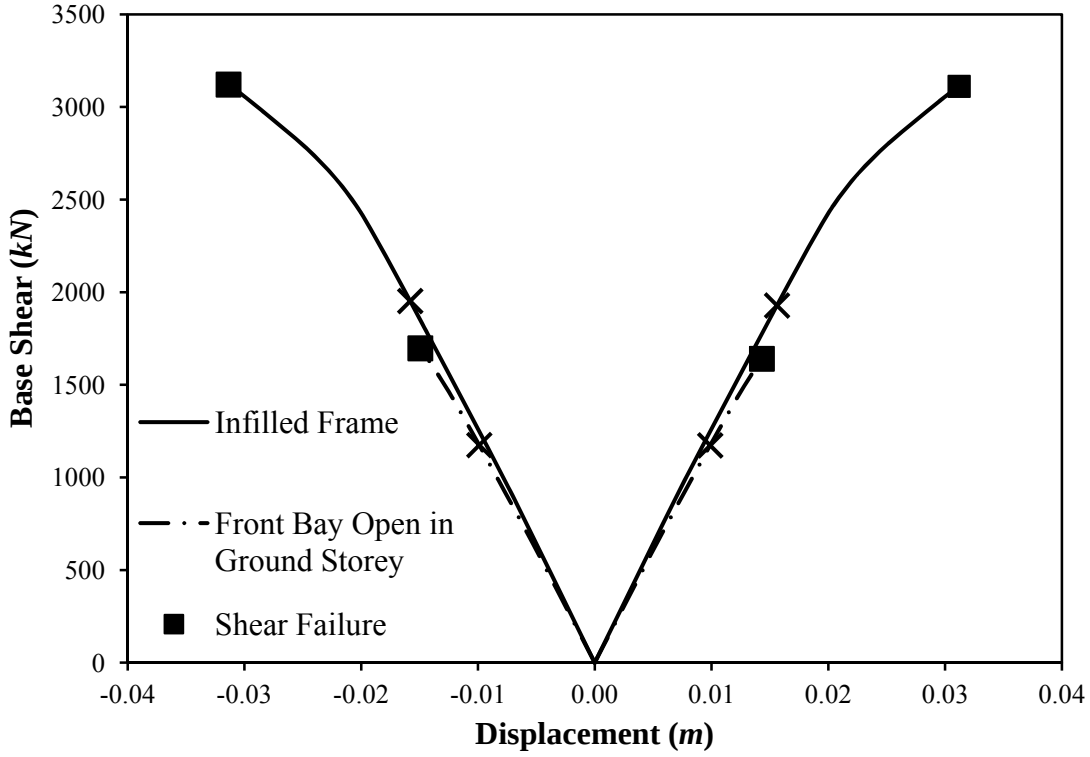

(a)

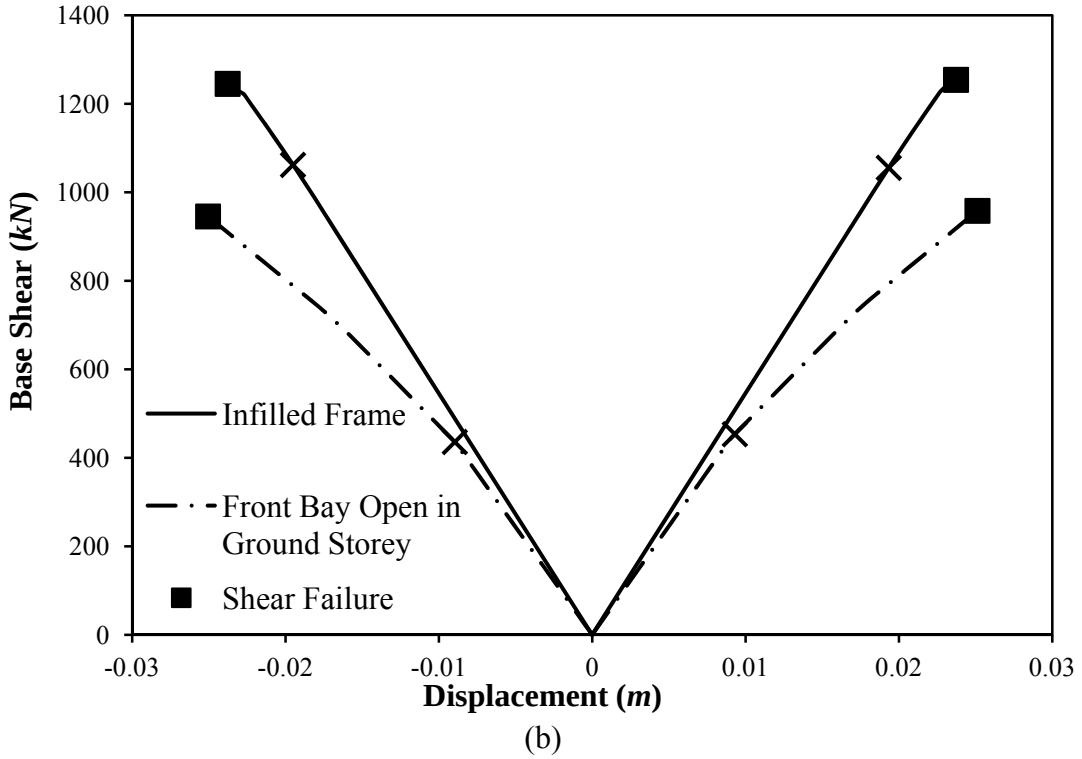

(b)

Fig. 5.19 Comparison of capacity curves for the ten storey RC frame building with uniform infills and infilled frame building with front bay open in ground storey, designed for gravity loads only as per relevant Indian Standards: (a) longitudinal direction; (b) transverse direction. The three crosses (×) represent IO, LS, and CP performance levels, consecutively.

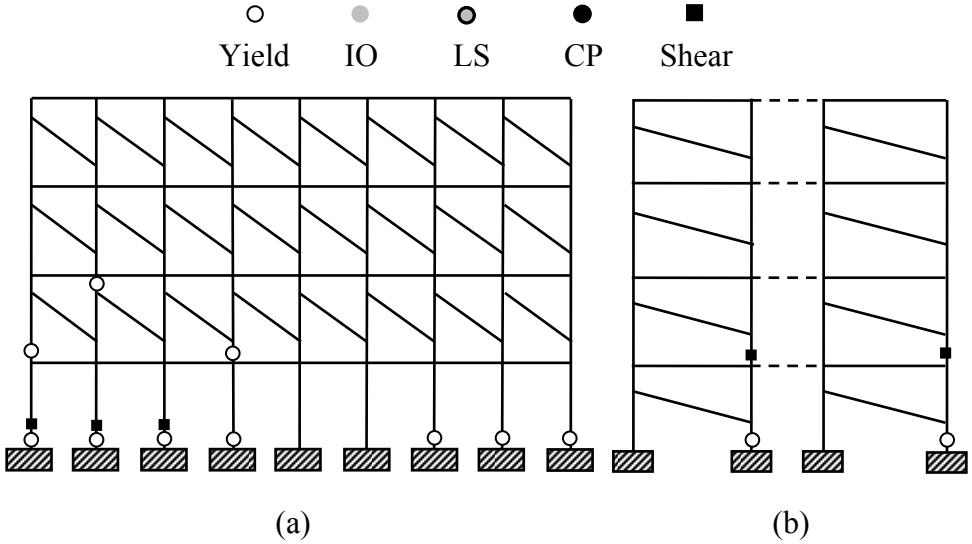

Fig. 5.20 Collapse mechanism of four storey RC infilled frame building with open front bay in ground storey, designed for gravity loads alone as per relevant Indian Standards: (a) open front bay in longitudinal direction; (b) typical transverse frame.

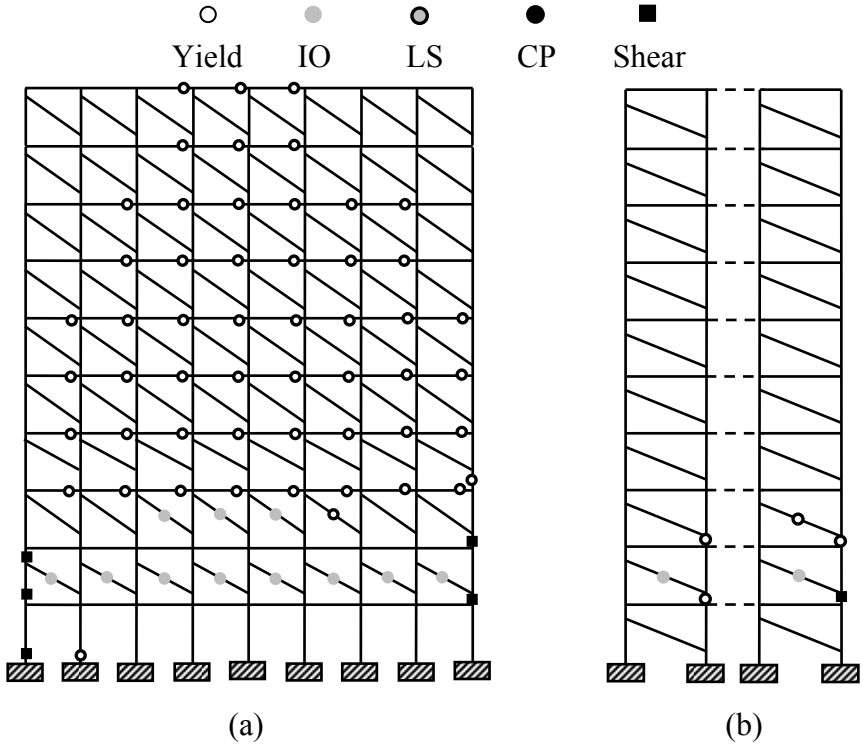

Fig. 5.21 Collapse mechanism of ten storey RC infilled frame building with open front bay in ground storey, designed for gravity loads alone as per relevant Indian Standards: (a) open front bay in longitudinal direction; (b) typical transverse frame.

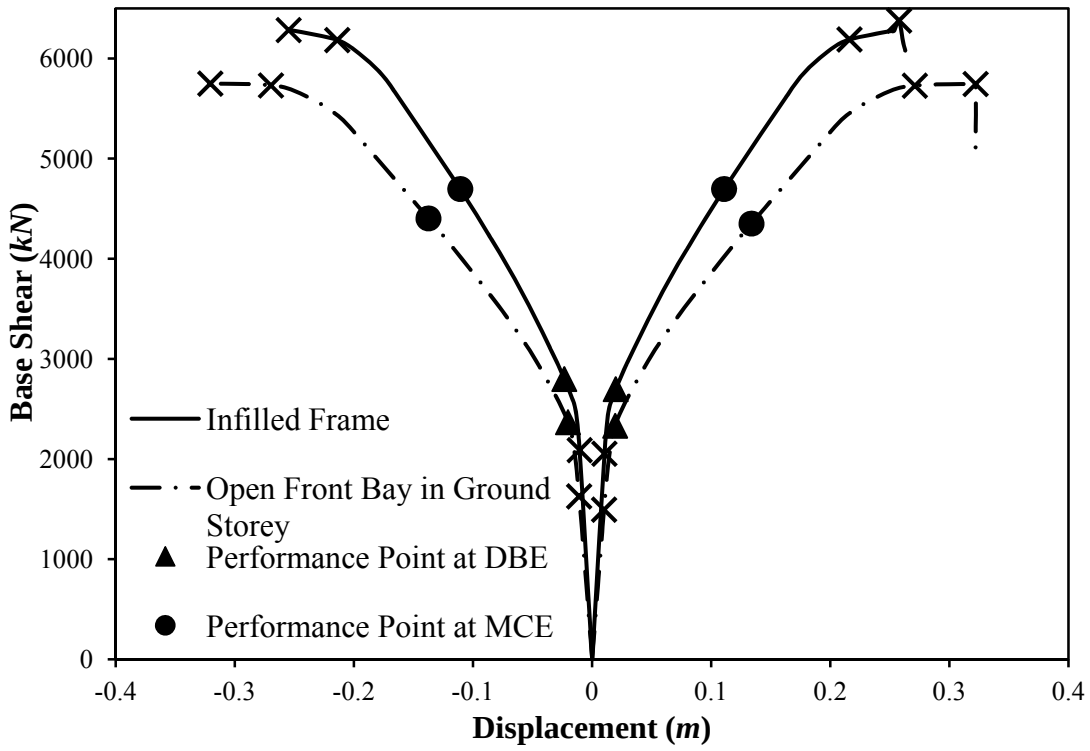

(a)

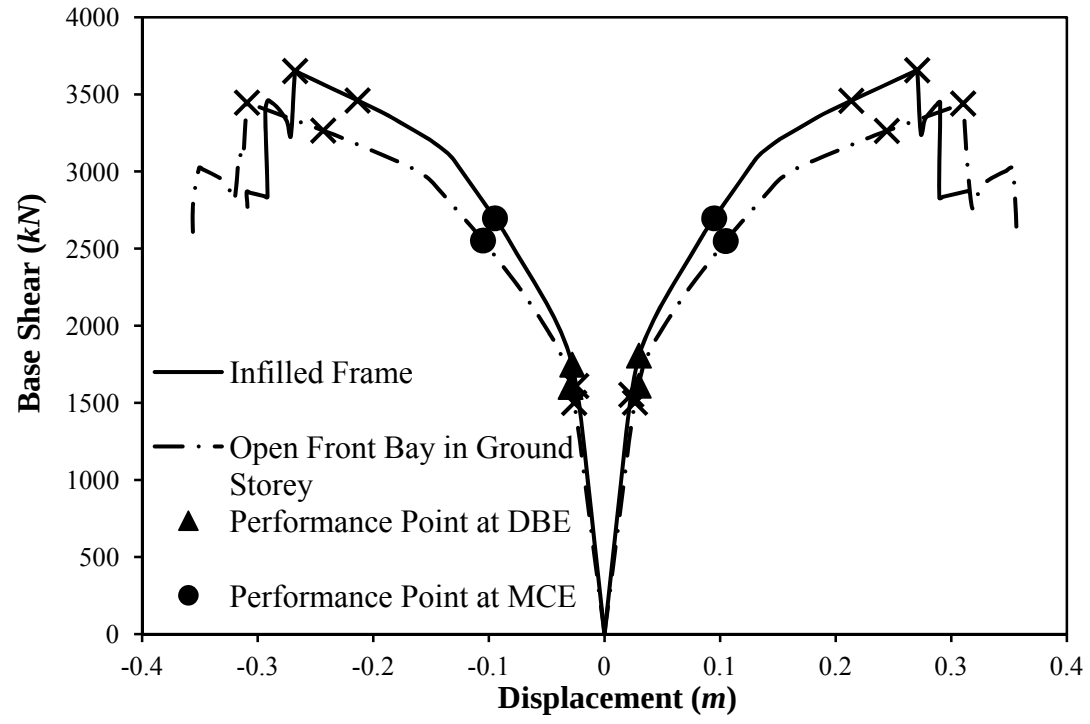

(b)

Fig. 5.22 Comparison of capacity curves and performance points for the four storey RC frame buildings with uniform infills, and infilled frame buildings with one front bay open in ground storey, designed as SMRF as per relevant Indian Standards: (a) longitudinal direction; (b) transverse direction. The three crosses (×) represent IO, LS, and CP performance levels, consecutively.

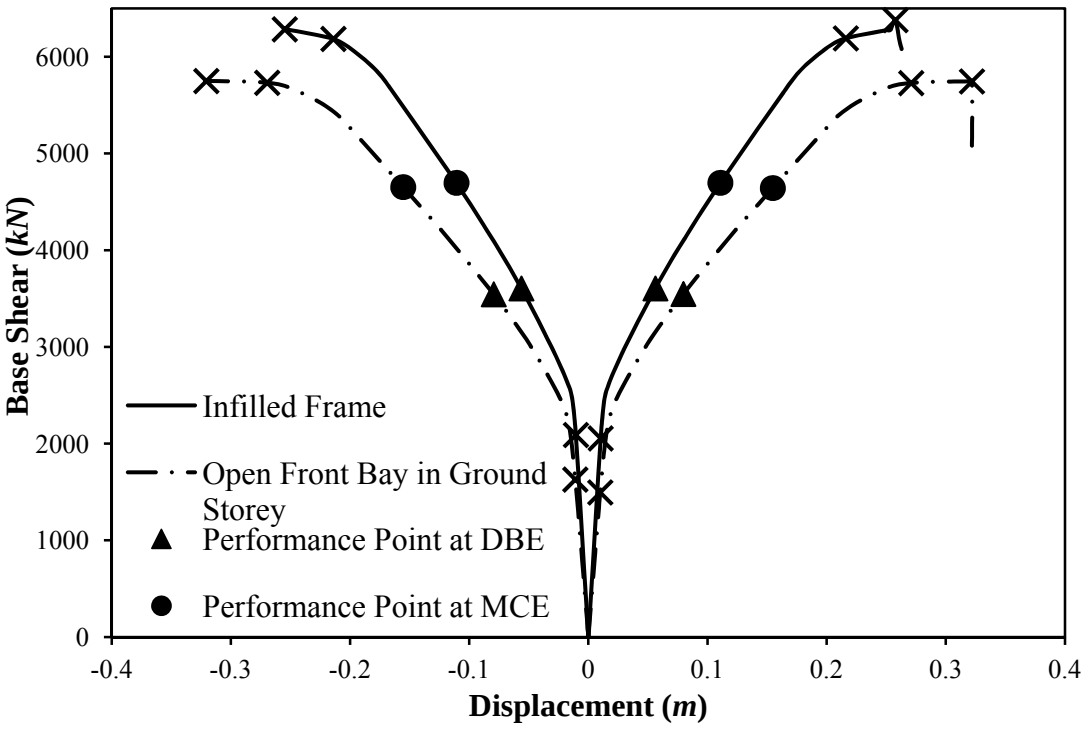

(a)

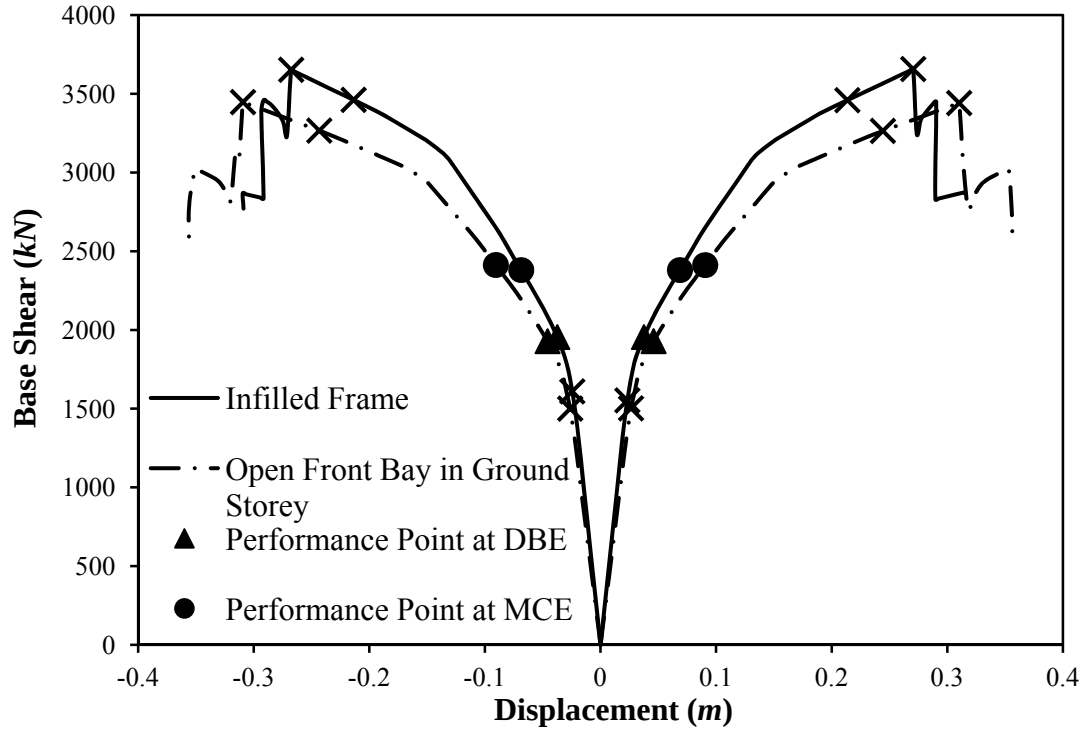

(b)

Fig. 5.23 Comparison of capacity curves and performance points for the ten storey RC frame buildings with uniform infills, and infilled frame buildings with one front bay open in ground storey, designed as SMRF as per relevant Indian Standards: (a) longitudinal direction; (b) transverse direction. The three crosses (×) represent IO, LS, and CP performance levels, consecutively.

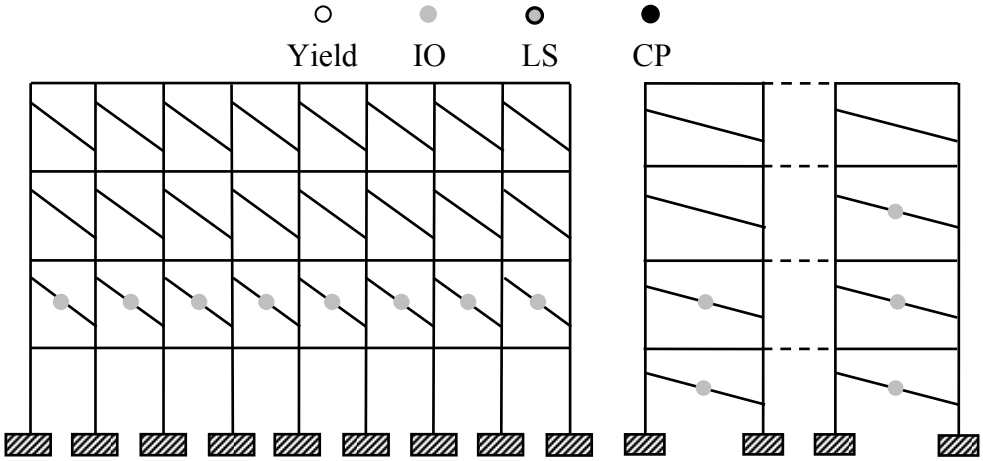

Fig. 5.24 Hinge pattern at performance point for DBE of four storey RC infilled frame building designed as SMRF as per relevant Standards with one front bay open in ground storey: (a) open front bay in longitudinal direction; (b) typical transverse frame.

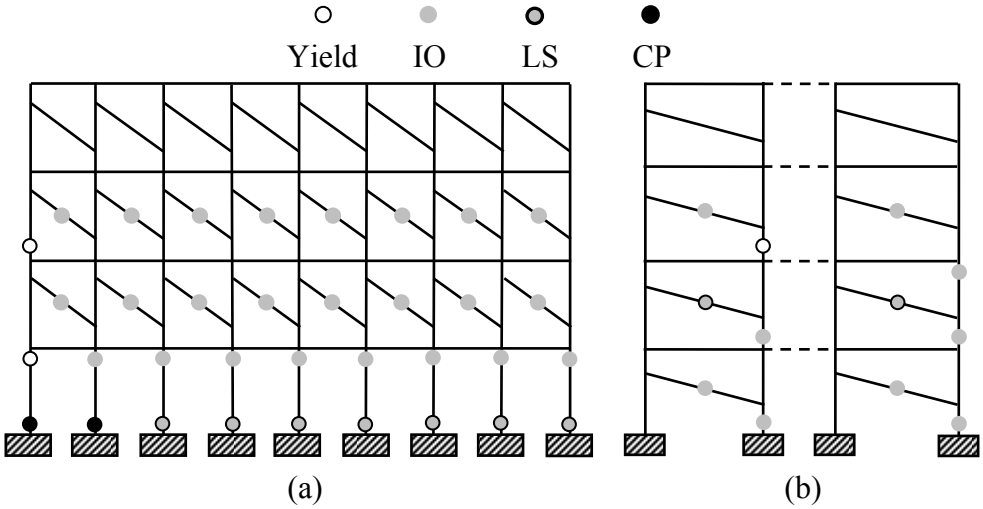

Fig. 5.25 Collapse mechanism of the four storey infilled RC frame building designed as SMRF as per relevant Standards with one front bay open in ground storey: (a) open front bay in longitudinal direction; (b) typical transverse frame.

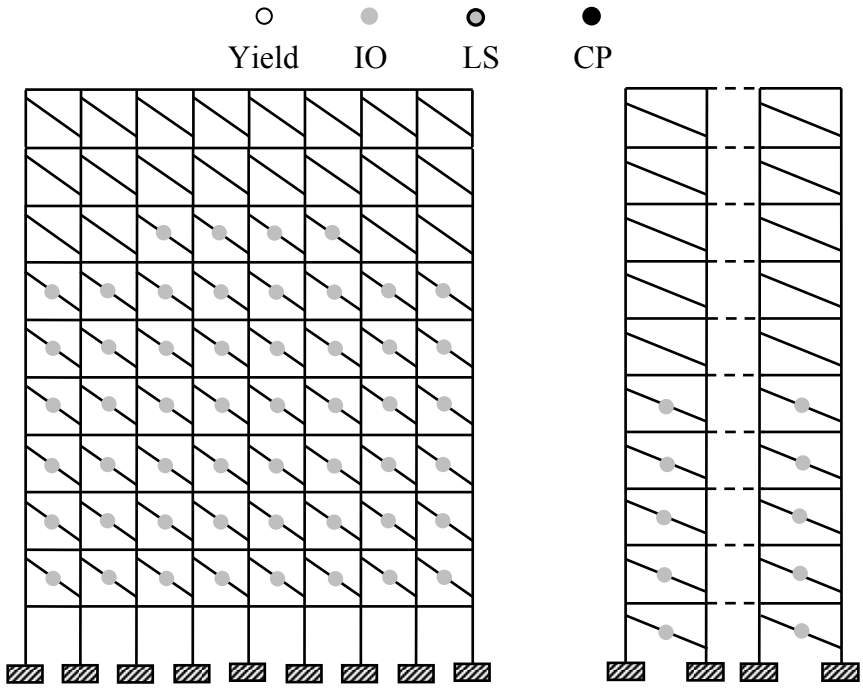

Fig. 5.26 Hinge pattern at performance point under DBE of the ten storey infilled RC frame buildings with one front bay open in ground storey: (a) open front bay in longitudinal direction; (b) typical transverse frame.

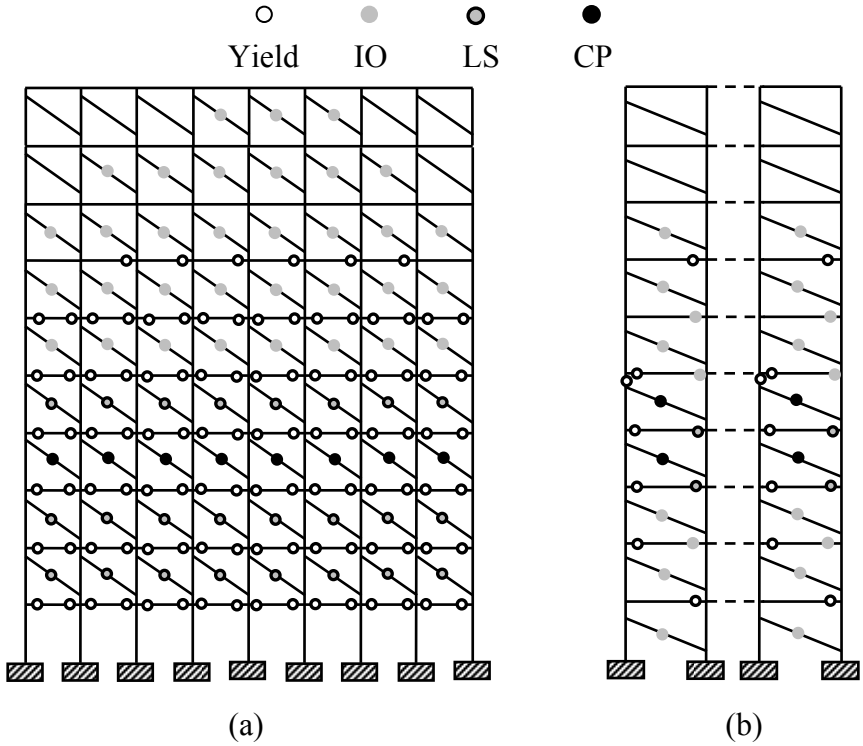

Fig. 5.27 Collapse mechanism of ten storey infilled RC frame buildings designed as SMRF as per relevant Standards with one front bay open in ground storey: (a) open front bay in longitudinal direction; (b) typical transverse frame.

Table 5.9

Effect of irregular placement of URM infills on strength and stiffness of infilled RC frame buildings designed for gravity loads only

Design Level	No. of Storey	Strength (*kN*)		Stiffness (*kN/m*)	
		Longitudinal	Transverse	Longitudinal	Transverse
RC frame buildings with uniformly placed URM infills	4	2445.50	1235.86	336908.72	180280.59
	10	2938.10	1235.20	124321.14	54594.26
URM infilled RC frame buildings with open ground storey	4	1606.98	1409.84	64401.36	56095.03
	10	2588.83	1204.74	64163.74	40813.84
URM infilled RC frame buildings with front bay open in ground storey	4	1665.10	1214.15	298563.53	199066.21
	10	1595.06	1235.01	119718.06	54498.73
URM infilled RC frame buildings with three bays open in ground storey	4	877.74	1125.58	169880.14	124418.71
	10	482.17	833.21	100301.80	47953.76

Table 5.10

Effect of irregular placement of URM infills on strength and stiffness of infilled RC frame buildings designed as SMRF

Design Level	No. of Storey	Strength (*kN*)		Stiffness (*kN/m*)	
		Longitudinal	Transverse	Longitudinal	Transverse
RC frame buildings with uniformly placed URM infills	4	5152.85	3969.80	423153.43	229896.93
	10	5801.55	3393.06	161296.53	64924.56
URM infilled RC frame buildings with open ground storey without any consideration of relevant provisions of Indian Standard (BIS 2002)	4	3212.17	2953.02	76317.54	67920.13
	10	5617.63	3243.27	100586.26	44245.08
URM infilled RC frame buildings with open ground storey, designed and detailed as per BIS (2002)	4	7095.64	4507.13	213584.85	118517.87
	10	6383.76	3712.00	196823.98	73591.21
URM infilled RC frame buildings with front bay open in ground storey	4	3930.51	3956.58	192017.57	224523.58
	10	5745.28	2945.59	135895.53	50065.24
URM infilled RC frame buildings with three bays open in ground storey	4	3103.23	3673.44	94983.48	117738.56
	10	5707.48	3233.63	109331.71	52520.55

Tables 5.11 and 5.12 summarize the capacity curve parameters of the RC frame buildings with different design levels, heights, and placement of infills. The Tables also present the performance point at DBE and MCE of Indian Seismic Zones IV and V. As evident from the pushover curves, the GLD buildings with irregular infills could not survive DBE excitation of Indian Seismic Zone IV, therefore the possibility of survival without collapse in the lower Indian Seismic Zone (III), is also explored as presented in Table 5.11. It is observed that none of the infilled frame buildings designed for gravity loads only could survive even DBE excitation of Seismic Zone III (0.08*g* PGA) and are expected to collapse. In case of four storey buildings with seismic action in longitudinal direction (i.e. the direction of asymmetry), the ratio of yield and collapse base shear to seismic weight is highest in uniformly infilled building (16.3% and 16.6%, respectively); and is lowest in case of O3B building (1.3% at yield as well as at collapse points). In case of the ten storey uniformly infilled frame building, the values at yield and collapse are 7% and 7.3%, respectively, whereas in case of the ten storey O3B building, the corresponding values are only 0.02% and 1.3% at yield and collapse points, respectively.

The SMRF buildings yield at higher base shear than its GLD counterpart. Similar to the GLD buildings, in this case also, the uniformly infilled buildings have the highest yield (23.3% of seismic weight) and collapse base shear (36% of seismic weight), except for OG (C) building, due to BIS (2002) design provision resulting in higher design base shear. It is interesting to observe that the buildings designed as SMRF for DBE of Indian Seismic Zone IV having uniform as well as irregular infills can sustain seismic excitation upto MCE of Indian Seismic Zone V without collapse, except for four storey RC frame buildings with three bays open in ground storey, subjected to earthquake in longitudinal direction.

5.4 . NONLINEAR DYNAMIC ANALYSIS

In the nonlinear dynamic procedure, the building model is similar to the one used in nonlinear static procedure. The main difference is that the seismic action is simulated using a time-history analysis, which involves time-step-by-time-step evaluation of the building response.

Table 5.11

Capacity curve parameters and performance point of RC frame buildings designed for gravity loads only as per relevant Indian Standards with uniform and irregular infills

Direction	Design Level	No. of Storey	Capacity Curve Parameters				Spectral Displacement at Performance Point (*m*)					
			Yield Capacity Point		Ultimate Capacity Point		Zone III (BIS 2002)		Zone IV (BIS 2002)		Zone V (BIS 2002)	
							DBE	MCE	DBE	MCE	DBE	MCE
			D_y/H	V_y/W	D_u/H	V_u/W	0.08 (*g*)	0.16(*g*)	0.12(*g*)	0.24(*g*)	0.18(*g*)	0.36(*g*)
Longitudinal	RC frame buildings with uniformly placed URM infills	4	0.001	0.163	0.001	0.166	0.005	0.013	0.008	0.020	0.011	0.021
		10	0.001	0.070	0.001	0.073	0.017	0.046	0.035	0.069	0.052	0.104
	RC frame buildings with open ground storey	4	0.002	0.100	0.003	0.109	0.018	0.084	0.028	0.057	0.042	0.085
		10	0.001	0.063	0.002	0.064	0.024	0.057	0.042	0.085	0.064	0.127
	RC frame buildings with front bay open in ground storey	4	0.0004	0.096	0.001	0.113	0.011	0.021	0.016	0.032	0.024	0.048
		10	0.0004	0.039	0.000	0.040	0.016	0.031	0.023	0.046	0.034	0.069
	RC frame buildings with three bays open in ground storey	4	0.0003	0.0546	0.0009	0.0633	0.010	0.019	0.027	0.053	0.040	0.080
		10	0.0002	0.0127	0.0001	0.0128	0.017	0.034	0.025	0.051	0.038	0.076
Transverse	RC frame buildings with uniformly placed URM infills	4	0.001	0.084	0.001	0.084	0.006	0.016	0.012	0.024	0.018	0.035
		10	0.001	0.030	0.001	0.031	0.036	0.071	0.053	0.101	0.080	0.160
	RC frame buildings with open ground storey	4	0.093	0.002	0.002	0.095	0.018	0.039	0.027	0.054	0.040	0.080
		10	0.001	0.028	0.002	0.030	0.034	0.068	0.051	0.101	0.076	0.152
	RC frame buildings with front bay open in ground storey	4	0.000	0.082	0.001	0.082	0.006	0.023	0.017	0.034	0.026	0.051
		10	0.001	0.030	0.001	0.031	0.029	0.058	0.043	0.087	0.065	0.130
	RC frame buildings with three bays open in ground storey	4	0.0003	0.0368	0.0016	0.0812	0.017	0.034	0.026	0.051	0.039	0.077
		10	0.0005	0.0210	0.0008	0.0221	0.031	0.062	0.046	0.093	0.070	0.139

Shaded cells show that performance point could not be achieved, i.e. building is expected to collapse.

where, D_y, D_u are yield and ultimate displacement, respectively; V_y and V_u are base shear corresponding to yield and ultimate displacement and H is height of the building.

Table 5.12

Capacity curve parameters and performance point of RC frame buildings designed as SMRF with uniform and irregular infills

Direction	Design Level	No. of Storey	Capacity Curve Parameters				Spectral Displacement at Performance Point (*m*)			
			Yield Capacity Point		Ultimate Capacity Point		Zone IV (BIS 2002)		Zone V (BIS 2002)	
							DBE	MCE	DBE	MCE
			D_y/H	V_y/W	D_u/H	V_u/W	0.12 (*g*)	0.24 (*g*)	0.18 (*g*)	0.36 (*g*)
Longitudinal	RC frame buildings with uniformly placed URM infills	4	0.001	0.233	0.012	0.359	0.005	0.064	0.048	0.096
		10	0.001	0.100	0.008	0.135	0.020	0.107	0.080	0.161
	URM infilled RC frame buildings with open ground storey without any consideration of relevant provisions of Indian Standard (BIS 2002)	4	0.003	0.213	0.009	0.224	0.024	0.068	0.036	0.102
		10	0.001	0.073	0.008	0.131	0.030	0.118	0.089	0.177
	URM infilled RC frame buildings with open ground storey, designed and detailed as per BIS (2002)	4	0.002	0.315	0.010	0.478	0.014	0.051	0.021	0.077
		10	0.001	0.096	0.008	0.142	0.019	0.096	0.072	0.144
	URM infilled RC frame buildings with front bay open in ground storey	4	0.002	0.175	0.007	0.216	0.006	0.091	0.009	0.137
		10	0.001	0.084	0.010	0.134	0.019	0.131	0.098	0.197
	URM infilled RC frame buildings with three bays open in ground storey	4	0.002	0.175	0.007	0.216	0.011	0.112	0.017	0.168
		10	0.001	0.085	0.010	0.133	0.019	0.131	0.098	0.197
Transverse	RC frame buildings with uniformly placed URM infills	4	0.001	0.190	0.010	0.277	0.006	0.062	0.047	0.093
		10	0.001	0.064	0.010	0.079	0.028	0.028	0.021	0.042
	URM infilled RC frame buildings with open ground storey without any consideration of relevant provisions of Indian Standard (BIS 2002)	4	0.003	0.007	0.007	0.206	0.021	0.064	0.032	0.096
		10	0.002	0.058	0.010	0.079	0.036	0.108	0.054	0.162
	URM infilled RC frame buildings with open ground storey, designed and detailed as per BIS (2002)	4	0.002	0.244	0.008	0.304	0.014	0.029	0.021	0.061
		10	0.001	0.065	0.008	0.083	0.026	0.090	0.039	0.135
	URM infilled RC frame buildings with front bay open in ground storey	4	0.001	0.154	0.007	0.256	0.011	0.131	0.098	0.197
		10	0.002	0.069	0.011	0.069	0.028	0.100	0.042	0.150
	URM infilled RC frame buildings with three bays open in ground storey	4	0.001	0.154	0.007	0.256	0.011	0.131	0.017	0.197
		10	0.001	0.050	0.008	0.075	0.030	0.099	0.075	0.149

Shaded cells show that performance point could not be achieved, i.e. building is expected to collapse.

where, D_y, D_u are yield and ultimate displacement, respectively; V_y and V_u are base shear corresponding to yield and ultimate displacement and H is height of the building.

Incremental Dynamic Analysis (IDA) is a relatively new concept of parametric analysis, first introduced by Vamvatsikos and Cornell (2002) and further developed by (Vamvatsikos and Cornell 2005b; Han and Chopra 2006; Vamvatsikos and Cornell 2006; Zarfam and Mofid 2009), in which sway collapse mechanism of the structure is simulated to estimate structural performance more thoroughly under seismic loads. In IDA, the analytical model of a structure is subjected to a ground motion record, and the non-linear dynamic analysis is repeated, each time increasing the scale factor on the ground motion's intensity, until that record causes structural collapse in a side-sway mode. This process is then repeated for an entire suite of ground motion records, to capture the record to record variability in the response. The outcome of the IDA procedure is a curve between the intensity measure (IM) (usually, S_a (T_1)) and the damage measure (DM) (usually, the spectral displacement, S_d). The IDA curves thus obtained can be combined statistically in multiple ways (Vamvatsikos and Cornell 2002). The advantage of IDA is that it addresses both demand and capacity of structures thus enabling thorough understanding of the nature of the structural response as the intensity range of ground motion increases e.g. changes in inter-storey drift, stiffness and strength degradation and their patterns, strength irregularities, considering record to record variability (Vamvatsikos and Cornell 2005b). This method is useful for determining structural behavior at multiple limit states. On the other hand, IDA is resource intensive (Vamvatsikos 2005a) requiring high level of skill and good understanding of inelastic behavior. IDA has been further extended by introducing a set of structural models in addition to the set of ground motion records to reflect epistemic (modeling) uncertainties. Liel et al. (2009) and Dolsek (2009) have considered both epistemic and aleatory uncertainties in the seismic response through a set of structural models and with extended IDA curves and dispersion measures. However, in the present study, Incremental Dynamic Analysis (IDA) method considering seismic hazard uncertainties with two design levels (GLD and SMRF), and two different heights (four and ten storey) is considered.

5.4.1 Selection of Ground Motion Records for IDA

Ground motion record selection is a major step in performing any nonlinear dynamic analyses due to the high sensitivity of dynamic response of the structure to the applied ground motions (Haselton 2009). The selected ground motions should be capable of

capturing all the intensity levels, frequency content, duration and all other parameters affecting seismic response of the structure. The ground motion parameters that affect structural performance depend on many factors such as source-site parameters, intensity, and duration of the event thus making it a challenging task to search for the most appropriate intensity measure with smaller dispersion in predicting seismic demand (Maniyar and Khare 2011). The influence of the number of records become important since the standard error of the mean estimate tends to fall with a rate of $1/\sqrt{N}$ where N is the number of records (Benjamin and Cornell 1970). Table 5.13 presents an overview of the requirement of minimum number of ground motion records for dynamic analysis, as prescribed in some major seismic building codes (BIS 2002; CEN 2004; NZS-1170.5 2004; ASCE-7 2010). Based on magnitude and source-site distance, different researchers have considered different numbers of ground motion records to estimate the IM corresponding to failure of frame structures under seismic action. Vamvatsikos and Cornell (2002) considered 20 time histories from a large magnitude and short distance suite. Similarly Ibarra and Krawinkler (2004) considered four different suites to represent a combination of large and small magnitude earthquakes with large and small source to site distances, resulting into a total of 80 time histories. Chopra and Chintanapakdee (2004) considered 13 suites for different magnitudes and source to site distances, which resulted in 232 time histories. Shome and Cornell (1999) mentioned that 10–20 records are usually enough to provide sufficient accuracy in the estimation of seismic demands for mid-rise buildings, assuming a relatively efficient IM, like spectral acceleration, S_a (T_1; 5%). They have also shown that to obtain an estimate of the median (geometric mean, defined as the exponential of the arithmetic mean of the log demand estimates) response within a factor of ± X (e.g. ± 0.1) with the accuracy of 95% confidence, the number of records (N) required for the dynamic analysis is given by

$$N = \frac{4\beta^2}{X^2} \tag{5.7}$$

where, β is the dispersion from the median.

Table 5.13

Requirement of the minimum number of ground motion records, in some major seismic building design codes

Reference	Minimum numbers of ground motion requirement
BIS (2002)	Appropriate ground motion
Eurocode-8 (2004)	7
NZS-1170.5 (2004)	3
ASCE-7 (2010)	3 and 7 records for using envelope and average response of the scaled selected records, respectively

In the absence of a consensus on the number of ground motion records required, in the present study, a total of 12 time histories have been randomly selected from available database of Indian earthquake records (Department of Earthquake Engineering, Indian Institute of Technology Roorkee, www.pesmos.in), as "the structural response is conditionally independent of the ground motion characteristics such as magnitude and source to site distance for a given seismic intensity level" even under the most extreme cases (Shome and Cornell 1999). Both the horizontal components of each record have been considered in orthogonal directions of the building, as the asymmetric O3B building has torsion irregularity. Details of the selected ground motions are presented in Table 5.14. Records having very low amplitude and duration were not considered. The selected records were classified into four magnitude (M) and source to site distance (R) bins. Bins have been designated as follows:

- Large Magnitude–Long Distance bin (LMLD; $M \geq 6.1$, $40\ km < R \leq 250\ km$)
- Large Magnitude–Short Distance bin (LMSD; $M \geq 6.1$, $R \leq 40\ km$)
- Small Magnitude–Long Distance bin (SMLD; $M \leq 6.0$, $40\ km < R \leq 250\ km$)
- Small Magnitude–Short Distance bin (SMSD; $M \leq 6.0$, $R \leq 40\ km$)

Table 5.14

Details of the ground motion records selected for IDA

Record ID	Sl No.	Earthquake Event	Direction	Station	Magnitude (*M*)	R (*km*)	PGA (*g*)
Bin 1 LMLD	1	1988 India Burma border	Longitudinal	Berlongfer	6.8	200.90	0.344
			Transverse		6.8	200.90	0.301
	2	1995 India Burma border	Longitudinal	Dimpu	6.4	215.91	0.102
			Transverse		6.4	215.91	0.081
	3	1990 India Burma border	Longitudinal	Berlongfer	6.1	230.00	0.145
			Transverse		6.1	230.00	0.142
Bin 2 LMSD	1	1991 Uttarkashi	Longitudinal	Uttarkashi	6.5	39.92	0.309
			Transverse		6.5	39.92	0.242
	2	1991 Uttarkashi	Longitudinal	Bhatwari	6.5	19.34	0.253
			Transverse		6.5	19.34	0.247
	3	1999 Chamoli	Longitudinal	Gopeshwar	6.4	8.70	0.359
			Transverse		6.4	8.70	0.199
Bin 3 SMLD	1	1986 N-E India	Longitudinal	Umsing	5.2	39.39*	0.101
			Transverse		5.2	39.39*	0.076
	2	1997 India Burma border	Longitudinal	Ummulong	5.7	70.63	0.155
			Transverse		5.7	70.63	0.101
	3	1988 India Bangladesh border	Longitudinal	Nogkhlaw	5.8	116.27	0.114
			Transverse		5.8	116.27	0.107
Bin 4 SMSD	1	1995 Chamba	Longitudinal	Chamba	4.9	8.20	0.146
			Transverse		4.9	8.20	0.125
	2	1986 N-E India	Longitudinal	Ummulong	5.2	12.83	0.113
			Transverse		5.2	12.83	0.064
	3	1986 Dhamashala	Longitudinal	Shahpur	5.5	9.98	0.248
			Transverse		5.5	9.98	0.204

* Marginal case between short and long distance.

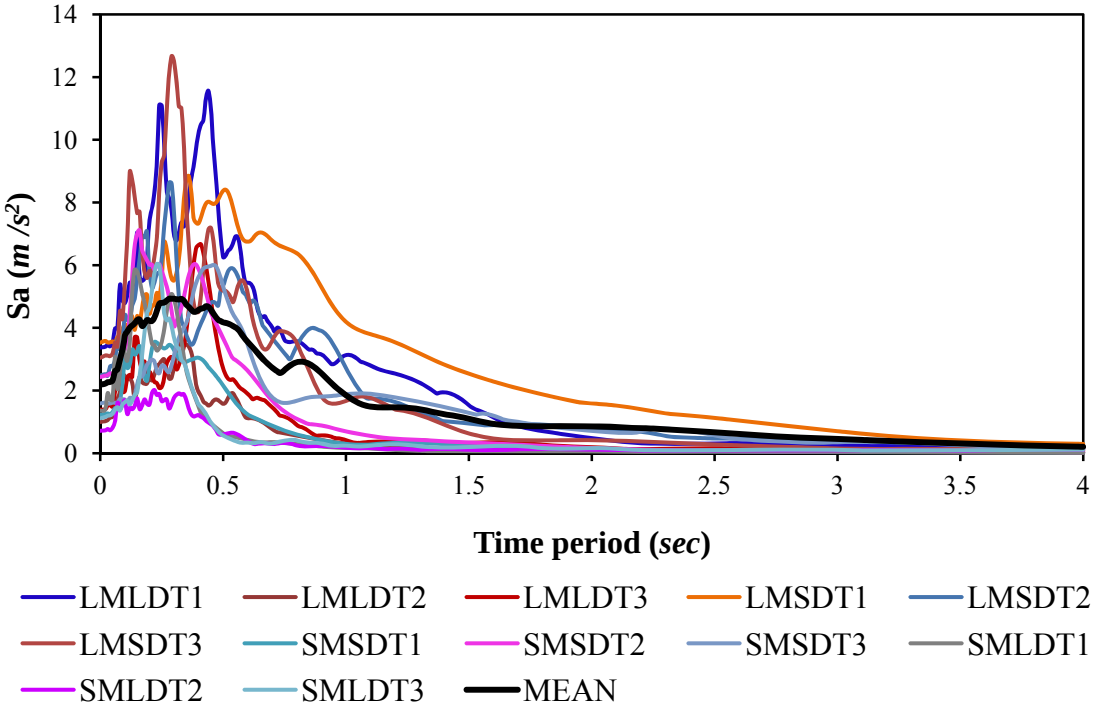

Fig. 5.28 Pseudo acceleration spectra of major components of ground motion records without scaling.

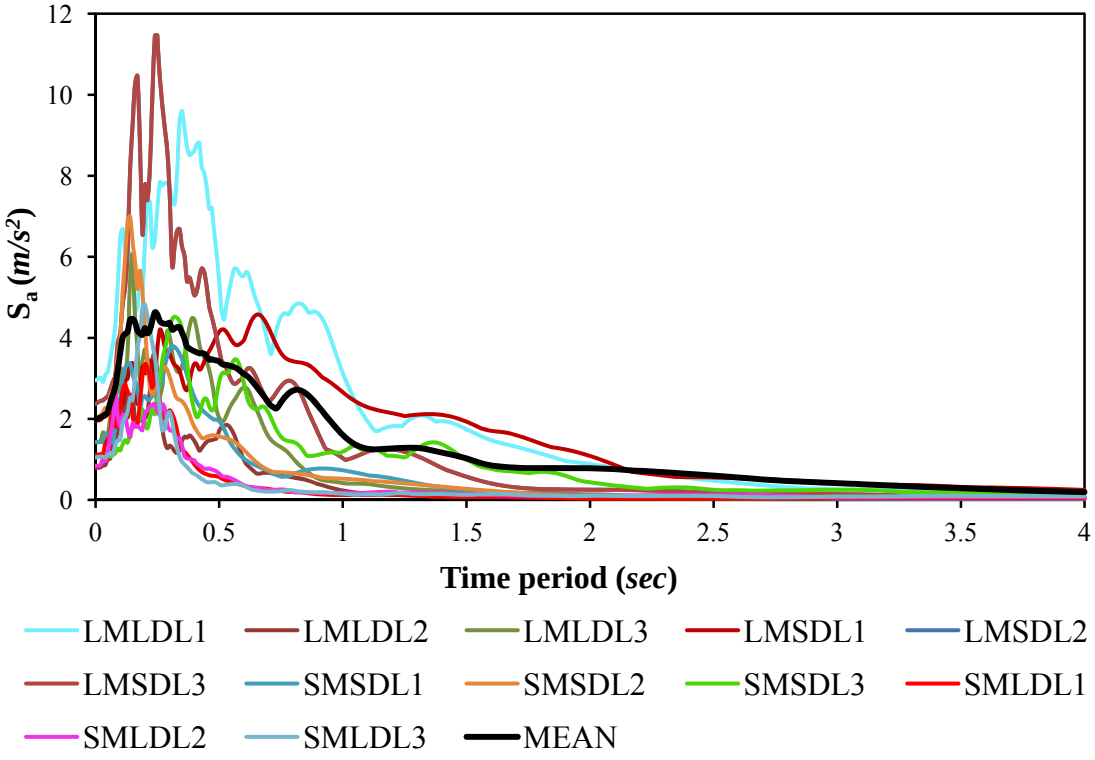

Fig 5.29 Pseudo acceleration spectra of minor components of ground motion records without scaling.

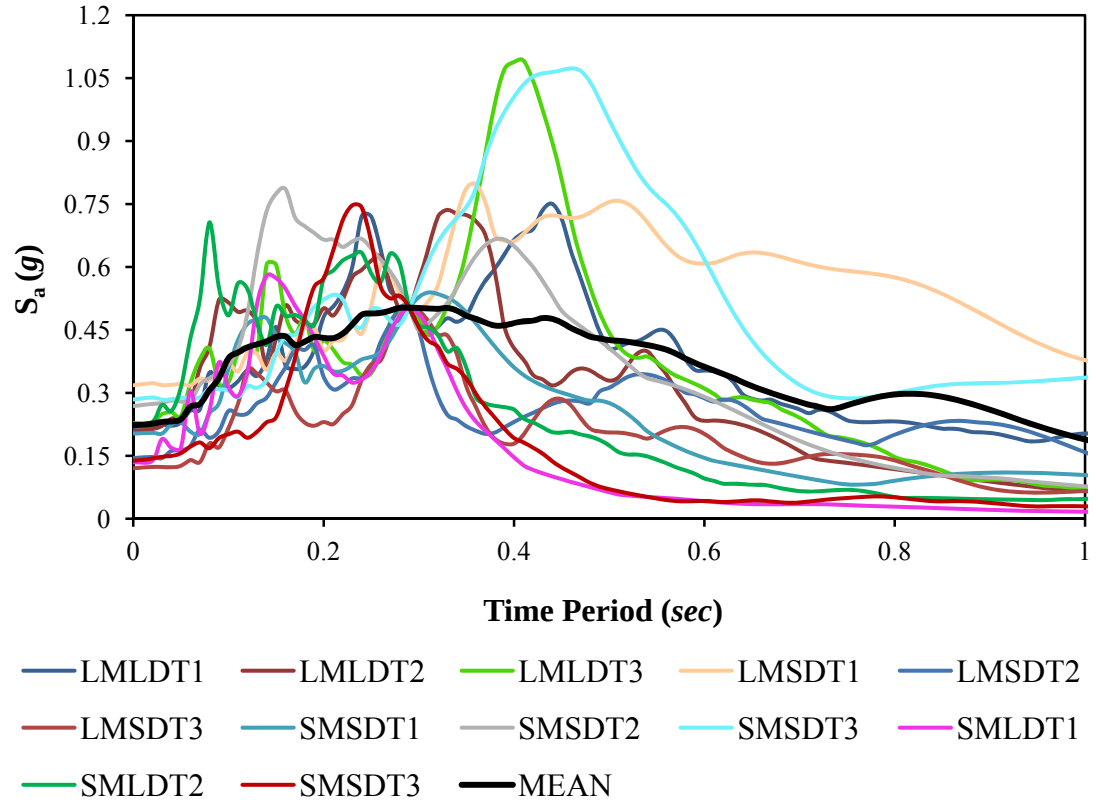

Fig 5.30 Pseudo acceleration spectra of the major components of the selected ground motions scaled to the mean spectral value at T_1=0.29 *sec*.

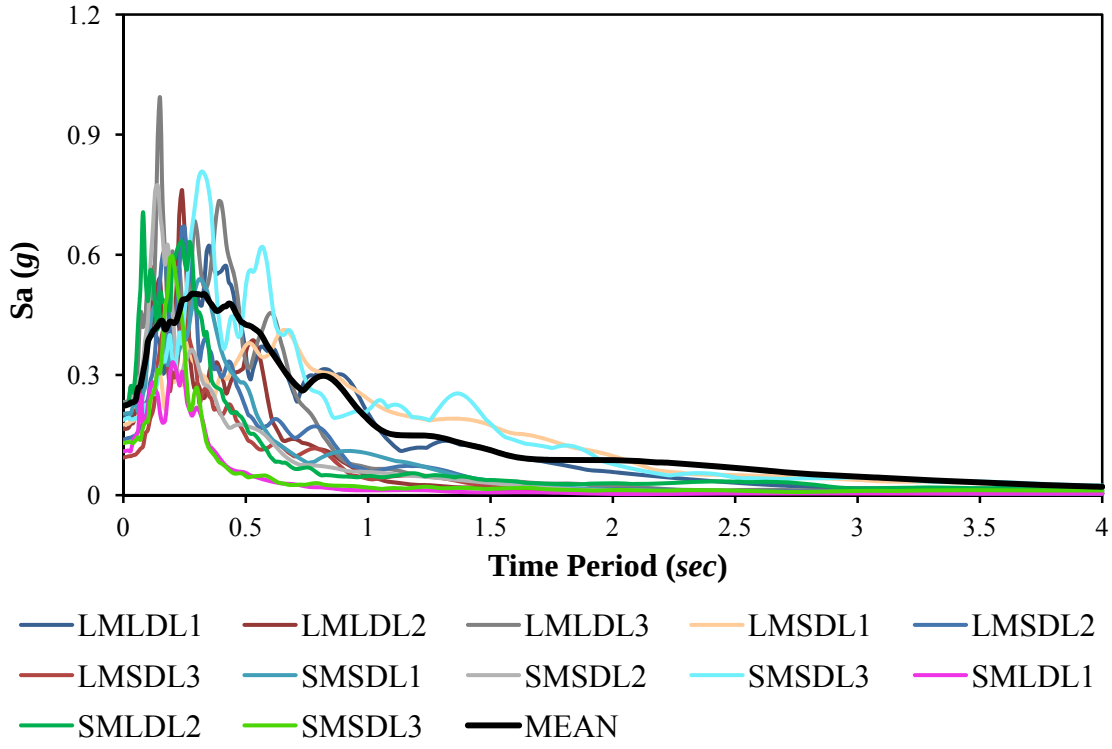

Fig 5.31 Pseudo acceleration spectra of the minor components of the selected ground motions, scaled by the factor of the major component spectral value at T_1 =0.29 *sec*.

Individual pseudo acceleration response spectra of major and minor components for all the twelve ground motion records selected in the present study for IDA are shown in Figures 5.28 and 5.29, respectively. The component having higher PGA value has been considered as the major component of the ground motion. Major component of each ground motion shown in Fig. 5.28 is normalized to the mean spectral acceleration of the major component of all the selected records, at the fundamental period of the building to be analyzed $[S_a(T_1)]$. The minor components of the selected ground motions are then normalized by the same scale factor as obtained for the major component of the particular ground motion. Figs. 5.30 and 5.31 show the pseudo acceleration spectra of major and minor components, respectively, of different ground motions considered in the present study, scaled to mean of the major spectral acceleration value at fundamental period (T_1=0.29 *sec*) of the four storey GLD building with three bays open in the ground storey (O3B). Similar scaling of the entire suite of selected ground motions has been done corresponding to the fundamental periods the other buildings with different design levels and heights. The analytical models of the buildings are then subjected to normalized ground motion records, and the non-linear dynamic analysis is repeated, each time increasing the scale factor on the ground motion's intensity, until that record causes structural collapse. This process is then repeated for an entire suite of ground motion records, to capture the record to record variability in the response.

5.4.2 Dynamic Capacity Curves of Irregularly Placed Infilled Frame Buildings

Figures 5.32 and 5.33 show the IDA curves of the four and ten storey RC frame buildings designed for gravity loads only (BIS 1987 (Part 1), 1987 (Part 2), 2000) with open three bays in the ground storey (O3B). Each curve represents the seismic demand imposed on the building by each time history at varying intensity (represented by spectral acceleration at fundamental period). Choice of intensity and damage measure is an important issue in IDA (Shome and Cornell 1999; Luco and Cornell 2007). Shome and Cornell (1999) have shown that first (fundamental) mode spectral acceleration $[S_a(T_1)]$ as intensity measure, reduces the scatter in response and can provide good demand and capacity estimates with a few ground motion records. Accordingly, $[S_a(T_1)]$ has been considered as the ground motion intensity measure in the present study. The IDA is used to find the response in terms of roof displacement

(damage measure) at each level of intensity measure. The IDA curves of the four and ten storey RC frame buildings designed as SMRF (BIS 1987 (Part 1), 1987 (Part 2), 1993, 2000, 2002) with three bays open in ground storey (O3B) are shown in Figs. 5.34 and 5.35.

It can be observed from Figs. 5.32-5.35 that IDA curves are linear within elastic range, whereas some of the ground motions result in weaving curves in the inelastic range of response. This weaving behaviour is more pronounced in case of SMRF buildings, as compared to those designed for gravity loads only, which reached collapse state immediate after yielding. The four storey SMRF building can sustain about 10 times higher seismic intensity $\left[S_a(T_1)\right]$ in both longitudinal and transverse directions; and the roof displacement in longitudinal and transverse direction is 17 times and 14 times, respectively, of the corresponding gravity load designed building (Figs. 5.32 and 5.34). The effect of seismic design and detailing is even more pronounced in IDA curves with increase in height of the building. The ten storey SMRF O3B building sustained up to 16 times higher seismic intensity with 24 times higher ultimate displacement (Figs. 5.33 and 5.35), as compared to the corresponding gravity load designed building. However this observation is not valid for all the ground motion records.

The typical collapse mechanism of gravity load designed buildings with major component of ground motions acting in longitudinal direction is shown in Fig. 5.36 (four storey) and Fig. 5.37 (ten storey). Similar collapse mechanisms of four and ten storey SMRF O3B buildings are presented in Figs. 5.38 and 5.39, respectively. Figs. 5.36-5.39 show that the collapse mechanisms of both the four and ten storey gravity designed buildings are governed by brittle shear failure of a number of columns (Fig. 5.36), particularly ground storey columns (Fig. 5.37) at a very early stage, due to the asymmetric placement of infills in ground storey. On the other hand, SMRF buildings exhibit ductile flexural failure, and collapse is observed due to excessive plastic rotation. In case of the four storey SMRF O3B building, the exterior ground storey columns reached collapse limit state, whereas in case of the ten storey SMRF O3B building, collapse mechanism is formed due to yielding of beams after collapse of a large number of infill panels. The start of weaving behavior of the IDA curves is used to mark the onset of global instability (incipient collapse) for the concerned ground motion record.

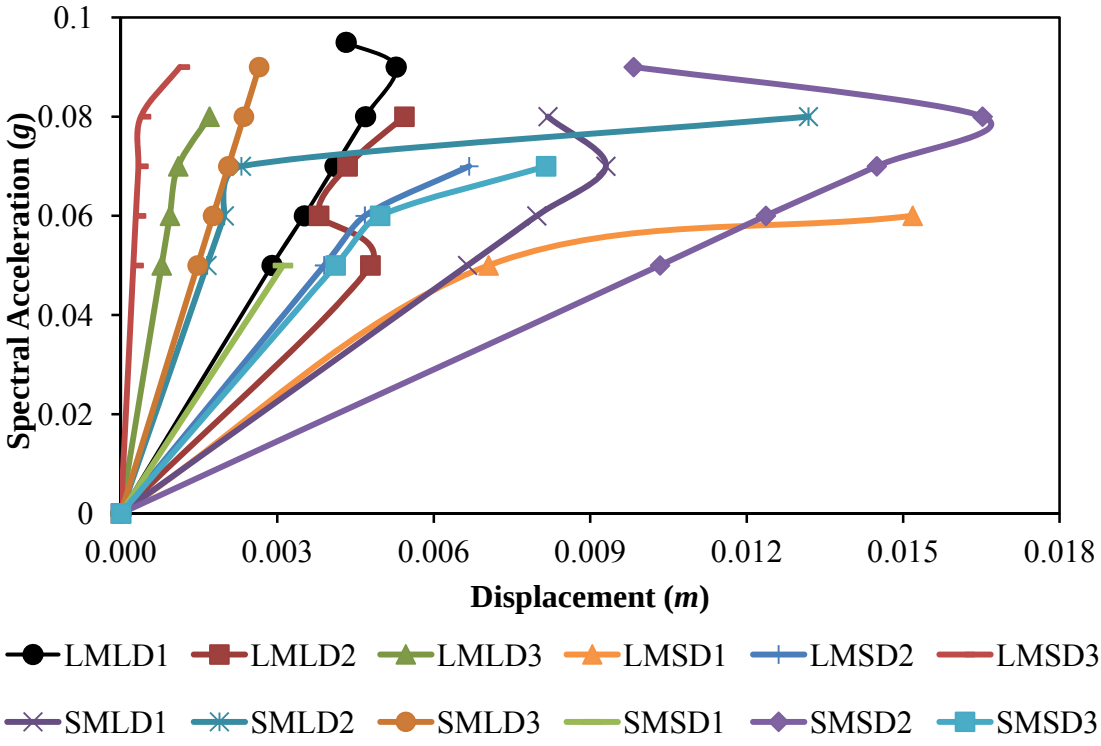

(a)

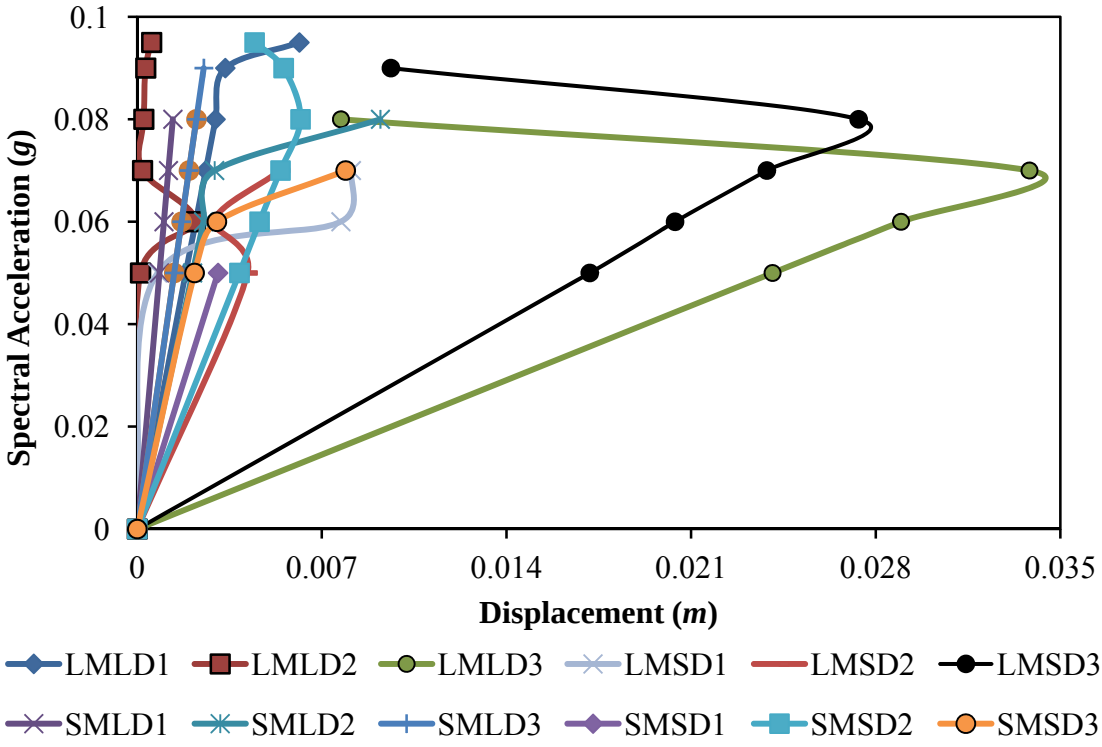

(b)

Fig 5.32 Dynamic response of the four storey building designed for gravity loads only, with open three bays in the ground storey, under the increasing excitation intensity of the four different bins of records scaled using the spectral acceleration at T_1=0.44 *sec*, in: (a) longitudinal direction; and (b) transverse direction.

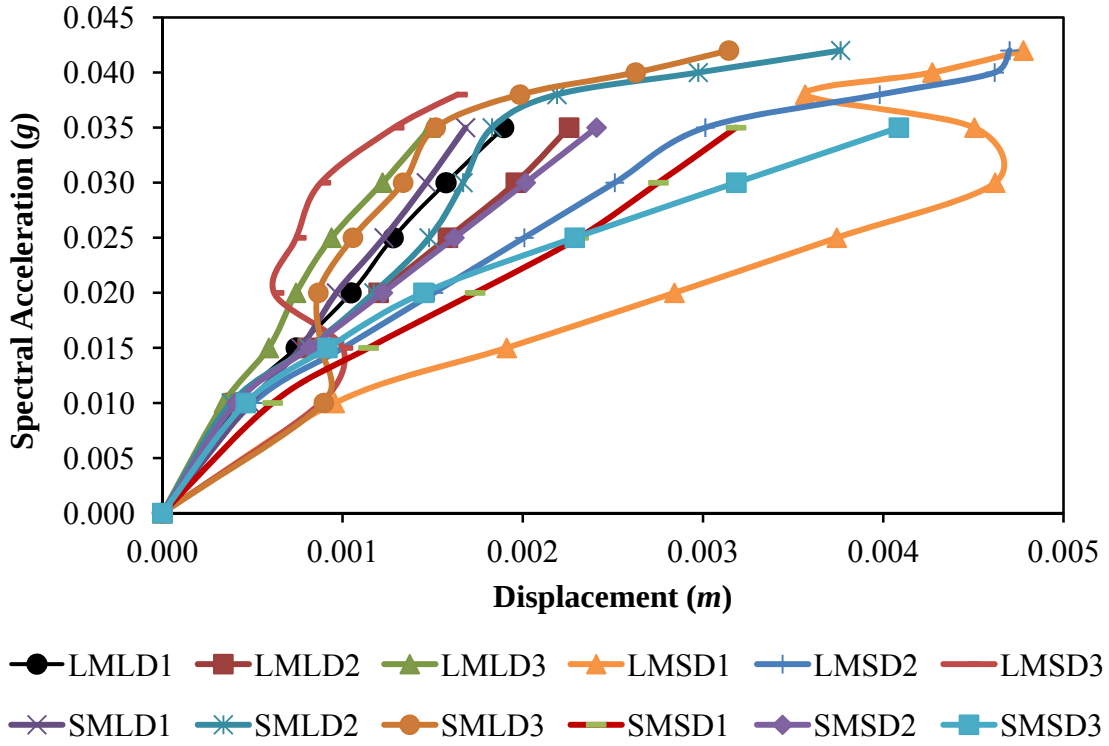

(a)

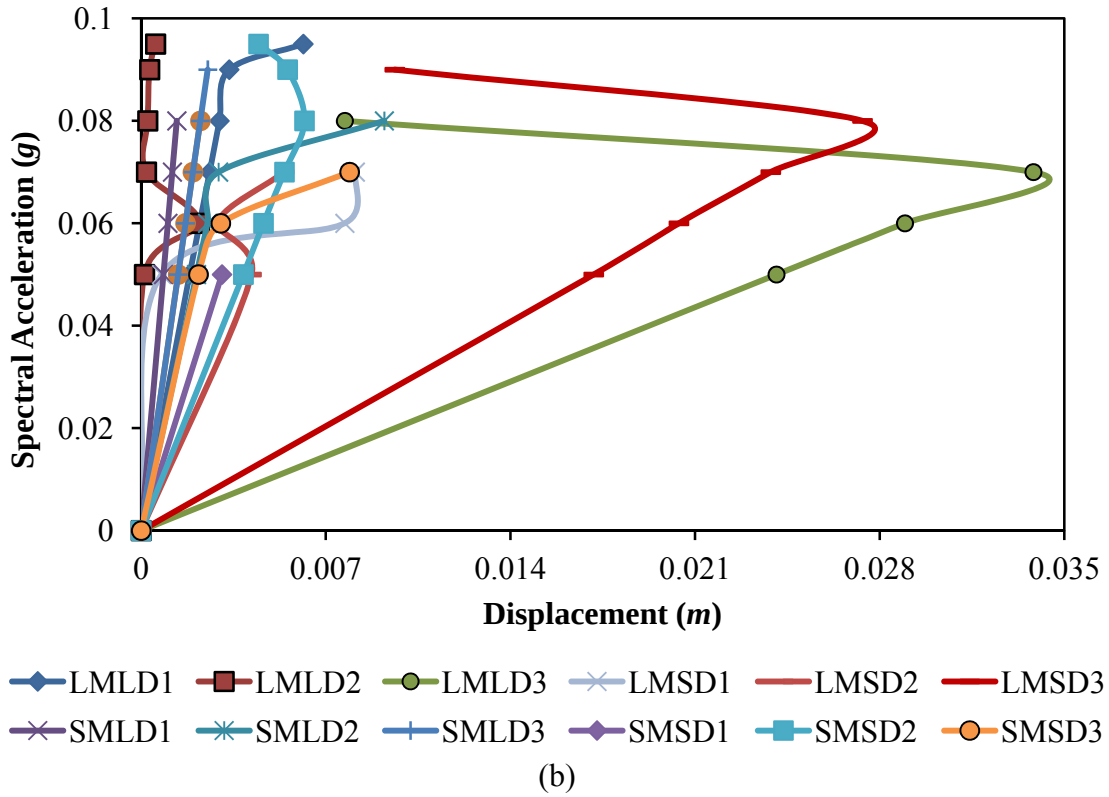

(b)

Fig 5.33 Dynamic response of the ten storey building designed for gravity loads only, with open three bays in the ground storey, under the increasing excitation intensity of the four different bins of records scaled using the spectral acceleration at T_1=0.93 *sec* in: (a) longitudinal direction; and (b) transverse direction.

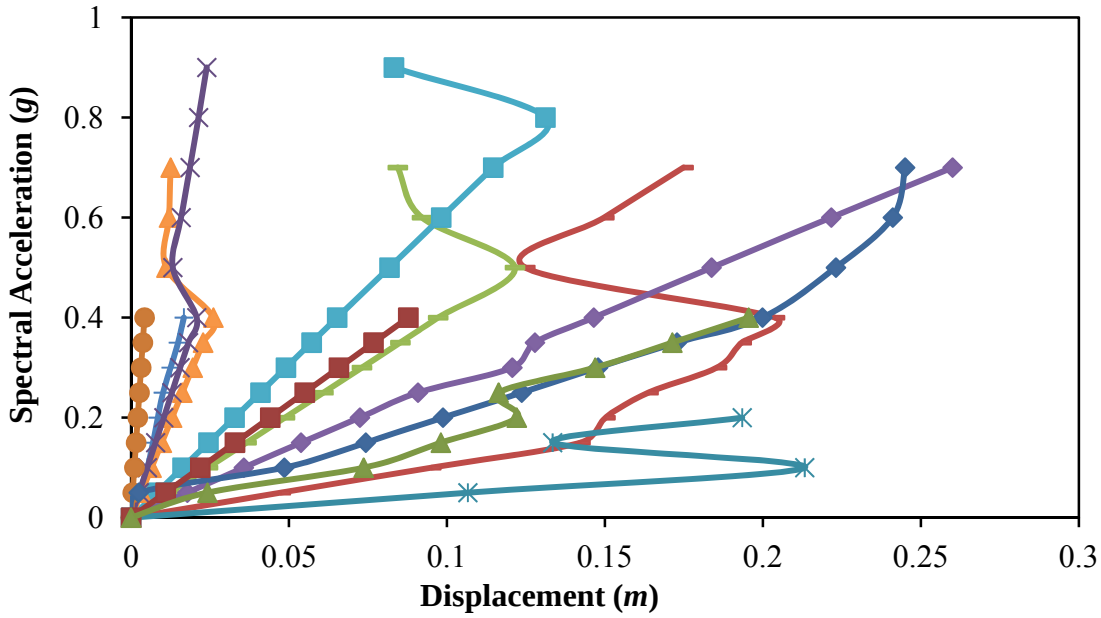

(a)

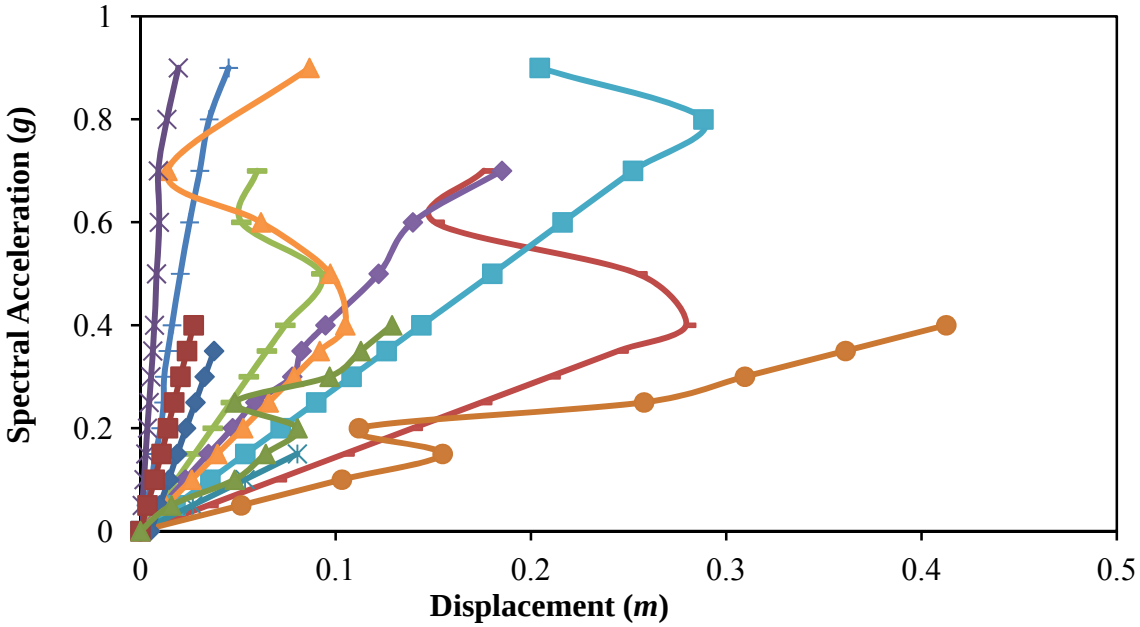

(b)

Fig 5.34 Dynamic response of the four storey SMRF building with open three bays in the ground storey, under the increasing excitation intensity of the four different bins of records, scaled using the spectral acceleration at T_1=0.29 *sec*, in: (a) longitudinal direction; and (b) transverse direction.

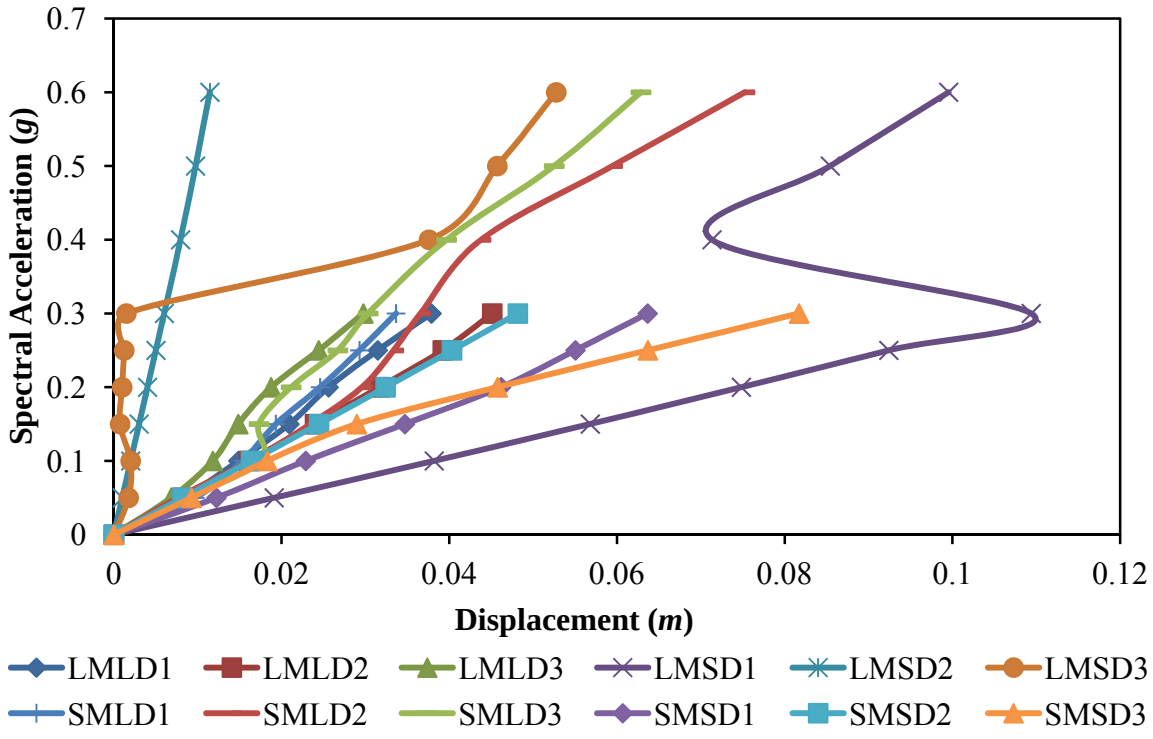

(a)

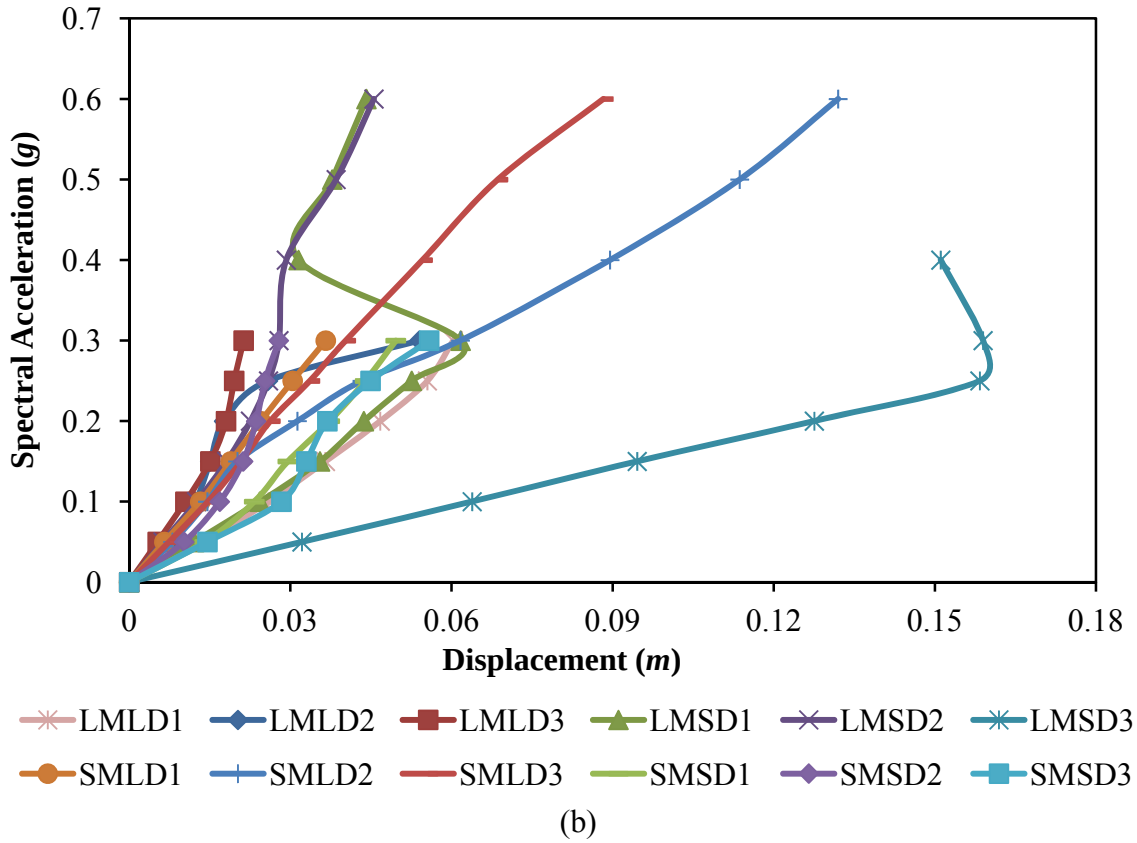

(b)

Fig 5.35 Dynamic response of the ten storey SMRF building with open three bays in the ground storey, under the increasing excitation intensity of the four different bins of records scaled using the spectral acceleration at T_1=0.75 *sec,* in: (a) longitudinal direction; and (b) transverse direction.

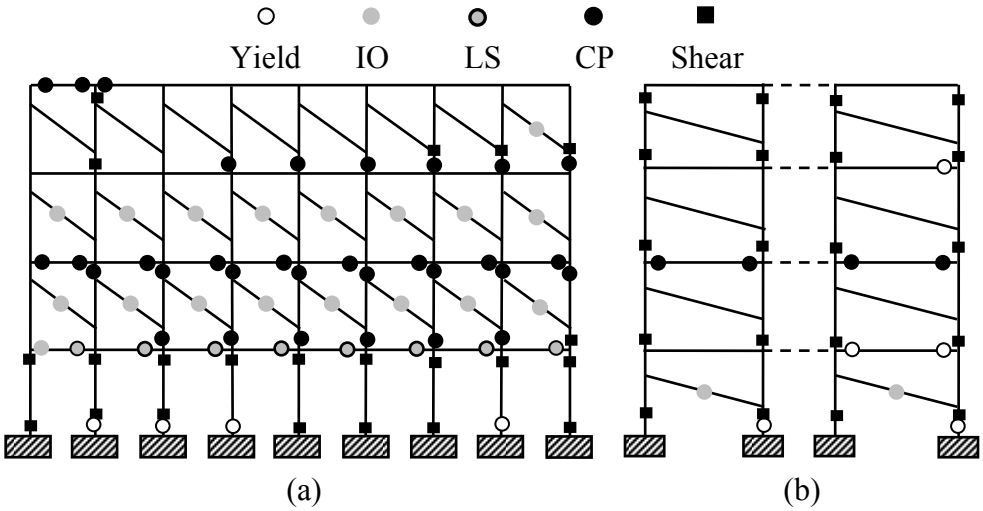

Fig. 5.36 Collapse mechanism of four storey gravity load designed RC frame building with three bays open in the ground storey under bi-axial seismic excitation with major component in longitudinal direction; typical exterior frame in: (a) longitudinal direction; (b) transverse direction.

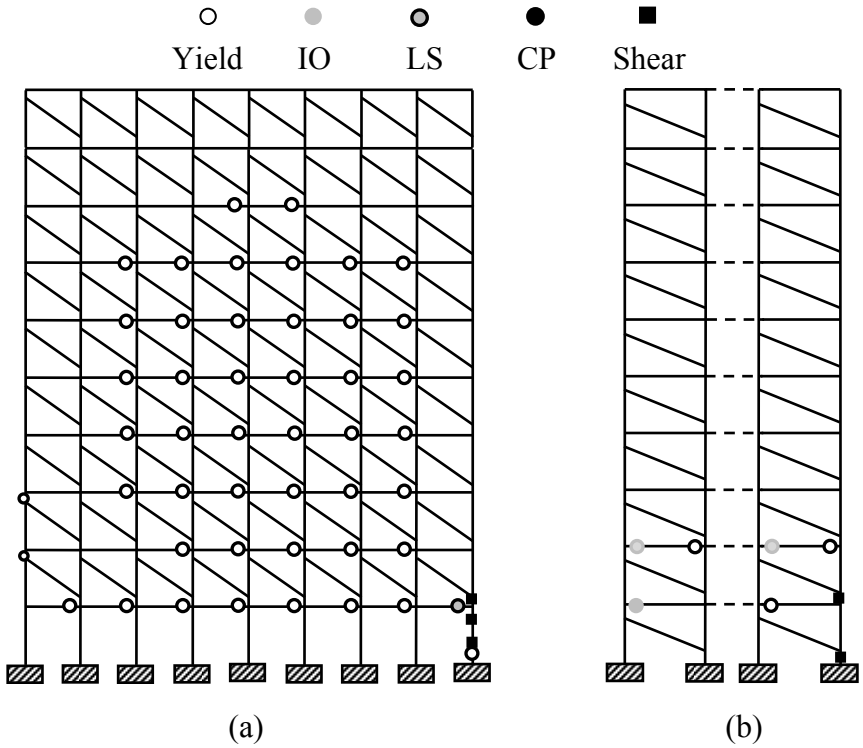

Fig. 5.37 Collapse mechanism of the ten storey gravity load designed RC frame building with three bays open in the ground storey under bi-axial seismic excitation with major component in longitudinal direction; typical exterior frame in: (a) longitudinal direction; (b) transverse direction.

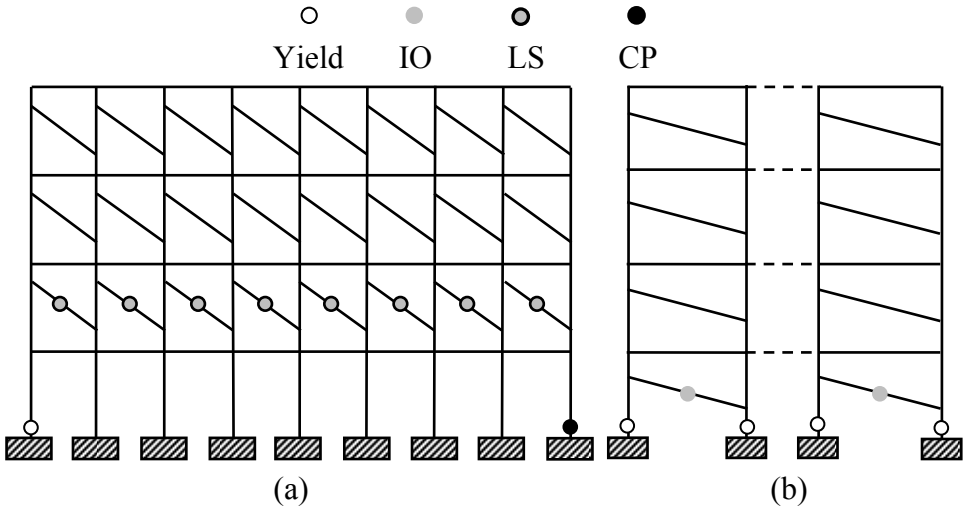

Fig. 5.38 Collapse mechanism of the four storey SMRF RC frame building with three bays open in the ground storey under bi-axial seismic excitation with major component in longitudinal direction; typical exterior frame in: (a) longitudinal direction; (b) transverse direction.

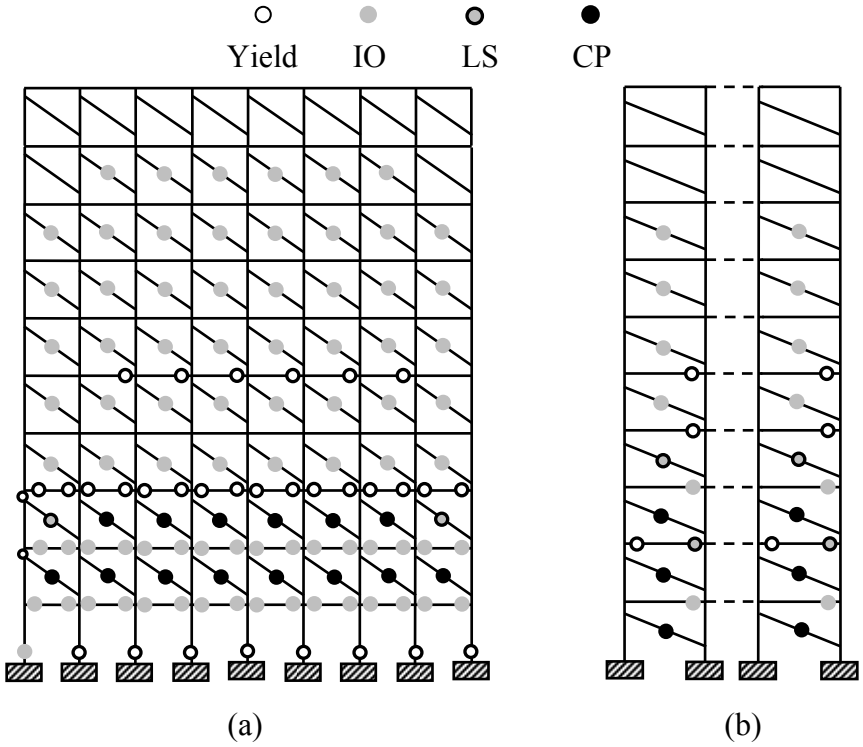

Fig. 5.39 Collapse mechanism of the ten storey SMRF RC frame building with three bays open in the ground storey under bi-axial seismic excitation with major component in longitudinal direction; typical exterior frame in: (a) longitudinal direction; (b) transverse direction.

The IDA curves presented in Figs. 5.32-5.35 show a large record-to-record variability. The ensemble of IDA curves is represented by the median, 16%, and 84% dynamic capacity curves presented in Figs. 5.40 and 5.41, for four and ten storey gravity load designed buildings, respectively. The dynamic capacity curves of four and ten storey SMRF O3B buildings are summarized in Figs. 5.42 and 5.43, respectively.

In case of four storey gravity load designed O3B building (longitudinal direction), 16%, 50% and 84% IDA curves remain linear up to elastic range till 0.03*g* but after yielding these started softening in the range of 0.05*g*–0.15*g* and finally, a collapse mechanism (as shown in Fig. 5.36) is formed. Beyond this point, numerical divergence has been encountered during analysis. Similar behaviour is observed in case of ten storey gravity load designed O3B building also. SMRF buildings sustain larger acceleration and undergo large drift before collapse. Both for four and ten storey SMRF O3B buildings, the softening and hardening behaviour is repeated several times. This weaving is attributed to the ductile failure mechanism of SMRF buildings as presented in Figs. 5.38 and 5.39.

The dynamic pushover curves obtained from IDA are compared with the static pushover curves of RC infilled frame buildings with three bays open in the ground storey designed as per BIS (2002), considering the torsional irregularity. Figs. 5.40-5.43 compare the dynamic pushover curves (16%, 50% and 84% IDA curves) with static pushover curve. For the purpose of comparison, static pushover curves (plot of base shear versus roof displacement) are transformed into the intensity and damage measure of IDA. The roof displacement is converted into average interstorey drift ratio by dividing with height of the building (H), while the base shear is converted to spectral demand acceleration by diving with seismic weight of the building (W) times modal mass coefficient (α_m) (or fraction of the building's weight effective in the pushover mode). By plotting static and dynamic pushover curves in a single graph, it is observed that the median dynamic curve and static curve matches well in the elastic range. But, as expected, after yielding, but the two curves diverge, however, the ultimate drift ratios obtained from the two methods are close.

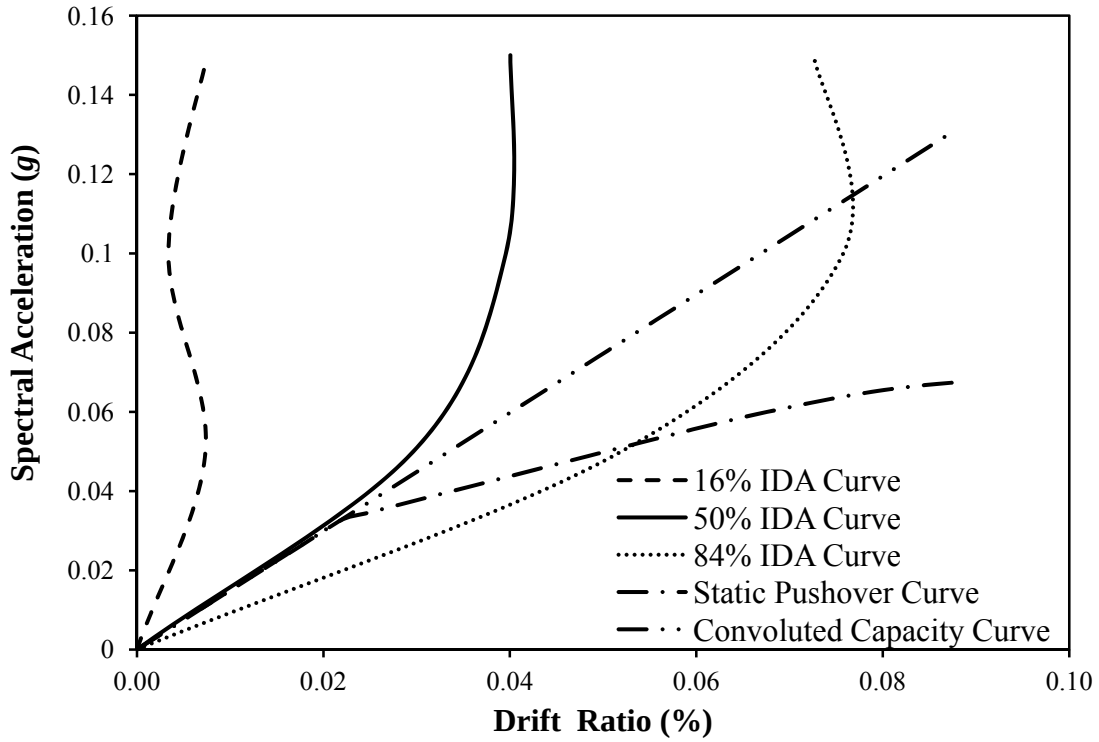

(a)

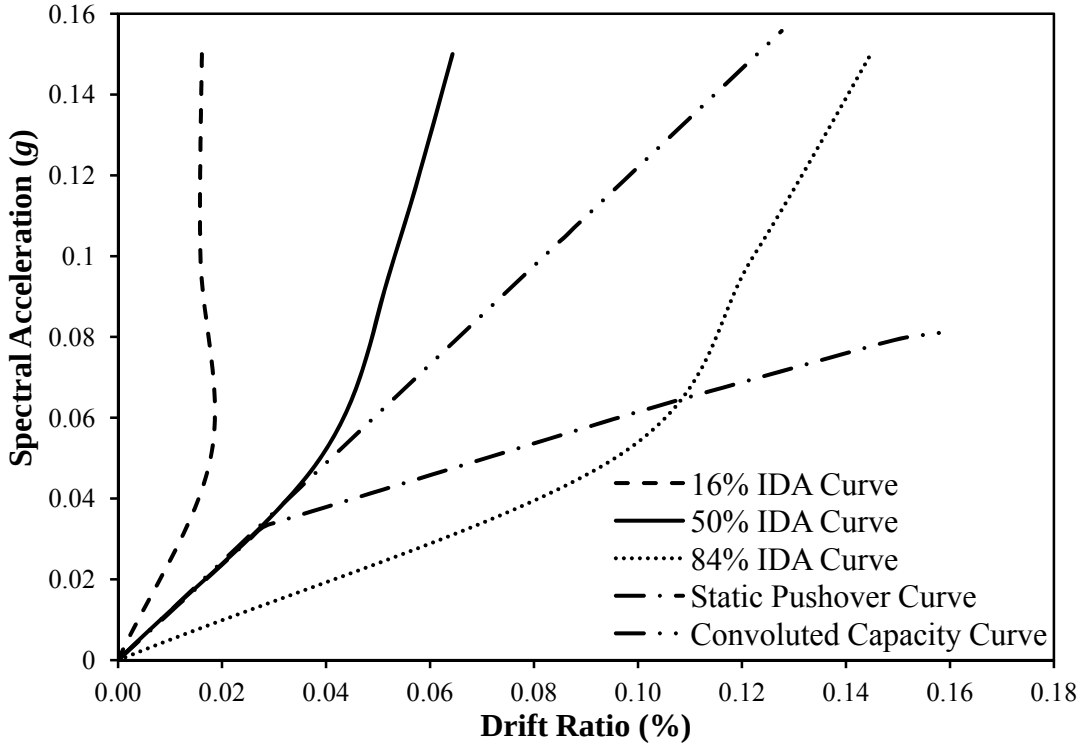

(b)

Fig. 5.40 Comparison of static and dynamic pushover curves for four storey gravity load designed infilled frame building, with three bays open in the ground storey: (a) longitudinal direction; and (b) transverse direction.

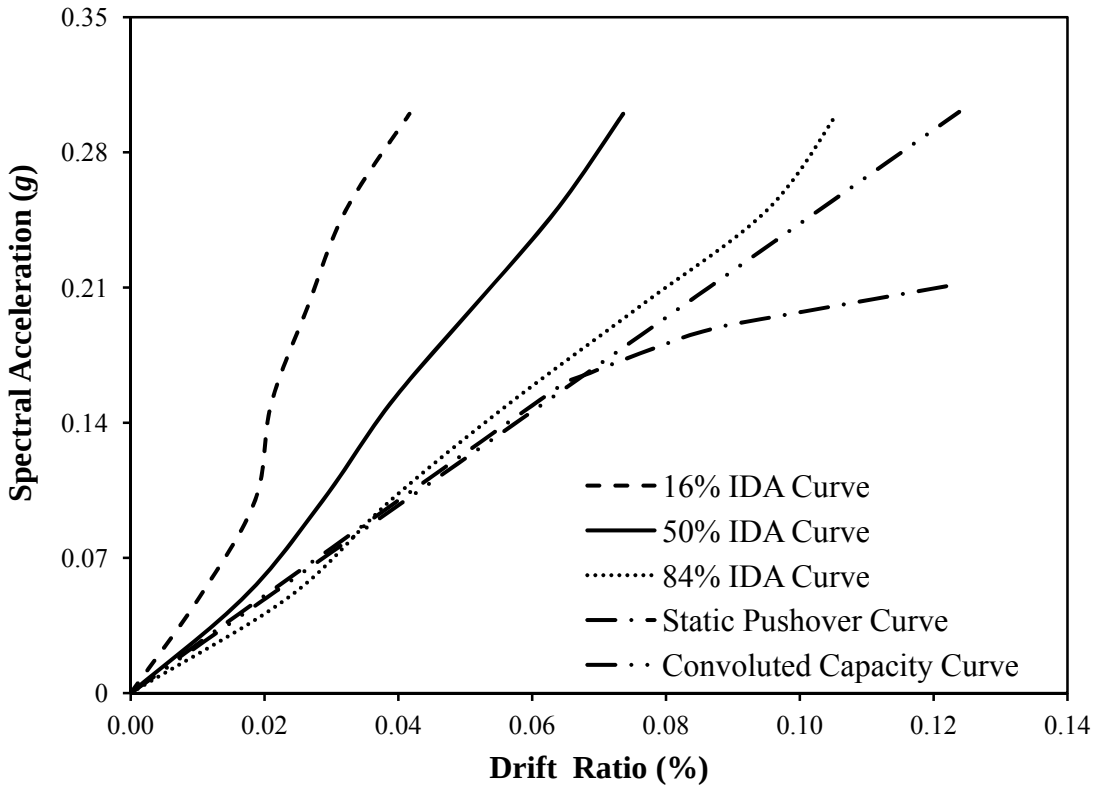

(a)

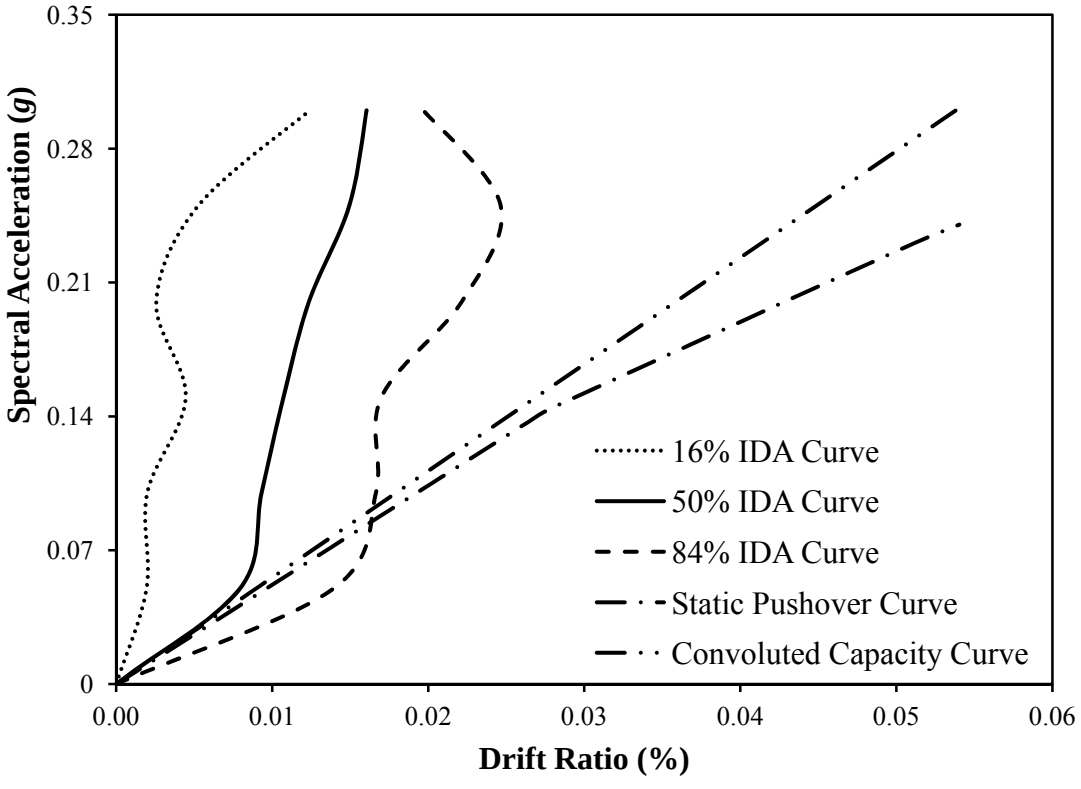

(b)

Fig. 5.41 Comparison of static and dynamic pushover curves for ten storey gravity load designed infilled frame building, with three bays open in the ground storey: (a) longitudinal direction; and (b) transverse direction.

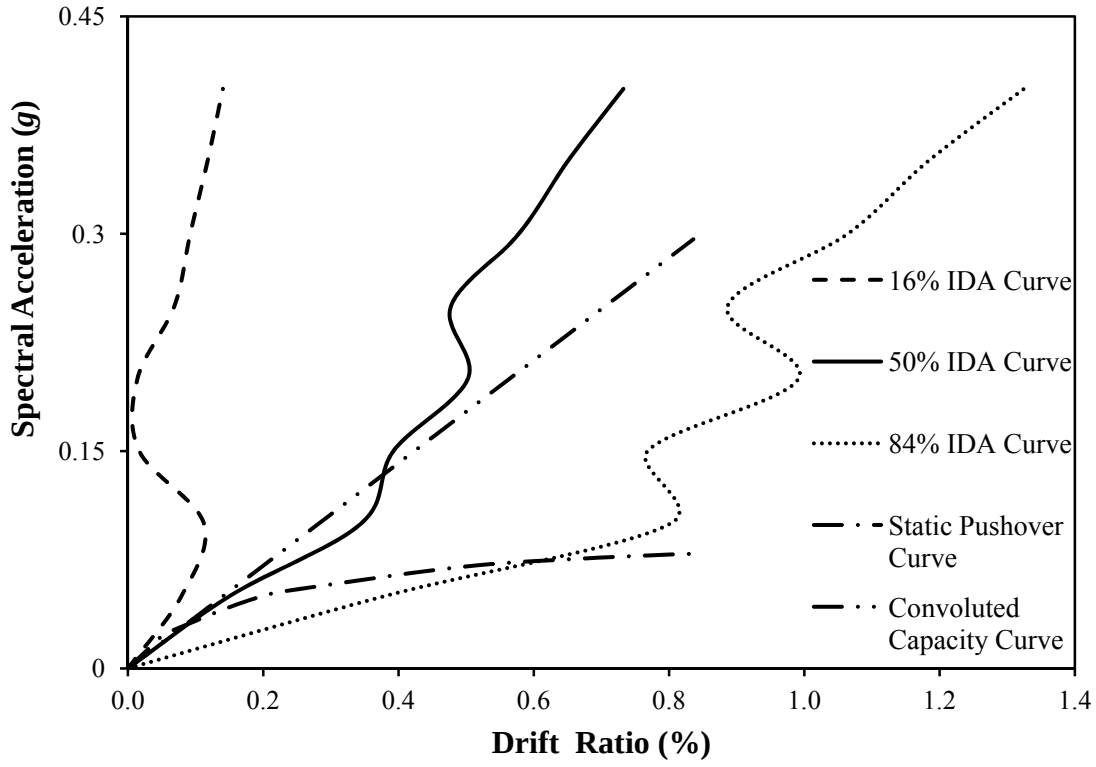

(a)

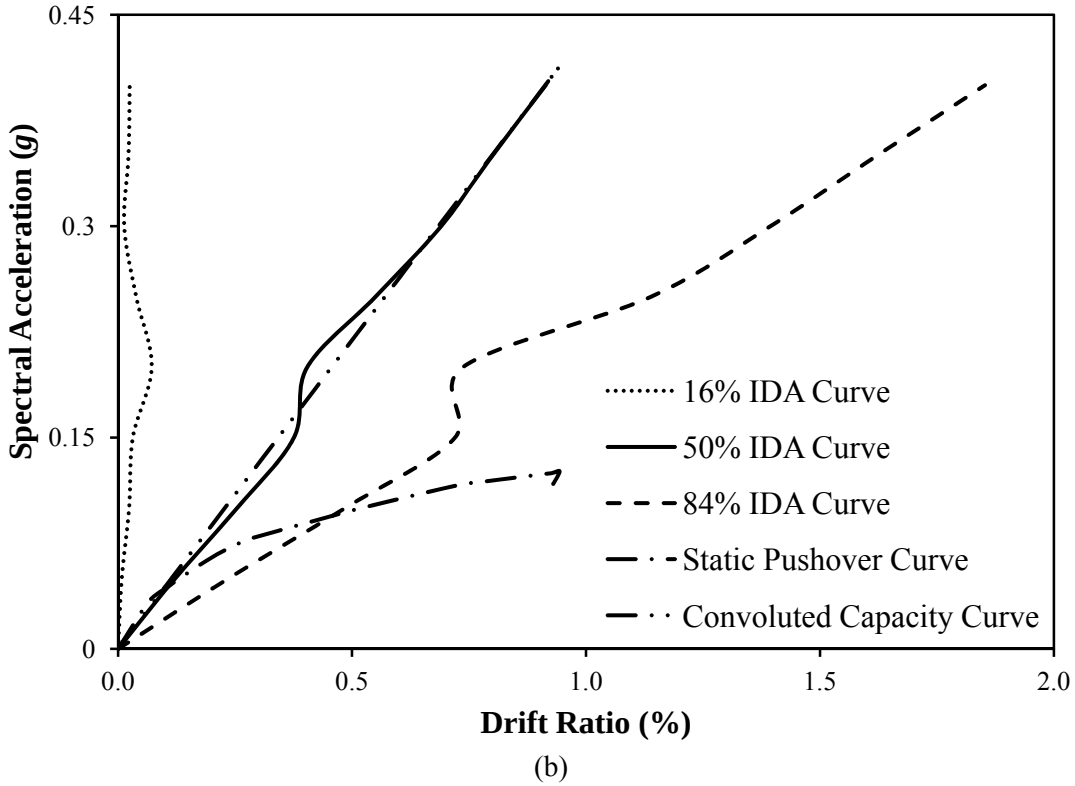

(b)

Fig. 5.42 Comparison of static and dynamic pushover curves for four storey SMRF infilled frame building, with three bays open in the ground storey: (a) longitudinal direction; and (b) transverse direction.

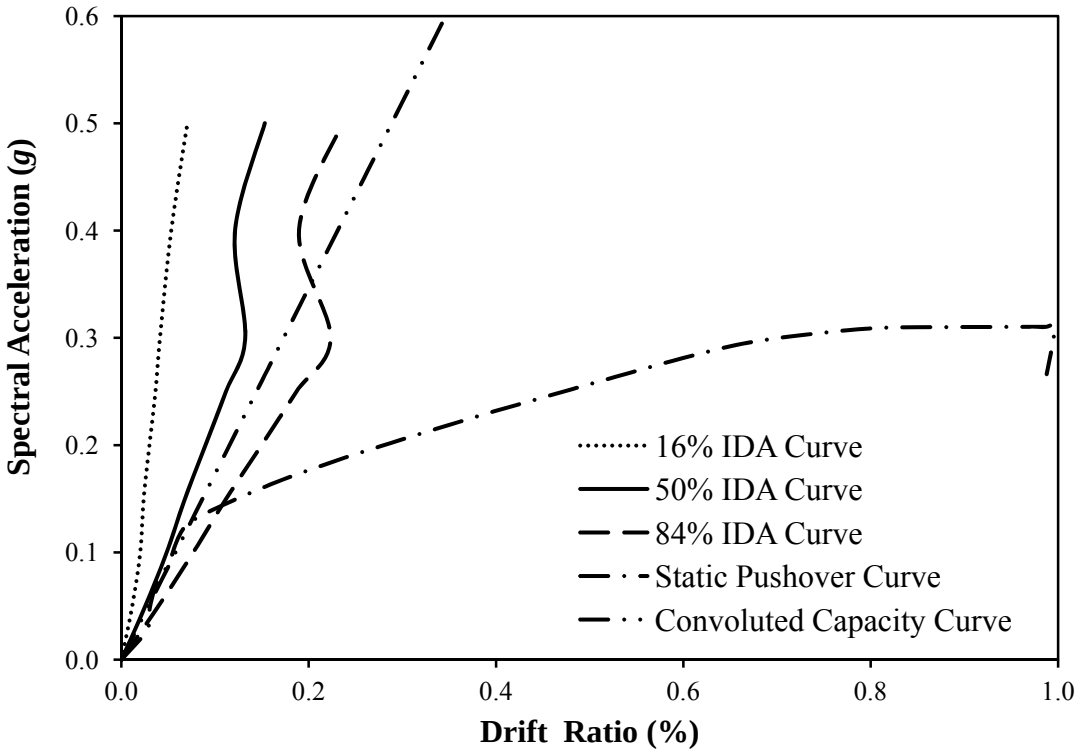

(a)

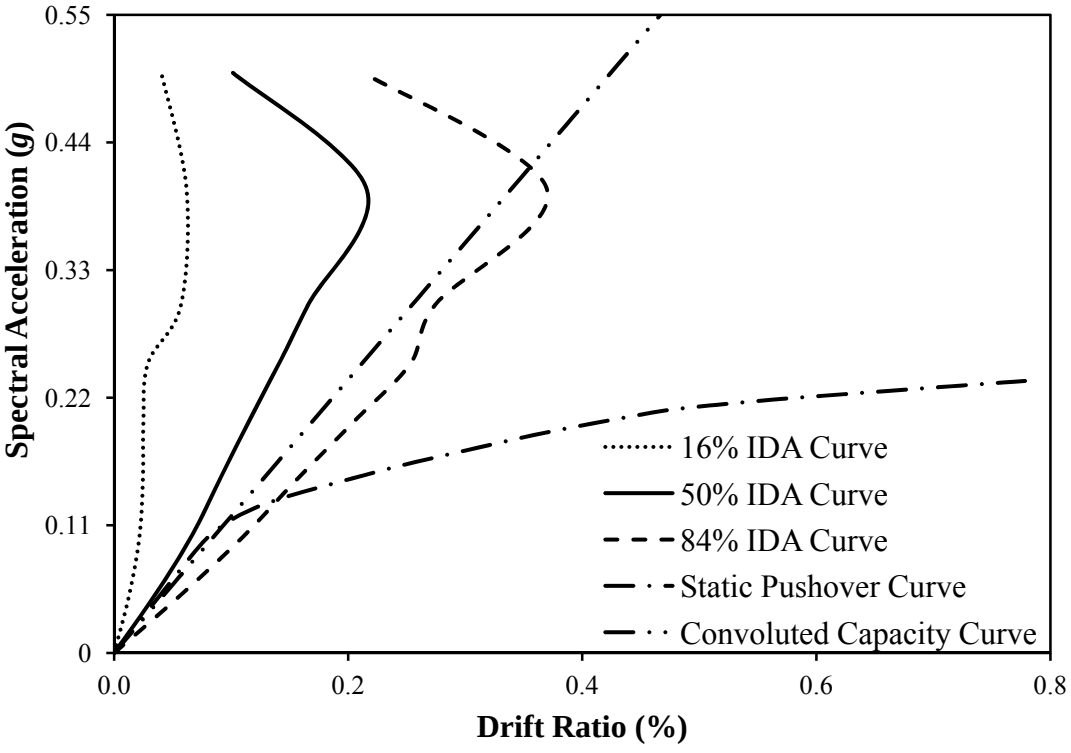

(b)

Fig. 5.43 Comparison of static and dynamic pushover curves for ten storey SMRF infilled frame building, with three bays open in the ground storey: (a) longitudinal direction; and (b) transverse direction.

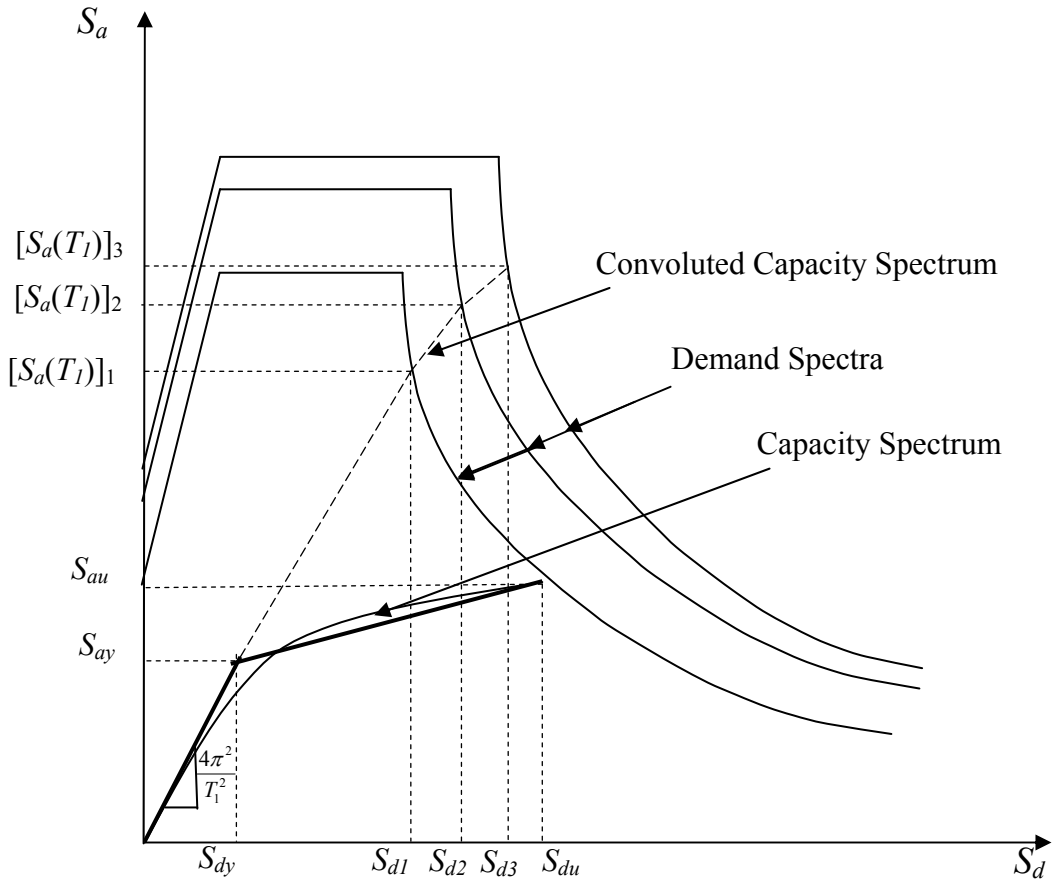

Fig. 5.44 Convolution of demand and capacity curves of a typical structure, represented in Acceleration-Displacement Response Spectra (ADRS) format.

However, it should be noted that the IDA curves represent a convolution of the demand on the structure and its capacity, whereas the pushover curves show only the capacity of the structure, and therefore cannot be compared directly. For the purpose of direct comparison, the pushover curves can be convoluted with the demand using Displacement Modification Method (Eqs. 4.10-4.13) or Equivalent Linearization Method. The convolution of demand with capacity of the building, converted to ADRS format (Capacity Spectrum) and idealized as a bilinear curve, is illustrated in Fig. 5.44. Capacity spectrum can be characterized by two control points, yield point (S_{dy}, S_{ay}), and ultimate point (S_{du} and S_{au}). $\left[S_a\left(T_1\right)\right]_i$ represent the seismic demand (in terms of 5% damped elastic spectral acceleration at fundamental period, T_1 corresponding to the inelastic spectral displacement S_{di}. Using the DMM of ASCE 41,

the elastic spectral acceleration demand corresponding to a given spectral displacement can be obtained as

$$\left[S_a(T_1)\right]_i = \frac{1}{C_1 C_2}\frac{4\pi^2}{T_1^2} S_{di} \tag{5.8}$$

where, T_1 is the effective fundamental period of the building, as shown in Fig. 5.45 and C_1 and C_2 are the modification coefficients as described in Section 4.6.1. Alternatively, the spectral acceleration can also be obtained directly from the roof displacement (Δ_{roof}), as

$$S_a(g) = \frac{\Delta_{\text{roof}}}{\left(C_0 C_1 C_2 \frac{T_1^{\,2}}{4\pi^2}\right)} \tag{5.9}$$

where, C_0 is modification factor to relate spectral displacement of an equivalent single degree of freedom (SDOF) system to the roof displacement of the building.

It can be observed from Figs. 5.40-5.43 that the convoluted capacity curve is quite close the median IDA curve, indicating that the static pushover method is adequate for the present case, despite being a torsionally irregular building.

5.5 SUMMARY

Seismic behavior of the three most common configurations of RC frame buildings with irregular placement of infills, viz. open ground storey, front bay open in the ground storey and three bays open in the ground storey, have been studied on the selected representative building with two design levels and two different heights. The eccentric single strut model of infills; and all possible failure modes of infill panels and surrounding frame members, identified earlier, have been considered for this purpose. It has been observed that the dynamic characteristics, strength and stiffness of the uniformly infilled frame are altered significantly by irregularly placed infills. SMRF open ground storey buildings designed as per relevant provisions of BIS (2002) for open ground storey have shown higher strength and plastic deformation capacity as compared to the SMRF open ground storey buildings designed without considering relevant provisions of BIS (2002) for open ground storey. The plastic

hinges in the ground storey columns lead to collapse in case of OG (NC) building, whereas, due to strengthening of the ground storey beams and columns of OG (C) buildings, collapse mechanism is caused by the plastic hinges in upper storey columns. The open ground storey buildings designed for code (i.e. ground storey columns and beams designed for 2.5 times the normal base shear) are able to attain the stiffness and strength close to those of the corresponding uniformly infilled frame building. The estimated performance of such buildings is slightly better than the uniformly infilled frame buildings, indicating the adequacy of the code provisions for open ground storey buildings. As expected, the OG (NC) buildings (both four and ten storey) have shown the lowest strength and plastic deformation capacities among the three cases, considered. It has been observed that none of the infilled frame buildings (with regular as well as irregular placement of infills) designed for gravity loads only could survive DBE excitation of Seismic Zone III whereas the buildings designed as SMRF for DBE of Indian Seismic Zone IV as per relevant Indian Standards having uniform and irregular infills can sustain seismic excitation upto MCE of Indian Seismic Zone V without collapse, except for the four storey RC frame buildings with three bays open in ground storey, subjected to earthquake in longitudinal (asymmetric) direction. Seismic performance of the RC buildings with three bays open in the ground storey has been studied using Incremental Dynamic Analysis, also, with bi-directional ground motions for a wide range of source and site parameters. Comparison of dynamic and static pushover curve revealed that the median dynamic pushover (IDA) curve and static pushover curve match quite well in the elastic range but there is divergence in the inelastic range. However, the ultimate drift ratios predicted by the static and dynamic procedure are of the same order. Since, the IDA curves represent a convolution of the demand on the structure and its capacity, whereas the pushover curves represent only the capacity of the structure, the static (pushover) capacity curves have been convoluted with the demand spectrum using DMM of ASCE 41. It has been observed that the convoluted static capacity curves are quite close to the median IDA curves, indicating reasonably accurate prediction of the seismic behaviour by pushover analysis, despite torsion irregularity in the considered building.

Chapter 6

SEISMIC VULNERABILITY OF INDIAN RC FRAME BUILDINGS

6.1 INTRODUCTION

Vulnerability assessment of existing housing stock is one of the crucial steps in seismic risk assessment of a community. A number of methodologies for vulnerability assessment based on empirical, analytical or hybrid approaches are available in literature. India has suffered several damaging earthquakes in past, but unfortunately adequate and systematic damage data for development of empirical vulnerability functions is not available. In such conditions, analytical vulnerability analysis is one of the available alternatives. Unreinforced Masonry (URM) buildings and URM infilled RC frame buildings are the most common building typologies in India. An attempt to develop the fragility functions for Indian URM buildings was made by Prasad (2009) and Singh et al. (2012). The present study is attempted at developing fragility functions for Indian RC frame buildings, which can be used in seismic risk assessment studies for Indian cities. The Indian RC frame buildings are characterized by widespread use of URM infills and a number of design and detailing deficiencies. In this study, effect of some of the common deficiencies on fragility of these buildings has also been investigated, vis-à-vis the buildings designed for Indian seismic codes.

Estimation of capacity curve parameters of representative buildings is a crucial step in fragility analysis. For reliable estimation of capacity curve parameters to develop analytical vulnerability functions, the ideal way is to carry out nonlinear analysis of a large sample of buildings of the chosen class and generate the statistical data to account for the variability in different parameters. It is numerically tedious and time expensive exercise, therefore to encompass the wide range of Indian infilled RC frame buildings; a field exercise was carried out to select representative building configurations, as presented in Section 3.5.1. The seismic behaviour of the representative buildings has

been simulated using the models proposed in Chapters 2 and 3, for URM infills and RC frames, and capacity spectra for different design levels and number of storeys have been developed in the previous Chapters. In this Chapter, an overview of the existing analytical methods for vulnerability assessment has been presented and the capacity spectra developed in Chapters 4 and 5 have been used to construct fragility functions for the RC frame buildings, with and without URM infills.

6.2 FRAGILITY ANALYSIS

Seismic vulnerability (or fragility) of a structure is described as its susceptibility to damage by the ground shaking of a given intensity. It is expressed as a relationship between the ground motion severity (i.e., intensity, PGA, or spectral displacement) and structural damage (expressed in terms of damage grades). For representing the vulnerability, fragility curves and Damage Probability Matrices (DPMs) are the most commonly used formats. Both methods describe the conditional probability of exceeding different levels of damage at given levels of ground motion intensity. Fragility curves express the data in a graphical format as continuous curve, whereas DPMs express it numerically in terms of discrete values. A number of approaches are available (Calvi et al. 2006) for developing the vulnerability relations for different types of buildings, ranging from those based on the empirical damage data from the past earthquakes to those based on the purely analytical simulations. Available vulnerability assessment methods have been classified (Calvi et al. 2006) into three generic groups, i.e., empirical (Whitman et al. 1973; Spence et al. 1992; Hassan and Sozen 1997; Rossetto and Elnashai 2003; Yakut 2004), analytical (Singhal and Kiremidjian 1996; Masi 2003; Rossetto and Elnashai 2005) and hybrid methods (Kappos et al. 1995; Barbat et al. 1996; Kappos et al. 1998; FEMA 1999, 2003b).

Empirical methods of vulnerability assessment are based on real post-earthquake damage scenarios and therefore are considered to be the most realistic approach of vulnerability assessment for any particular region. However, lack of adequate and reliable damage data for various building typologies subjected to different earthquake intensities, restricts its applicability. Considering the lack of sufficient empirical post-earthquake damage data,

and prohibitive cost of experimental tests, the analytical methods are the most attractive approach for vulnerability assessment. This method of vulnerability analysis undertake a detailed assessment of the analytical model under earthquake loading considering different parameters of building stock that may influence its vulnerability. The main disadvantage of analytical methods is that these are computationally very intensive and time consuming, and therefore not suitable for a large area or country with widely varying construction practices. Further, it is very difficult with the available techniques of analytical modeling to simulate and replicate the real behaviour of structures under earthquake shaking. The instability of solution algorithm used "may lead to completely divergent results if not handled with caution" (Kappos et al. 2006). Hybrid approach of vulnerability assessment is the combination of the available empirical data with the results of numerical analysis and thus bridges the gap between lack of empirical data and uncertainty of analytical estimation. The main difficulty of hybrid methods is to calibrate analytical results based on the observed data, because the two sets of data have two different sources of uncertainty, and therefore cannot be compared directly.

Although, India has suffered several devastating earthquakes (1897 Great Assam earthquake, 1991 Uttarkashi earthquake, 1993 Killari earthquake, 1997 Jabalpur earthquake, 1999 Chamoli earthquake, 2001 Bhuj earthquake, and 2005 Kashmir earthquake, etc.) in the past, unfortunately, very few systematic post-earthquake damage surveys have been conducted in India and the available data is highly inadequate and is not in a format suitable for development and calibration of reliable vulnerability estimates. Based on the available information for Indian earthquakes, Prasad (2009) has proposed intensity based DPMs for Indian buildings. In the absence of adequate empirical data, these need to be supported and supplemented by extensive analytical studies for different Indian building types.

Considering the scarcity of empirical damage data for Indian building typologies, in the present study, HAZUS methodology (FEMA 2003a, 2006) has been used to develop fragility functions for the RC frame buildings with and without URM infills. HAZUS methodology was originally developed for seismic risk assessment in the USA, but has

been extensively used world-over. In this methodology, the fragility curves follow a lognormal distribution representing probability of being in or exceeding a given damage state, given as

$$P[ds / S_d] = \Phi\left[\frac{1}{\beta_{ds}} ln\left(\frac{S_d}{\overline{S}_{d,ds}}\right)\right] \tag{6.1}$$

where, $\overline{S}_{d,ds}$ is median spectral displacement for damage state *ds*, Φ is normal cumulative distribution function, and β_{ds} is the standard deviation of the natural logarithm of the spectral displacement for damage state *ds*, which describes the total (combined) variability, given as

$$\beta_{ds} = \left\{\left(CONV\left[\beta_C, \beta_D, \overline{S}_{d,ds}\right]\right)^2 + \left(\beta_{M(ds)}\right)^2\right\}^{(1/2)} \tag{6.2}$$

where, β_C is the lognormal standard deviation parameter representing variability in the capacity properties of the building, β_D represents the variability in the demand spectrum due to spatial variability of the ground motion, and $\beta_{M(ds)}$ represents the uncertainty in the estimation of damage state threshold.

As discussed earlier, the three bays open buildings suffer torsion irregularity. For these buildings, IDA has also been performed in addition to the Pushover Analysis. The results of the two analyses have been compared in the previous Chapter. The fragility functions of these buildings have also been obtained using the two approaches. For developing the fragility functions using the dynamic capacity (IDA) curves, the methodology proposed by Wen et al. (2004) has been used in this Thesis. Similar to HAZUS methodology, the fragility curves by (Wen et al. 2004) also follow normal distribution, represented in a slightly different form, given as

$$P[LS / S_a] = 1 - \phi\left[\left(\frac{\lambda_c - \lambda_{D/S_a}}{\beta_T}\right)\right] \tag{6.3}$$

where, λ_c = natural logarithm of median drift capacity for a particular limit state; $\lambda_{D/Sa}$ = natural logarithm of calculated median demand drift for given spectral acceleration; and β_T is total uncertainty which is given as

$$\beta_T = \left\{\left(\beta_{D(S_a)}\right)^2 + \left(\beta_C\right)^2 + \left(\beta_M\right)^2\right\}^{(1/2)} \tag{6.4}$$

$$\beta_{D(Sa)} = \text{demand uncertainty} = \ln\left(1 + s^2\right)^{1/2} \tag{6.5}$$

$$s^2 = \text{standard error} = \frac{\sum\left[\ln\left(B_i\right) - \ln\left(C_i\right)\right]^2}{\left(N_d - 2\right)} \tag{6.6}$$

where, B_i, and C_i are the observed and power law predicted median demand drifts, respectively, given the spectral acceleration, and N_d is the number of sample demand data points. Similarly,

$$\beta_C = \text{capacity uncertainty} = \ln\left(1 + COV^2\right)^{1/2} \tag{6.7}$$

where, COV is the coefficient of variation of estimated drift capacity, and β_M is the modelling uncertainty, which is generally assumed based on the previous studies/experience.

6.3 DAMAGE STATE DEFINITION

An important step in developing fragility functions (DPMs/fragility curves) is definition of various 'damage severity levels' and their corresponding threshold parameters. In Intensity Scales, these damage states are defined in descriptive terms, but for fragility analysis, these need to be defined in terms of engineering parameters. Intensity scales define five Damage Grades, whereas HAZUS provides fragility functions for four Damage States, and the probability of fifth Damage State (i.e., "Collapse"), is specified as a fraction of Damage State 4 ("Complete Damage"). The specified fractions vary for different MBTs. In HAZUS, a two criteria approach based on the 'Performance Levels' of individual members is used, for the definition of damage state thresholds, as shown in Table 6.1. Based on yield and ultimate displacement parameters of the buildings, Barbat

et al. (2006) have proposed a four grade damage classification (Table 6.2). Similarly, Kappos et al. (2006) have proposed a five grade damage classification based on yield and ultimate spectral displacement parameters (S_{dy} and S_{du}) of the buildings. Table 6.3 shows the damage state definition proposed by Kappos et al. (2006).

Table 6.1
Damage state definition as per FEMA (2003a, 2006)

Damage Grade	Damage State	Criteria No. 1			Criteria No. 2		
		Fraction	Limit	Factor	Fraction	Limit	Factor
Gr1	Slight	> 0%	C	1.0	50%	B	1.0
Gr2	Moderate	> 5%	C	1.0	50%	B	1.5
Gr3	Extensive	> 25%	C	1.0	50%	B	4.5
Gr4	Complete	> 50%	E	1.0-1.5	50%	B	12

Table 6.2
Damage state definition as per Barbat et al. (2006)

Damage Grade	Damage State	Spectral Displacement
Gr1	Slight Damage	$0.7S_{dy}$
Gr2	Moderate Damage	S_{dy}
Gr3	Extensive Damage	$S_{dy}+0.25(S_{du}- S_{dy})$
Gr4	Complete Damage	S_{du}

Table 6.3
Damage state definition by Kappos et al. (2006)

Damage Grade	Damage State	Spectral Displacement
Gr1	Slight	$0.7\ S_{dy} < S_d < S_{dy}$
Gr2	Moderate	$S_{dy} < S_d < 2\ S_{dy}$
Gr3	Substantial to heavy	$0.7\ S_{dy} < S_d < S_{dy}$
Gr4	Heavy to very heavy	$0.7\ S_{du} < S_d < S_{du}$
Gr5	Collapse	$> S_{du}$

The approach by Barbat et al. (2006) is simpler, and the damage grade definitions are quite similar to those considered in HAZUS, therefore, the same has been used in the present study. As the damage state definition of Barbat et al. (2006) is based on the yield

and ultimate spectral displacement, it is not possible to use it directly in the fragility analysis using IDA. In case of IDA, a single damage state "Incipient Collapse" (IC) has been used, which represents either of the three conditions, whichever is reached first: (i) a column suffering shear failure or a set of members reaching collapse limit state as per ASCE-41 (2007) criteria, (ii) instability of the structure due to formation of collapse mechanism, or (iii) instability of the structure shown by a drastic change in the slope of the IDA curve.

6.4 CAPACITY CURVE PARAMETERS

To obtain the capacity curve parameters, the capacity curves/ pushover curves of the buildings for the selected design levels, as shown in previous Chapters, have been idealized as bilinear capacity spectra, as shown in Fig. 5.45, using the ASCE-41 (2007) guidelines.

The capacity curves (base shear vs. roof displacement) obtained in the previous Chapters are first transformed into capacity spectra (S_a vs. S_d) and then the bilinearized. The transformation from capacity curves to capacity spectra is performed using the following relationships:

$$S_a(g) = \frac{V_B}{W\alpha_m} \tag{6.8}$$

$$S_d = \frac{\Delta_{roof}}{\Gamma\phi_{roof}} \tag{6.9}$$

where,

$$\alpha_m = \frac{\sum(W_i\phi_i)^2}{\sum W_i \sum W_i\phi_i^2} \tag{6.10}$$

$$\Gamma = \frac{\sum W_i\phi_i}{\Sigma W_i\phi_i^2} \tag{6.11}$$

V is the base shear representing the building lateral load resistance, W is the total weight of building, W_i is the lumped storey weight at i^{th} floor level, Δ_{roof} is the roof displacement, ϕ_i is the modal shape coefficient for i^{th} floor, α_m is the modal mass coefficient (or fraction of the buildings weight effective in the pushover mode), and Γ is the modal participation factor for the pushover mode.

It is to be noted that the yield spectral displacement (S_{dy}) on the bi-linearized capacity curve shown in Fig. 5.45, does not represent the point where the first member of the building has reached yield point, but the point where a sizable number of members has yielded, resulting in significant reduction in structural stiffness. Similarly, ultimate spectral displacement (S_{du}) represents the point where either the building becomes unstable due to formation of a failure mechanism, or the strength of the building degrades below 80% of the peak strength of the building.

Table 6.4 shows the average capacity curve parameters of the four and ten storey buildings designed for gravity loads only, as per relevant Indian Standards, BIS (2000), BIS (1987 (Part 1)), BIS (1987 (Part 2)), without any consideration for earthquake forces. Different regular and irregular placements of infills are considered. Similar capacity curve parameters for the four and ten storey buildings designed and detailed for earthquake loading (BIS 1993, 2002) along with gravity loads are shown in Table 6.5. Table 6.6 and 6.7 show the median spectral displacements of gravity designed buildings and buildings designed as SMRF, respectively, corresponding to different damage grades, obtained analytically from the capacity spectra using the criteria of Table 6.2.

Figures 6.1-6.2 present the demand displacement for varying spectral acceleration corresponding to fundament period, and displacement corresponding to incipient collapse, as obtained from IDA of four and ten storey gravity load designed O3B buildings. The figures also show the median displacement demand and a power law fit to the median. The same plots for the four and ten storey buildings, designed as SMRF, with open three bays in the ground storey, are presented in Figs. 6.3 and 6.4, respectively.

Table 6.4
Average capacity spectrum parameters for Indian Model RC building types designed for gravity loads only

S. No.	Design Level	No. of Storey	Capacity Spectrum Parameters			
			Yield Point		Ultimate Point	
			S_{dy} (mm)	S_{ay} (g)	S_{du} (mm)	S_{au} (g)
1	RC frame buildings without infills	4	60	0.127	123	0.132
2		10	97	0.032	195	0.032
3	RC frame buildings with uniformly placed URM infills	4	5	0.215	6	0.217
4		10	14	0.093	17	0.095
5	URM infilled RC frame buildings with open ground storey	4	15	0.167	24	0.178
6		10	20	0.083	31	0.087
7	URM infilled RC frame buildings with front bay open in ground storey	4	4	0.155	8	0.170
8		10	11	0.064	9	0.065
9	URM infilled RC frame buildings with three bays open in ground storey (Parameters are obtained from static pushover analysis)	4	3	0.075	10	0.118
10		10	7	0.029	12	0.030

Table 6.5
Average capacity spectrum parameters for Indian Model RC building types designed as SMRF

S. No.	Design Level	No. of Storey	Capacity Spectrum Parameters			
			Yield Point		Ultimate Point	
			S_{dy} (mm)	S_{ay} (g)	S_{du} (mm)	S_{au} (g)
1	RC frame buildings without infills	4	114	0.259	219	0.281
2		10	202	0.136	403	0.136
3	RC frame buildings with uniformly placed URM infills	4	7	0.342	89	0.553
4		10	21	0.152	176	0.200
5	URM infilled RC frame buildings with open ground storey, designed and detailed as per Indian Standard (BIS 2002), but without special provisions for open ground storey	4	24	0.300	63	0.348
6		10	26	0.120	182	0.192
7	URM infilled RC frame buildings with open ground storey, designed and detailed as per Indian Standard (BIS 2002), including special provisions for open ground storey	4	17	0.488	78	0.684
8		10	19	0.156	159	0.218
9	URM infilled RC frame buildings with front bay open in ground storey	4	8	0.310	75	0.465
10		10	26	0.142	207	0.189
11	URM infilled RC frame buildings with three bays open in ground storey (Parameters are obtained from static pushover analysis)	4	15	0.278	61	0.399
12		10	23	0.126	178	0.194

Table 6.6
Median spectral displacement corresponding to different damage grades of Indian Model RC building types designed for gravity loads only

S. No.	Design Level	No. of Storey	Median S_d (mm)			
			Damage Grade, Gr1	Damage Grade, Gr2	Damage Grade, Gr3	Damage Grade, Gr4
1	RC frame buildings without infills	4	42	60	76	123
2		10	68	97	122	195
3	RC frame buildings with uniformly placed URM infills	4	4	5	5	6
4		10	10	14	15	17
5	URM infilled RC frame buildings with open ground storey	4	11	15	17	24
6		10	14	20	23	31
7	URM infilled RC frame buildings with front bay open in ground storey	4	3	4	5	8
8		10	8	11	10	9
9	URM infilled RC frame buildings with three bays open in ground storey (Parameters are obtained from static pushover analysis)	4	2	3	5	10
10		10	5	7	8	12

Table 6.7
Median spectral displacement corresponding to different damage grades of Indian Model RC building types designed as SMRF

S. No.	Design Level	No. of Storey	Median S_d (mm)			
			Damage Grade, Gr1	Damage Grade, Gr2	Damage Grade, Gr3	Damage Grade, Gr4
1	RC frame buildings without infills	4	80	114	140	219
2		10	141	202	252	403
3	RC frame buildings with uniformly placed URM infills	4	5	7	27	89
4		10	15	21	60	176
5	URM infilled RC frame buildings with open ground storey, designed and detailed as per Indian Standard (BIS 2002), but without special provisions for open ground storey	4	17	24	34	63
6		10	18	26	65	182
7	URM infilled RC frame buildings with open ground storey, designed and detailed as per Indian Standard (BIS 2002), including special provisions for open ground storey	4	12	17	32	78
8		10	13	19	54	159
9	URM infilled RC frame buildings with front bay open in ground storey	4	6	8	25	75
10		10	18	26	71	207
11	URM infilled RC frame buildings with three bays open in ground storey (Parameters are obtained from static pushover analysis)	4	10	15	26	61
12		10	16	23	61	178

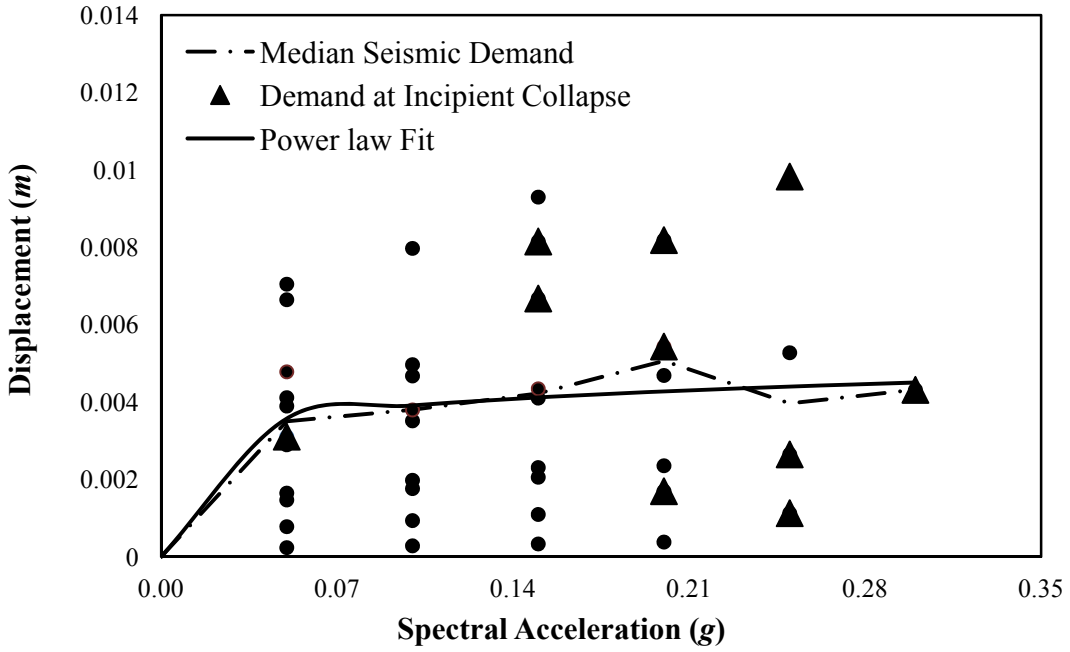

(a)

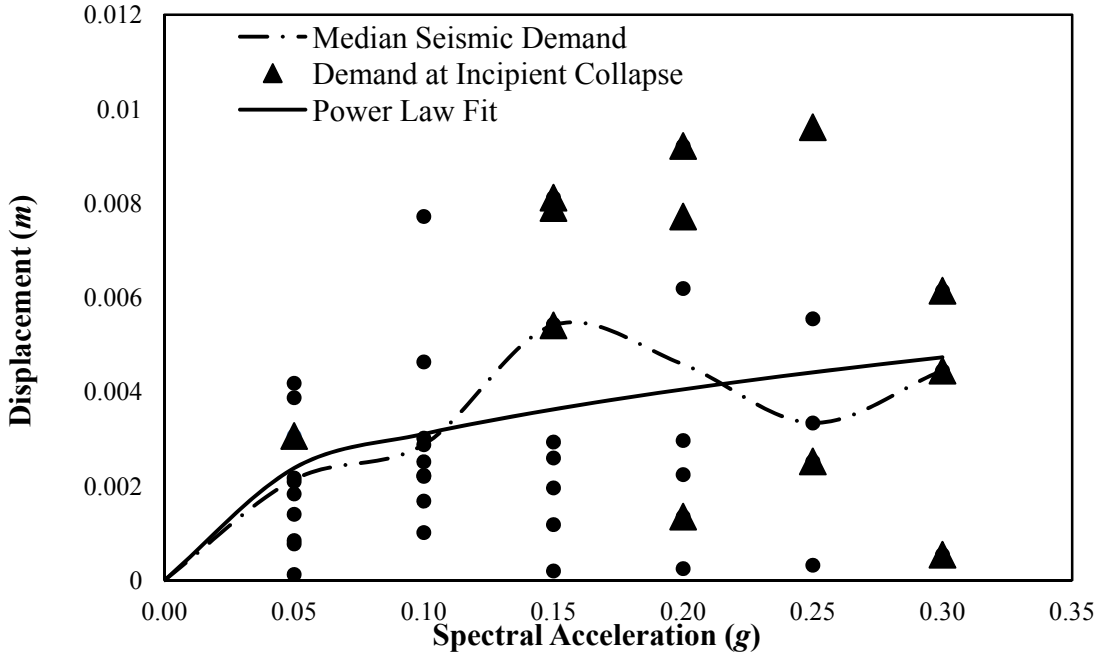

(b)

Fig. 6.1 Displacement demand corresponding to spectral acceleration at fundamental period for four storey infilled frame building designed for gravity load only, with three bays open in the ground storey: (a) longitudinal direction; and (b) transverse direction.

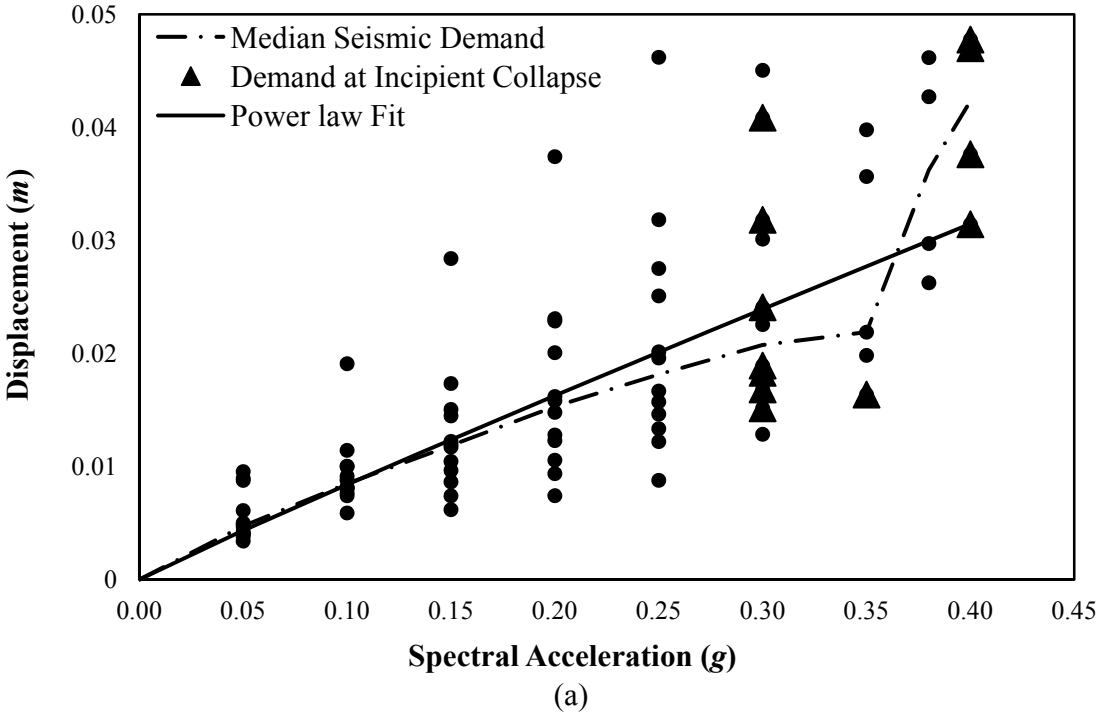

(a)

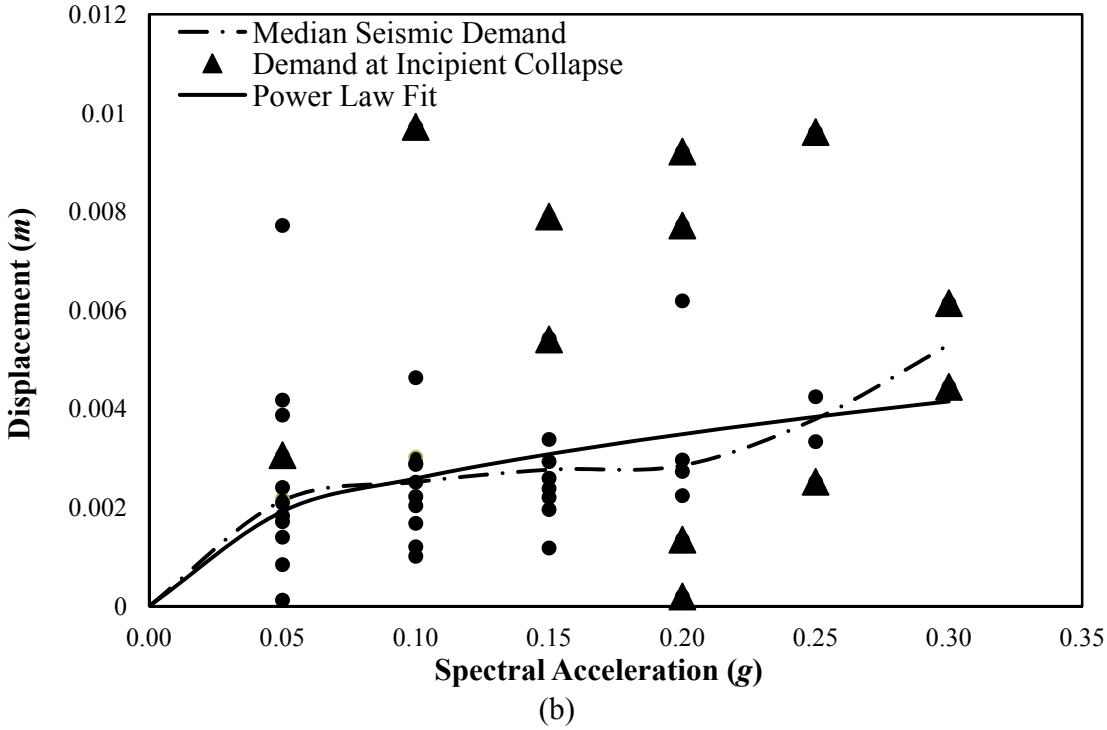

(b)

Fig. 6.2 Displacement demand corresponding to spectral acceleration at fundamental period, for ten storey infilled frame building designed for gravity load only, with three bays open in the ground storey: (a) longitudinal direction; and (b) transverse direction.

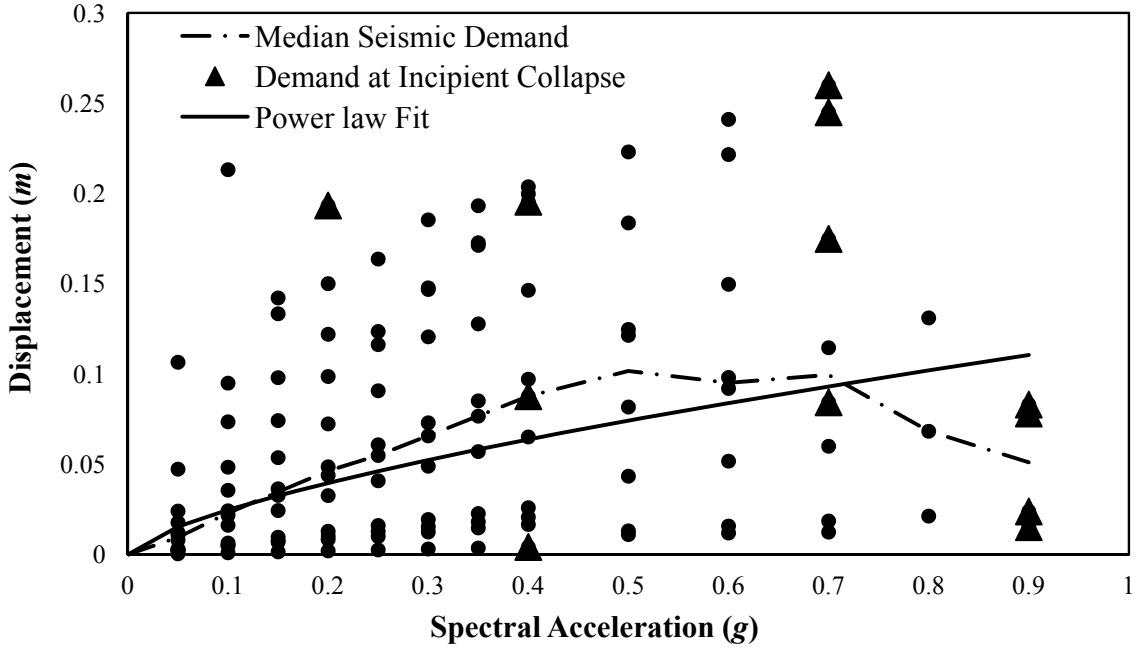

(a)

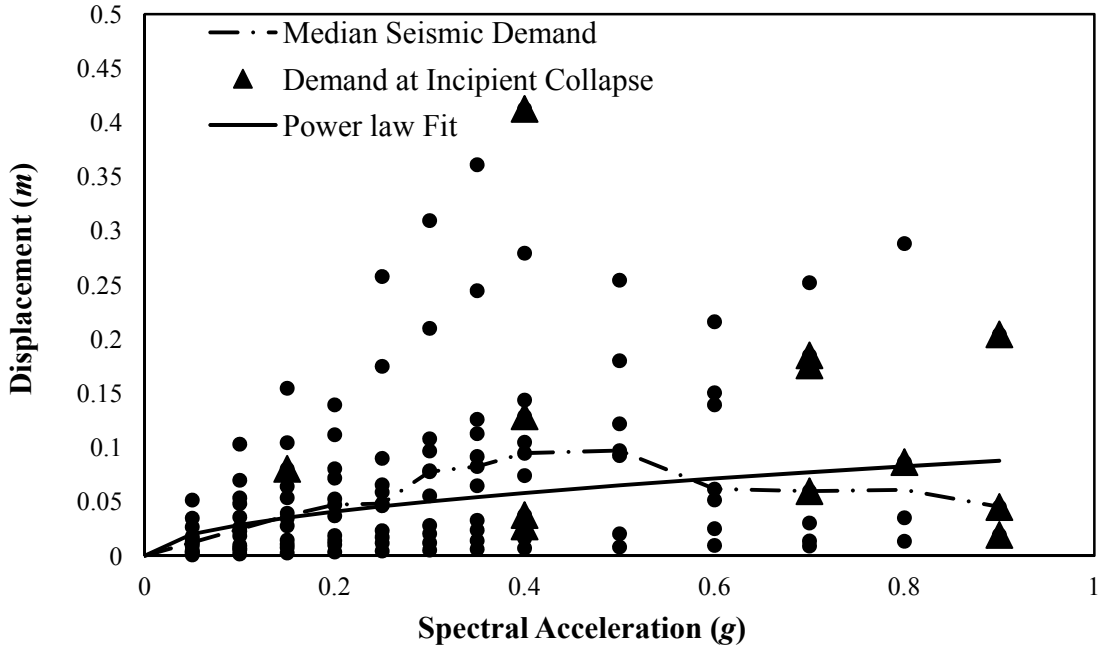

(b)

Fig. 6.3 Displacement demand corresponding to spectral acceleration at fundamental period for four storey infilled frame building designed as SMRF, with three bays open in the ground storey: (a) longitudinal direction; and (b) transverse direction.

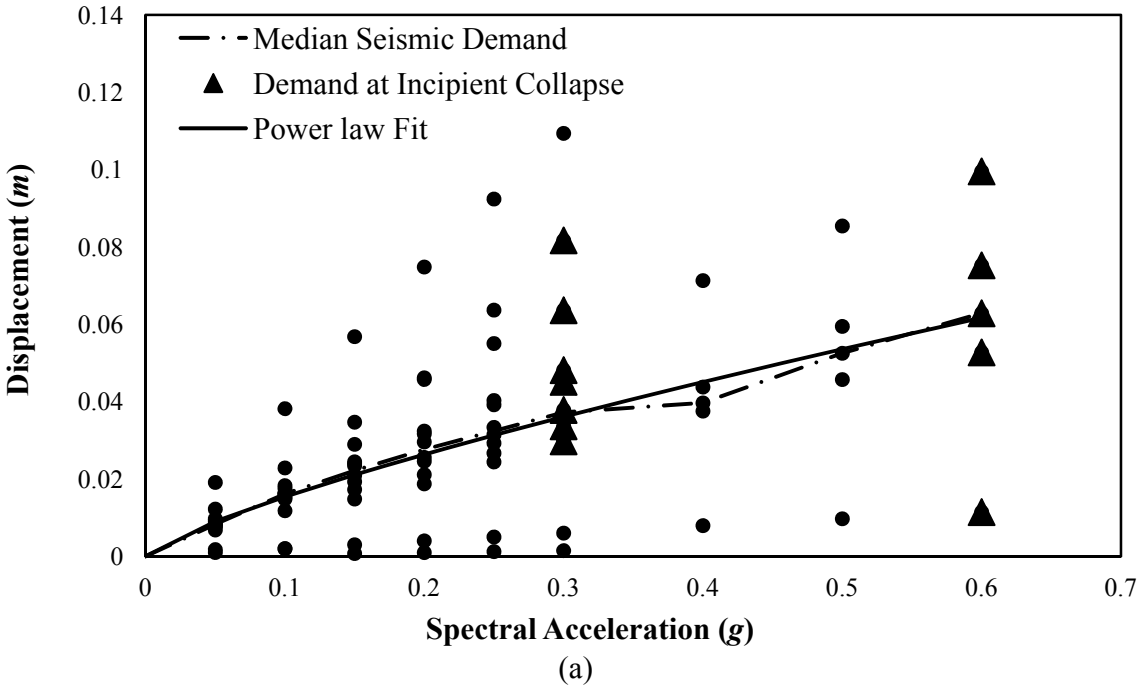

(a)

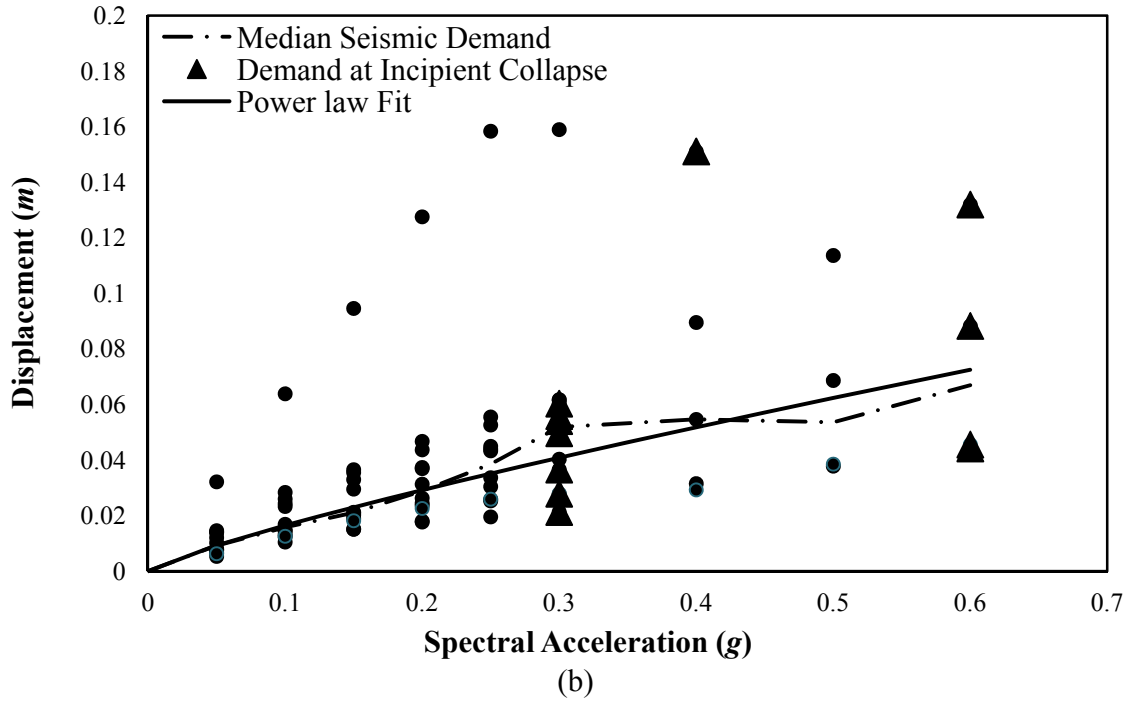

(b)

Fig. 6.4 Displacement demand corresponding to spectral acceleration at fundamental period for ten storey infilled frame building designed as SMRF, with three bays open in the ground storey: (a) longitudinal direction; and (b) transverse direction.

6.5 CONSIDERATION OF VARIABILITY

Another important issue in the estimation of fragility functions is the quantification of variability associated with different processes in vulnerability assessment. This includes uncertainty in ground motion, variability in capacity curve parameters, and uncertainty in the definition of damage state thresholds. Estimation of variability in fragility analysis is a complex process requiring large amount of statistical data. FEMA (2003a) has presented variability for fragility estimation of U.S. American (Californian) buildings, where total variability in structural damage is considered to be contributed by the three sources as described in Eq. 6.1.As demand and capacity are interdependent, uncertainty in ground motion β_D, and variability in capacity curve parameters β_C is combined using a convolution process. The variability in damage state threshold, $\beta_{M(ds),}$ is assumed to be independent of β_C and β_D and is therefore combined with the result of convolution by square-root-of-sum-of-the squares (SRSS) method. As the variability in different parameters for Indian conditions is not available, HAZUS (FEMA 2003a) values of variability for the corresponding classes of buildings as reproduced in Table 6.10 and 6.11, have been considered.

HAZUS has considered uniform variability (lognormal standard deviation parameter) in demand spectrum as 0.45 and 0.5, for acceleration and velocity sensitive ranges of spectrum, respectively. In the present study, moderate variability of 0.3 in capacity curve and 0.4 in the damage state threshold, for all the structural damage states, as suggested by HAZUS, has been considered for all the buildings. As gravity designed buildings are constructed without any considerations for ductile detailing, these are expected to experience major degradation after yielding. Accordingly, a variability of 0.5 corresponding to major post yield degradation has been considered. Whereas, buildings designed and detailed as SMRF are expected to experience minor degradation after yielding. Therefore, variability of 0.9 corresponding to minor post yield degradation has been considered for SMRF buildings. However, presence of infills and moreover irregular placement of infills in plan and/or elevation results in rapid post yield degradation of these buildings and the same has been accounted for using increased variability as shown in Tables 6.8 and 6.9.

Table 6.8
Variability parameters considered in the present study as per FEMA (2003a) for buildings designed for gravity loads only

Building Design Levels	Damage State	Post-yield Degradation	Damage State Variability ($\beta_{M(ds)}$)	Capacity Curve Variability (β_c)	Total Variability (β_{ds})	
					4 Storey Buildings	10 Storey Buildings
RC frame buildings without infills	Gr1	Minor Degradation (0.9)	Moderate (0.4)	Moderate (0.3)	0.75	0.70
	Gr2					
	Gr3	Major Degradation (0.5)			0.85	0.80
	Gr4					
RC frame buildings with uniformly placed URM infills	Gr1	Minor Degradation (0.9)			0.75	0.70
	Gr2					
	Gr3	Major Degradation (0.5)			0.85	0.80
	Gr4	Extreme Degradation (0.1)			1.00	1.00
URM infilled RC frame buildings with open ground storey	Gr1	Minor Degradation (0.9)			0.75	0.70
	Gr2	Major Degradation (0.5)			0.85	0.80
	Gr3	Extreme Degradation (0.1)			1.00	1.00
	Gr4					
URM infilled RC frame buildings with front bay open in ground storey	Gr1	Minor Degradation (0.9)			0.75	0.70
	Gr2					
	Gr3	Major Degradation (0.5)			0.85	0.80
	Gr4	Extreme Degradation (0.1)			1.00	1.00
URM infilled RC frame buildings with three bays open in ground storey	Gr1	Minor Degradation (0.9)			0.75	0.70
	Gr2	Major Degradation (0.5)			0.85	0.80
	Gr3	Extreme Degradation (0.1)			1.00	1.00
	Gr4					

Table 6.9
Variability parameters considered in present study as per FEMA (2003a) for buildings designed as SMRF

Building Design Levels	Damage State	Post-yield Degradation	Damage State Variability ($\beta_{M(ds)}$)	Capacity Curve Variability (β_c)	Total Variability (β_{ds})	
					4 Storey Buildings	10 Storey Buildings
RC frame buildings without infills	Gr1	Minor Degradation (0.9)	Moderate (0.4)	Moderate (0.3)	0.75	0.70
	Gr2					
	Gr3					
	Gr4	Major Degradation (0.5)			0.85	0.80
RC frame buildings with uniformly placed URM infills	Gr1	Minor Degradation (0.9)			0.75	0.70
	Gr2					
	Gr3	Major Degradation (0.5)			0.85	0.80
	Gr4					
URM infilled RC frame buildings with open ground storey without consideration of BIS (2002)	Gr1	Minor Degradation (0.9)			0.75	0.70
	Gr2	Major Degradation (0.5)			0.85	0.80
	Gr3					
	Gr4	Extreme Degradation (0.1)			1.00	1.00
URM infilled RC frame buildings with open ground storey, designed and detailed as per BIS (2002)	Gr1	Minor Degradation (0.9)			0.75	0.70
	Gr2					
	Gr3	Major Degradation (0.5)			0.85	0.80
	Gr4					
URM infilled RC frame buildings with front bay open in ground storey	Gr1	Minor Degradation (0.9)			0.75	0.70
	Gr2					
	Gr3	Major Degradation (0.5)			0.85	0.80
	Gr4					
URM infilled RC frame buildings with three bays open in ground storey	Gr1	Minor Degradation (0.9)			0.75	0.70
	Gr2	Major Degradation (0.5)			0.85	0.80
	Gr3					
	Gr4	Extreme Degradation (0.1)			1.00	1.00

On the other hand, in case of IDA, the demand and capacity are convoluted in the process of analysis itself, and accordingly Wen et al. (2004) combined the three variabilities β_C, $\beta_{D/Sa}$, and β_M using the SRSS rule. The fragility parameters for 'IC' damage state of RC buildings having three bays open in the ground storey, have been estimated using Eqs. 6.3-6.6, and are summarized in Table 6.10. It is interesting to note that the total variability for 'IC' damage state estimated using Wen et al. (2004) procedure for IDA is of the same order as obtained using HAZUS guidelines for capacity spectrum procedure (Tables 6.8 and 6.9) for Gr4 ("Complete Damage") damage state, except in case of the ten storey gravity load designed O3B building.

Table 6.10
Fragility parameters for "Incipient Collapse" damage state of URM infilled RC buildings with three bays open in the ground storey

Design Levels	No. of Storey	λ_c	β_c	β_m	$\beta_{D/Sa}$	β
Gravity load designed	4	-5.11	0.15	0.3	0.88	0.95
	10	-3.58	0.12		0.37	0.49
SMRF	4	-2.45	0.46		0.99	1
	10	-2.99	0.19		0.86	0.93

6.6 FRAGILITY CURVES AND DAMAGE PROBABILITY MATRICES (DPMs)

Fragility curves of bare and uniformly infilled frame buildings have been compared to study the effect of URM infills on the damageability of RC frame buildings. Figs. 6.5 and 6.6 show the fragility curves of four storey bare and infilled frames for the two considered design levels. Similar comparison for ten storey bare frame and uniformly infilled frame buildings designed for gravity loads only and as SMRF, is shown in Figs. 6.7 and 6.8, respectively. It can be observed from the Figures that the fragility curves for the buildings with and without infills are visually separated in to two groups. The fragility curves for infilled frame buildings show high probability of damage at much lower spectral displacement as compared to the bare frame buildings. This is due to the much higher stiffness of infilled frame buildings. Very small dispersion in the fragility curves of both four and ten storey gravity load designed infilled frame buildings, as compared to their SMRF counterparts, indicates a

quick complete damage within a short range of spectral displacement in case of gravity load designed infilled frames.

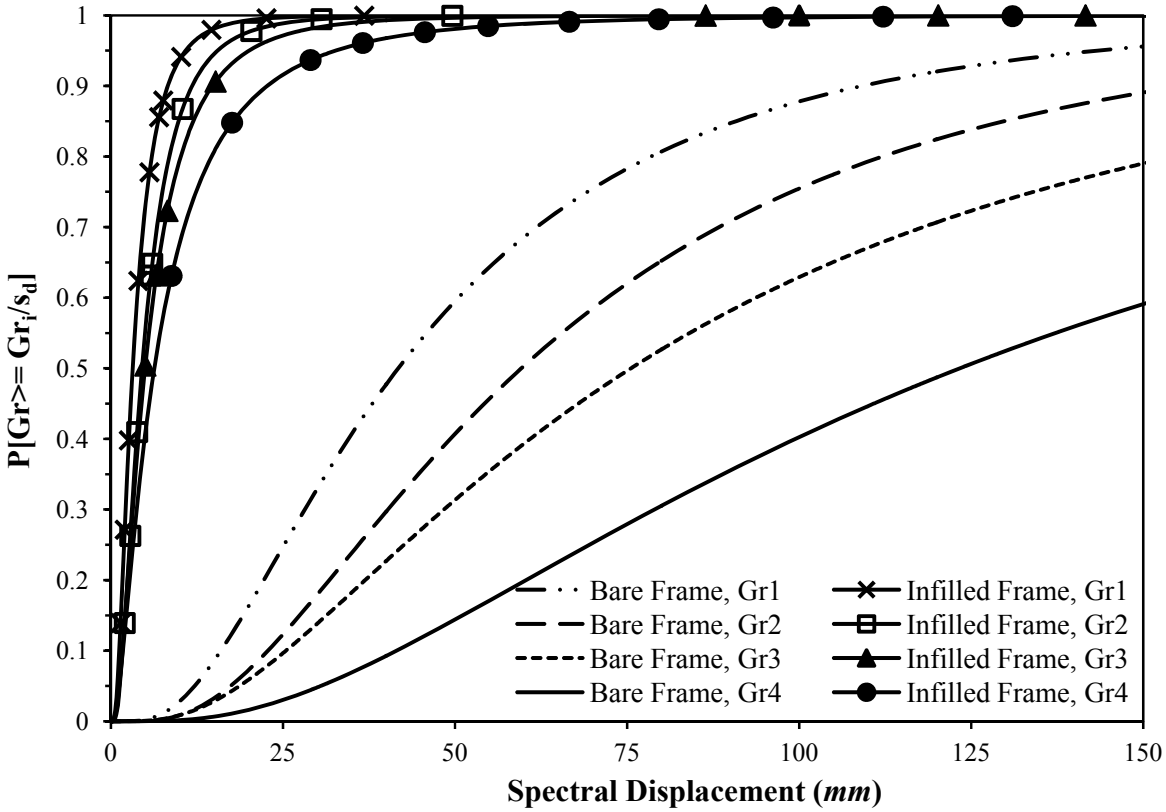

Fig. 6.5 Fragility curves for four storey bare frame and uniformly infilled frame buildings, designed for gravity loads only.

The fragility curves indicate increased damage probabilities of infilled frames as compared to bare frames, for gravity load designed buildings as well as for SMRF buildings. At a spectral displacement of 10 *mm,* 87% and 80% of four storey, and 67% and 12% of ten storey gravity load designed infilled frame buildings suffer moderate (Gr2) and heavy (Gr3) damages, respectively, whereas both four and ten storey bare frame buildings have no damage at all, at the same spectral displacement. Further, at the same spectral displacement, the infilled SMRF buildings suffer much less damage than their counterparts designed for gravity load alone. The gravity load designed infilled frame buildings show the worst performance and

have the highest damage probability for all the damage grades and for all values of spectral displacement. However, it should be noted that fragility curves compare the probability of damage for a given spectral displacement, but as the dynamic characteristics of infilled frame buildings are significantly different from those of bare frames, the damage probabilities need to be expressed in terms of some other intensity measure, such as Peak Ground Acceleration (PGA), for direct comparison.

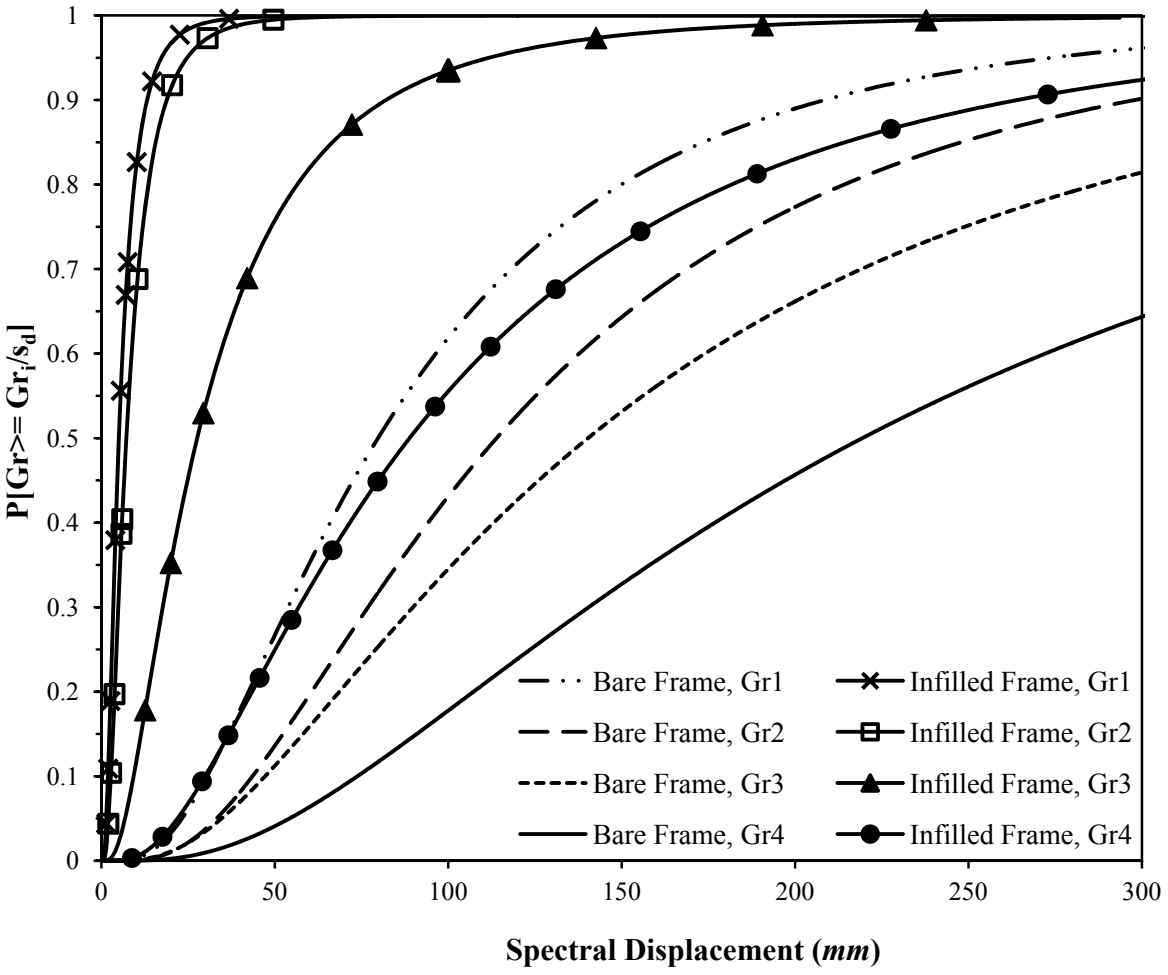

Fig. 6.6 Fragility curves for four storey bare and uniformly infilled frame buildings, designed as SMRF.

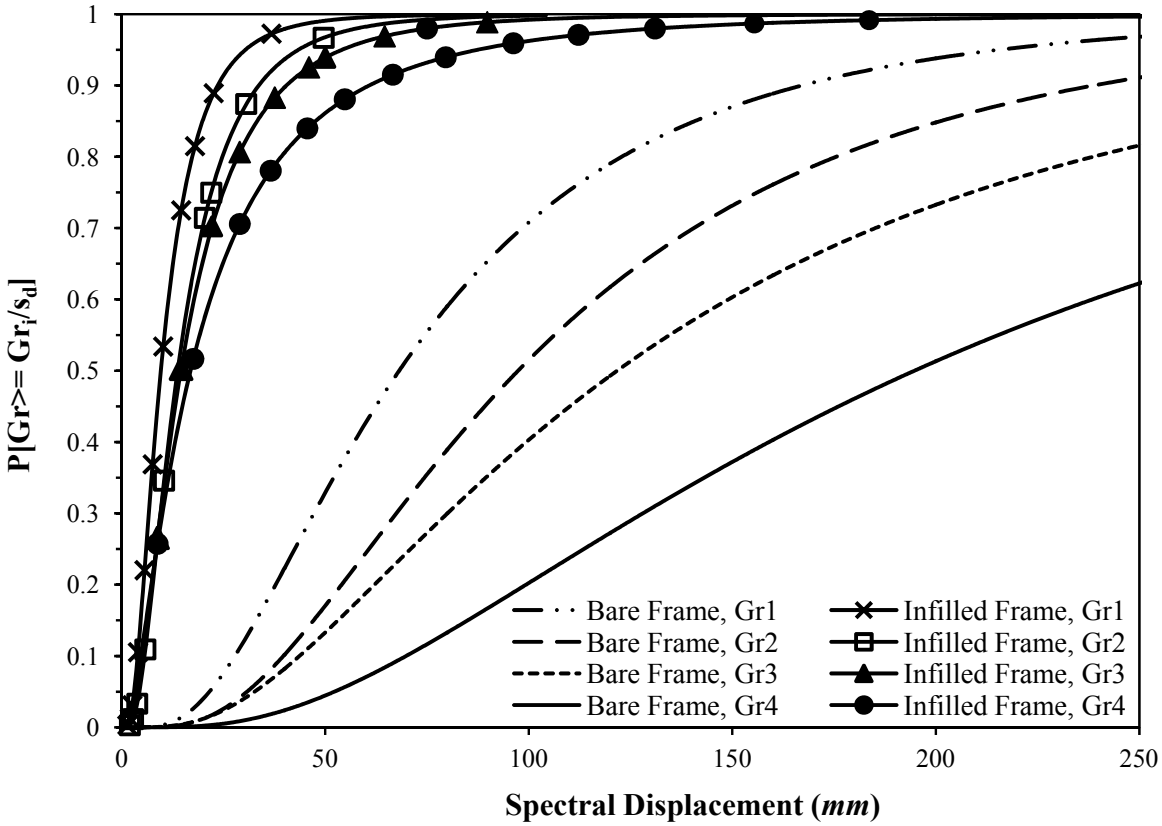

Fig. 6.7 Fragility curves for ten storey bare frame and uniformly infilled frame buildings, designed for gravity loads.

To study the effect of design provisions of BIS (2002) on damageability of open ground storey buildings, the fragility curves for four and ten storey infilled frame buildings with open ground (OG) storey, have been compared for the three design levels viz., designed as SMRF without considering provisions of BIS (2002) for open ground storey (designated as SMRF (NC)), designed as SMRF as per BIS (2002) considering the provisions for open ground storey (designated as SMRF (C)), and designed for gravity loads alone (designated as GLD), in Figs. 6.9 and 6.10. It is observed that at a given spectral displacement, the probability of damage is highest in case of gravity load designed RC buildings with open ground storey, for all the damage grades and range of spectral displacement. The probability of slight damage (Gr1) of the three design levels does not differ much; but it increases significantly for the higher damage states (Gr3 and Gr4), in case of GLD open ground storey

(OG) buildings. The probability of complete damage of four storey GLD OG building is higher than the probability of moderate damage (Gr3) of SMRF OG (NC) building and the probability increases with increase in building height. Fragility curves of four storey SMRF OG (NC) and SMRF OG (C) buildings are identical showing equal moderate damage probability for both the design levels. The probability of moderate damage for ten storey SMRF OG (NC) building is slightly higher than the ten storey SMRF OG (C) building.

The effect of asymmetric placement of infills on the damageability of URM infilled RC frame buildings is studied in Figs. 6.11-6.16. Fragility curves for four and ten storey URM infilled RC frame buildings with front bay open (O1B) in the ground storey are presented in Figs. 6.11 and 6.12, respectively.

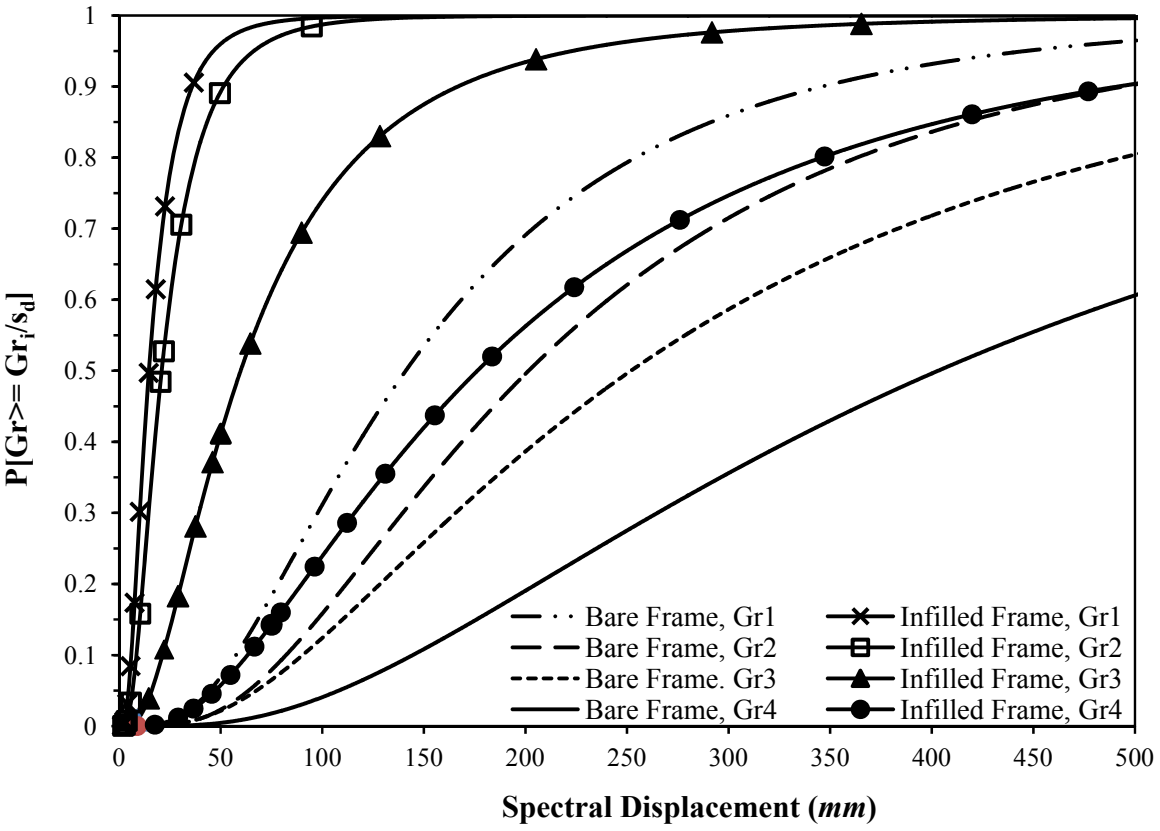

Fig. 6.8 Fragility curves for ten storey bare frame and uniformly infilled frame buildings, designed as SMRF.

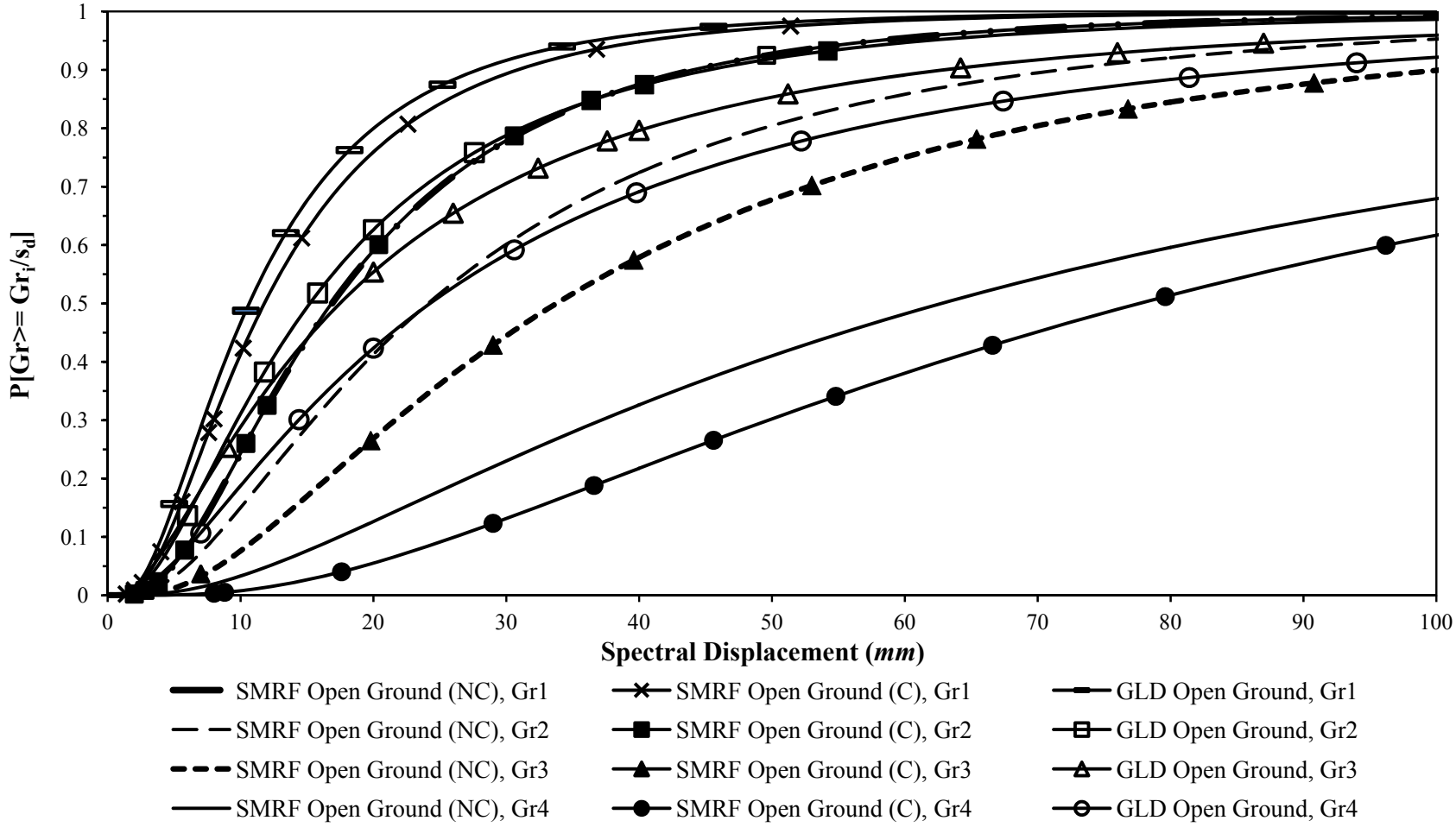

Fig. 6.9 Fragility curves for four storey building having open ground storey, with different design levels.

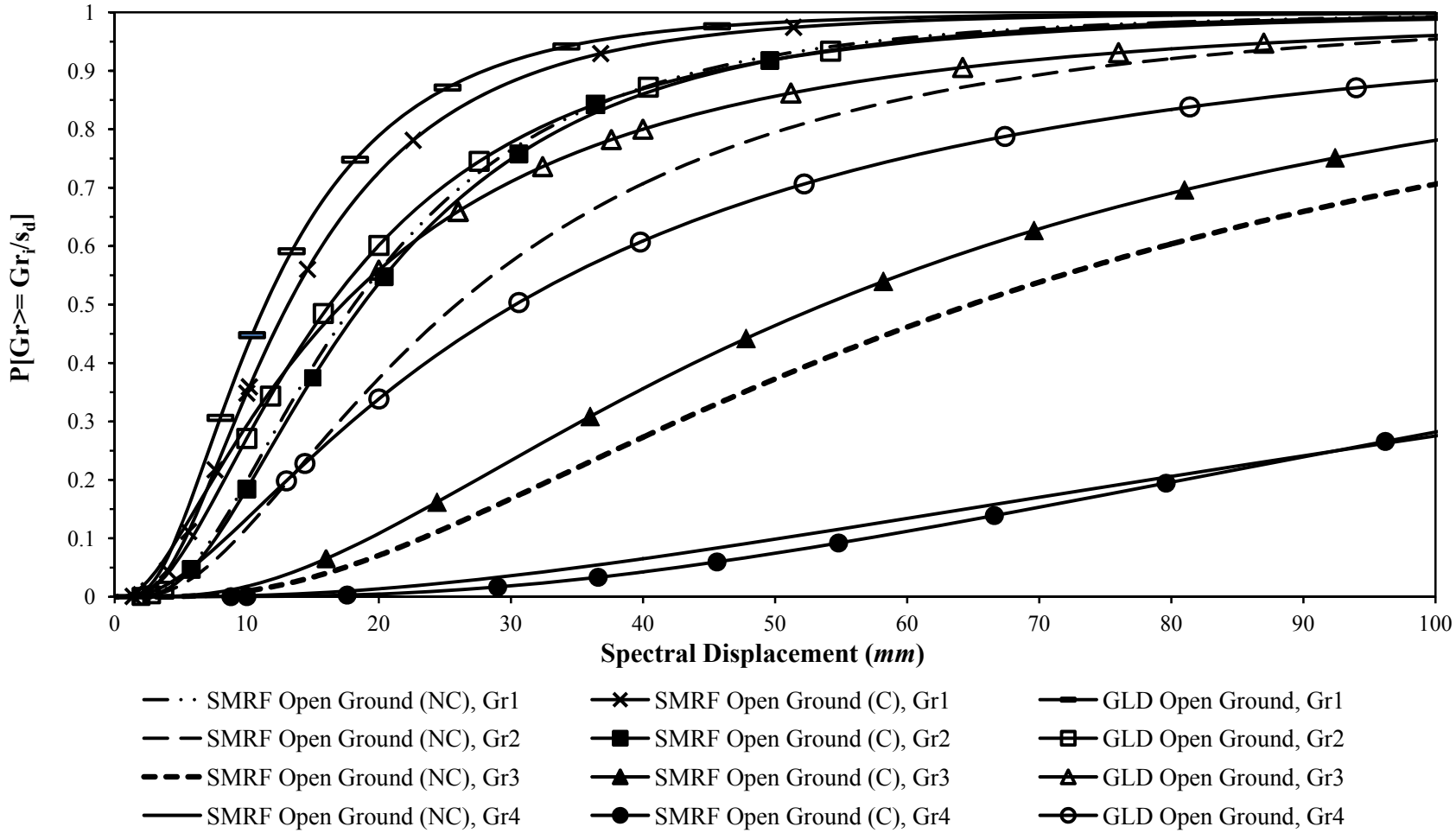

Fig. 6.10 Fragility curves for ten storey building having open ground storey, with different design levels.

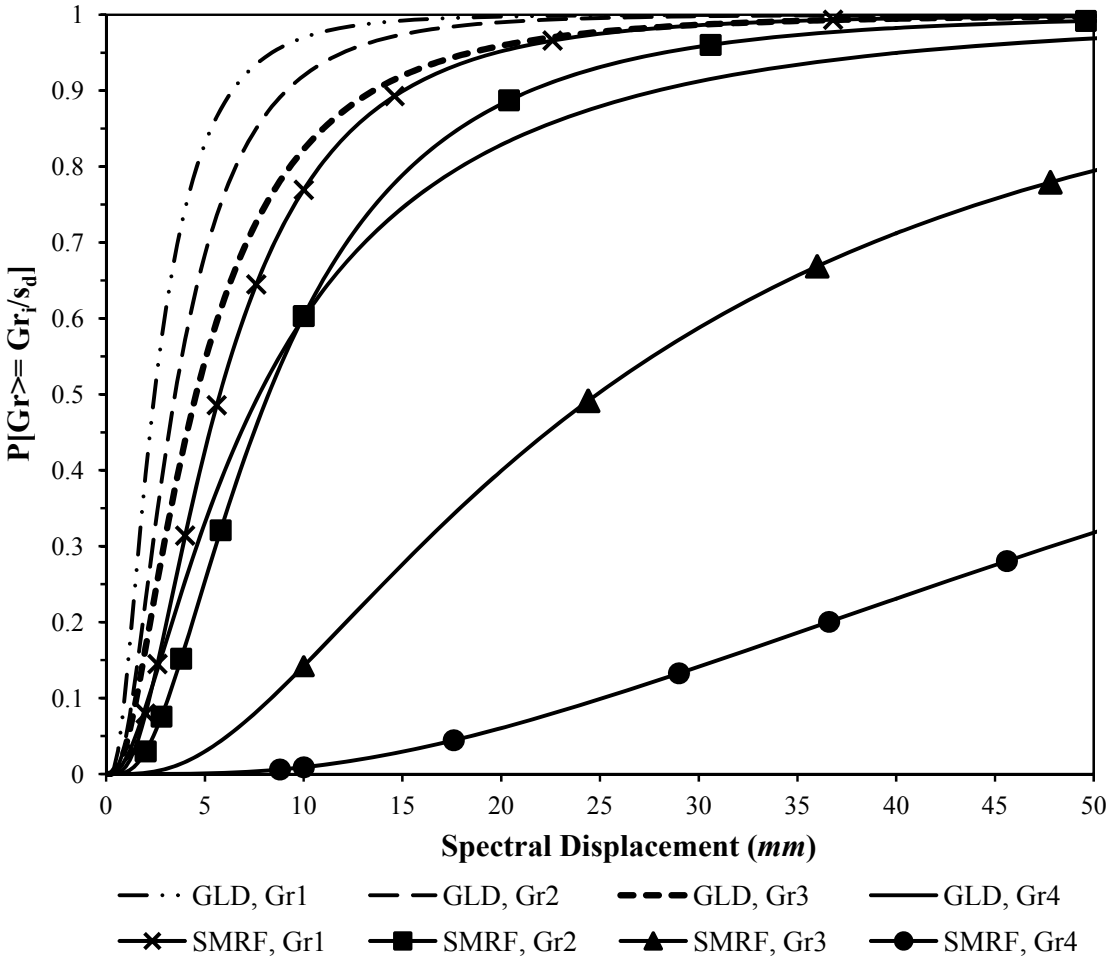

Fig. 6.11 Fragility curves for four storey infilled frame buildings with open front bay in the ground storey.

Both the four and ten storey gravity load designed O1B buildings are showing poorer performance for all the grades. At 10*mm* spectral displacement, the four and ten storey gravity load designed O1B buildings suffers complete damage in 60% and 43% cases, respectively; whereas the corresponding probabilities in case of SMRF O1B buildings, are only 1% and 0.7%, for four and ten storey buildings, respectively.

Fragility curves of the four and ten storey URM infilled RC frame buildings with three bays open in the ground storey (O3B), derived from pushover curve parameters, are shown in Figs. 6.13 and 6.14, respectively. Effect of earthquake resistant design on the fragility of

buildings can be prominently seen in this case also. Buildings designed for gravity loads alone are showing a sharp increase in damage with a slight increase in spectral displacement. At a spectral displacement of 10*mm,* the four storey GLD O3B building shows 49% probability of damage of Gr4, whereas 3.5% buildings designed as SMRF are expected to suffer Gr4 damage. The corresponding values for ten storey GLD and SMRF O3B buildings are 53% and 0.2%, respectively.

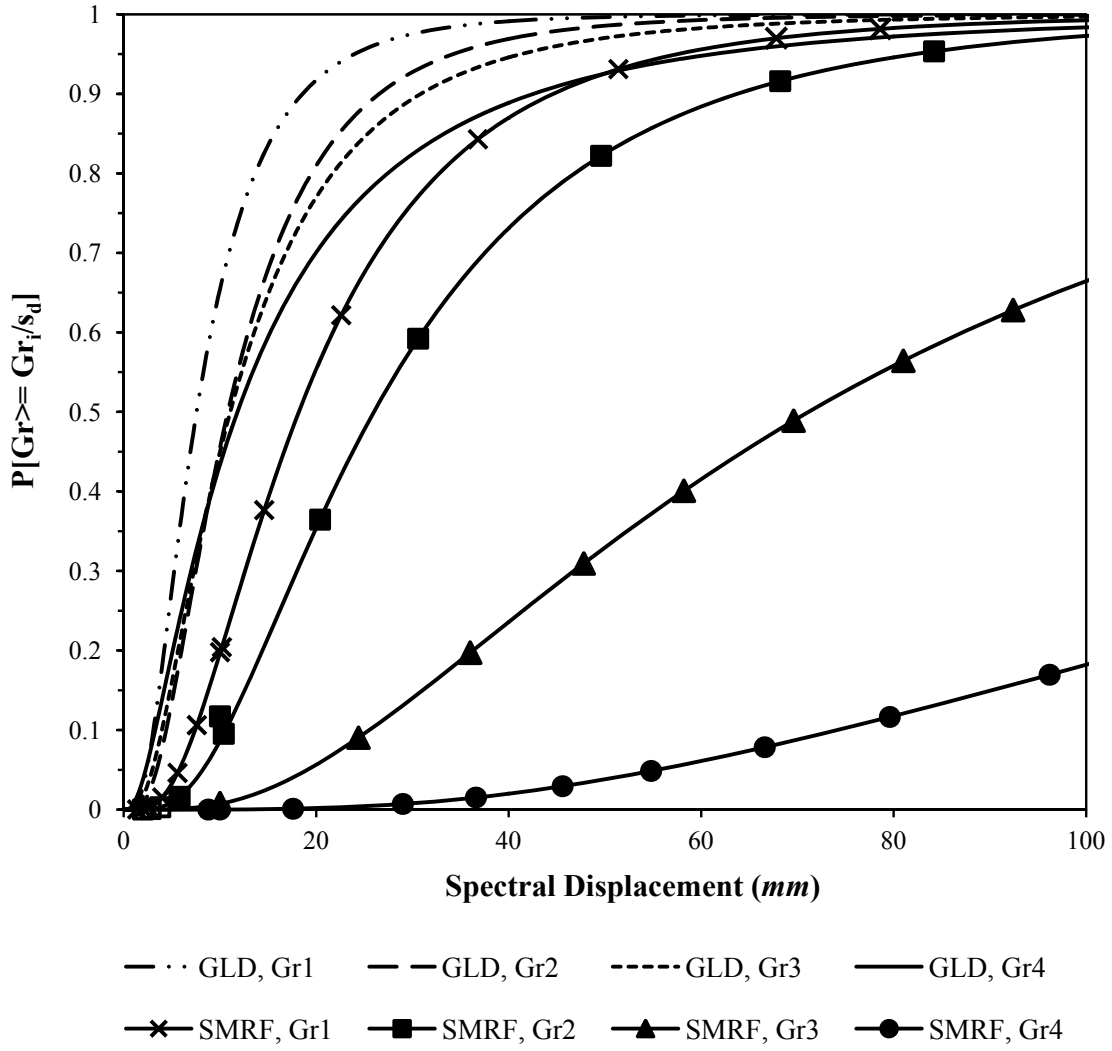

Fig. 6.12 Fragility curves for ten storey infilled frame buildings with open front bay in the ground storey.

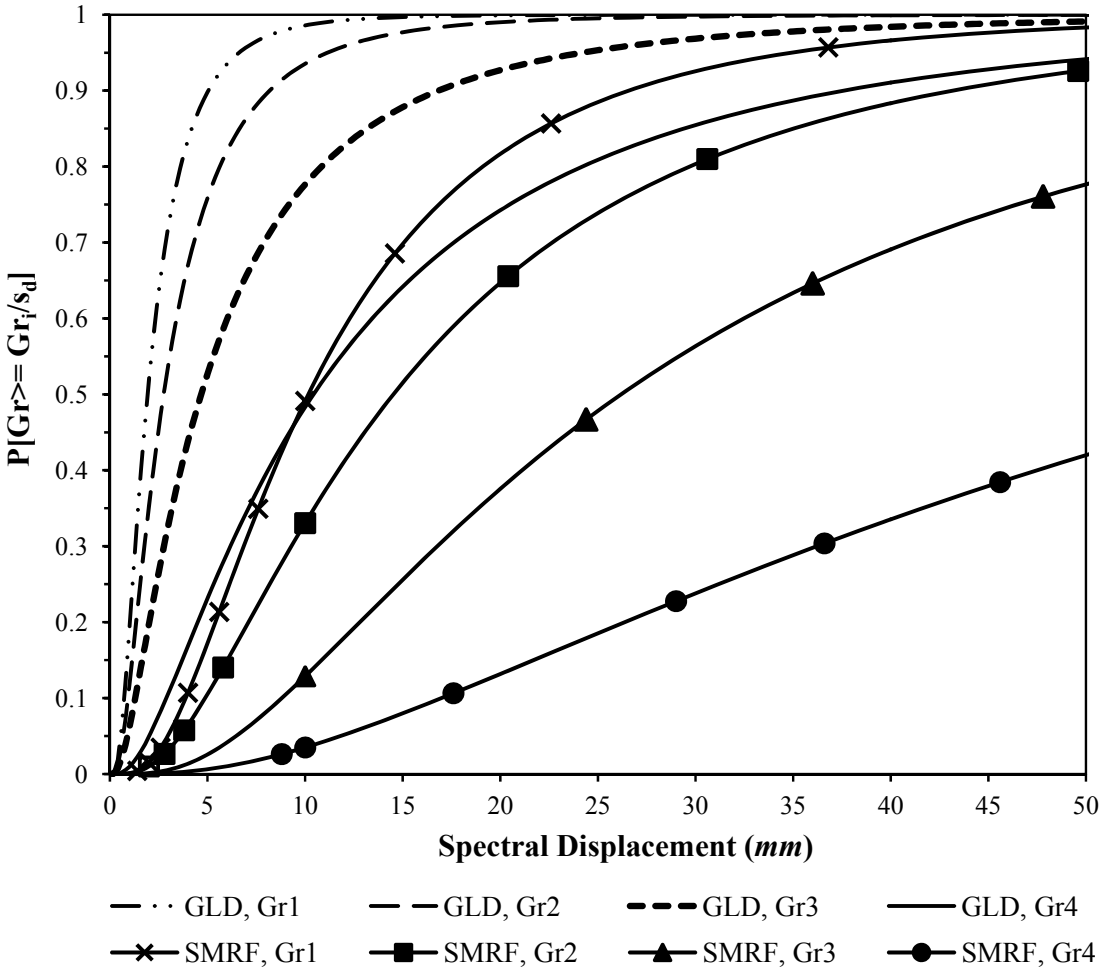

Fig. 6.13 Fragility curves for four storey infilled frame buildings with three bays open in the ground storey.

Fragility curves for the "Incipient Collapse" damage state obtained from the IDA results are compared with those for "Complete Damage" state (Gr4) obtained using static pushover (HAZUS) methodology. Fragility curves for four and ten storey O3B buildings designed for gravity loads only and as SMRF are presented in Figs. 6.15 and 6.16, respectively. It is to be noted that the damage probabilities are expressed as a function of spectral displacement in case of HAZUS methodology (Eq. 6.1) and as a function of spectral acceleration in case of IDA methodology (Eq. 6.3). Therefore, for the purpose of comparison, the damage probabilities need to be expressed in terms of a common parameter (S_a in the present study).

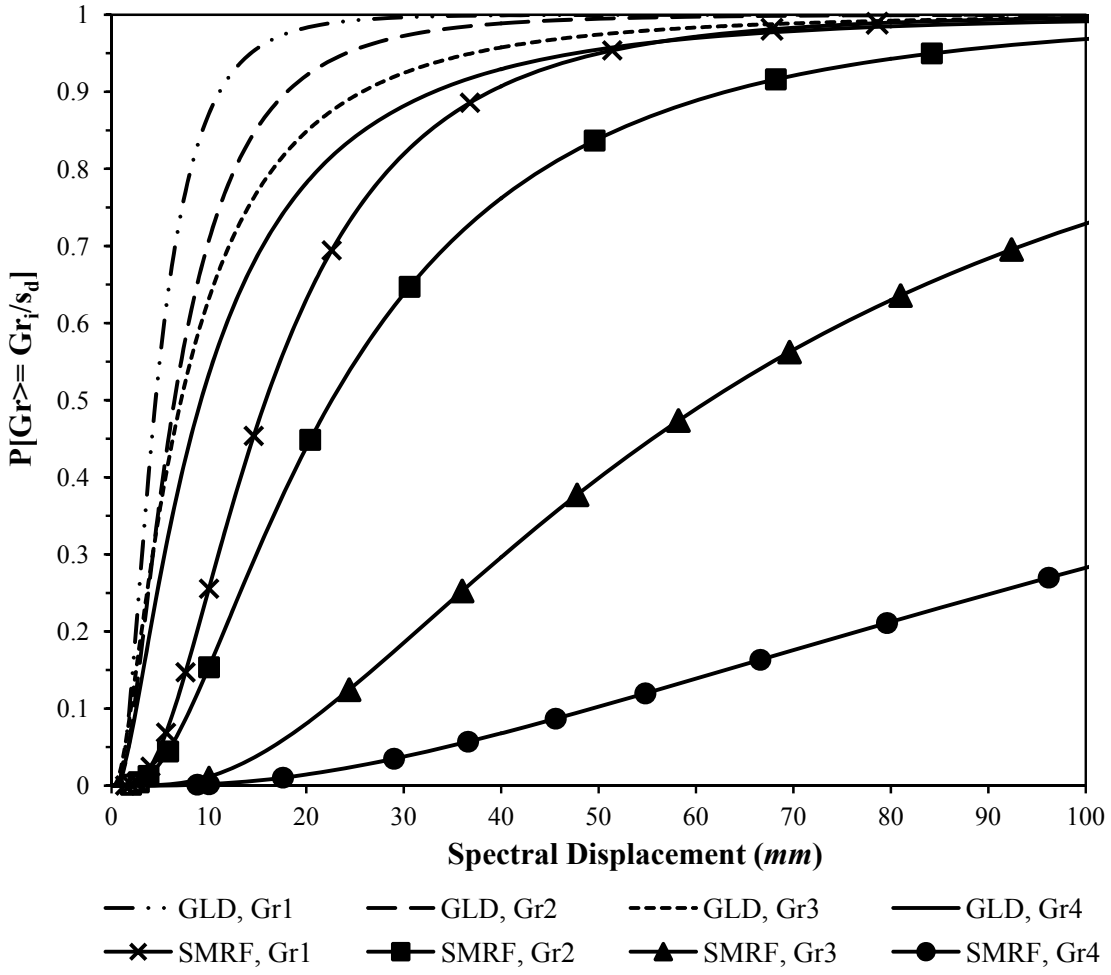

Fig. 6.14 Fragility curves for ten storey infilled frame buildings with three bays open in the ground storey.

In addition to the spectral shape, initial period and material damping of the structure play an important role in the relationship between spectral acceleration and spectral displacement. In the present study, spectral shape of BIS (2002) for Soil Type-I has been used in the Displacement Modification Method (DMM) of ASCE-41 (2007) to obtain the spectral displacement corresponding to different values of spectral acceleration and the damage probability at any given spectral acceleration is estimated using Eq. 6.1 for the two directions. The damage probabilities in the two directions are combined using mean to obtain the damageability of the building. The initial periods as obtained from Table 5.1 and material damping of 5% and 10% for bare and infilled frames, respectively, have been used.

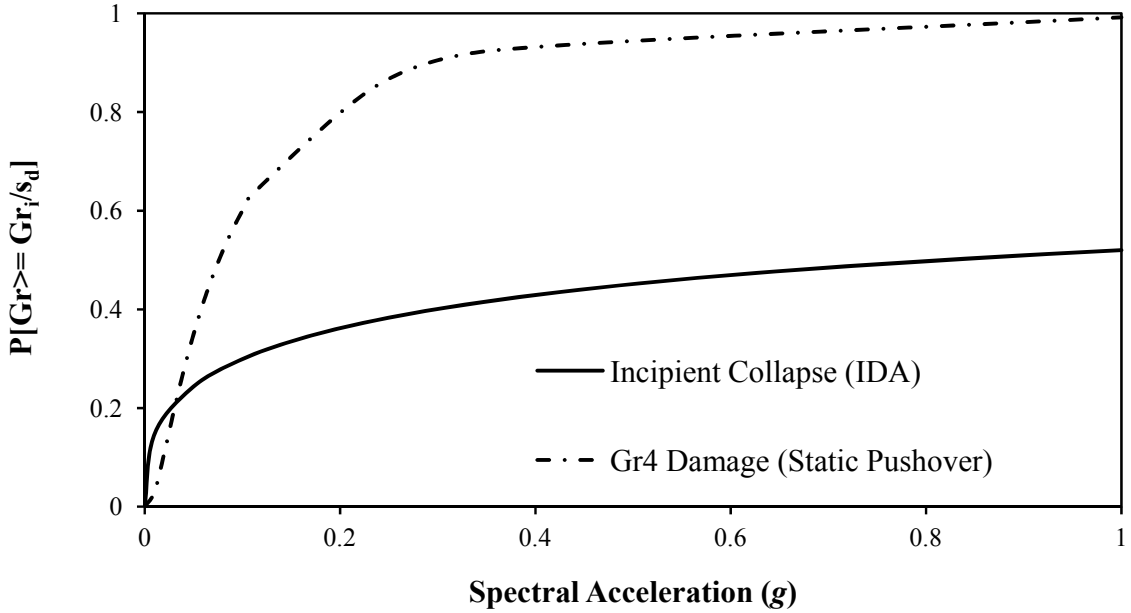

(a)

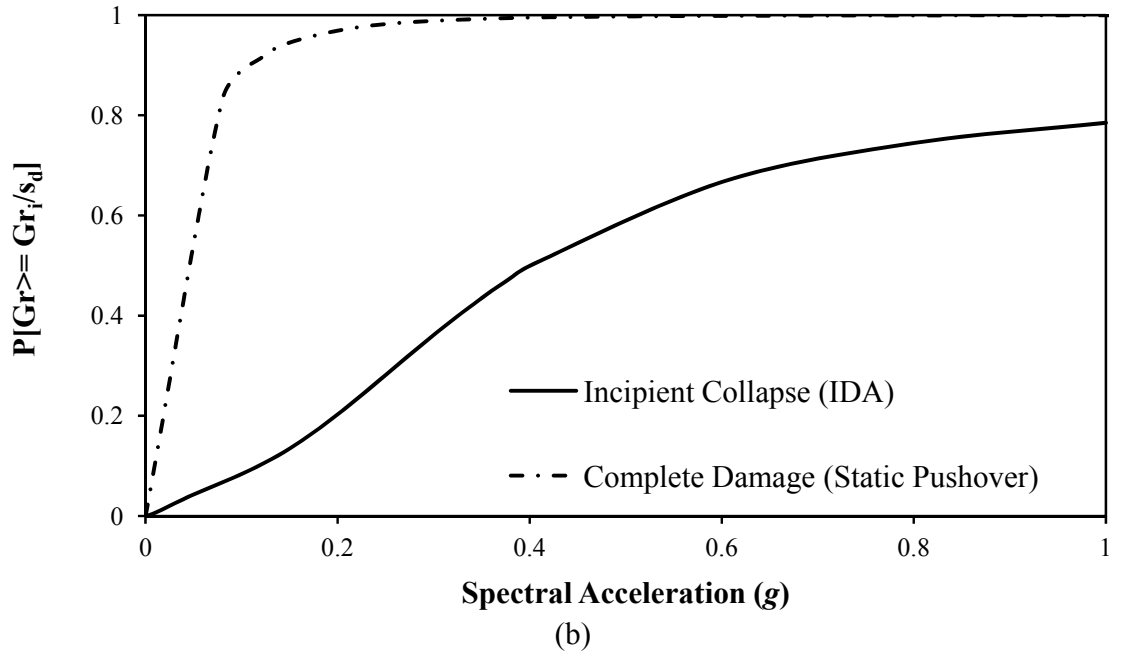

(b)

Fig. 6.15 Comparison of fragility curves obtained from IDA and Static Pushover, for infilled frame building designed for gravity loads only, with three bays open in the ground storey: (a) four; and (b) ten storey.

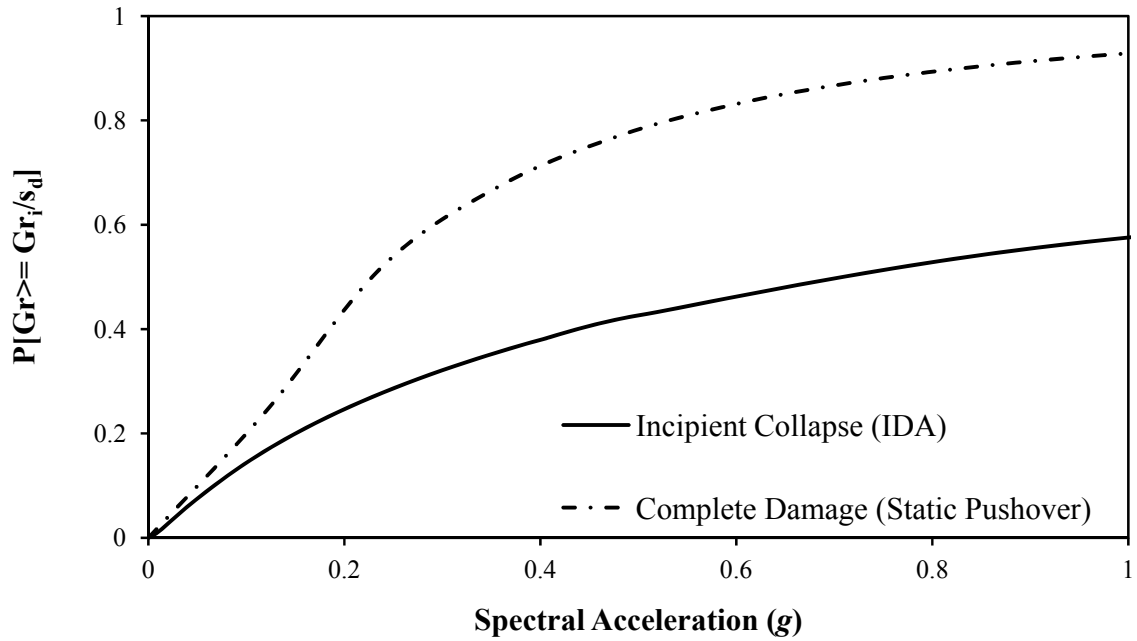

(a)

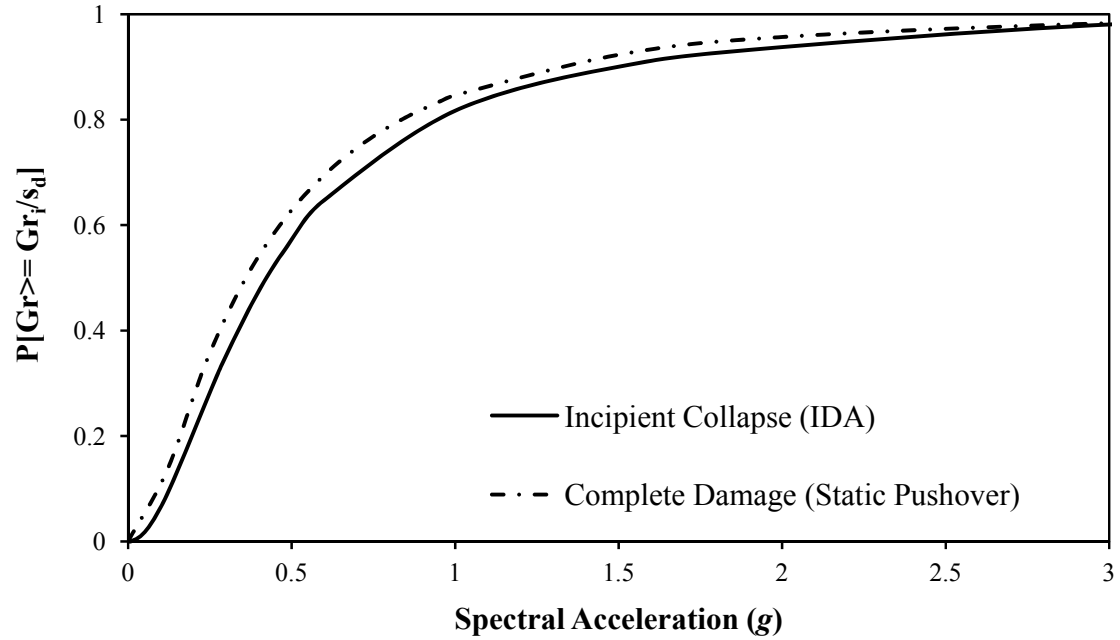

(b)

Fig. 6.16 Comparison of fragility curves obtained from IDA and static pushover for infilled frame building designed as SMRF, with three bays open in the ground storey: (a) four; and (b) ten storey.

It is observed that in case of the buildings designed for gravity loads only, the probability of 'Collapse', obtained from static pushover analysis is much higher than that of 'Incipient Collapse' obtained using IDA, for a given spectral acceleration. The difference can be attributed to the relatively larger difference between the convoluted capacity curves and IDA curves (Figs. 5.41 and 5.42) and variability (Tables 6.9 and 6.10) in case of GLD buildings. The difference in the fragility curves obtained from the two methods is much reduced in case of SMRF design, as the convoluted (static) capacity curves were quite close to the IDA curves (Fig. 5.42-5.43) in this case.

6.7 DAMAGE PROBABILITY MATRICES

As mentioned earlier, the fragility curves plotted in terms of spectral displacement cannot be compared directly as the spectral displacements of two buildings (particularly with and without infills) may be quite different for a given seismic intensity. Comparison of discrete damage probabilities for different values of Effective Peak Ground Acceleration (EPGA), conventionally used in the design codes as zone factor, can provide a clearer picture of the relative damageability of different buildings with varying structural systems, design levels, and number of storeys. In case of IDA, the EPGA can be directly related to spectral acceleration, using a chosen spectral shape (a common choice may be design spectral shape of a seismic code). On the other hand, in case of static pushover analysis, the spectral displacements corresponding to the chosen values of EPGA needs to be evaluated using any of the available procedures, involving spectral shape, elastic damping, and initial/effective period of the structure. In the present study, spectral shape of BIS (2002) for Soil Type-I and Displacement Modification Method (DMM) of ASCE-41 (2007) have been used. Further, considering the increased energy dissipation in case of infilled buildings, due to cracking and friction sliding of masonry infills, 10% elastic damping has been considered, as compared to the 5% damping in case of bare frames. Table 6.11 shows the damage probabilities of gravity load designed RC frame buildings for EPGA levels (0.08*g*, 0.12*g*, 0.18*g*) corresponding to the Design Basis Earthquake (DBE) of Indian Seismic Zones III, IV and V. Similarly, Table 6.12 shows the damage probabilities of RC frame buildings designed as SMRF, for EPGA

levels corresponding to DBE (0.12*g*, 0.18*g*) and MCE (0.24*g*, 0.36*g*) of Indian seismic zones IV and V, respectively. It is interesting to note that in the deterministic performance analysis presented in the previous section, the buildings which survived MCE of Zone IV (PGA = 0.24*g*) without collapse, show more than 50% probability of extensive damage (except in case of four and ten storey SMRF bare frame which has 37% and 33%, respectively, chances of extensive damage) in fragility analysis. This demonstrates the effect of inherent variabilities on expected performance of buildings. Again, the gravity designed infilled frame buildings show the worst performance and have the highest damage probability for all values of EPGA. It can also be observed from Table 6.12 that inclusion of infills increases the damage probability of the frame buildings significantly, irrespective of design level. The adverse effect of infills on performance of frame buildings has been recognized in FEMA (2003a, 2006), which assigns only "low code" design levels to the frame buildings with URM infills, and does not consider these as "moderate" or "high code" design.

6.8 SUMMARY

The fragility curves indicate higher damage probability of infilled frames as compared to bare frame for both gravity designed buildings as well as SMRF buildings designed as per relevant Indian Standards. Gravity designed infilled frame buildings have the worst performance and highest damage probability for all the grades of damages. Even the SMRF buildings designed and detailed as per Indian Standards have more than 50% probability of extensive damage under MCE of the same seismic zone for which these have been designed. The damage probability of infilled frame increases further for all the damage states due to irregularly placed infills. Considering the significant undesirable effect of URM infills on seismic performance, it is very important to give proper attention to the infill-frame interaction in design of URM infilled RC frame buildings. Further, the study shows that the deterministic performance analysis does not provide complete insight into expected performance of buildings, and a probabilistic framework for performance-based design is required.

Table 6.11
Damage probabilities (%) of Indian model RC building types designed for gravity loads only as per relevant Indian Standards

Design Level	No. of Storeys	Damage ≥Gr1 for EPGA (*g*)				Damage ≥Gr3 for EPGA (*g*)				Damage ≥Gr4 for EPGA (*g*)			
		Zone III (BIS 2002)		Zone IV (BIS 2002)	Zone V (BIS 2002)	Zone III (BIS 2002)		Zone IV (BIS 2002)	Zone V (BIS 2002)	Zone III (BIS 2002)		Zone IV (BIS 2002)	Zone V (BIS 2002)
		DBE	MCE	DBE	DBE	DBE	MCE	DBE	DBE	DBE	MCE	DBE	DBE
		0.08	0.16	0.12	0.18	0.08	0.16	0.12	0.18	0.08	0.16	0.12	0.18
RC frame buildings without infills	4	38	77	59	91	17	49	31	68	6	27	14	46
	10	59	92	89	99	30	70	64	89	13	48	41	74
RC frame buildings with uniformly placed URM infills	4	75	98	93	99	72	89	87	94	38	80	55	79
	10	93	100	99	100	77	96	92	99	67	89	83	95
URM infilled RC frame Buildings with open ground storey	4	75	99	90	99	51	90	68	87	43	82	66	89
	10	85	98	96	100	60	98	93	100	78	92	86	97
URM infilled RC frame buildings with one front bay open in ground storey	4	95	100	99	100	76	97	94	99	52	85	78	93
	10	94	99	98	100	82	96	91	99	74	91	85	96

Table 6.12
Damage probabilities (%) of Indian model RC building types designed as SMRF as per relevant Indian Standards

Design Level	No. of Storeys	Damage ≥Gr1 for EPGA (*g*)				Damage ≥Gr3 for EPGA (*g*)				Damage ≥Gr4 for EPGA (*g*)			
		Zone IV (BIS 2002)		Zone V (BIS 2002)		Zone IV (BIS 2002)		Zone V (BIS 2002)		Zone IV (BIS 2002)		Zone V (BIS 2002)	
		DBE	MCE	DBE	MCE	DBE	MCE	DBE	MCE	DBE	MCE	DBE	MCE
		0.12	0.24	0.18	0.36	0.12	0.24	0.18	0.36	0.12	0.24	0.18	0.36
RC frame buildings without infills	4	24	66	43	83	7	37	18	58	1	14	4	32
	10	28	65	49	83	8	33	20	56	1	10	4	27
RC frame buildings with uniformly placed URM infills	4	55	100	100	100	7	83	74	93	1	34	23	53
	10	76	99	96	100	13	56	42	75	1	12	6	25
URM infilled RC frame buildings with open ground storey without any consideration of relevant provisions of Indian Standard (BIS 2002)	4	65	97	82	99	32	78	50	90	15	52	27	68
	10	80	100	98	100	20	76	55	89	4	32	18	47
URM infilled RC frame buildings with open ground storey, designed and detailed as per BIS (2002)	4	59	95	78	99	16	60	31	82	2	22	6	44
	10	78	100	98	100	14	75	52	88	1	25	9	44
URM infilled RC frame buildings With one front bay open in ground storey	4	70	100	100	100	10	96	82	99	1	68	35	83
	10	64	100	97	100	13	73	50	87	1	23	9	41

Chapter 7

AN OPEN TOOL FOR SEISMIC RISK ASSESSMENT

7.1 INTRODUCTION

Seismic safety of the built environment in seismically active regions has been on the national and international agenda since earthquakes have been identified to be a serious threat to human development. In developing countries, this challenge is continually increasing due to the rapid growth of vulnerable housing stock resulting from lack of awareness and effective enforcement. As the assessment of earthquake risk for a region or community is a costly and time-consuming task, software tools which make effective use of different techniques and forms of available information are necessary. For this purpose, several software tools have been developed in recent years. Differences in underlying approaches, loss computation methodologies and format of the required input information generally result in large variations of the derived risk estimates. Comparative studies using common building inventory are required for identifying the significance of different parameters and possible convergence of different approaches. In the past, only a few studies have been undertaken to compare different approaches of seismic risk assessment (Erdik et al. 2003; Strasser et al. 2008; Lang et al. 2012). The need of a comparative study of risk assessment based on macroseismic intensity and spectrum-based approaches was recognized by Erdik et al. (2003), who compared risk estimates using the two different approaches for the common building inventory of Istanbul metropolitan area in order to quantify the range of uncertainties involved. Later, using the identical building inventory of Istanbul, Strasser et al. (2008) compared building damage and social losses provided by five European Earthquake Loss Estimation (ELE) methodologies: KOERILOSS (Erdik and Aydinoğlu 2002), SELENA (Molina et al. 2010), ESCENARIS (Giovinazzi 2005; Mouroux and Le Brun 2006; Roca et al. 2006), SIGEDPC (Sabetta et al. 1998), and DBELA (Crowley et al. 2004), in order to assess the applicability of the selected software packages in European urban centers. However, due to differences in the damage state classifications and casualty models

incorporated in the selected software packages, no satisfactory conclusions on the effect of different parameters could be made. Lang et al. (2012) presented risk estimates for the city of Dehradun (northern India) which were computed using the spectrum-based approach and compared them with previously derived risk estimates that were based on macroseismic intensity (Prasad et al. 2009). For the spectrum-based risk estimates, Lang et al. (2012) made use of the elastic design spectrum of Indian code (BIS 2002). Adhikary and Singh (2011) have pointed out limitations of Indian code design spectra and soil amplification provisions, vis-à-vis other seismic building codes and the Next Generation Attenuation (NGA) relationships. It has been observed that differences in soil amplification models and different magnitude-distance (M-R) pairs can result in widely varying response spectra even for the same Peak Ground Acceleration (PGA). Differences in soil amplification models in different codes, result in widely varying spectral shapes and hence are expected to result in significant variation in seismic loss estimates, as well. Further, several researchers (Bommer and Elnashai 1999; Chopra and Goel 2001; Bozorgnia and Campbell 2004) have highlighted the limitations of elastic response spectrum in representing the response of an inelastic system and considered inelastic response spectrum as a step closer to reality than its elastic counterpart (Bozorgnia et al. 2010a). Therefore, it is pertinent to study the effect of source-site parameters, spectral shapes, soil amplification models, and inelastic spectra on the estimated losses.

In the present study, a software tool 'SeisVARA (**Sei**smic **V**ulnerability **A**nd **R**isk **A**ssessment)' has been developed to facilitate comparative studies using a common building inventory and risk model, while specifying the seismic demand in any of the three forms, i.e. macroseismic intensity, PGA with choice of spectral shapes and soil amplification models of various seismic building codes (BIS 2002; Eurocode-8 2004; NZS-1170.5 2004; ASCE-7 2006), and inelastic displacement spectra using the NGA relationships (Bozorgnia et al. 2010b). The use of an identical building inventory and loss model thereby helps in bringing out the effect of hazard and vulnerability models on the risk estimates, more clearly.

Table 7.1 summarizes the main features and methodologies adapted for damage estimation by different seismic risk estimation software tools. The initial development in seismic risk assessment tools, such as SIGE-DPC (Sabetta et al. 1998) or RADIUS (IDNDR 1999), was based on intensity scales which was then followed by advent of

spectrum-based approaches such as HAZUS-MH (FEMA 1999, 2006), RISK-UE (Mouroux and Le Brun 2006), HAZ-Taiwan (Yeh et al. 2006), etc. HAZUS-MH (FEMA 1999, 2006), that was developed for FEMA to plan seismic risk mitigation strategies in the United States is one of the most significant developments in this direction. It deals with nearly all aspects of the built environment and provides estimates of a wide range of losses. The HAZUS-MH methodology has been applied to other parts of the world with hazard and vulnerability adapted as per local conditions, as in case of RISK-UE (Mouroux and Le Brun 2006) and HAZ-Taiwan (Yeh et al. 2006). The open-source risk assessment software SELENA (Molina et al. 2010) adapts the core of the HAZUS methodology but is open to any input data and thus can be applied to any built environment worldwide. A slightly different analytical loss estimation approach is implemented in the software DBELA (Crowley et al. 2004), which computes demand and capacity of building classes in terms of displacement at different damage limit states.

Table 7.1
Summary of available seismic risk estimation tools

Software tool	Seismic hazard parameter for damage estimation			Use of proprietary software
	Macro-seismic intensity	Elastic spectrum	Inelastic spectrum	
SIGE-DPC (Sabetta et al. 1998)	√	×	×	×
RADIUS (IDNDR 1999)	√	×	×	√
ELER (Hancilar et al. 2010)	√	√	×	√
HAZUS-MH (FEMA 2006)	×	√	×	√
RISK-UE (Mouroux and Le Brun 2006)	√	√	×	√
HAZ-Taiwan (Yeh et al. 2006)	×	√	×	√
DBELA (Crowley et al. 2004)	×	√	×	×
ESCENARIS (Giovinazzi 2005; Mouroux and Le Brun 2006; Roca et al. 2006)	√	×	×	√
RISK.iitb (Sinha et al. 2008)	√	×	×	√
SEISMOCARE (Anagnostopoulos et al. 2008)	×	√	×	√
SELENA (Molina et al. 2010)	×	√	×	√
IVARA (Haldar et al. 2010)	√	×	×	×
SeisVARA (Haldar et al. 2013)	√	√	√	×

However, tools that are based on the analytical approach require elaborate data on building exposure and vulnerability, which is generally not available in many parts of the world. Therefore, the use of macroseismic intensity in earthquake loss estimation is still prevalent and a number of loss estimation software make use of macroseismic intensity to derive estimates for building damage, e.g., ESCENARIS (Giovinazzi 2005; Mouroux and Le Brun 2006; Roca et al. 2006), SIGE-DPC (Sabetta et al. 1998), RADIUS (IDNDR 1999), etc. Aware of the fact that either earthquake hazard or structural vulnerability may be available in terms of different ground motion parameters, some software tools provide separate modules for conducting intensity-based and spectrum-based loss assessments, e.g., ELER (Hancilar et al. 2010). Considering the lack of vulnerability information on the Indian housing stock, particularly in terms of spectral parameters, RISK.iitb (Sinha et al. 2008) first computes the hazard in terms of PGA and then converts it into MSK intensity (Medvedev et al. 1965) for damage assessment.

Most of the available risk assessment tools require additional (often commercial or proprietary) software packages (e.g. MATLab, ArcGIS, etc.) or advanced programming skills to be able to adapt these software tools to local conditions. The potential of Microsoft Excel (MS Excel) (Microsoft-Corp. 2010) as a platform for a widely applicable risk analysis tool was explored during the RADIUS project (IDNDR 1999). Its simplicity, transparency through spreadsheet-based calculations, and popularity makes it in a way an ideal platform for easy adaptation and modification for local conditions. The truly open characteristic of MS Excel-based tools was demonstrated in 'IVARA' (Seismic **V**ulnerability **A**nd **R**isk **A**ssessment of **I**ndian Housing) – a seismic intensity based risk assessment tool for Indian housing (Haldar et al. 2010), which can be easily adapted for any other housing stock by simple manipulation of the data in tabular format. The tool has been further developed to include the Capacity Spectrum Methodology (CSM) (ASCE-41 2007) using spectral shapes of various national design codes (BIS 2002; Eurocode-8 2004; NZS-1170.5 2004; ASCE-7 2006) as well as inelastic displacement spectra using the NGA relationships (Bozorgnia et al. 2010b). The current version of the software, called 'SeisVARA', has been customized for Indian housing stock but can be easily adapted to any other region by simple modification of the building classification scheme and

by providing corresponding vulnerability information in the tabular (spreadsheet) format.

The software utilizes a common housing database and loss model for risk assessment and hence allows a direct comparison of loss estimates derived by the three different approaches. The software derives estimates of physical damage, direct economic loss, life loss and injuries at day and night time, as well as number of homeless people. During the development of the software tool, 34 different model building types (MBTs) representing the major building typologies on the Indian subcontinent have been identified (Prasad et al. 2009) and implemented in the software. A detailed comparative study of risk estimates using the three different approaches of damage assessment, for Dehradun, a typical north Indian city is also presented. Deterministic risk scenarios based on MSK-EMS, and PSI intensity scales, PGA with spectral shapes of four different national design codes, and inelastic displacement spectra for varying source-site parameters, are presented and discussed in the present manuscript.

7.2 THE OPEN-SOURCE SOFTWARE TOOL SeisVARA

The schematic outline of the developed software is presented in Fig. 7.1. As it is shown, the software consists of the main risk engine (processor) and four program modules. The input module consists of information on the building inventory and hazard scenario. As mentioned earlier, SeisVARA allows specifying hazard either in terms of macroseismic intensity (SeisVARA-Intensity), response spectrum/PGA (SeisVARA-Spectrum) or alternatively in terms of source-site parameters of the scenario earthquake (SeisVARA-NGA). Fig. 7.2 shows the main output pages of the software for the three different options of hazard specification. The input data required for building inventory are total floor area, indoor occupancy at day and night time, replacement costs of the structural system and nonstructural components, and building contents for each MBT exposed to the seismic impact. Currently, four occupancy classes are distinguished, i.e., residential, low commercial, medium commercial and high commercial, which represent a typical Indian urban habitat. However, any occupancy class can be substituted or added by the user following local conditions or available information.

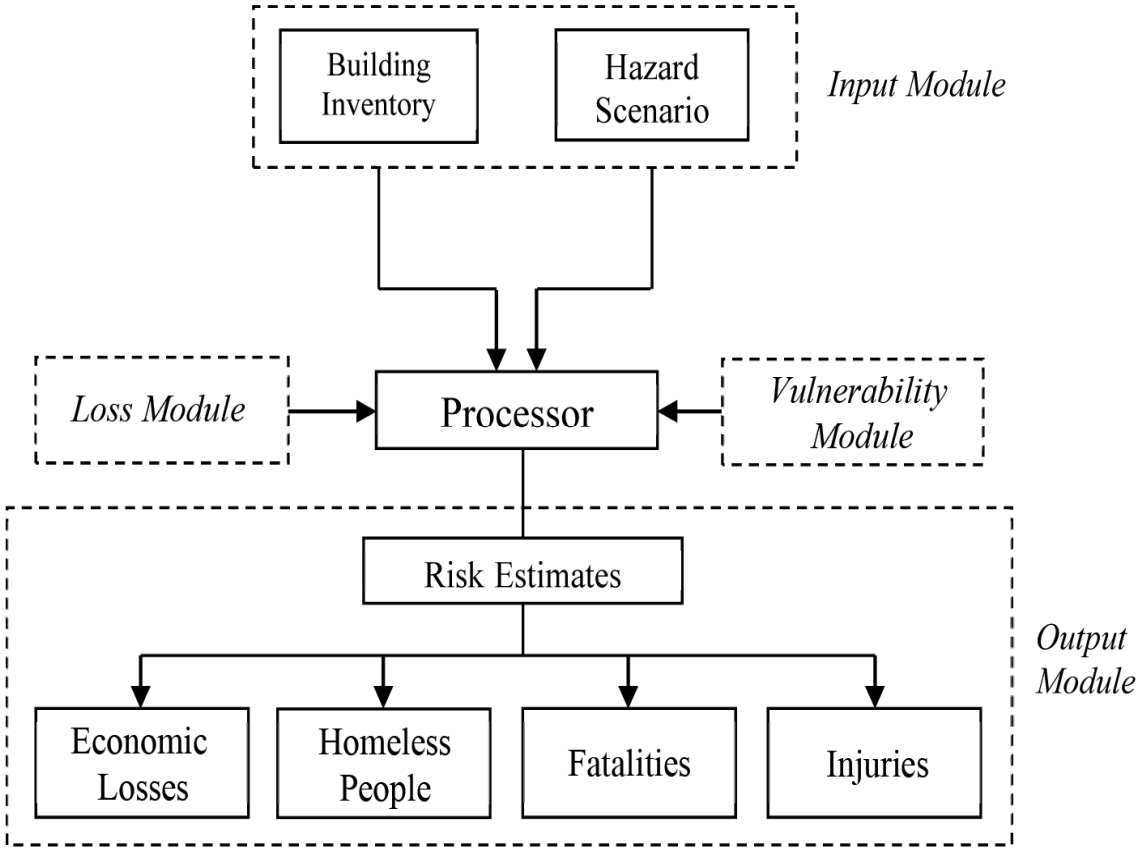

Fig. 7.1 Schematic outline of SeisVARA. All the modules, except for the processor are available in tabular format of the spreadsheet. The processor module consists of simple mathematical relationships in MS Excel format, which can be openly accessed by the user and easily modified if required.

The vulnerability module provides the damage probabilities of the defined MBTs using the procedure described in Section 7.4. Vulnerability of Indian buildings has been estimated considering three alternative approaches - Upper-Bound and Lower-Bound Damage Probability Matrices (DPMs) based on MSK (Medvedev et al. 1965) and EMS (Grünthal ed.1998) intensity scales, continuous vulnerability functions of PSI (Spence et al. 1991) intensity scale, and the analytical capacity spectrum-based approach. The capacity spectrum approach used in SeisVARA is similar to the one applied in HAZUS, except for the fact that the Displacement Modification Method (DMM) of ASCE-41 (2007) has been used instead of the iterative Acceleration-Displacement Response Spectrum method of ATC-40 (1996). The DMM is an improvement over the original Displacement Coefficient Method (DCM) of FEMA-273 (1997). Further, unlike the ATC-40 (1996) method, it provides a direct estimation (without iterations) of the target displacement and hence is more suitable for

spreadsheet-based programming. In case of the scenario earthquake-based approach (SeisVARA-NGA), the Next Generation Attenuation (NGA) model (Bozorgnia et al. 2010b) has been used to obtain the inelastic displacement response spectrum for the given source-site parameters, and ductility ratios corresponding to the target displacement. This process generally requires two to three iterations to converge to the target displacement.

The loss module is responsible for the computation of social and economic loss for each MBT at any particular damage grade, as discussed in Section 7.5. Since a loss model that is customized to Indian conditions is not yet available, the loss model of HAZUS for comparable building typologies has been incorporated in the software.

The output module provides aggregated loss estimates for the entire study area for which input data is provided. As illustrated in Fig. 7.2, SeisVARA provides risk estimates in terms of direct economic loss, life loss and injuries (both at day and night time) and number of homeless people. The software uses physical damage (i.e., building floor area affected by different damage severity) as an intermediate step to derive loss estimates.

The software consists of self-explanatory spreadsheets with adequate documentation to provide details of theoretical formulation, with appropriate references. The second spreadsheet (after the "Main Page") provides "Instructions to users". The software can be downloaded freely from the website <www.eqrisk.info> and can be easily used and adapted for any building typology, vulnerability, and risk model, using the instructions provided within the spreadsheets.

7.3 CLASSIFICATION OF HOUSING STOCK

In total, 34 different MBTs (Prasad et al. 2009) representing the wide range of Indian housing stock have been implemented in the software. These vary from traditional construction practices, over low-strength masonry constructions dominated by locally available materials to modern multi-story RC constructions. In this classification scheme, existing constructions have been broadly categorized into three main classes according to the lateral load-resisting frame (wall) system, namely adobe and random rubble stone construction, masonry consisting of rectangular units, and framed

structures. These three classes are further subdivided according to wall/framing typology and height range (i.e., number of storeys). Table 7.2 lists the 12 identified wall types in increasing order of lateral load-resisting capacity.

SeisVARA-Intensity (V.1.0) — Seismic Vulnerability And Risk Assessment of Housing using Intensity

CITY:	Dehradun
WARD / TRACT NO:	91038
MOHALLA / COLONY NAME:	Palton Bazar Dehradun

SEISMIC RISK SCENARIO FOR MSK INTENSITY: VIII

BASED ON: PARAMETERLESS SCALE OF INTENSITY (PSI) ESTIMATES

SEISMIC RISK SCENARIO FOR MSK INTENSITY - VIII

DIRECT ECONOMIC LOSS =	65802,66	Rs./m²		
TOTAL DIRECT ECONOMIC LOSS =	Rs. 2 420 455 386			
NO. OF HOMELESS PEOPLE =	5443	PERSONS		
	DAY TIME		NIGHT TIME	
TOTAL POPULATION =	38839	Persons	36405	Persons
EXPECTED CASUALITIES =	86	Persons	78	Persons
EXPECTED INJURIES =	644	Persons	604	Persons

(a)

SeisVARA-Spectrum (V.1.0) — Seismic Vulnerability And Risk Assessment of Housing, using Response Spectrum

CITY:	Dehradun
WARD / TRACT NO:	91035
NAME OF LOCALITY :	Nehru Colony Old Dehradun

SEISMIC RISK SCENARIO FOR EFFECTIVE PEAK GROUND ACCELERATION (EPGA) =	0,12	g	
PARAMETERS REQUIRED FOR RISK ESTIMATION BASED ON ASCE STANDARD			
Mapped,5% Damped Acceleration Parameter (S_S) at 0.2 Sec Time Period	0,12	g	Required Field
Mapped,5% Damped Acceleration Parameter (S_1) at 1 Sec Time Period	0,4	g	Required Field
Long Period Transition Period (T_L)	4	sec	Required Field

SITE CLASS: ASCE STANDARD-ASCE/SEI 7-05 SITE CLASS B

SEISMIC RISK SCENARIO FOR EFFECTIVE PEAK GROUND ACCELERATION (EPGA) = 0,12 g

DIRECT ECONOMIC LOSS =	8 526	Rs./m² of constructed area		
TOTAL DIRECT ECONOMIC LOSS =	Rs. 337 548 253			
NO. OF HOMELESS PEOPLE =	754	PERSONS		
	DAY TIME		NIGHT TIME	
TOTAL POPULATION =	38840	Persons	36404	Persons
EXPECTED CASUALITIES =	0	Persons	0	Persons
EXPECTED INJURIES =	52	Persons	45	Persons

(b)

Fig. 7.2 (contd.)

SeisVARA-NGA (V.1.0) — Seismic Vulnerability And Risk Assessment of Housing, using NGA

CITY:	Dehradun
WARD / TRACT NO:	91035
NAME OF LOCALITY :	Nehru Colony Old Dehradun

SEISMIC RISK FOR GIVEN SITE-SOURCE PARAMETERS
USING NEXT GENERATION ATTENUATION RELATIONSHIP

DIRECT ECONOMIC LOSS =	92 191 Rs./m² of constructed area	
TOTAL DIRECT ECONOMIC LOSS =	Rs. 3 308 569 055	
NO. OF HOMELESS PEOPLE =	7 425 Persons	
	DAY TIME	NIGHT TIME
TOTAL POPULATION =	38840 Persons	36404 Persons
EXPECTED CASUALITIES =	95 Persons	91 Persons
EXPECTED INJURIES =	926 Persons	872 Persons

(c)

Input data required in SeisVARA-NGA for Scenario

INPUT DATA REQUIED FOR NEXT GENERATION ATTENUATION RELATIONSHIP (Bozorgnia et al., 2010)

M	R_{RUP} (km)	R_{JB} (km)	F_{RV}	F_{NM}	Z_{TOR} (km)	δ (Degree)	V_{s30} (m/sec)	$Z_{2.5}$ (km)			
6	20	5	1	0	3	30	1070	0,5452			

Where,

- M = Moment magnitude
- R_{RUP} = Closest distance to coseismic rupture (km)
- R_{JB} = Closest distance to surface projection of coseismic rupture (km)
- F_{RV} = Reverse-faulting factor: 0 for strike slip, normal, normal-oblique; 1 for reverse, reverse-oblique and thrust
- F_{NM} = Normal-faulting factor: 0 for strike slip,reverse,reverse-oblique and thrust; 1 for normal and normal-oblique
- Z_{TOR} = Depth to top of coseismic rupture (km)
- δ = Average dip of rupture plane (degrees)
- V_{S30} = Average shear-wave velocity in top 30m of site profile
- A_{1100} = PGA on rock with Vs30 = 1100 m/s (g)
- $Z_{2.5}$ = Depth of 2.5 km/s shear-wave velocity horizon (km)

(d)

Fig. 7.2 Main pages of SeisVARA for the three different formats of hazard inputs: (a) macroseismic intensity, (b) design response spectrum, and (c) and (d) scenario earthquake parameters for the NGA relationship (Bozorgnia et al. 2010b).

Table 7.2
Identified wall types commonly used on the Indian subcontinent shown in order of increasing lateral load resistance

No.	Label	Description of Wall/Framing Type
1	W_1	Rammed mud/ sun-dried bricks/ rubble stones in mud mortar
2	W_2	Rubble stones in lime-surkhi[a)] mortar
3	W_3	Rubble stones in cement mortar
4	W_4	Burnt clay bricks/ rectangular stones in mud mortar
5	W_5	Burnt clay bricks/ rectangular stones in lime-surkhi [a)] mortar
6	W_6	Burnt clay bricks/ rectangular stones/ concrete blocks in cement mortar
7	W_7	Burnt clay bricks/ rectangular stones/ concrete blocks in cement mortar and provided with seismic bands and vertical reinforcement at corners and jambs
8	W_8	RC frames/shear walls with URM infill walls – constructed without any consideration of earthquake forces
9	W_9	RC frames/ shear walls with URM infill walls – earthquake forces considered in design but detailing of reinforcement and execution not as per earthquake-resistant guidelines (C_L / C_M)[b)]
10	W_{10}	RC frames/ shear walls with URM infill walls – designed, detailed and executed as per earthquake-resistant guidelines (C_L / C_M / C_H) [b)]
11	W_{11}	Steel moment frames with URM infill walls (C_L / C_M / C_H) [b)]
12	W_{12}	Steel braced frames (C_L / C_M / C_H)[b)]

a) 'Surkhi' is powdered burnt clay, commonly used with lime and other ingredients in historical masonry constructions on the Indian subcontinent. It has good pozzolanic properties, which result in reasonably strong and durable constructions.

b) C_L, C_M, C_H represent low-code, moderate-code and high-code design levels, respectively (see Section 7.4.2.1).

Table 7.3 specifies the six different roof/floor systems commonly found in India in ascending order of their expected seismic performance with respect to their crucial role in distributing lateral loads and in providing lateral support to the walls in out-of-plane action. The number of storeys is another key parameter which controls the seismic vulnerability of buildings, since both the building's natural period of vibration and base shear strongly depend on their height.

Table 7.4 illustrates the commonly used combinations of the wall/framing systems with roof/floor types and number of storeys leading to a total number of 34 different MBTs. Low-strength adobe, random rubble stone masonry and mud mortar buildings (generally limited to two storeys) as well as buildings constructed with rectangular brick units and cement mortar (up to 4 storeys) are prevailing in India. The current

Indian seismic building code (BIS 2002) recommends a unique form of confined masonry with horizontal RC bands at lintel level (in some cases at plinth and roof level as well) and vertical reinforcement at corners, joints and jambs. Other common construction practice in urban India consists predominantly of RC frame buildings with unreinforced masonry (URM) infill walls.

Table 7.3
Identified roof/floor types commonly used on the Indian subcontinent, shown in ascending order of expected seismic performance

No.	Label	Roof/Floor Type
1	R_1	Heavy sloping roofs – stones/burnt clay tiles/ thatch on sloping rafters
2	R_2	Heavy flat flexible roofs – wooden planks, stone/burnt clay tiles supported on wooden/steel joists with thick mud overlay
3	R_3	Light sloping roofs – corrugated asbestos cement or GI sheets on sloping rafters without cross bracing
4	R_4	Trussed roof with light weight sheeting (without cross bracing)
5	R_5	Trussed/hipped roof with light-weight sheeting (with cross bracing)
6	R_6	Flat rigid reinforced-concrete or reinforced-masonry slab

7.4 VULNERABILITY OF HOUSING STOCK

As discussed in Chapter 6, despite several devastating earthquakes in India, systematic information on building damage for the development and calibration of reliable vulnerability estimates is lacking. A similar situation does exist in many other parts of the world and several efforts (e.g. PAGER[http://earthquake.usgs.gov/ earthquakes/pager/], GEM [http://www.globalquakemodel.org/]) have been initiated to develop a consensus on the vulnerability functions (and of course, on other issues related to seismic risk assessment methodologies) for different MBTs in different parts of the world. As long as such consensus vulnerability information is not available for all parts of the world, it should be legitimate to use vulnerability functions developed for comparable MBTs in other parts of the world. However, the parity between MBTs of different regions requires expert judgment based on good understanding of the lateral load resistance of the comparable MBTs.

Table 7.4

Identified Model Building Types (MBTs) on the Indian subcontinent based on prevalent combinations between wall and roof types and number of storeys; and the details of building inventory of Dehradun

Classification Basis			MBT Label	PSI Class	PAGER Class[a]	Building inventory of Dehradun		
Wall/ Framing Type	Roof/Floor Type	No. of Stories				Floor area (m^2)	No. of occupants at day time	No. of occupants at night time
Adobe and Random Rubble Stone Masonry								
W_1	R1, R2	1	AM11	AA1	A4/RS2	6441	916	1346
		2	AM12			507	82	110
	R3	1	AM21		A2/RS2	1041	64	190
		2	AM22			-	-	-
W_2	R1, R2	1	AL11	AR1	RS3	35312	3587	5034
		2	AL12			542	12	18
	R3, R4	1	AL21			5551	878	1173
		2	AL22			-	-	-
	R5	1	AL31			2083	134	442
		2	AL32			13308	555	534
W_3	R1, R2	1	AC11		RS	5640	455	1073
		2	AC12			3648	156	146
	R3, R4	1	AC21			14640	2019	2804
		2	AC22			1845	101	152
	R5, R6	1	AC31			3900	83	139
		2	AC32			7800	167	277
Masonry consisting of Rectangular Units								
W_4	R1, R2	1	MM11	AA1	UFB1	56602	7086	9636
		2	MM12			395	25	84
	R3, R4	1	MM21			56810	6437	10825
		2	MM21			-	-	-
	R5	1	MM31			14047	1645	3015
		2	MM32			1090	23	39
W_5	R1, R2	1	ML11	BB2	*not defined*	118802	7167	12051
		2	ML12			144254	7003	11560
	R3, R4	1	ML21			26848	1856	2984
		2	ML22			17646	901	1337
	R5, R6	1	ML31			149704	6055	9564
		2	ML32			307263	12288	15924
W_6	R1,R2	1	MC11	BC1	UFB3/UCB	88156	5136	11384
		2	MC12			143621	7592	15810
	R3, R4	1	MC21			110040	7522	13755
		2	MC22			58149	2773	4535
	R5, R6	1	MC3L1	BB2	UFB4/UCB	1901875	76480	127124
		2	MC3L2			2241803	84142	131508
		3-4	MC3M			327128	11700	15348
W_7	R5, R6	1	ME1L1	*(DB1)*[b]	UFB4	100459	2947	4655
		2	ME1L2			252538	8311	12949
		3-4	ME1M			65385	1399	2324
Framed Structures								
W_8	R6	1-3	RC1L	CC1	C2L/C3L	1235535	36209	58040
		4-7	RC1M		C2M/C3M	293806	6285	10397
		10	RC1H		*not defined*			
W_9		1-3	RC2L	(between CC1& DC-UBC-2)[b]	C2	-	-	-
		4-7	RC2M			-	-	-
		8+	RC2H			-	-	-
W_{10}		1-3	RC3L	(DC-UBC-2)[b]	*not defined*	-	-	-
		4-7	RC3M			-	-	-
		8+	RC3H			-	-	-
W_{11}		1-3	ST1L	(DC-UBC-3)[b]	*S5L*	-	-	-
		4-7	ST1M		S5M	-	-	-
		8+	ST1H		S5H	-	-	-
W_{12}		1-3	ST2L		S2L	-	-	-
		4-7	ST2M		S2M	-	-	-
		8+	ST3H		S2H	-	-	-

[a] Sub-typologies according to the PAGER classification of global building types (Jaiswal and Wald 2008)

[b] The corresponding classes are not defined in PSI scale. Judgments have been used to establish parity between Indian MBTs and PSI classes based on expected seismic performance.

In order to estimate the vulnerability of Indian housing stock, Prasad et al. (Prasad et al. 2009) have explored the parity between Indian MBTs with the building vulnerability classes defined in MSK (Medvedev et al. 1965), EMS (Grünthal ed.1998), and PSI (Spence et al. 1992) intensity scales as well as HAZUS (FEMA 2003), based on construction material, roof type, number of stories and seismic design level. Lang et al. (2012) extended this parity to other building typologies available in literature. A global building classification scheme for the purpose of compiling the inventory and vulnerability information for the building stock across the globe was provided by PAGER (Jaiswal and Wald 2008). Table 7.4 shows and allocates the corresponding building classes according to PAGER to the identified Indian MBTs.

7.4.1 Intensity-Based Approach

The correlations of Indian MBTs with the building vulnerability classes defined in MSK, EMS and PSI scales have been used to develop damage probability matrices for the intensity-based module SeisVARA-Itensity. During past damage surveys in India, the MSK intensity scale was traditionally used (GSI 1995; BMTPC 1997/2006; DEQ 1999; GSI 2003). In principle, the classification scheme of EMS scale follows MSK scale in terms of the intensity severity definition. Most of the building types in Class 'A', 'B' and 'C' of EMS-98 scale (Grünthal ed.1998) are similar to those of MSK scale (Medvedev et al. 1965) classification. The only difference between the two scales is that EMS-98 scale has upgraded masonry buildings with RC floors to Class 'C'. Accordingly, in the building classification for the present study, the MBT labels 'MC3' and 'RC1' are considered as equivalent to Class 'C' of EMS-98 scale (Table 7.5). Considering the similarities in the two scales, MSK and EMS-98 scales have been interpreted together. PSI presents an even more detailed classification of load-bearing walls and framed structures depending on the degree of earthquake resistant design as shown in Table 7.4. A detailed discussion on the parity of different Indian MBTs with the EMS-98, MSK, and PSI vulnerability classes is available elsewhere (Prasad 2009). In MSK and EMS intensity scales, the extent of damage is not provided in terms of definite probabilities, rather probable ranges of damage have been described in terms of ‘few’, ‘many’ and ‘most’. Keeping in mind the uncertainty associated with the descriptive damage ranges, it should be avoided to define a

definite Damage Probability Matrix (DPM) based on these intensity scales. Therefore, the 'Upper-Bound' and 'Lower-Bound' DPMs proposed by Prasad et al. (2009) have been implemented in SeisVARA-Intensity. Probability ranges provided by EMS, i.e., 10–20%, 15–55% and 55–100% (with ±5% uncertainty), for the descriptive terms 'few', 'many' and 'most', respectively, have been used to define the Lower and Upper-Bound DPMs (Table 7.5) for the identified MBTs. While defining Upper-Bound DPMs, first, the corresponding probability of the most severe grade of damage has been assigned, and then the probabilities of less severe grades have been adjusted to keep the sum equal to 100%. The similar procedure was applied for estimating the Lower-Bound DPMs. Further, the Lower-Bound and Upper-Bound probabilities for 'few' have been interpreted as 10% and 20%, respectively, in order to avoid the Lower-Bound interpretation of 0% probability of damage in case of 'few'. Arya (2003) suggested some modifications in the damage probability distribution for Indian MBTs according to the EMS scale, corresponding to Intensities VI-IX. These suggestions were based on his experience of past earthquake damage surveys in India. Arya (2003) assigned slightly higher damage expectancy to Indian buildings and also proposed a broader damage distribution covering lower damage grades, as compared to MSK and EMS scales. These modifications have also been incorporated in the Lower- and Upper-Bound DPMs. Table 7.5 reproduces the Lower- and Upper-Bound DPMs for groups of Indian MBTs for MSK intensity VIII.

To avoid subjectivity and difficulties associated to the use of different macroseismic intensity scales while assigning discrete intensity values of the same area according to observed damage by different survey groups, Spence et al. (1992) have developed the parameterless scale of Seismic Intensity (PSI). Unlike MSK and EMS scales, PSI is a continuous scale based on earthquake damage data of 70,000 buildings in 13 different earthquakes, worldwide. Vulnerability functions for a range of common building types and damage states have been provided by Coburn and Spence (2006) in terms of the values of the Gaussian distribution parameters M and σ. The probability of an expected damage state, D_i for a certain building class and for a given value of the PSI intensity, Ψ can be obtained as:

$$[\mathrm{P}(D_i)/\psi]_j = \int_{-\infty}^{\Psi} \frac{1}{\sqrt{2\pi}\sigma_{ij}} \exp\left[-\frac{1}{2}\left(\frac{\psi - M_{ij}}{\sigma_{ij}}\right)\right] \tag{7.1}$$

Where, σ_{ij} is the value of standard deviation for damage state, D_i and building type j, and M_{ij} is the mean value of intensity for the damage state D_i and building type j.

The relationship between MSK and PSI intensities has been given by Coburn and Spence (2006) graphically. Giovinazzi (2005) used this information to deduce the following expression, to correlate the two intensities:

$$\text{MSK Intensity } (I) = 0.54 \cdot \psi + 3.25 \tag{7.2}$$

Using Eqs. 7.1 and 7.2 and correlations between Indian MBTs and PSI classes, the DPMs for the Indian MBTs have been evaluated and implemented in the module-SeisVARA-Intensity.

Table 7.5
Lower and Upper Bound Damage Probability Matrices of Indian MBTs for MSK intensity VIII

Indian MBTs	Vulnerability class as per		Damage Probability (%)									
			Lower-Bound					Upper-Bound				
	MSK	EMS	Gr1	Gr2	Gr3	Gr4	Gr5	Gr1	Gr2	Gr3	Gr4	Gr5
AM1,AM2, AL1,AL2,AL3, AC1,AC2,AC3, MM1,MM2, MM3	A	A	0	18	17	55	10	0	0	0	80	20
ML1,ML2,ML3, MC1, MC2	B	B	0	35	55	10	0	0	0	80	20	0
MC3L,MC3M, RC1L, RC1M	B	C	35	55	10	0	0	0	80	20	0	0
RC2L,RC2M, RC2H	C	C	35	55	10	0	0	0	80	20	0	0
ME1L,ME1M, C3L,RC3M, RC3H,ST1L, ST1M,ST1H, ST2L,ST2M, ST3H	-	D	0	0	0	0	0	0	15	0	0	0

Table 7.6 shows the equivalence of Indian MBTs with PSI classes; mean value, M of PSI intensity corresponding to different damage grades and a typical DPM for MSK intensity VIII, obtained using the PSI scale. Similar DPMs have been obtained for other intensities.

Table 7.6
Damage probabilities of Indian MBTs for MSK intensity VIII using PSI scale

Indian MBTs	PSI Class	Mean of intensity ψ (M)					Damage Probabilities (%)				
		Gr1	Gr2	Gr3	Gr4	Gr5	Gr1	Gr2	Gr3	Gr4	Gr5
AM1, AM2, MM1, MM2, MM3	AA1	3.9	6.6	8.9	10.5	12.4	16	33	24	17	7
AL1, AL2, AL3, AC1, AC2, AC3	AR1	3.2	5.9	8.2	9.8	11.7	11	28	25	22	12
MC1, MC2	BC1	5.6	8.5	10.7	12.3	14.0	35	32	14	6	2
ML3, MC3L, MC3M	BB2	6.5	9.4	11.6	13.2	14.9	42	27	9	3	1
ML1, ML2	BB1	4.9	7.8	10.0	11.6	13.3	29	34	18	10	4
ME1M, ME1L	*(DB1)*	7.5	10.6	13.0	15.0	17.0	46	19	4	1	0
RC1L, RC1M	CC1	7.9	10.3	11.3	12.9	14.1	37	12	11	3	2
RC2L, RC2M, RC2H	(between CC1& DC-UBC-2)	8.4	10.4	11.9	13.5	31.0	15	8	2	1	31
RC3L, RC3M, RC3H	(DC-UBC-2)	8.8	10.5	12.5	14.1	15.2	25	18	5	1	1
ST1L, ST1M, ST1H, ST2L, ST2M, ST3H	(DC-UBC-3)	*9.4*	11.1	13	14.7	16.4	23	13	4	1	0

Table 7.4 indicates that no counterpart exists in the PSI scale for Indian earthquake-resistant masonry construction denoted as ME. The same applies to RC frame buildings (RC2) designed for earthquake forces but not constructed as per earthquake resistance guidelines. The PSI scale does not provide damage probabilities for steel buildings as well. It will be shown later (Section 7.4.2) that the design forces considered in high Seismic Zones of India are comparable to the design forces considered in low Seismic Zones of UBC (1994) (Table 7.9). Accordingly, Indian RC frame buildings (RC3) designed and constructed as per earthquake-resistance guidelines and steel buildings (ST) are equated with PSI classes DC-UBC2 and DC-UBC3, respectively. To complete the DPM, Indian MBT, ME has been considered

equivalent to 'Reinforced Unit Masonry (DB1)' of PSI classification, and the damage probability of RC2 has been obtained as average of CC1 and DC-UBC-2 of PSI scale.

7.4.2 Capacity Spectrum-Based Approach

SeisVARA follows the HAZUS approach (FEMA 2003) in order to estimate the fragility of identified MBTs, using capacity spectrum methodology. The three major steps of this methodology, in context of the present study, are discussed below:

7.4.2.1 Estimation of capacity curve parameters

The capacity curve parameters and fragility functions for URM infilled RC frame buildings of different design levels, developed in the previous Chapters, have been implemented in SeisVARA. Prasad (2009) has performed a similar fragility analysis for masonry building types (MM3, ML3 and MC3L) consisting of rectangular units in different types of mortar and with rigid floor/roof diaphragms. He has considered the building configurations and material properties, typical for northern India and the capacity curve parameters obtained by him have also been implemented in SeisVARA.

Since, reliable analytical models for all Indian model building typologies are not yet available, capacity curve parameters of the other MBTs have been obtained from building typologies available in literature, which are closest to the Indian MBTs on the basis of design force level, as well as material and quality of construction. However, as soon as enhanced models for different local MBTs are available, these parameters can be easily substituted in the software. Table 7.7 summarizes capacity curve parameters considered in the current version of SeisVARA, based on the parity established (Prasad et al. 2009; Lang et al. 2012) with available building typologies.

The low-strength Indian building typologies, i.e., adobe (AM) and random rubble stone masonry (AL, AC), are regarded to be comparable with adobe (M2) and rubble stone (M1) building typologies, respectively, as defined by Cattari et al. (2004). The code-compliant Indian masonry construction denoted as ME (i.e. buildings of wall type W_7 according to Table 7.2) can be equated to MBT 'M6'of Cattari et al. (2004). Reinforced-concrete frames with URM infills (RC1) and without any consideration

for earthquake resistant design are comparable to 'RC3.1 - low-code design' building typology defined by Kappos et al. (2006). The legitimacy of applying these curves for Indian building typologies is discussed in detail by Lang et al. (2012).

Table 7.7
Capacity curve parameters considered in SeisVARA

Indian MBTs	Storeys	Reference	Index of referred building type	Capacity Curve Parameters			
				D_y [mm]	A_y [m/s^2]	D_u [mm]	A_u [m/s^2]
AM1, AM2	1	Cattari et al. (2004)	M2-1	1.01	1.408	10.70	1.408
AM1, AM2	2		M2-2	1.82	0.940	11.40	0.940
AL1, AL2, AL3, AC1, AC21,AC3	1		M1-1	1.01	2.288	11.10	2.288
AL1, AL2, AL3, AC1, AC2, AC3	2		M1-2	1.82	1.527	11.80	1.527
MM1, MM2, MM3	1	Prasad (2009)	MM31	1.50	1.079	8.40	1.472
MM1, MM2, MM3	2		MM32	2.70	0.700	14.60	1.177
ML1, ML2, ML3	1		ML31	1.00	1.570	8.30	2.158
ML1, ML2, ML3	2		ML32	2.60	1.275	14.60	1.766
MC1, MC2, MC3L	1		MC3L1	1.30	1.962	8.00	2.453
MC1, MC2, MC3L	2		MC3L2	2.60	1.570	14.60	2.158
MC3M	3+		MC3L2	2.60	1.570	14.60	2.158
ME1L	1	Cattari et al. (2004)	M6-1	2.28	5.470	25.18	5.470
ME1L	2		M6-2	4.21	3.652	26.81	3.652
ME1M	3+		M6-3	5.78	2.743	28.38	2.743
RC1L (C_N)	1–3	Kappos et al. (2006)	RC3.1LL	5.30	4.234	67.40	5.136
RC1M (C_N)	4-7	Present study	GLD-UI	5.00	2.11	6.00	2.13
			GLD-OG	15.00	1.64	24.00	1.75
			GLD-O1B	4.00	1.52	8.00	1.67
			GLD- O3B	3.00	0.74	10.00	1.16
RC1H (C_N)	8+	Present study	GLD-UI	14.00	0.91	17.00	0.93
			GLD-OG	20.00	0.81	31.00	0.85
			GLD-O1B	11.00	0.63	9.00	0.64
			GLD- O3B	7.00	0.28	12.00	0.29
RC2L, RC3L (C_L & C_M)	1–3	HAZUS-MH MR2 (2006)	C3L (Pre & Low Code)	3.05	0.981	34.29	2.207
RC2L (C_H)	4-7	Present study	SMRF-UI	7.00	3.35	89.00	5.42
			SMRF-OG (C)	24.00	2.94	63.00	3.41
			SMRF-OG (NC)	17.00	4.79	78.00	6.71
			SMRF-O1B	8.00	3.04	75.00	4.56

Indian MBTs	Storeys	Reference	Index of referred building type	Capacity Curve Parameters			
				D_y [mm]	A_y [m/s^2]	D_u [mm]	A_u [m/s^2]
			SMRF-O3B	15.00	2.73	61.00	3.91
RC2M (C_H)	8+	Present study	SMRF-UI	21.00	1.49	176.00	1.96
			SMRF-OG (C)	26.00	1.18	182.00	1.88
			SMRF-OG (NC)	19.00	1.53	159.00	2.14
			SMRF-O1B	26.00	1.39	207.00	1.85
			SMRF-O3B	23.00	1.24	178.00	1.90
ST1L (C_L & C_M)	1–3	HAZUS-MH MR2 (2006)	S5L (Pre & Low Code)	3.05	0.981	30.48	1.961
ST1M (C_L & C_M)	4-7		S5M (Pre & Low Code)	8.64	0.814	57.66	1.638
ST1H (C_L & C_M)	8+		S5H (Pre & Low Code)	27.69	0.618	138.43	1.245
ST2L (C_L & C_M)	1–3		S2L (Pre & Low Code)	4.06	0.981	47.75	1.961
ST2L (C_H)	1–3		S2L (Moderate Code)	7.87	1.961	95.50	3.923
ST2M (C_L & C_M)	4-7		S2M (Pre & Low Code)	15.49	0.814	102.62	1.638
ST2M (C_H)	4-7		S2M (Moderate Code)	30.73	1.638	246.38	3.266
ST3H (C_L & C_M)	8+		S2H (Pre & Low Code)	49.28	0.618	295.15	1.245
ST3H (C_H)	8+		S2H (Moderate Code)	98.30	1.245	590.30	2.491

At present, HAZUS capacity curve parameters for comparable building typologies have been adapted for earthquake-resistant steel frames. While comparing the Indian MBTs with HAZUS (and for that matter with any other region), three parameters – design force level, detailing, and quality of construction, are important. For this purpose, a detailed comparison of Indian RC frame buildings with the US construction has been performed by Prasad (2009) and it has been concluded that Indian design and construction practices differ significantly from those of the US practices. However, parity between comparative building classes can be established. In order to compare the design seismic forces of two different building codes, it is necessary to consider the differences in soil classification and associated amplification

factors. Table describes the three soil types defined in BIS (2002) and their equivalent site classes in UBC (1994).

Table 7.8
Comparison of soil classes of Indian Standard BIS (2002) and UBC (1994)

Soil Classification of BIS (2002)		**Soil Classification of UBC (1994)**	
Soil Type	**Description**	**Soil Profile**	**Description V_{s30} (m/s)**
I	Rock or Hard Soil: Well graded gravel and sand gravel mixtures with or without clay binder, and clayey sands poorly graded or sand clay mixtures having $N > 30$	S_B	Rock ($760 < V_{s30} < 1{,}500$)
		S_C	Very Dense Soil and Soft Rock ($N > 50$) ($360 < V_{s30} < 760$)
II	Medium Soils: All soils with $10 < N < 30$ poorly graded sands or gravelly sands with little or no fines with $N > 15$	S_D	Stiff Soil Profile ($15 > N > 50$) ($180 < V_{s30} < 360$)
III	Soft Soils: All soils with $N < 10$	S_E	Soft Soil Profile ($N < 15$) ($V_{s30} < 180$)

It can be seen from Table 7.8 that the Indian soil type I represents a much wider site class encompassing the soil profile types S_B and S_C of UBC (1994), whereas soil types II and III are comparable with Soil Profiles S_D and S_E, respectively.

Table 7.9 compares the zone factors and design base shear coefficients of BIS (2002) and UBC (1994) for different Seismic Zones. The comparison of design base shear coefficients is done for two periods of vibration, viz., 0.2 *sec* and 1.0 *sec*, representing the acceleration- and velocity-controlled range of the design spectrum, respectively. It should be considered that the detailing and response reduction factor, R for Indian RC frame constructions 'Ordinary Moment Resisting Frames (OMRF)' (R = 3) and 'Special Moment Resisting Frames (SMRF)' (R = 5) are comparable with UBC 94 ductility classes 'OMRF' and 'IMRF', respectively. It can be observed from Table 7.9 that the design base shear coefficients of BIS (2002) for short-period structures (0.2 *sec* period) are constant for all types of soil, which are comparable to UBC (1994) design coefficients for Soil Profile S_B, but are considerably lower for softer soils. This because BIS (2002) does not consider the effect of soil amplification in the short-period range. However, for 1.0 *sec* period, the design base shear coefficients of Indian Seismic Zones III, IV and V are comparable with the UBC (1994) zones 1, 2A, and 2B, respectively, for the equivalent site and ductility classes (shown in Table 7.9 by

bold font and underlain with gray background for OMRF and SMRF of BIS (2002), respectively).

Table 7.9
Comparison of design base shear coefficients of BIS (2002) and UBC (1994)

		BIS (2002)				**UBC (1994)**				
Seismic Zone		**II**	**III**	**IV**	**V**	**1**	**2A**	**2B**	**3**	**4**
Intensity (MSK64)		VI	VII	VIII	≥ IX	V,VI	VII	VIII	>VIII	-
Zone Factor		0.1	0.16	0.24	0.36	0.075	0.15	0.2	0.3	0.4
Soil type I of IS 1893 (2002) equivalent to soil profile type S_B (UBC 94)										
T = 0.2 *sec*	OMRF	0.042	**0.067**	**0.1**	**0.15**	**0.057**	**0.107**	**0.142**	0.214	0.285
	IMRF	–	–	–	–	0.036	0.068	0.09	0.136	0.182
	SMRF	0.025	0.04	0.06	0.09	0.023	0.044	0.058	0.08	0.118
T = 1.0 *sec*	OMRF	0.017	0.027	0.04	0.06	0.023	0.043	0.057	0.086	0.114
	IMRF	–	–	–	–	0.014	0.027	0.036	0.054	0.073
	SMRF	0.01	0.016	0.024	0.036	0.009	0.018	0.024	0.035	0.047
Soil type II of IS 1893 (2002) equivalent to soil profile type S_D (UBC 94)										
T = 0.2 *sec*	OMRF	0.042	0.067	0.10	0.150	0.129	0.229	0.286	0.386	0.457
	IMRF	–	–	–	–	0.082	0.145	0.182	0.245	0.291
	SMRF	0.025	0.040	0.06	0.090	0.053	0.094	0.118	0.159	0.188
T = 1.0 *sec*	OMRF	0.023	**0.0363**	**0.054**	**0.082**	**0.026**	**0.046**	**0.057**	0.077	0.091
	IMRF	–	–	–	–	0.016	0.029	0.036	0.049	0.058
	SMRF	0.014	0.0218	0.033	0.049	0.011	0.019	0.024	0.032	0.038
Soil type III of IS 1893 (2002) equivalent to soil profile type S_E (UBC 94)										
T = 0.2 *sec*	OMRF	0.042	0.067	0.1	0.15	0.186	0.357	0.457	0.6	0.686
	IMRF	–	–	–	–	0.118	0.227	0.291	0.382	0.436
	SMRF	0.025	0.04	0.06	0.09	0.076	0.147	0.188	0.247	0.282
T = 1.0 *sec*	OMRF	0.028	**0.045**	**0.067**	**0.10**	**0.037**	**0.071**	**0.091**	0.12	0.137
	IMRF	–	–	–	–	0.024	0.045	0.058	0.076	0.087
	SMRF	0.017	0.027	0.040	0.06	0.015	0.029	0.038	0.049	0.056

Considering the quality of construction and equivalence of design forces in different zones, the correspondence of code design level (C_L, C_M and C_H) of Indian MBTs has been established with the code design levels of HAZUS (Table 7.10) and the considered fragility curve parameters are shown in Table 7.11. Considering the Indian construction standards, no building class exists which can qualify for the superior quality of construction as described/targeted by UBC (1994). Therefore, Indian construction is equated to 'ordinary' and 'inferior' quality of construction denoted by

HAZUS. Accordingly, the HAZUS nomenclature of pre-code, low-code and moderate-code has been interpreted as low code (C_L), moderate code (C_M), and high code (C_H), respectively, in the context of Indian buildings. In India, a large proportion of buildings are still being constructed without any consideration for seismic forces. Such buildings have been assigned a 'no code (C_N)' design level.

Table 7.10
Comparison of Indian MBTs' design code level with HAZUS classification, considering the quality of construction and design seismic force

Quality of design	Indian Seismic Zones (BIS 2002)				UBC (1994) Seismic Zones				
	II	III	IV	V	1	2A	2B	3	4
Superior	not available				moderate Code		high code		special
Ordinary	C_L	C_M		C_H	low code		moderate code		high code
Inferior	C_N	C_L		C_M	pre code		low code		moderate code

7.4.2.2 Evaluation of displacement demand

Displacement demand for different classes of buildings can be estimated either by using code specified design spectrum in conjunction with PGA estimated using appropriate attenuation relationship or by direct construction of an inelastic displacement demand spectrum using the NGA relationship. As shown in Table 7.1, until now, SeisVARA is the only tool providing risk estimates directly using the inelastic displacement spectrum. The procedure used for the evaluation of displacement demand using elastic and inelastic displacement spectra are discussed in subsequent Sections.

7.4.2.2.1 Using PGA and code design spectrum

The inelastic response of the structure is obtained in SeisVARA-Spectrum using the Displacement Modification Method (DMM) (ASCE-41 2007), in which the response of an equivalent elastic Single Degree of Freedom (SDOF) system is multiplied with some modification factors to obtain the inelastic response of the structure. The elastic response of the equivalent SDOF system is read directly from the response spectrum which is constructed using PGA and the standard elastic spectral shapes and soil amplification models available in design codes.

Table 7.11
Fragility parameters considered in SeisVARA for Indian MBTs

Building Typology (MBTs)	No. of storey	Damage Grade							
		Gr1		Gr2		Gr3		Gr4	
		μ_{Gr1} (mm)	β_{Gr1}	μ_{Gr2} (mm)	β_{Gr2}	μ_{Gr3} (mm)	β_{Gr3}	μ_{Gr4} (mm)	β_{Gr4}
AM1, AM2	1	0.86	1.062	1.51	1.062	4.76	1.06	9.10	1.062
AM1, AM2	2	1.57	0.825	2.73	0.825	5.81	0.82	9.69	0.825
AL1, AL2, AL3, AC1, AC2, AC3	1	0.86	1.079	1.51	1.079	4.90	1.078	9.44	1.079
AL1, AL2, AL3, AC1, AC2, AC3	2	1.57	0.841	2.73	0.841	5.95	0.841	10.03	0.841
MM1, MM2, MM3	1	1.27		2.25		4.44		7.14	
MM1, MM2, MM3	2	2.30		4.05		7.81		12.41	
ML1, ML2, ML3	1	0.85		1.50		3.91		7.05	
ML1, ML2, ML3	2	2.21	0.800	3.90	0.950	7.71	1.050	12.41	1.050
MC1, MC2, MC3L	1	1.11		1.95		4.10		6.80	
MC1, MC2, MC3L2	2	2.21		3.90		7.71		12.41	
MC3M	3+	2.21		3.90		7.71		12.41	
ME1L1	1	1.94	0.961	37.77	0.961	11.10	0.961	21.40	0.961
ME1L2	2	3.58	0.833	40.21	0.833	13.60	0.833	22.79	0.833
ME1M	3+	4.91	0.716	42.57	0.716	15.71	0.716	24.12	0.716
RC1L	1–3	4.51	0.733	7.95	0.733	28.89	0.733	57.29	0.733

Building Typology (MBTs)	No. of storey	Damage Grade							
		Gr1		Gr2		Gr3		Gr4	
		μ_{Gr1} (mm)	β_{Gr1}	μ_{Gr2} (mm)	β_{Gr2}	μ_{Gr3} (mm)	β_{Gr3}	μ_{Gr4} (mm)	β_{Gr4}
RC1M (C_N)	4–7	4.15	0.750	4.50	0.750	4.95	0.850	6.30	1.000
RC1M (OG) (C_N)		10.64	0.750	15.20	0.850	17.48	1.000	24.3	1.000
RC1M (O1B) (C_N)		2.45	0.750	3.50	0.750	4.55	0.850	7.70	1.000
RC1M (O3B) (C_N)		1.96	0.750	2.8	0.850	4.70	1.000	10.40	1.000
RC1H (C_N)	8+	9.59	0.700	13.70	0.700	14.50	0.800	16.90	1.000
RC1H (OG) (C_N)		14.14	0.700	20.20	0.800	22.80	1.000	30.60	1.000
RC1H (O1B) (C_N)		7.56	0.700	10.80	0.700	10.40	0.800	9.20	1.000
RC1H (O3B) (C_N)		4.55	0.700	6.50	0.800	7.83	1.000	11.80	1.000
RC2L (C_H)	4-7	4.90	0.750	7.00	0.750	27.45	0.850	88.80	0.850
RC2L (OG, NC) (C_H)		16.87	0.750	24.20	0.850	33.75	0.850	62.70	1.000
RC2L (OG, C) (C_H)		11.76	0.750	16.80	0.750	32.03	0.850	77.70	0.850
RC2L (O1B) (C_H)		5.74	0.750	8.20	0.750	24.85	0.850	74.80	0.850
RC2L (O3B) (C_H)		10.15	0.750	14.50	0.850	26.18	0.850	61.20	1.000
RC2M (C_H)	8+	14.70	0.700	21.00	0.700	59.83	0.800	176.30	0.800
RC2M (OG, NC) (C_H)		18.13	0.700	25.90	0.800	64.83	0.800	181.60	1.000
RC2M (OG, C) (C_H)		13.16	0.700	18.80	0.700	53.78	0.800	158.70	0.800
RC2M (O1B) (C_H)		18.20	0.700	26.00	0.700	71.18	0.800	206.70	0.800
RC2M (O3B) (C_H)		15.82	0.700	22.60	0.800	61.38	0.800	177.70	1.000
For all other framed structures	-	Fragility functions have been taken from HAZUS-MH MR2 (2006) for equivalent MBTs (Table 7.7).							

where, μ and β are mean spectral displacement and total variability, respectively.

Currently, SeisVARA-Spectrum incorporates spectral shapes and soil amplification models of four seismic building codes, i.e. Indian code (BIS 2002), Eurocode-8 (2004), U. S. American code (ASCE-7 2006), and New Zealand code (NZS-1170.5 2004). The software provides options for specifying the PGA at rock outcrop or at the soil surface. In the first case, amplification of PGA as well as change in spectral shape (due to changes in the frequency content of ground motion) corresponding to the given site class is considered using the site amplification factors from the respective design codes. Most of the attenuation relationships inherently consider the site amplification effect and provide PGA directly at the soil surface. Therefore, in the second case, the amplified PGA is obtained directly from the attenuation relationships, whereas the spectral shape is taken from the code provision given the respective site class and ground motion level (in case of ASCE-7 (2006)).

7.4.2.2.2 Using NGA relationships

Bozorgnia and Campbell (2004) pointed out the limitation of elastic response spectra to predict nonlinear structural displacement response under severe ground motions. As mentioned in Chapter 4, the conversion of elastic acceleration spectra to inelastic displacement spectra is subjected to not only the uncertainties of conversion, but also those of elastic spectrum itself (Bommer and Elnashai 1999; Akkar and Bommer 2007). To obtain the inelastic spectrum directly using the governing earthquake parameters, for the estimation of nonlinear structural displacement response, recently a few Ground Motion Prediction Equations (GMPEs) (Akkar and Bommer 2007; Rupakhety and Sigbjörnsson 2009; Bozorgnia et al. 2010b), as shown in Table 7.12, have been developed for different regions.

The GMPEs proposed by Bozorgnia et al. (Bozorgnia et al. 2010a; Bozorgnia et al. 2010b) are based on the largest set of records from the world-over earthquake database and consider the largest number of governing source-site parameters. Further, this model provides inelastic spectra for the longest period range (up to 7.5 *sec*). The model is gaining widespread acceptability and the same has been implemented in the developed tool SeisVARA-NGA. Based on this model, inelastic demand spectra for ductility factors ranging from 1.0 to 8.0 are generated and the displacement demand is obtained by iterating on ductility demand.

Table 7.12
Overview of various Ground Motion Prediction Equations (GMPEs) for inelastic spectrum

Model reference	Region	Nos. of ground motion records considered	Period of records	Soil types	Governing parameters
Akkar and Bommer (2007)	Europe and Middle East	532	1973–2003	1. Rock 2. Stiff soil 3. Soft soil 4. Very soft soil	1. Moment Magnitude 2. Joyner–Boore distance 3. Site factor 4. Fault mechanism
Rupakhety and Sigbjörnsson (2009)	Continental Europe and Middle East	186	1983–2008	1. Rock 2. Stiff soil	1. Moment Magnitude 2. Distance to the surface projection of fault 3. Site factor
Bozorgnia et al. (2010a); (Bozorgnia et al. 2010b)	World-over	3122	1952–2003	All site classes	1. Magnitude 2. Fault distance 3. Fault mechanism *4.* $V_{s,30}$ **a)** 5. Hanging wall effect 6. Basin effect

a) Average shear wave velocity in top 30 *m*.

7.4.2.3 Estimation of Fragility Functions

The process of estimating Fragility Functions from the Capacity Curve parameters has been discussed in details in Chapter 6. Importance of definition of various 'damage severity levels' and their corresponding threshold parameters is discussed in Section 6.3. Intensity scales define five Damage Grades, whereas HAZUS provides fragility functions for four Damage States, while the probability of fifth Damage State - (i.e., 'Collapse'), is specified as a fraction of Damage State 4 ('complete damage'). The specified fractions vary for different MBTs. Damage state proposed by Kappos et al. (2006) have a five grade damage classification which is quite similar to the one used by intensity scales. This approach is simpler, and can be used for direct comparison of damage with intensity scales; Due to this reason the same has been used in the present study.

Another important issue in the estimation of fragility functions is the quantification of variability associated with different processes in vulnerability assessment. This includes uncertainty in ground motion, variability in capacity curve parameters, and uncertainty in

the definition of damage state thresholds. Estimation of variability is a complex process requiring reliable and adequate statistical data. Considering the lack of systematic data for Indian conditions, the variability for the comparable MBTs from literature, based on the parity discussed earlier, has been used (Table 7.11).

7.5 LOSS ESTIMATION

The computation of connected losses is conducted using the same loss model for all the three components of the software, i.e. SeisVARA-Intensity, SeisVARA-Spectrum and SeisVARA-NGA. Thereby, estimates of expected life losses, injuries, direct economic losses as well as number of homeless people for the study area are derived. Due to the lack of statistical data with respect to these parameters for India, the loss model of HAZUS-MH (FEMA 2003) has been used in the present study. Therein, indoor and outdoor casualty rates for the different MBTs to estimate the expected life-loss and injuries are defined.

7.5.1 Estimation of Life Loss and Injuries

Table 7.13 shows the indoor casualty rates for the two most common building typologies in India. However, any loss model suitable for a region can be easily implemented in the software. Therein, indoor and outdoor casualty rates for the different MBTs to estimate the expected life-loss and injuries are defined. Table 7.13 shows the indoor casualty rates for the two most common building typologies in India. However, any loss model suitable for a region can be easily implemented in the software.

The probability of a severity level due to different damage states for a building type can be obtained by summation of the product for different damage grades, given as

$$P(S_i)_{MBT} = \sum_{j=1}^{5} \left(P(S_i / Gr_j) \times P(Gr_j)_{MBT} \right) \tag{7.3}$$

where, $P(S_i)_{MBT}$ = Probability of Severity Level *i* in a *MBT,* $P(S_i / Gr_j)$ = Casualty rate of severity *i* for damage grade *j,* and $P(Gr_j)_{MBT}$ = Probability of occurrence of damage

grade *j* in a *MBT*. For a group of similar buildings, the total number of injuries or life loss can be obtained by multiplying this probability with the total number of occupants.

Table 7.13
Indoor casualty rates (%) of different building types (FEMA 2006)

Casualty Severity Level [a)]	Masonry Buildings					Reinforced Concrete Buildings				
	Gr1	Gr2	Gr3	Gr4	Gr5	Gr1	Gr2	Gr3	Gr4	Gr5
Severity 1	0.05	0.35	2	10	40	0.05	0.2	1	5	40
Severity 2	0	0.4	0.2	2	20	0	0.025	0.1	1	20
Severity 3	0	0.001	0.002	0.02	5	0	0	0.001	0.01	5
Severity 4	0	0.001	0.002	0.02	10	0	0	0.001	0.01	10

a) Severity 1: Injuries requiring basic medical aid, but without hospitalization
Severity 2: Injuries requiring medical attention and hospitalization but not considered to be life threatening
Severity 3: Injuries that pose an immediate life threatening condition if not treated adequately and expeditiously
Severity 4: Instantaneously killed or mortally injured

7.5.2 Estimation of Direct Economic Losses

During an earthquake, the main share of direct economic loss is caused by three types of damages, i.e., structural damage, non-structural damage and damage to contents. HAZUS provides loss ratios as percentages of building replacement cost for all the three damage types. However, the contribution of non-structural components in the reconstruction costs of conventional Indian buildings is rather low and not known explicitly. Therefore, loss ratios for structural and non-structural (both acceleration- and drift-sensitive) components have been considered jointly for the present study (Table 7.14). HAZUS has considered the structural and non-structural loss ratios for the 'complete damage' state (which includes 'collapse') as 100% of a building's replacement cost. However, recent research on 'demand surge' (Olsen and Porter 2010) suggests that the actual replacement cost for complete damage state may be higher than the normal reconstruction cost, considering scarcity of construction materials and labor, due to high demand after an earthquake. The total reconstruction cost may also increase due to turning down extensively damaged or partly collapsed buildings as well as removing and disposing the debris.

The total expected loss due to building damage for a given occupancy class can be estimated as

$$CBD_i = \sum_{MBT=1}^{N} \left[FA_{MBT,i} \times TBA_i \times \sum_{j=1}^{5} \left(P(Gr_j)_{MBT} \times LR_j \right) \times RV_{MBT} \right] \quad (7.4)$$

where, CBD_i = Cost of building damage in Occupancy Class *i*, $FA_{MBT,i}$ = Percentage floor area of a *MBT* in Occupancy Class *i*, TBA_i = Total built-up area of Occupancy *i*, $P(Gr_j)_{MBT}$ = Probability of Damage Grade *j* in a *MBT*, LR_j = Building Loss Ratio for Damage Grade *j*, including structural and non-structural damage, RV_{MBT} = Building Replacement Value for a MBT.

The total loss due to damage of contents in a given occupancy class can be estimated as,

$$CCD_i = \sum_{MBT=1}^{N} \left[FA_{MBT,i} \times TBA_i \times \sum_{j=1}^{5} \left(P(Gr_j)_{MBT} \times CLR_j \right) \times RV_{MBT} \right] \quad (7.5)$$

where, CCD_i = Cost of Contents Damage in Occupancy Class *i*, $FA_{MBT,i}$ = Percentage floor area of a *MBT* in Occupancy Class *i*, TBA_i = Total built-up area of Occupancy *i*, $P(Gr_j)_{MBT}$ = Probability of Damage Grade *j* in a *MBT*, CLR_j = Contents Loss Ratio for Damage Grade *j*, CVR_i = Contents Value of a MBT in Occupancy Class *i*.

Table 7.14
Loss Ratios at different damage states considered in SeisVARA

Damage State	Structural and non-structural loss (%) in terms of building replacement cost	Content loss (%) in terms of building content value
Slight	2.0	1.0
Moderate	10.0	5.0
Extensive	50.0	25.0
Complete	100.0	50.0

Quantification of uncertainty in estimated losses is an important though difficult task. In addition to the uncertainty in hazard and vulnerability, the uncertainty in loss estimates depends on many other factors including local conditions and construction practices, awareness of occupants in the hazard strike area, preparedness of local authorities, etc.

The objective of the present study is not to present the most realistic risk estimate, but to compare the loss estimates obtained using different approaches, to identify some of the factors contributing to the differences, and to move a step towards possible convergence. The consideration of the very same loss model and casualty severity rates in all the approaches, leads to an equal contribution to the uncertainty in losses estimated by the different approaches, and brings out the differences due to hazard and vulnerability models more clearly.

7.6 CASE STUDY

To compare the process and results of the three different approaches offered by SeisVARA, a realistic study area was chosen. In earlier studies (Prasad 2009; Lang et al. 2012), Dehradun, the capital city of the state of Uttarakhand in northern India, was subject for detailed computations of expected losses during scenario earthquakes. The city of Dehradun is located in the seismically active Himalayan region with a building stock that consists of a variety of building typologies ranging from old adobe/stone buildings to newly constructed RC buildings, generally without any consideration for seismic forces. The city also has a variety of occupancy classes with significant variation in day and night time population, as shown in Table 7.4. It is to be noted that the data shown in Table 7.4 does not include institutional and industrial occupancies, as these could not be surveyed due to logistic problems and permissions from the concerned authorities. Table 7.4 shows that the building inventory in Dehradun mainly consists of unreinforced brick masonry walls with flat RC roofs (about 68%), followed by the RC frame buildings with unreinforced masonry infills (about 20%). No steel building was found in the surveyed area of the city, since the use of steel is generally limited to industrial buildings in India. Further, most of the buildings in the city are in the category of low-rise buildings. A closer look at Tables 7.4 and 7.7 show that the majority (74%) of the total building inventory is covered by the fragility functions developed by Prasad (2009) for typical northern Indian buildings.

For the estimation of seismic losses, the whole city has been subjected to the code (BIS 2002) specified seismic hazard. Spatial variation of ground shaking in the city due to topographical variations, local soil conditions, etc. has not been considered as the purpose of the present manuscript is not to present the most realistic risk scenario for Dehradun city but to compare the loss estimates from the three approaches using a common building

inventory. Thereby, the sensitivity of loss estimates to different input parameters is investigated. First, a comparative study of the intensity-based and capacity spectrum-based approaches is presented and afterwards a comparison is made between the loss estimates obtained using the design spectra of different seismic building codes and those obtained using the NGA model.

7.7 RESULTS AND DISCUSSION

7.7.1 Intensity-Based Approach vs. Spectrum-Based Approach

As described earlier, the developed software provides options for both intensity-based and capacity spectrum-based approaches of loss estimation. As the two approaches are completely different in specifying the hazard and vulnerability, it is interesting to compare the estimates derived from the two approaches for the same building inventory with a common loss model. However, the main difficulty in comparing these results lies in specifying a common hazard level. Even though a number of relationships between macroseismic intensity and PGA are available, large uncertainties are involved which lead to a wide variation of PGA for a given intensity. According to the Indian seismic zonation map (BIS 2002) the whole country is divided into four Seismic Zones II, III, IV and V, each corresponding to an expected MSK intensity of VI, VII, VIII and IX and a design PGA of 0.05*g*, 0.08*g*, 0.12*g*, 0.18*g*, respectively. According to this zonation map of India, the city of Dehradun is located in Seismic Zone IV. Fig. 7.3 correlates the five intensity-PGA relationships compiled in ATC-13 (1985) as well as intensity-compatible PGA values used in BIS (2002) to define the various Seismic Zones. It can be observed from Fig. 7.3 that PGA estimates of BIS (2002) are below the mean of the five relationships for all the four Seismic Zones and differences increase for higher Seismic Zones. In the absence of adequate empirical data, it is difficult to choose any single relationships for Indian conditions. Therefore, in the present study, seismic losses for Dehradun have been evaluated for MSK intensity VIII and for two values of PGA equal to 0.12*g* (corresponding to Indian Seismic Zone IV) and 0.26*g* (corresponding to the mean of the five intensity-PGA relationships shown in Fig. 7.3). Further, in order to avoid differences arising from the change in spectral shapes due to local site effects, first the Indian standard design spectrum for soil type I (NEHRP site class B (FEMA-368 2000)),

has been considered, and the effect of site class and spectral shape has been discussed later.

Figure 7.4 shows a comparison of the estimated floor area of different damage grades for Dehradun city using MSK-EMS and PSI scales for an MSK intensity VIII and using the spectrum-based approach for 0.12*g* PGA on Indian Soil Type I. It can be observed that the damage predicted by the Lower- and Upper-Bound DPMs based on MSK-EMS intensity scales is limited to a narrow band of three grades (Gr2, Gr3 and Gr4), whereas the damage predicted by PSI scale and the spectrum-based (analytical) approach is distributed over all damage grades. Further, the intensity scales, particularly MSK-EMS intensity scales predict higher damage in the lower grades whereas in the higher damage grades (Gr4 and Gr5), the damage predicted by the analytical approach is higher. Estimation of life-loss, injuries, number of homeless people/shelter needed, and direct economic loss using the Lower- and Upper-Bound vulnerability matrices based on MSK-EMS scales, PSI scale, and capacity spectrum approach are shown in Table 7.15.

It can be observed from Table 7.15 that PSI derives approximately about 20% higher estimates of life-loss than the Upper-Bound MSK-EMS estimates, whereas the injuries and economic loss obtained from PSI scale are within the Upper-Bound and Lower-Bound estimates. The difference between the loss estimates based on the two intensity scales is due to a more refined building classification and better distributed vulnerability functions in case of PSI (Fig. 7.4). It is interesting to note that the loss estimates for intensity VIII are quite close to those for PGA equal to 0.12*g* (Indian code, BIS (2002), specified hazard level for Dehradun), but much lower (up to one third) than the loss estimated for PGA equal to 0.26*g* (corresponding to the mean of the five intensity-PGA relationships shown in Fig. 7.3). However, the parity of losses with 0.12*g* PGA appears to be only coincidental since 0.12*g* is quite low PGA than that corresponding to MSK Intensity VIII, as obtained from most of the available intensity-PGA relationships. The difference in the risk estimates for MSK Intensity VIII and for the corresponding mean PGA (0.26*g*) are due to the difference in the vulnerability functions used in the two approaches and the uncertainties in establishing parity between intensity and PGA.

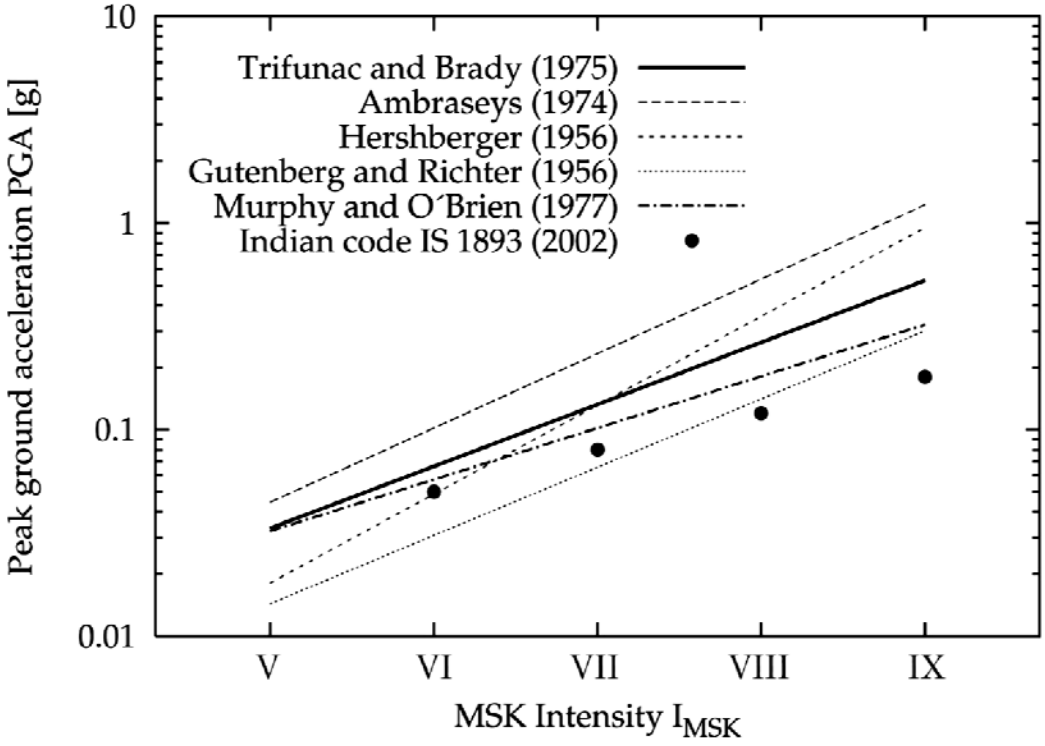

Fig. 7.3 Peak Ground Acceleration versus intensity relationships.

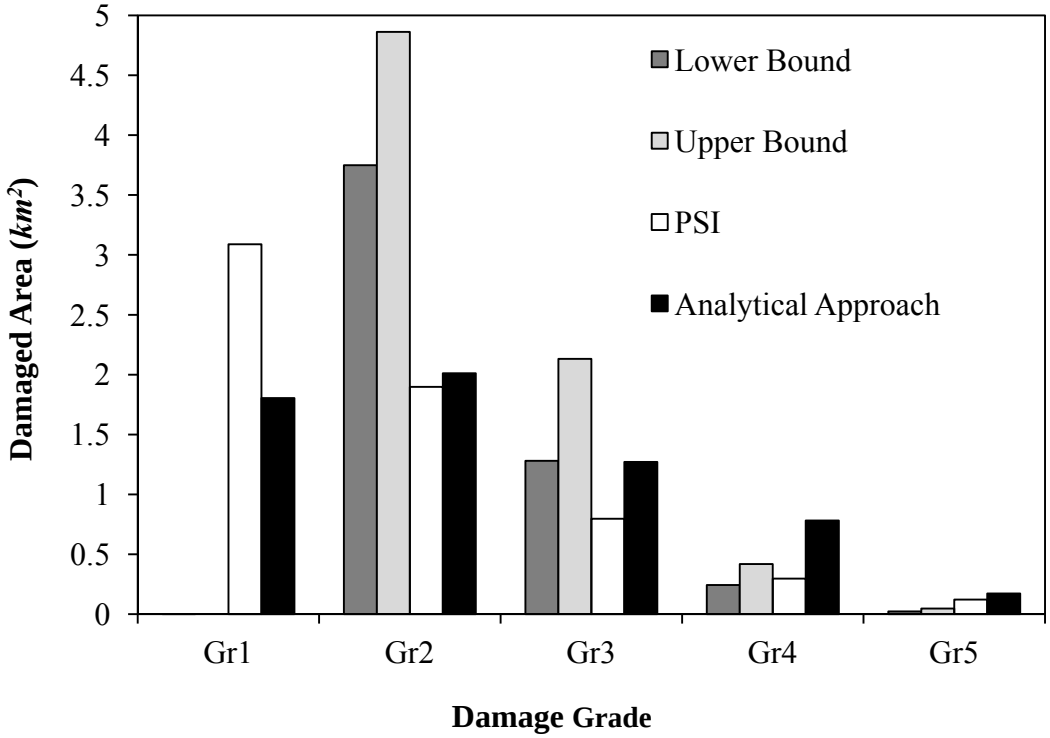

Fig. 7.4 Comparison of estimated building floor area of different grades for Dehradun city obtained using Lower-Bound and Upper-Bound DPMs, PSI, and analytical approach for a PGA of 0.12*g* on Indian Soil Type I (rock).

Table 7.15
Loss estimates for Dehradun city for MSK intensity VIII and PGA equal to 0.12*g* and 0.26*g* on Indian Soil Type I

Estimated Parameter	SeisVARA-Intensity				SeisVARA-Spectrum			
	MSK-EMS Lower-Bound-Upper-Bound Estimates		PSI Estimates		PGA = 0.12*g*		PGA = 0.26*g*	
	Night Time	Day Time	Night Time	Day Time	Night Time	Day Time	Night Time	Day Time
Life-loss	572 - 1,142	375 - 748	1,449	913	1,363	835	4,778	2,970
Injuries	9,762 - 15,694	6,156 - 9,950	10,861	6,796	14,154	7,338	39,787	26,533
Homeless People	122,930 - 204,426		88,898		119,717		288,013	
Direct Economic Loss in billion INR(10^9)	7.14-12.03		9.71		14.11		36.68	

7.7.2 Code Spectra vs. Scenario Earthquake Spectra

While representing the seismic hazard in terms of response spectrum, the two main parameters are PGA and spectral shape, representing the amplitude (level) and frequency content of ground shaking, respectively. Traditionally, seismic building codes specify hazard in terms of PGA or spectral ordinates at the rock outcrop and then generate the design response spectrum at the soil surface by multiplication with empirical factors to consider the amplification of ground motion due to the underlying soil. Modern attenuation relationships (including the NGA relationships), however, directly incorporate the amplification of ground motion due to underlying soil and provide PGA or spectral accelerations at the soil surface. In addition, code design spectra represent some sort of envelope or uniform hazard spectra, whereas scenario earthquake spectra explicitly represent effects of individual sources and their shape varies greatly for different magnitude-distance combinations, even for the same PGA as illustrated in Fig. 7.5. Therefore, it is expected that the loss estimated using the code spectra and scenario earthquake spectra will be different, and it will be interesting to study the relative influence of different parameters.

ASCE-7 (2006) anchors the design response spectrum using two spectral ordinates, while the vast majority of codes anchor the design spectrum solely to PGA. To obtain parity between ASCE-7 and other codes, the spectral ordinates, S_S and S_1 on rock (site class B) have been considered equal to 2.5 times PGA and PGA, respectively, as is the case in all other codes. For other site classes, ASCE-7 spectra have been obtained using the recommended amplification factors. While considering the effect of underlying soil on the response spectra, two aspects are important: (i) amplification of PGA, and (ii) change in frequency content and hence in the spectral shape. The two effects have been studied separately by considering two different cases for loss estimates on the soil surface. In the first case, PGA on rock (NEHRP site class B) (FEMA-368 2000) and on soil (NEHRP site class E) have been kept the same, i.e., 0.12*g* PGA, thereby considering solely the effect of change of spectral shape on the estimated seismic risk as shown in Table 7.17. In the second case, however, the amplification of PGA as well as the change in spectral shape is considered. Figs. 7.5 (a) and (b) show thereby obtained demand response spectra using the provisions of different codes and the NGA model, for Indian soil type III

(NEHRP site class E) for a given PGA (0.12*g*) at soil surface and at rock outcrop, respectively.

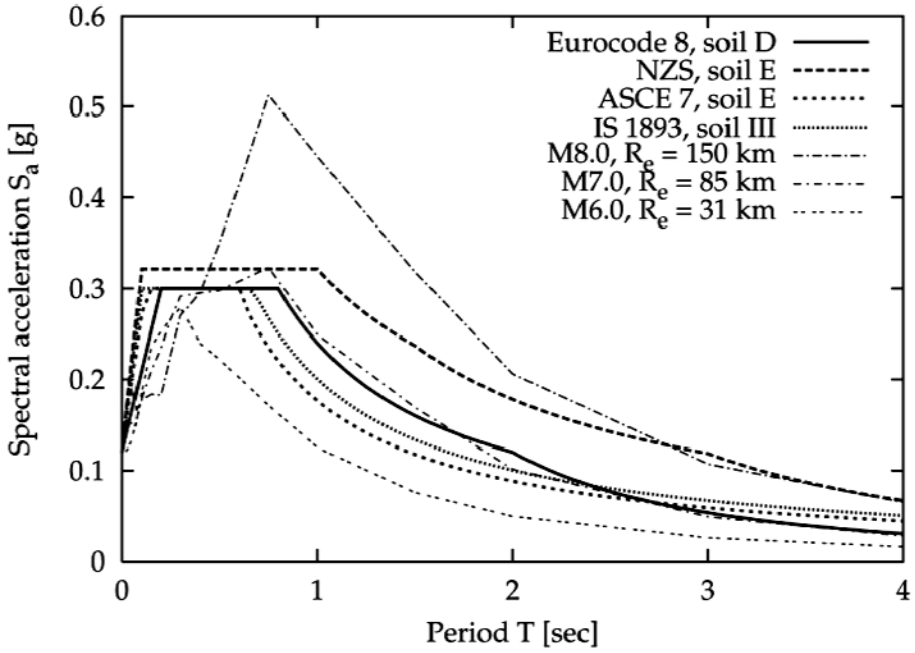

(a)

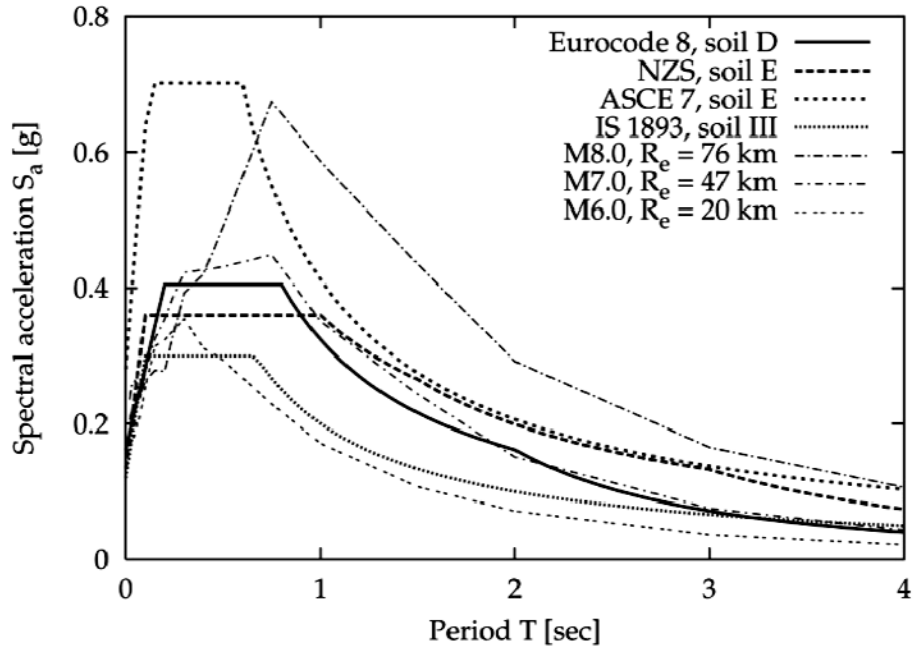

(b)

Fig. 7.5 Comparison of demand spectra obtained using different code provisions and the NGA model for Indian Soil Type III (NEHRP Site Class E): (a) PGA = 0.12*g* at soil surface; (b) PGA = 0.12*g* at rock outcrop. The first set of spectra shows the effect of change in spectral shape alone, whereas the second set of spectra shows the effect of soil amplification as well as change in spectral shape.

To obtain the inelastic demand spectra from the NGA relationships (Bozorgnia et al. 2010a; Bozorgnia et al. 2010b) corresponding to Indian code (BIS 2002) recommended PGA of 0.12*g*, two different sets of magnitude-distance (M-R) pairs have been selected to result in the same PGA (PGA= 0.12*g*) at rock outcrop (Indian Soil Type I or NEHRP site Class B) and at soil surface (Indian Soil Type III or NEHRP Site Class E), respectively. In both sets, three magnitudes (M_w = 6.0, 7.0, and 8.0) have been considered and the corresponding co-seismic rupture lengths have been adjusted (R_{Rup} =20 *km*, 47 *km,* and 76 *km* in case of rock, and 31 *km*, 85 *km,* and 150 *km* in case of soil) to get the target PGA (0.12*g*) at rock and soil sites, respectively. The other input parameters for the NGA relationships have been kept constant (e.g. reverse faulting with 30° dipping rupture plane, and depth to top of co-seismic rupture = 3 *km*). The values of $V_{s,30}$ have been considered as 1070 *m/s* and 150 *m/s* for NEHRP site classes B and E, respectively, as recommended by Campbell and Bozorgnia (2008).

To examine the sensitivity of estimated seismic losses due to amplification effects of the underlying soil materials explicitly, the shear wave velocity in the NGA model has been modified to 150 *m/s* for the same M-R pairs (i.e., 6-20, 7-47, 8-85) which were chosen to result in the targeted PGA (0.12*g*) at rock outcrop. Due to the modified shear wave velocity, these pairs result in amplified PGA values of 0.16*g*, 0.18*g*, and 0.18*g*, respectively on the soil surface (Indian soil type III or NEHRP site class E). The demand spectra obtained on soil surface (NEHRP site class E) using the NGA model and the soil amplification models of different codes, are compared in Figure 5.5(b).

It can be concluded from Fig. 7.5 that contrary to the common expectation, code spectra are not conservative in all the cases, as compared to scenario earthquake spectra (given the same PGA). Naturally, this difference in the spectra is reflected in the estimated risk. Table 7.16 shows the risk estimated on rock site for PGA= 0.12*g*, whereas Tables 7.17 and 7.18 show the estimated risk on NEHRP site class E with reference PGA (0.12g) considered at soil surface (and using the demand spectra of Fig. 7.5(a)) and at rock outcrop (using the demand spectra of Fig. 7.5(b)), respectively. It can be noted that the buildings present in Dehradun city mainly consist of 1-2 storey masonry buildings and a small number of low-rise RC buildings with fundamental periods of vibration below 0.5 *sec*. This is one of the reasons for the good agreement of the risk estimates between different spectra for rock/hard soil (Table 7.16), as there is little difference in the response

spectra of different codes for rock, particularly in the short-period range. Similarly, the risk estimates using the different code spectra with reference PGA considered at soil surface (i.e. considering the effect of changes in spectral shape alone) are also close (Table 7.17). However, significant differences exist in the estimated risk (Table 7.18) given that the reference PGA (0.12*g*) is considered at rock outcrop which gets amplified due to underlying soil layers depicting the significance of differences in soil amplification considered in different codes. Fig. 7.5 (b) shows that for the uniform PGA of 0.12*g* at rock outcrop, the estimated spectral acceleration in the short-period range at NEHRP site class E varies from 0.3*g* to 0.7*g* for different codes. It can be noted that this difference is of the same order as in case of the two PGA values (0.12*g* and 0.26*g*) considered for the same intensity (i.e., intensity VIII). This difference is reflected in the estimated risk, where the risk estimates using ASCE-7 spectrum are about three times of those estimated using the BIS (2002) spectrum. In case of the NGA model for demand spectra, as expected, the estimated risk is significantly affected (more than 1.5 times) by the choice of M-R pairs resulting in the same PGA. This indicates that considering only PGA as the hazard parameter is not adequate to obtain reliable risk estimates as the magnitude and distance of the scenario earthquake can cause significant variations in the resulting spectra and hence in the estimated risk.

Another interesting observation, which can be made from Tables 7.16-7.18, is that there is no effect of site class on the risk estimated using Indian code spectra. This is because unlike other seismic building codes, Indian code accounts for the effect of soil only on the spectral shape, ignoring the amplification of PGA (Adhikary and Singh 2011). This results in identical demand spectra in the short-period range ($T < 0.67$ *sec*) for all soil types, while buildings present in Dehradun predominantly have periods below 0.5 *sec*. However, except for the Indian code, the effect of soil amplification on estimated risk is clearly visible and may be more than 3 times as in case of ASCE-7.

7.8 SUMMARY

A user-friendly, open source, spreadsheet-based seismic risk estimation software 'SeisVARA' has been developed to facilitate the comparative study of different risk assessment approaches, using a common building inventory and loss model.

Table 7.16
Loss estimates for Dehradun city for 0.12*g* PGA on Indian Soil Type I (NEHRP Site Class B (FEMA-368 2000))

Estimated Parameter	SeisVARA-Spectrum								SeisVARA-NGA					
	Indian code		Eurocode 8		ASCE-7		New Zealand code		M6, R=20 *km*		M7, R=47 *km*		M8, R=76 *km*	
	Night Time	Day Time	Night Time	Day Time	Night Time	Day Time	Night Time	Day Time	Night Time	Day Time	Night Time	Day Time	Night Time	Day Time
Life-loss	1,363	835	1,363	835	1,364	837	1,268	776	1,284	794	1,291	793	1,301	797
Injuries	14,154	7,338	14,135	7,328	14,154	7,338	12,570	6,496	12,452	6,510	12,996	6,398	12,705	6,626
Homeless People	119,717		119,507		119,717		105,794		105,620		109,761		106,544	
Direct Economic Losses in billion INR (10^9)	14.11		14.06		14.11		12.61		13.13		13.40		12.67	

Table 7.17
Loss estimates for Dehradun city on Indian Soil Type III (NEHRP Site Class E (FEMA-368 2000)) for 0.12*g* PGA on ground surface

Estimated Parameter	SeisVARA-Spectrum								SeisVARA-NGA					
	Indian code		Eurocode 8		ASCE-7		New Zealand code		M6, R=31 *km*		M7, R=85 *km*		M8, R=150 *km*	
	Night Time	Day Time	Night Time	Day Time	Night Time	Day Time	Night Time	Day Time	Night Time	Day Time	Night Time	Day Time	Night Time	Day Time
Life-loss	1,348	825	1,348	824	1,348	825	1,994	1,227	2,091	1,672	2,174	1,749	2,368	1,868
Injuries	14,782	7,700	14,468	7,483	14,782	7,700	18,382	9,564	20,280	14,211	21,293	14,593	22,883	15,199
Homeless People	128,836		124,521		128,836		629,460		109,746		116,108		108,750	
Direct Economic Losses in billion INR(10^9)	15.06		14.52		15.06		16.95		14.50		15.57		13.69	

Table 7.18
Loss estimates for Dehradun city on Indian Soil Type III (NEHRP Site Class E (FEMA-368 2000)) for 0.12*g* PGA on rock outcrop

Estimated Parameter	SeisVARA-Spectrum								SeisVARA-NGA					
	Indian code		Eurocode 8		ASCE-7		New Zealand code		M6, R=20 *km*		M7, R=47 *km*		M8, R=76 *km*	
	Night Time	Day Time	Night Time	Day Time	Night Time	Day Time	Night Time	Day Time	Night Time	Day Time	Night Time	Day Time	Night Time	Day Time
Life-loss	1,348	825	2,594	1,598	6,108	3,804	2,141	1,324	2,502	1,538	4,400	2,713	4,292	2,636
Injuries	14,782	7,700	24,883	12,814	53,670	28,042	20,870	10,923	23,529	12,112	38,967	19,855	38,559	19,424
Homeless People	128,836		189,454		339,979		165,358		179,369		267,886		262,792	
Direct Economic Losses in billion INR (10^9)	15.06		22.90		44.73		19.72		22.20		33.77		33.20	

The software provides three options for specifying seismic hazard in terms of macroseismic intensity, PGA with choice of spectral shape and soil amplification models of various seismic design codes, and inelastic displacement spectra. The software also provides the option for specifying the PGA at rock outcrop or at the soil surface in order to allow an easy comparison with loss estimates based on macroseismic intensity. Currently, the tool has been tailored to Indian housing stock and fragility functions developed in the present study for medium rise RC frame buildings, have been implemented. For other building types, fragility functions available in literature have been used. However, the software can be easily adapted to any region worldwide. The tool can be used for estimating direct economic and social losses for any geographical unit, but can be easily integrated with a GIS platform for spatially visualizing the results.

A comparison of deterministic seismic risk scenarios using the three approaches has been conducted and the sensitivity of the estimated losses to PGA, spectral shape, source-site parameters, and soil amplification models has been studied, using a case study of a typical northern Indian city. It is observed that the variation in the loss estimates results mainly from the lack of correlation between the different definitions of seismic hazard and different vulnerability models. It has been observed that the loss estimated for Dehradun city for MSK intensity VIII is close to that obtained for PGA equal to 0.12*g*. However, this parity is only coincidental, as the PGA provided by Indian Standard is considerably lower than that obtained from most of the available intensity-PGA relationships. The losses estimated for a PGA of 0.26*g* corresponding to the mean of the Intensity-PGA relationships selected in ATC-13, is about three times the losses estimated for an MSK Intensity VIII.

The risk estimated using design spectra of different codes for the same PGA at rock outcrop, reveals variations up to 3 times, primarily because of the difference in soil amplification models adapted by different codes. Significant differences are also observed for the code design spectra and NGA model. Further, it is not adequate to consider the PGA predicted by an attenuation relationship with code-prescribed spectral shapes, as the magnitude and distance of the scenario earthquake can cause significant variation in the resulting spectra and hence in the estimated risk. However, in the present study, the difference in estimated losses for different M-R pairs is not that prominent, since the building stock of the test bed Dehradun consists of mostly low-rise (short-period)

buildings, where the difference in spectra is not so prominent. The open-source software tool SeisVARA is available on the website www.eqrisk.info.

Chapter 8

CONCLUSIONS AND RECOMMENDATIONS FOR FUTURE WORK

In this Thesis, an attempt has been made to develop modeling guidelines and to estimate seismic vulnerability of RC frame buildings with and without URM infills. A cost effective methodology and software tool for seismic risk assessment using different sources of information, have also been developed. Particular focus has been on the effect of infills and their placement on seismic performance and associated vulnerability of RC frame buildings, considering all possible failure modes of infill panels and surrounding frame members. Possible shear failure of joints has also been considered in the present study. Effect of different deficiencies on the estimated seismic vulnerability, has been discussed. Capacity spectrum parameters and fragility functions have been developed for URM infilled RC frame buildings with construction typical to India, with open ground storey and asymmetric placing of infills. Effect of different design levels and number of storeys on seismic vulnerability has also been studied. An open-source, user-friendly spreadsheet-based software 'SeisVARA' has been developed for estimation of seismic risk in order to plan short-term and long-term mitigation measures to reduce risk from future earthquakes. The software has been developed to make use of the information available in various forms, viz. Macro-seismic Intensity scales, design codes, and fragility functions obtained analytically and from studies on comparable building typologies in other parts of the world.

The major conclusions of this Thesis are as following:

- Construction sequence of infills relative to frame has a drastic impact on the failure modes of infilled frames, as the ideal contact between the beam and infill, as assumed in most of the analytical studies, is not practically possible. The gap and sliding at the top of the infill explains the shear failure of columns, observed in most of the post earthquake damage surveys.

- Simulation of construction sequence of infills relative to frame also has a drastic impact on the estimated capacity curve of an infilled frame and the conventional simultaneous analysis ignoring the construction sequence can almost nullify the effect of infills. This effect of construction sequence increases with the height of the building.

- Comparison of analytical results with the field and laboratory observations suggests that simulation of infills using single equivalent strut, eccentrically connected to columns, can realistically predict the failure modes in infilled frames.

- Sliding shear has been observed as the most probable mode of failure in URM infills, which is in agreement with the provisions of ASCE-41 (2007).

- Based on the available literature, a macro model for simulation of the URM infill panels with initial lack of fit has been proposed and validated with the field and laboratory observations.

- Using the developed model of infills, various probable modes of failure in RC frame buildings with and without URM infills, have been explored, and it has been observed that presence of infills significantly alters the combination of interacting axial force and moment in the columns. It increases (and reduces on tension side) axial force but reduces the bending moment in columns. This is expected to affect not only the strength, but also the ductility of columns, due to alteration of failure mode.

- Resulting net tension significantly reduces the shear strength of columns on tension side of the building. Further, there may be sudden drop in axial force accompanied by sudden gain in bending moment, in columns, due to simultaneous failure of a sizeable number of infills. This phenomenon has been particularly noticed in the taller building.

- Chances of shear failure in beam-column joints have been found to reduce in presence of infills due to reduction in shear force in the joint. The observed failures of beam-column joints in infilled frames during past earthquakes may be attributed to bond-slip failure and/or collapse of infills in out-of-plane

action rendering the behavior of the remaining frame similar to that of a bare frame.

- In case of ductile RC frame buildings (SMRF) having closely spaced stirrups in plastic hinge regions and joints, the shear failure of columns as well as joints is avoided, even in presence of infills of 'fair' quality (ASCE-41 2007) of masonry.

- Static Pushover Analysis of four and ten storey buildings, using the developed model for simulation of infills and considering all the identified failure modes of infill panels and surrounding frame, shows that infills have drastic effect on capacity curves of the RC frame and their stiffness and strength have been found to increase up to 35 times and 7.3 times, respectively, as compared to the bare frames.

- Seismic performance of gravity load designed as well as SMRF buildings has been found to deteriorate significantly in presence of URM infills, due to significant reduction in the plastic deformation capacity, resulted from failure of a sizable number of infills at very small drift as infills are attracting large forces due to much higher stiffness in comparison to columns.

- The RC bare frame buildings designed and constructed properly for the gravity loads alone, as per the relevant Indian Standards without any consideration for earthquake force, have sufficient overstrength and ductility to survive, without collapse, even the MCE level of ground shaking specified by BIS (2002) for Seismic Zone IV.

- Performance of URM infilled RC frames, designed for gravity loads alone, deteriorated significantly due to undesired brittle shear failure of columns and no performance point could be achieved for the DBE of Seismic Zone IV, indicating collapse.

- The SMRF bare frame buildings detailed and designed for DBE of Zone IV, as per the relevant Indian Standards, show 'IO' performance for MCE.

- RC bare frames as well as uniformly infilled frame buildings designed as SMRF for DBE of Indian Seismic Zone IV survive even MCE of Seismic Zone V excitation, without collapse.

- The open ground storey buildings designed for code (i.e. ground storey columns and beams designed for 2.5 times the normal base shear) are able to attain the stiffness and strength close to those of the corresponding uniformly infilled frame building. The estimated performance of such buildings is slightly better than the uniformly infilled frame buildings, indicating the adequacy of the code provisions for open ground storey buildings.

- URM infilled RC frame buildings with three bays open in the ground storey, considered in the study, have been found to suffer extreme torsional irregularity.

- Even the SMRF buildings designed and detailed as per Indian codes have more than 50% probability of extensive damage under MCE of the same seismic zone for which these have been designed. This shows that the deterministic performance analysis does not provide complete insight into expected performance of buildings, and a probabilistic framework for performance-based design is required.

- An open-source, user-friendly spreadsheet-based software ‘SeisVARA’ is developed and used for comparison of deterministic seismic risk scenarios using three different approaches. Sensitivity of the estimated losses to PGA, spectral shape, source-site parameters, and soil amplification models has been studied.

- Variation in the loss estimates results mainly from the lack of correlation between the different definitions of seismic hazard and different vulnerability models.

- The risk estimated using design spectra of different codes for the same PGA at rock outcrop, reveals variations up to 3 times, primarily because of the difference in soil amplification models adapted by different codes. Significant differences are also observed for the loss estimates using code design spectra

and NGA model. Therefore, it is not adequate to use the PGA predicted by an attenuation relationship with code-prescribed spectral shapes, to estimate seismic risk.

8.1 RECOMMENDATIONS FOR FUTURE WORK

Present study is based on analytical simulation of the seismic behaviour, which needs to be validated by experimental results. Therefore, large scale tests of bare and infilled RC frames with regular and irregular infills in plan and/or elevation are required to be undertaken.

In the present study, uniformly placed URM infills and the three most common configurations of RC frame buildings with irregular placement infills are addressed. There are different other configurations of RC frames with irregularly placed infills, which need to be studied further.

In case of URM infills, both in-plane and out-of-plane actions are important. The out-of-plane failure of infills is not considered in the present study. Such failure can drastically alter the seismic behavior of the infilled buildings, due to irregular pattern of remaining infills. This issue needs to be investigated.

Analytical approaches considering both in-plane and out-of-plane actions of infills in a single model are not available, at present. Models need to be developed for simulating the combined action of infills in the two modes and the failure probabilities considering the combined effect of two actions should be estimated.

The present study focuses on infills without openings. This represents an extreme case, as far as influence of infills on failure modes of RC frames is concerned. Effect of the presence of openings and its location on the seismic performance and associated vulnerability can be further studied.

Variabilities in different input parameters for fragility analysis, using static and dynamic capacity curves, have been adopted, in this Thesis, from HAZUS and Wen et al. (2004). These variabilities in Indian constructions need to be evaluated using extensive field studies. Further, there are several deficiencies in buildings which crop

up during construction. The effect of these deficiencies should also be simulated based on field studies.

Present study is limited to residential and office buildings only. This can be extended to commercial buildings, having large span floor systems, low strength partitions and large shear wall cores.

REFERENCES

1. ACI 318. 2008. *Building Code Requirements for Structural Concrete and Commentary (ACI 318M-08)*. American Concrete Institute, Detroit, Michigan.

2. ACI 352R-02. 2002. *Recommendations for Design of Beam-Column Connections in Monolithic Reinforced Concrete Structures*. Detroit, Michigan, American Concrete Institute.

3. ACI 530. 2005 *Building Code Requirements for Masonry Structures*, *ACI 530-05/ASCE 5-05/TMS 402-05*. Masonry Standards Joint Committee, USA.

4. Adhikary, S., and Singh, Y. 2011. Limitations of Soil Amplification Provisions in the 2002 Indian Seismic Code. *Journal of Earthquake Engineering*, **16** (1):1-14.

5. Akkar, S., and Bommer, J. J. 2007. Prediction of Elastic Displacement Response Spectra in Europe and the Middle East. *Earthquake Engineering & Structural Dynamics*, **36**:1275-1301.

6. Alath, S., and Kunnath, S. K. 1995. Modeling Inelastic Shear Deformation in RC Beam-Column Joints In *Engineering mechanics proceedings of 10th Conference*, at University of Colorado, Boulder, Colorado, 822-825.

7. Al-Chaar, G. 1998. Non-Ductile Behavior of Reinforced Concrete Frames with Masonry Infill Panels Subjected to In-Plane Loading, Civil Engineering, University of Illinois at Chicago, Chicago, Illinois.

8. Al-Chaar, G. 2002. *Evaluating Strength and Stiffness of Unreinforced Masonry Infill Structures* Report no. ERDC/CERL TR-02-1. Champaign, Ill,, U.S. Army Corps of Engineers

9. Ali, S. S., and Page, A. W. 1987. Finite Element Model for Masonry Subjected to Concentrated Loads *American Society of Civil Engineers, Journal of Structural Engineering*, **114** (8):1761-1784.

10. Alire, D. A. 2002. Seismic Evaluation of Existing Unconfined Reinforced Concrete Beam-Column Joints, Department of Civil and Environmental Engineering, University of Washington.

11. Anagnostopoulos, S., Providakis, C., Salvarieschi, P., Athanasopoulos, G., and Bonacina, G. 2008. SEISMOCARE: An Efficient GIS Tool for Scenario-Type Investigations of Seismic Risk of Existing Cities. *Soil Dynamics and Earthquake Engineering*, **28** (2):73-84.

12. Anderson, J. C., and Townsend, W. H. 1977. Models for RC Frames with Degrading Stiffness. *Journal of the Structural Division, ASCE*, **103** (ST12):1433-1449.

13. Anderson, L., Ruthford, M., Perlea, V., Serafini, D., Montgomery, J., and Bowles, D. 2011. Risk Assessment of Success Dam, California: Flood Related Potential Failure Modes, at Atlanta, GA, 96.

14. Anderson, M., Lehman, D., and Stanton, J. 2008. A cyclic shear stress-strain model for joints without transverse reinforcement. *Engineering Structures*, **30** (4):941-954.

15. Angel, R. 1994. Behavior of Reinforced Concrete Frames with Masonry Infills, Department of Civil Engineering, University of Illinois at Urbana-Champaign.

16. Arya, A. S. 2003. *Rapid Visual Screening of Buildings in Various Seismic Zones in India* New Delhi, India, Capacity Building Advisor, GOI-UNDP (DRM)

17. ASCE 41-06. 2007. *Seismic rehabilitation of existing buildings*, American Society of Civil Engineers, Virginia, USA.

18. ASCE/SEI-41 Supplement-1. 2007. *Update to ASCE/SEI 41 Concrete Provisions*. Reston, Virginia, American Society of Civil Engineers

19. ASCE-7. 2006. *Minimum Design Loads for Buildings and Other Structures, (ASCE/SEI 7-05)*. Reston, Virginia, American Society of Civil Engineers.

20. Asteris, P. G. 2003. Lateral Stiffness of Brick Masonry Infilled Plane Frames. *Journal of Structural Engineering; American Society of Civil Engineers (ASCE)*, **129** (8):1071-1079.

21. Asteris, P. G., Antoniou, S. T., Sophianopoulos, D. S., and Chrysostomou, C. Z. 2011. Mathematical Macromodeling of Infilled Frames: State of the Art. *Journal of Structural Engineering; American Society of Civil Engineers (ASCE)*, **137** (12):1508-1517.

22. ATC-13. 1985. *Earthquake Damage Evaluation Data for California. ATC-13 report*. Redwood City, California, Applied Technology Council.

23. ATC-40. 1996. *Seismic Evaluation and Retrofit of Concrete Buildings (ATC-40, Vol. 1)*. Redwood City, California, Applied Technology Council.

24. Axley, J. W., and Bertero, V. V. 1979. *Infill Panels: Their Influence on Seismic Response of Buildings*. Vol. UCB/EERC - 79/28, University of California, Berkeley.

25. Bakir, P. G., and Boduroglu, H. M. 2002. A New Design Equation for Predicting the Joint Shear Strength of Monotonically Loaded Exterior Beam-Column Joints. *Engineering Structures*, **24** (8):1105-1117.

26. Barbat, A. H., Pujades, L. G., and Lantada, N. 2006. Performance of Buildings under Earthquakes in Barcelona, Spain. *Computer-Aided Civil and Infrastructure Engineering*, **21** (8):573-593.

27. Barbat, A. H., Yépez Moya, F., and Canas, J. A. 1996. Damage Scenarios Simulation for Seismic Risk Assessment in Urban Zones. *Earthquake Spectra*, **12** (3):371-394.

28. Benjamin, J. R., and Cornell, C. A. 1970. *Probability, Statistics, and Decision for Civil Engineers*, McGraw-Hill.

29. Beres, A., White, R., and Gergely, P. 1992. *Seismic Behavior of Reinforced Concrete Frame Structures with Nonductile Details: Part I - Summary of Experimental Findings of Full Scale Beam-Column Joint Tests* Report

NCEER-92-0024, NCEER, State University of New York at Buffalo.

30. Bertero, V. V., and Collins, R. G. 1973. *Investigation of the Failures of the Olive View Stair Towers during the San Fernando Earthquake and Their Implications on Seismic Design*. Vol. UCB/EERC-73/26 Earthquake Engineering Research Center, University of California, Berkeley, pp 276.

31. Biddah, A., and Ghobarah, A. 1999. Modelling of shear deformation and bond slip in reinforced concrete joints. *Structural Engineering and Mechanics*, **7** (4):413-432.

32. Biot, M. S. 1933. Theory of Elastic Systems Vibrating under Transient Impulse with an Application to Earthquake-Proof Buildings. *Proc. National Academy of Sciences*, **19** (2):262-268.

33. BIS. 1987 (Part 1). *IS: 875 (Part 1) Indian Standard Code of Practice for Design Loads (Other than Earthquake) for Buildings and Structures, Pari 1: Dead Loads—Unit Weights of Building Materials and Stored Materials (Second Revision)*. New Delhi, Bureau of Indian Standards.

34. BIS. 1987 (Part 2). *IS: 875 (Part 2) Indian Standard Code of Practice for Design Loads (Other than Earthquake) for Buildings and Structures, Part 2: Imposed Loads (Second Revision)*. New Delhi, Bureau of Indian Standards.

35. BIS. 1993. *IS: 13920 Ductile Detailing of Reinforced Concrete Structures Subjected to Seismic Forces – Code of Practice*. New Delhi, Bureau of Indian Standard.

36. BIS. 2000. *IS 456 Indian Standard Plain and Reinforced Concrete-Code of Practice (Fourth Revision)*. New Delhi, Bureau of Indian Standards.

37. BIS. 2002. *IS 1893 (Part 1) Indian Standard Criteria for Earthquake Resistant Design of Structures, Part 1: General Provisions and Buildings (Fifth Revision)*. New Delhi, Bureau of Indian Standards.

38. BMTPC. 1997/2006. *Vulnerability Atlas of India*, Building Materials and Technology Promotion Council New Delhi, India, Ministry of Urban

Development, Government of India.

39. Bommer, J. J., and Elnashai, A. S. 1999. Displacement Spectra for Seismic Design. *Journal of Earthquake Engineering*, **3** (1):1 - 32.

40. Bozorgnia, Y., and Campbell, K. W. 2004. Engineering Characterization of Ground Motion in Earthquake Engineering. In *Engineering Seismology to Performance-Based Engineering*, edited by Y. Bozorgnia and V. V. Bertero. Boca Raton, Florida: CRC Press.

41. Bozorgnia, Y., Hachem, M. M., and Campbell, K. W. 2010a. Ground Motion Prediction Equation ("Attenuation Relationship") for Inelastic Response Spectra *Earthquake Spectra*, **26** (1):1-23.

42. Bozorgnia, Y., Hachem, M. M., and Campbell, K. W. 2010b. Deterministic and Probabilistic Predictions of Yield Strength and Inelastic Displacement Spectra. *Earthquake Spectra*, **26** (1):25-40.

43. Browning, J. P. 2001. Proportioning of Earthquake-Resistant RC Building Structures. *Journal of Structural Engineering; American Society of Civil Engineers (ASCE)*, **127** (2):145-151.

44. CALTRANS. 2010. Caltrans Seismic Design Criteria. Sacramento, California: California Department of Transportation.

45. Calvi, G. M., Pinho, R., Magenes, G., Bommer, J. J., Restrepo-Vélez, L. F., and Crowley, H. 2006. Development of Seismic Vulnerability Assessment Methodologies over the Past 30 Years. *ISET Journal of Earthquake Technology*, **43** (3):75-104.

46. Campbell, K. W., and Bozorgnia, Y. 2008. NGA Ground Motion Model for The Geometric Mean Horizontal Component of PGA, PGV, PGD and 5% Damped Linear Elastic Response Spectra for Periods Ranging from 0.01 to 10 s. *Earthquake Spectra*, **24** (1):139-171.

47. Cattari, S., Curti, E., Giovinazzi, S., Lagomarsino, S., Parodi, S., and Penna, A. 2004. Un Modello Meccanico per L'analisi Di Vulnerabilità Del

Costruito in Muratura a Scala Urbana. In *Proceedings, VI Congreso nazionale. L'ingegneria Sismica in Italia*, at Genova, Italy,

48. Celik, O. C., and Ellingwood, B. R. 2008. Modeling Beam-Column Joints in Fragility Assessment of Gravity Load Designed Reinforced Concrete Frames. *Journal of Earthquake Engineering*, **12** (3):357-381.

49. Chen, P. F., and Powell, G. H. 1982. *Generalized Plastic Hinge Concepts for 3D Beam-Column Elements*, Report No. UCB/EERC-82/20, University of California, Berkeley, Earthquake Engineering Research Center, pp 274.

50. Chopra, A. K., and Chintanapakdee, C. 2004. Inelastic Deformation Ratios for Design and Evaluation of Structures: Single-Degree-of-Freedom Bilinear Systems. *Journal of Structural Engineering; American Society of Civil Engineers (ASCE)*, **130** (9):1309-1319.

51. Chopra, A. K., and Goel, R. K. 2001. Direct Displacement Based Design: Use of Inelastic vs. Elastic Design Spectra. *Earthquake Spectra*, **17** (1):47-64.

52. Chopra, A. K., and Goel, R. K. 2002. A Modal Pushover Analysis Procedure for Estimating Seismic Demands for Buildings. *Earthquake Engineering & Structural Dynamics*, **31**:561-582.

53. Chrysostomou, C. Z. 1991. Effects of Degrading Infill Walls on The Non-Linear Seismic Response of Two-Dimensional Steel Frames, Cornell University, Ithaca, New York, U.S.A.

54. Chrysotomou, C. Z., Gergely, P., and Abel, J. F. 1992. Non-linear Seismic Response of Infilled Steel Frames. Paper read at Proceedings of the 10th World Conference on Earthquake Engineering, at Madrid, Spain, 4435-4437.

55. Coburn, A., and Spence, R. 2006. In *Earthquake Protection*: John Wiley & Sons, Ltd.

56. Coenraads, A. C. 1991. Numerieke Detailberekeningen Van Penanten in Metselwerk - Underzoek Naar Modelleringsaspecten Binen DIANA (in Dutch).

57. Crisafulli, F. 1997. Seismic Behaviour of Reinforced Structures with Reinforced Masonry Infiills, University of Canterbury, New Zealand.

58. Crowley, H., Pinho, R., and Bommer, J. J. 2004. A Probabilistic Displacement-Based Vulnerability Assessment Procedure for Earthquake Loss Estimation. *Bulletin of Earthquake Engineering*, **2** (2):173-219.

59. CSI Analysis Reference Manual for SAP2000 (2010). Computers and Structures Inc., Berkeley, California.

60. Cuesta, I., Aschheim, M. A., and Fajfar, P. 2003. Simplified R-Factor Relationships for Strong Ground Motions. *Earthquake Spectra*, **19** (1):25-45.

61. Deng, C.-G., Bursi, O. S., and Zandonini, R. 2000. A Hysteretic Connection Element and its Applications. *Computers & Structures*, **78** (1–3):93-110.

62. DEQ. 1999. *A Report on Chamoli Earthquake of March 29, 1999* Roorkee, India, , Department of Earthquake Engineering, University of Roorkee

63. DEQ. 2009. *Seismic Vulnerability of Multistorey Buildings in Noida* Roorkee, India, Department of Earthquake Engineering, Indian Institute of Technology Roorkee, pp 1-118.

64. Dhanasekar, M., et al. 1985. Behaviour of Brick Masonry under Biaxial Stress with Particular Reference to Infilled Frames. Paper read at Proceedings of *7th International Conference on Brick Masonry*, at Melbourne, Australia, 815-824.

65. Dogangun, A. 2004. Performance of reinforced concrete buildings during the May 1, 2003 Bingol earthquake in Turkey. *Engineering Structures*, **26**:841-856.

66. Dolsek, M. 2009. Incremental Dynamic Analysis with Consideration of Modeling Uncertainties. *Earthquake Engineering & Structural Dynamics*, **38** (6):805-825.

67. Doudoumis, I. N., and Mitsopoulou, E. N. 1986. Non-Linear Analysis of Multistorey Infilled Frames for Unilateral Contact Conditions. Paper read at Proceedings of the *8th European Conference on Earthquake Engineering*, at Lisbon, 63-70.

68. Durrani, A. J., Elnashai, A. S., Hashash, Y. M. A., Kim, S. J., and Masud, A. 2005. *The Kashmir Earthquake of October 8, 2005, A Quick Report, MAE Center Reprt No. 05-04* Mid-America Earthquake Center, University of Illinois at Urbana-Champaign.

69. Dwairi, H. M., Kowalsky, M. J., and Nau, J. M. 2007. Equivalent Damping in Support of Direct Displacement-Based Design. *Journal of Earthquake Engineering*, **11** (4):512-530.

70. EERI. 1994. Northridge Earthquake, January 17, 1994, Reconnaissance Report Vol. 1. *Earthquake Spectra, Suppl. C*, **11** (J. H. Hall, ed).

71. EERI. 2002. *Bhuj, India Earthquake of January 26, 2001 Reconnaissance Report*. Supplement a to volume 18 vols. Vol. Earthquake Spectra, Earthquake Engineering Research Institute.

72. El-Dakhakhni, W. W., Elgaaly, M., and Hamid, A. A. 2003. Three-Strut Model for Concrete Masonry-Infilled Steel Frames. *Journal of Structural Engineering; American Society of Civil Engineers (ASCE)*, **129** (2):177-185.

73. El-Metwally, S. E., and Chen, W. F. 1988. Moment-Rotation Modeling of Reinforced Concrete Beam-Column Connections. *ACI Structural Journal*, **85** (4):384-394.

74. Elwood, K. J., and Eberhard, M. O. 2006. *Effective Stiffness of Reinforced Concrete Columns*. Vol. No. 2006-1, *PEER Research Digest*. Pacific Earthquake Engineering Research Center University of California-Barkeler, CA.

75. Elwood, K. J., and Eberhard, M. O. 2009. Effective Stiffness of Reinforced Concrete Columns. *ACI Structural Journal*, **106** (4):476-484.

76. Erdik, M., and Aydinoğlu, N. 2002. Earthquake Risk to Buildings in Istanbul and a proposal Towards Its Mitigation. Paper read at Proceedings Second Annual IIASA-DPRI Meeting on Integrated Disaster Risk Management: Megacity Vulnerability and Resilience, at Laxenburg, Austria, 1-10.

77. Erdik, M., Aydinoglu, N., Fahjan, Y., Sesetyan, K., Demircioglu, M., Siyahi, B., Durukal, E., Ozbey, C., Biro, Y., Akman, H., and Yuzugullu, O. 2003. Earthquake Risk Assessment for Istanbul Metropolitan Area. *Earthquake Engineering and Engineering Vibration*, **2** (1):1-23.

78. Erduran, E., and Yakut, A. 2007. Vulnerability Assessment of Reinforced Concrete Moment Resisting Frame Buildings. *Journal of Structural Engineering; American Society of Civil Engineers (ASCE),* **133** (4):576-586.

79. Eurocode-8. 2004. *BS EN 1998-1: Design of Structures for Earthquake Resistance- Part 1: General Rules, Seismic Actions and Rules for Buildings*. Brussels, Belgium, European Committee for Standardization (CEN).

80. FEMA. 1999. *HAZUS-99 Technical Manual*. Washington, DC, U.S.A, Federal Emergency Management Agency.

81. FEMA. 2003. *HAZUS-MH MR1, Multi-Hazard Loss Estimation Methodology Earthquake Model*. Washington, DC, U.S.A, Federal Emergency Management Agency.

82. FEMA. 2003a. *HAZUS-MH Technical Manual*. Washington, DC, U.S.A, Federal Emergency Management Agency (FEMA).

83. FEMA. 2006. *HAZUS-MH MR2, Multi-Hazard Loss Estimation Methodology, Earthquake Model*. Washington, DC, U.S.A., Federal Emergency Management Agency.

84. FEMA-273. 1997. *NEHRP Guidelines for the Seismic Rehabilitation of Buildings*. Washington, DC, Federal Emergency Management Agency.

85. FEMA-306. 1998. *Evaluation of Earthquake Damaged Concrete and Masonry Wall Buildings*. Washington, DC, Federal Emergency Management Agency.

86. FEMA-310. 1998. *Handbook for the Seismic Evaluation of Buildings*. Washington, DC, Federal Emergency Management Agency.

87. FEMA-356. 2000. *Prestandard and Commentary for the Seismic Rehabilitation of Buildings*. Washington, DC, U. S. A., Federal Emergency Management Agency.

88. FEMA-368. 2000. *NEHRP Recommended Provisions for Seismic Regulations for New Buildings and Other Structures, 2000 Edition, Part 1: Provisions*. Washington, D.C., Building Seismic Safety Council (BSSC) for the Federal Emergency Management Agency.

89. FEMA-440. 2006. *Improvement of Nonlinear Static Seismic Analysis Procedures (FEMA 440)*. Washington, DC, U.S.A., Federal Emergency Management Agency.

90. Fillipou, F. C., Popov, E. P., and Bertero, V. V. 1983. *Effects of Bond Deterioration on Hysteretic Behaviour of Reinforced Concrete Joints*, EERC

91. Fiorato, A. E., Sozen, M. A., and Gamble, W. L. 1970. *An Investigation of the Interaction of Reinforced Concrete Frames with Masonry Filler Walls*. Civil Engineering Studies SRS- 370 vols,U. o. I. E. E. S. C. o. Engineering. University of Illinois at Urbana-Champaign, Civil Engineering Studies SRS-370, University of Illinois Engineering Experiment Station. College of Engineering.

92. Firat Alemdar, B. S. 2007. Evaluation and Prediction of Shear Behaviour of Reinforced Concrete Beam-Column Joints, The Ohio State University.

93. Flanagan, R. D., and Bennett, R. M. 1999. In-Plane Behavior of Structural Clay Tile Infilled Frames. *Journal of Structural Engineering, ASCE*, **125** (6):590-599.

94. Flanagan, R. D., and Bennett, R. M. 2001. In-Plane Analysis of Masonry Infill Materials. *Practice Periodical on Structural Design and Construction, American Society of Civil Engineers*, **6** (4):176-182.

95. Flores, L. E., and Alcocer, S. M. 1996. Calculated Response of Confined Masonry Structures, Paper no. 1830. In *Proceedings of the 11th World Conference on Earthquake Engineering*, at Mexico.

96. Gambarotta, L., and Lagomarsino, S. 1997a. Damage Models for the Seismic Response of Brick Masonry Shear Walls. Part I: The Mortar Joint Model and Its Applications. *Earthquake Engineering & Structural Dynamics*, **26** (4):423-439.

97. Gambarotta, L., and Lagomarsino, S. 1997b. Damage Models for the Seismic Response of Brick Masonry Shear Walls. Part II: The Continuum Model and Its Applications. *Earthquake Engineering & Structural Dynamics*, **26**:441-462.

98. Ghosh, C. 2008. Earthquake Risk Mitigation Strategies in India. In *Proc. of 12th International Association for Computer Methods and Advances in Geomechanics (IACMAG)*, at Goa, 2985-2991.

99. Giberson, M. F. 1969. Two Nonlinear Beams with Definition of Ductility. *Journal of the Structural Division; American Society of Civil Engineers (ASCEz*, **95** (ST2):137-157.

100. Giovinazzi, S. 2005. The Vulnerability Assessment and the Damage Scenario in Seismic Risk Analysis, Braunschweig Technical University, Germany.

101. Goodman, R. E., Taylor, R. L., and Brekke, T. L. 1968. A Model for the Mechanics of Jointed Rock. *American Society of Civil Engineers, Journal of the Soil Mechanics and Foundations Division*, **94** (SM3): 637-659.

102. Grant, D. N., Blandon, C. A., and Priestley, M. J. N. 2005. *Modelling Inelastic Response in Direct Displacement-Based Design*, Report 2005/03 IUSS Press, Pavia, Italy, pp 104.

103. Grünthal, G. ed.1998. *European Macroseismic Scale1998*. Edited by G. Grünthal. Vol. 15 Luxembourg Centre Européen de Géodynamique et de Séismologie.

104. GSI. 1995. *Report on Uttarkashi Earthquake (20th October 1991)* Memoir 30, Bangalore, India, Geological Society of India (GSI).

105. GSI. 2003. *Kutch (Bhuj) Earthquake 26 January 2001*. Vol. Special Publication No. 76 Lucknow, India, Geological Survey of India.

106. Gulkan, P., and Sozen, M. A. 1974. Inelastic Responses of Reinforced Concrete Structure to Earthquake Motions. *ACI Journal*, **71** (12):604-610.

107. Haldar, P., and Singh, Y. 2009. Seismic Performance and Vulnerability of Indian Code Designed RC Frame Buildings. *ISET Journal of Earthquake Engineering*, **46** (1:502):29-45.

108. Haldar, P., Singh, Y., Lang, D. H., and Paul, D. K. 2010. IVARA - A Tool for Seismic Vulnerability and Risk Assessment of Indian Housing. In *14th Symposium on Earthquake Engineering*, at Department of Earthquake Engineering, IIT Roorkee,, 1405-1415.

109. Haldar, P., Singh, Y., Lang, D. H., and Paul, D. K. 2013. Comparison of Seismic Risk Assessment Based on Macroseismic Intensity and Spectrum Approaches using 'SeisVARA'. *Soil Dynamics and Earthquake Engineering*, **48** (0):267-281.

110. Han, S. W., and Chopra, A. K. 2006. Approximate incremental dynamic analysis using the modal pushover analysis procedure. *Earthquake Engineering & Structural Dynamics*, **35** (15):1853-1873.

111. Hancilar, U., Tuzun, C., Yenidogan, C., and Erdik, M. 2010. ELER Software - A New Tool for Urban Earthquake Loss Assessment. *Natural*

Hazards and Earth System Sciences, **10** (12):2677-2696.

112. Haselton, C. B., ed. 2009. *Evaluation of Ground Motion Selection and Modification Methods: Predicting Median Interstory Drift Response of Buildings, Report no. PEER 2009/01*. Pacific Earthquake Engineering Research Center: PEER Ground Motion Selection and Modification Working Group.

113. Hashemi, A., and Mosalam, K. M. 2007. *Seismic Evaluation of Reinforced Concrete Buildings Including Effects of Masonry Infill Walls* University of California, Berkeley, Pacific Earthquake Engineering Research Center.

114. Hassan, A. F., and Sozen, M. A. 1997. Seismic Vulnerability Assessment of Low-Rise Buildings in Regions with Infrequent Earthquakes. *ACI Structural Journal*, **94** (1):31-39.

115. Hegger, J., Sherif, A., and Roeser, W. 2003. Nonseismic Design of Beam-Column Joints. *ACI Structural Journal*, **100** (5):654-664.

116. Holmes, M. 1961. Steel Frames with Brickwork and Concrete Infilling. Paper read at Proceedings of the *Institution of Civil Engineers - Structures and Buildings*, 19 (4), 473-478.

117. Hsu, T. T. C. 1988. Softened Truss Model-Theory for Shear and Torsion. *ACI Structural Journal*, **85** (6):624-635.

118. Ibarra, L. F., and Krawinkler, H. 2004. Global Collapse of Detoriorating MDOF Systems. In *13th World Conference on Earthquake Engineering*, at Vancouver, Canada.

119. IDARC2D Version 4.0- A Program for the Inelastic Damage Analysis of Buildings, Technical Report NCEER-96-0010. National Centre for Earthquake Engineering Research, State University of New York, Buffalo, New York.

120. IDNDR. 1999. *RADIUS: Risk Assessment Tool for Diagnosis of Urban Areas against Seismic Disasters*, United Nations office for the Coordination

of Humanitarian Affairs, Geneva, Switzerland, International Decade for Natural Disaster Reduction (IDNDR).

121. Inc. ABAQUS, Pawtucket, Rhode Island.

122. Inel, M., Ozmen, H. B., and Bilgin, H. 2008. Re-evaluation of Building Damage during Recent Earthquakes in Turkey. *Engineering Structures*, **30**:412-427.

123. Iwan, W. D. 1980. Estimating Inelastic Response Spectra from Elastic Spectra. *Earthquake Engineering & Structural Dynamics*, **8** (4):375-388.

124. Jaiswal, K., and Wald, D. J. 2008. *Creating a Global Building Inventory for Earthquake Loss Assessment and Risk Management* U.S. Geological Survey, pp 103.

125. Johansson, J., Mayorca, P., Torres, T., and Leon, E. 2007. *A Reconnaisance Report on The Pisco, Peru Earthquake of August 15, 2007* http://shake.iis.u-tokyo.ac.jp/Peru2007/JSCE_JAEE_Report/Index.htm, Japan Society of Civil Engineers (JSCE), Japan Association for Earthquake Engineering (JAEE), and Institute of Industrial Science, University of Tokyo.

126. Kadir, M. R. A. 1974. The Structural Behaviour of Masonry Infill Panels in Framed Structures, Ph.D. Thesis, University of Edinburgh.

127. Kappos, A. J., Panagopoulos, G., Panagiotopoulos, C., and Penelis, G. 2006. A Hybrid Method for the Vulnerability Assessment of R/C and URM Buildings. *Bulletin of Earthquake Engineering*, **4** (4):391-413.

128. Kappos, A. J., Pitilakis, K., and Stylianidis, K. C. 1995. Cost-Benefit Analysis for the Seismic Rehabilitation of Buildings in Thessaloniki, Based on a Hybrid Method of Vulnerability Assessment. In *Proceedings of the Fifth International Conference on Seismic Zonation*, at France, 406-413.

129. Kappos, A. J., Stylianidis, K. C., and Pitilakis, K. 1998. Development of Seismic Risk Scenarios Based on a Hybrid Method of Vulnerability Assessment. *Natural Hazards*, **17** (2):177-192.

130. Kaushik, H. B., and Manchanda, S. V. 2010. Influence of Ductile Detailing on Behavior of Masonry Infilled RC Frames. Paper read at Proceedings of the *14th European Conference on Earthquake Engineering*, at Ohrid, Macedonia.

131. Kaushik, H. B., Rai, D. C., and Jain, S. K. 2007. Stress-strain characteristics of clay brick masonry under uniaxial compression. *Journal of Materials in Civil Engineering*, **19** (9):728-739.

132. Khose, V. N., and Singh, Y. 2012. An Anomaly in Equivalent Linearization Approach for Estimation of Inelastic Response (Accepted). *Earthquake Spectra*.

133. Khuntia, M., and Ghosh, S. K. 2004. Flexural Stiffness of Reinforced Concrete Columns and Beams: Analytical Approach. *ACI Structural Journal*, **101** (3):351-363.

134. Kim, J., and LaFave, J. M. 2007. Key Influence Parameters for the Joint Shear Behaviour of Reinforced Concrete (RC) Beam–Column Connections. *Engineering Structures*, **29** (10):2523-2539.

135. King, G. J. W., and Pandey, D. C. 1978. The Analysis of Infilled Frames Using Finite Elements. Proceedings of the *Institution of Civil Engineers*, **65**:749-760.

136. Kitayama, K., Otani, S., and Aoyama, H. 1991. *Development of Design Criteria for RC Interior Beam–Column Joints*. Edited by J. O. Jirsa, Design of beam–column joints for seismic resistance (SP123) Michigan, American Concrete Institute, pp 97–123.

137. Klinger, R. E., and Bertero, V. V. 1978. Earthquake Resistance of Infilled Frames. *Journal of Structural Division,* Proceedings of the *American Society of Civil Engineers*, **104** (ST6):973-989.

138. Kowalsky, M. J. 1994. Displacement-Based Design-a Methodology for Seismic Design Applied to Rc Bridge Columns, Master's Thesis, University of California at San Diego, La Jolla, California.

139. Krawinkler, H., and Nassar, A. A. 1992. Seismic design based on ductility and cumulative damage demands and capacities. In *Nonlinear seismic analysis and design of reinforced concrete buildings*, edited by P. Fajfar and H. Krawinkler. New York. Elsevier.

140. Kumar, A. 2010. Effects of Torsion in Seismic Response of Buildings, Master's Thesis, Department of Earthquake Engineering, Indian Institute of Technology Roorkee, Roorkee, India.

141. Kumar, R., and Singh, Y. 2010. Stiffness of Reinforced Concrete Frame Members for Seismic Analysis. *American Concrete Journal*, **107** (5):607-615.

142. Kwan, W.P., and Billington, S. L. 2003. Influence of Hysteretic Behavior on Equivalent Period and Damping of Structural Systems. *Journal of Structural Engineering; American Society of Civil Engineers (ASCE)*, **129** (5):576-585.

143. LaFave, J. M., and Shin, M. 2005. Discussion of "Modeling reinforced-concrete beam-column joints subjected to cyclic loading" *Journal of Structural Engineering; American Society of Civil Engineers (ASCE)*, **131** (6):992-993.

144. Lang, D. H., Singh, Y., and Prasad, J. S. R. 2012. Comparing Empirical and Analytical Estimates of Earthquake Loss Assessment Studies for the City of Dehradun, India. *Earthquake Spectra*, **28** (2):595-619.

145. Lehman, D. E., and Moehle, J. P. 2000. *Seismic Performance of Wellconfined Concrete Bridge Columns*, PEER Rep. 98/01 University of California at Berkeley, Pacific Earthquake Engineering Research Center.

146. Leon, R. T. 1990. Shear Strength and Hysteretic Behavior of Interior Beam-Column Joints. *ACI Structural Journal, American Concrete Institute*, **87** (1):3-11.

147. Liauw, T. C., and Kwan, K. H. 1984. New Developments in Research on Infilled Frames. In *Proceedings of the 8th World Conference on Earthquake Engineering*, at San Fransisco, 623-630.

148. Liauw, T. C., and Kwan, K. H. 1985b. Unified Plastic Analysis for Infilled Frames. *Journal of Structural Engineering; American Society of Civil Engineers (ASCE)*, **111** (7):1427-1448.

149. Liauw, T. C., and Lee, S. W. 1977. On the Behaviour and the Analysis of Multi-Storey Infilled Frames Subject to Lateral Loading. Proceedings of the *Institution of Civil Engineers*: 641-656.

150. Liel, A. B., Haselton, C. B., Deierlein, G. G., and Baker, J. W. 2009. Incorporating Modeling Uncertainties in the Assessment of Seismic Collapse Risk of Buildings. *Structural Safety*, **31** (2):197-211.

151. Lofti, H. R., and Shing, P. B. 1994. Interface Model Applied to Fracture of Masonry Structures. Proceedings of the *American Society of Civil Engineers, Journal of Structural Engineering*, **120** (1):63-80.

152. Lourenco, P. B. 1996. Computatinal Strategies for Masonry Structures, Delft University of Technology, Netherlands.

153. Lowes, L. N., and Altoontash, A. 2003. Modeling Reinforced-Concrete Beam-Column Joints Subjected to Cycling Loading. *Journal of Structural Engineering; American Society of Civil Engineers (ASCE)*, **129** (12):1686–1697.

154. Luco, N., and Cornell, C. A. 2007. Structure-Specific Scalar Intensity Measures for Near-Source and Ordinary Earthquake Ground Motions. *Earthquake Spectra*, **23** (2):357-392.

155. M.J.N. Priestley, G.M. Calvi, and M.J. Kowalsky. 2007. *Displacement Based Seismic Design of Structures*. Pavia, Italy, IUSS Press.

156. Madan, A., Reinhorn, A. M., Mander, J. B., and Valles, R. E. 1997. Modeling of Masonry Infill Panels for Structural Analysis. *Journal of Structural Engineering; American Society of Civil Engineers (ASCE)*, **123** (10):1295-1302.

157. Mainstone, R. J. 1971. On the Stiffnesses and Strengths of Infilled Frames. Proceedings of the *Institution of Civil Engineers, Supplement IV*: 57-90.

158. Mallick, D. V., and Severn, R. T. 1967. The Behavior of Infilled Frames Under Static Loading. Proceedings of the *Institution of Civil Engineering*, **39**:639-656.

159. Mander, J. B., Priestley, M. J. N., and Park, R. 1988. Theoretical Stress-Strain Model for Confined Concrete. *Journal of Structural Engineering; American Society of Civil Engineers (ASCE)*, **114** (8):1804-1826.

160. Maniyar, M. M., and Khare, R. K. 2011. Selection of Ground Motion for Performing Incremental Dynamic Analysis of Existing Reinforced Concrete Buildings in India. *Current Science*, **100** (5).

161. Masi, A. 2003. Seismic Vulnerability Assessment of Gravity Load Designed R/C Frames. *Bulletin of Earthquake Engineering*, **1** (3):371-395.

162. MCEER. 2000. *The Chi-Chi, Taiwan earthquake of September 21, 1999: Reconnaissance Report*. Vol. Technical Report MCEER-00-0003.

163. Medvedev, S. W., Sponheuer, W., and Karnik, V. 1965. *Seismic intensity scale version MSK 1964*, United Nation Educational, Scientific and Cultural Organization Paris, pp 7.

164. Mehrabi, A. B., and Shing, P. B. 1994. *Performance of Masonry-Infilled R/C Frames Under In-Plane Lateral Loads: Analytical Modelling* 1vols San Francisco, California, Proceedings from the NCEER Workshop on Seismic Response of Masonry, pp 44-50.

165. Mehrabi, A. B., Shing, P. B., Schuller, M. P., and Noland, J. L. 1996. Experimental Evaluation of Masonry-Infilled RC Frames. *Journal of Structural Engineering*, **122** (3):228-237.

166. Microsoft-Corp. 2010. *Excel 2010 (version 14)*, http://office.microsoft.com/en-us/excel/.

167. Miranda, E. 1993. Site Dependent Strength Reduction Factors. *Journal of Structural Engineering; American Society of Civil Engineers (ASCE)*, **119** (12):3503-3519.

168. Miranda, E. 2000. Inelastic Displacement Ratios for Structures on Firm Sites. *Journal of Structural Engineering; American Society of Civil Engineers (ASCE)*, **126** (10):1150-1159.

169. Mirza, S. A. 1990. Flexural Stiffness of Rectangular RC Columns. *ACI Structural Journal*, **87** (4):425-435.

170. Mitra, N., and Lowes, L. N. 2007. Evaluation, Calibration, and Verification of a Reinforced Concrete Beam–Column Joint Model. *Journal of Structural Engineering; American Society of Civil Engineers (ASCE)*, **133** (1105-120).

171. Moghaddam, H. A., and Dowling, P. J. 1987. *The State of the Art in Infilled Frames* London, Civil Engineering Department, Imperial College, ESEE Research Report No 87-2.

172. Molina, S., Lang, D. H., and Lindholm, C. D. 2010. SELENA - An Open-Source Tool for Seismic Risk and Loss Assessment using a Logic Tree Computation Procedure. *Computers & Geosciences*, **36** (3):257-269.

173. Mondkar, D. P., and Powell, G. H. 1975. *ANSR 1: General Purpose Program for Analysis of Nonlinear Structures Response*, EERC Report 75-37 UC Berkeley.

174. Moroni, M., Astroza, M., and Mesias, P. 1996. Displacement Capacity Required Storey Drift in Confined Masonry Buildings, Paper no. 1059. In *Proceedings of the 11th World Conference on Earthquake Engineering*, at Mexico.

175. Mosalam, K. M., P. Gergely, R.N. White, and Zawilinski, D. 1993. The Behavior of Frame with Concrete Block Infill Walls. Paper read at First Egyptian Conference on Earthquake Engineering at Hurghada, Egypt, 283-292.

176. Mouroux, P., and Le Brun, B. 2006. RISK-UE project: An Advanced Approach to Earthquake Risk Scenarios with Application to Different European Towns. In *Assessing and Managing Earthquake Risk*, edited by C. S. Oliveira, A. Roca and X. Goula: Springer Netherlands.

177. Muhsen, B. A., and Umemura, H. 2011. New Model for Estimation of Shear Strength of Reinforced Concrete Interior Beam-Column Joints. Paper read at The 12th East Asia-Pacific Conference on Structural Engineering and Construction, 2151-2159.

178. Naiem, F. 1989. *The Seismic Design Handbook*, *First Edition*. Van Nostrand Reinhold, New York.

179. Newmark, N. M., and Hall, W. J. 1982. *Earthqukae Spectra and Design*, Earthquake Engineering Research Institute, Berkeley, California 94704.

180. NZS-1170.5. 2004. *Structural Design Actions Part 5: Earthquake Actions-New Zealand*. Wellington, Standards Association of New Zealand.

181. NZS-3101:Part1. 2006. *Concrete Structures Standard*, *Part 1, Design of Concrete Structures*. Wellington, New Zealand, Standards Association of New Zealand.

182. NZS-4230. 2004. *Design of Reinforced Concrete Masonry Structures*. Wellington, New Zealand, Standards Association of New Zealand.

183. Ockleston, A. J. 1955. Load Tests on a Three Storey Reinforced Concrete Building in Johannesburg. *The Structural Engineer*, **33** (10):304-322.

184. Olsen, A. H., and Porter, K. A. 2010. *What We Know About Demand and Surge* University of Colorado, Colorado, Structural Engineering and Structural Mechanics SESM-10-1

185. Ordaz, M., and Pérez-Rocha, L. E. 1998. Estimation of strength-reduction factors for elastoplastic systems: a new approach. *Earthquake Engineering & Structural Dynamics*, **27** (9):889-901.

186. Otani, S. 1974. Inelastic Analysis of R/C Frame Structures. *Journal of the Structural Divisio; American Society of Civil Engineers (ASCE)*, **100** (7):1433-1449.

187. Özcebe, G., Ramirez, J., Wasti, S. T., and Yakut, A. 2003. *1 May 2003 Bingöl Earthquake Engineering Report* , http://www.seru.metu.edu.tr/archives.html, http://www.anatolianquake.org

188. Page, A. W. 1978. Finite Element Model for Masonry. *Journal of the Structural Division, ASCE*, **104**:1267-1285.

189. Pagni, C. A., and Lowes, L. N. 2004. *Predicting Earthquake Damage in Older Reinforced Concrete Beam-Column Joints*, Pacific Earthquake Engineering Research Center.

190. Pampanin, S., Magenes, G., and Carr, A. J. 2003. Modelling of Shear Hinge Mechanism in Poorly Detailed RC Beam-Column Joints. In *Fib Symposium on Concrete Structures in Seismic Regions*, at Athens, Greece.

191. Panagiotakos, T. B., and Fardis, M. N. 1996. Seismic Response of Infilled RC Frames Structures, Paper no. 225. In Proceedings of the *11th World Conference on Earthquake Engineering*, at Mexico.

192. Park, R., and Paulay, T. 1975. *Reinforced Concrete Structures*, John Wiley & Sons.

193. Park, S., and Mosalam, K. M. 2009. *Shear Strength Models of Exterior Beam–Column Joints without Transverse Reinforcement*, PEER report 2009/106 Berkeley, Pacific Earthquake Engineering Research Center, University of California.

194. Park, S., and Mosalam, K. M. 2012. Analytical Model for Predicting Shear Strength of Unreinforced Exterior Beam-Column Joints. *ACI Structural Journal*, **109** (2):149-159.

195. Paul, D. K., Singh, Y., Dube, R. N., and Sekar, K. 2004. *Damage to Andaman & Nicobar Island Due to Tsunamigenic Earthquake of December*

26, 2004 National Disaster Management Division, Ministry of Home Affairs, Government of India, Department of Earthquake Engineering, Indian Institute of Technology Roorkee.

196. Paulay, T., and Priestley, M. J. N. 1992. *Seismic Design of Reinforced Concrete and Masonry Buildings*. New York, U.S.A., John Wiley & Sons.

197. Pennucci, D., Sullivan, T. J., and Calvi, G. M. 2011. Displacement Reduction Factors for the Design of Medium and Long Period Structures. *Journal of Earthquake Engineering*, **15** (sup1):1-29.

198. Polyakov, S. V. 1956. Masonry in Framed Buildings (An Investigation into the Strength and Stiffness of Masonry Infilling). In *Gosudarstvennoe izdatel'stvo Literatury po stroitel'stvu i arkhitekture*, at Moscow (English translation by G. L. Cairns, National Lending Library for Science and Technology, Boston, Yorkshire, England, 1963).

199. Polyakov, S. V. 1960. *On the Interaction between Masonry Filler Walls and Enclosing Frame When Loaded in the Plane of the Wall*, San francisco, Earthquake Engineering Research Institute, pp 36-42.

200. Powell, G., and Chen, P. 1986. 3D Beam-Column Element with Generalized Plastic Hinges. *Journal of Engineering Mechanics, American Society of Civil Engineers (ASCE)*, **112** (7):627-641.

201. Prasad, J. S. R. 2009. Seismic Vulnerability and Risk Assessment of Indian Urban Housing, Ph.D. Thesis, Department of Earthquake Engineering, Indian Institute of Technology Roorkee, India.

202. Prasad, J. S. R., Singh, Y., Kaynia, A. M., and Lindholm, C. 2009. Socioeconomic Clustering in Seismic Risk Assessment of Urban Housing Stock. *Earthquake Spectra*, **25** (3):619-641.

203. Priestley, M. J. N. 1980. Chapter 6: Masonry Structures in Design of Earthquake Resistant Structures, edited by E. Rosenbleeth: Pentech Press, London.

204. Priestley, M. J. N. 1993. Myths and Fallacies in Earthquake Engineering. *Bulletin of NZ National Society for Earthquake Engineering*, **26** (3):329-341.

205. Priestley, M. J. N. 2000. Direct Displacement Based Design. In *12t^h Conference on Earthquake Engineering*,

206. Priestley, M. J. N. 2003. *Myths and Fallacies in Earthquake Engineering, Revisited*. Pavia, Italy, 9th Mallet-Milne Lecture, IUSS Press.

207. Priestley, M. J. N., and Calvi, G. M. 1991. Towards a Capacity-Design Assessment Procedure for Reinforced Concrete Frames. *Earthquake Spectra*, **7** (3):413-437.

208. Priestley, M. J. N., Calvi, G. M., and Kowalsky, M. J. 2007. *Displacement Based Seismic Design of Structures*. Pavia, Italy, IUSS Press.

209. Priestley, M. J. N., Verma, R., and Xiao, Y. 1994. Seismic Shear Strength of Reinforced Concrete Columns. *Journal of Structural Engineering; American Society of Civil Engineers (ASCE)*, **120** (8):2310-2329.

210. Qi, X., and Moehle, J. P. 1991. *Displacement Design Approach for Reinforced Concrete Structures Subjected to Earthquakes*. Vol. UCB/EERC-91/02.

211. Riddell, R., Garcia, J. E., and Garces, E. 2002. Inelastic deformation response of SDOF systems subjected to earthquakes. *Earthquake Engineering & Structural Dynamics*, **31** (3):515-538.

212. Riddell, R., Hidalgo, P., and Cruz, E. 1989. *Response Modification Factors for Earthquake Resistant Design of Short Period Buildings*. Vol. 5, EERI.

213. Riddington, J. R. 1984. The Influence of Initial Gaps on Infilled Frame Behavior. Proceedings of the *Institution of Civil Engineers*, **part 2**:295-310.

214. Rivero, C. E., and Walker, W. H. 1984. An Analytical Study of the Interaction of Frames and Infill Masonry Walls. In Proceedings of *8th World Conference on Earthquake Engineering*, 591-598.

215. Roca, A., Goula, X., Susagna, T., Chávez, J., González, M., and Reinoso, E. 2006. A Simplified Method for Vulnerability Assessment of Dwelling Buildings and Estimation of Damage Scenarios in Catalonia, Spain. *Bulletin of Earthquake Engineering*, **4** (2):141-158.

216. Rosenbleath, E., and Herrera, I. 1964. On a Kind of Hysteretic Damping. *Journal of Engineering Mechanics Division; American Society of Civil Engineers (ASCE)*, **90**:37-48.

217. Rossetto, T., and Elnashai, A. 2003. Derivation of Vulnerability Functions for European-Type RC Structures Based on Observational Data. *Engineering Structures*, **25** (10):1241-1263.

218. Rossetto, T., and Elnashai, A. 2005. A New Analytical Procedure for the Derivation of Displacement-Based Vulnerability Curves for Populations of RC Structures. *Engineering Structures*, **7** (3):397-409.

219. Rots, J. G. 1991. Numerical Simulation of Cracking in Structural Masonry. *Heron*, **36** (2):49-63.

220. RUAUMOKO. Inelastic Dynamic Analysis Program. Department of Civil Engineering, University of Canterbury, Christchurch, New Zealand.

221. Ruiz-García, J., and Miranda, E. 2004. *Inelastic Displacement Ratios for Design of Structures on Soft Soils Sites*. Vol. 130, *American Society of Civil Engineers (ASCE)*.

222. Rupakhety, R., and Sigbjörnsson, R. 2009. Ground-Motion Prediction Equations (GMPEs) for inelastic Displacement and Ductility Demands of Constant-Strength SDOF Systems. *Bull Earthquake Eng.*, **7**:661-679.

223. Saatcioglu, M., Mitchell, D., Tinawi, R., Gardner, N. J., Gillies, A. G., Ghobarah, A., Anderson, D. L., and Lau, D. 2001. The August 17, 1999, Kocaeli (Turkey) earthquake — damage to structures. *Canadian Journal of Civil Engineering*, **28**:715–737.

224. Sabetta, F., Goretti, A., and Lucantoni, A. 1998. Empirical Fragility Curves from Damage Surveys and Estimated Strong Ground Motion. In *11th European Conference on Earthquake Engineering*, at Paris.

225. Sahota, M. K., and Riddington, J. R. 2001. Experimental Investigation into Using Lead to Reduce Vertical Load Transfer in Infilled Frames. *Engineering Structures*, **23** (1):94-101.

226. Saneinejad, A., and Hobbs, B. 1995. Inelastic Design of Infilled Frames. *Journal of Structural Engineering; American Society of Civil Engineers (ASCE)*, **121** (4):634-650.

227. Schnobrich, W. C. 1985. The Role of Finite Element Analysis of Reinforced Concrete Structures. Paper read at Proceedings of Seminar on Finite Element Analysis of Reinforced Concrete Structures, at Tokyo, Japan, 1-24.

228. Schriver, A. B. et al. 1989. Dynamic Loading of Brick Panel Infills. *Proceedings of 5th Canadian Masonry Symposium*: 415-424.

229. Sezen, A., A.S., W., K.J., E., and K.M., M. 2003. Performance of reinforced concrete buildings during the August 17, 1999 Koceli, Turkey earthquake, and seismic design and construction practice in Turkey. *Engineering Structures*, **25** (103-114).

230. Sezen, H. 2002. Seismic Behavior and Modeling of Reinforced Concrete Building Columns, University of California, Berkeley.

231. Sezen, H., and Moehle, J. P. 2004. Shear Strength Model for Lightly Reinforced Concrete Columns. *Journal of Structural Engineering; American Society of Civil Engineers (ASCE)*, **130** (11):1692-1703.

232. Sharma, A., Eligehausen, R., and Reddy, G. R. 2011a. A New Model to Simulate Joint Shear Behavior of Poorly Detailed Beam-Column Connections in RC Structures under Seismic Loads, Part I: Exterior Joints. *Engineering Structures*, **33** (3):1034-1051.

233. Sharma, M. L., Sinhval, A., Singh, Y., and Maheshwari, B. K. 2011b. *Damage Survey Report for Sikkim Earthquake of September 18, 2011* India, Indian Institute of Technology Roorkee.

234. Shin, M., and LaFave, J. M. 2004. Testing and Modelling for Cyclic Joint Shear Deformations in RC Beam-Column Connections. In *13th World Conference on Earthquake Engineering*.

235. Shing, P. B., Lotfi, H. R., Barzegarmehrabi, A., and Brunner, J. 1992. Finite Element Analysis of Shear Resistance of Masonry Wall Panels with and without Confining Frames. Paper read at Proceedings of 10th World Conference on Earthquake Engineering, at Madrid, Spain, 2581-2586.

236. Shome, N., and Cornell, C. A. 1999. *Probabilistic Seismic Demand Analysis of Nonlinear Structures*, RMS-35, RMS Program. Stanford University, Stanford. URL http://pitch.stanford.edu/rmsweb/Thesis/NileshShome.pdf.

237. Singh, H., Paul, D. K., and Sastry, V. V. 1998. Inelastic Dynamic Response of Reinforced Concrete Infilled Frames. *Computers & Structures*, **69** (6):685-693.

238. Singh, Y., Lang, D. H., Prasad, J. S. R., and Deoliya, R. 2012. An Analytical Study on the Seismic Vulnerability of Masonry Buildings in India. *Journal of Earthquake Engineering*, **17** (3):399-422.

239. Singhal, A., and Kiremidjian, A. S. 1996. Method for Probabilistic Evaluation of Seismic Structural Damage. *Journal of Structural Engineering; American Society of Civil Engineers (ASCE)*, **122** (12):1459-1467.

240. Sinha, R., Aditya, K. S. P., and Gupta, A. 2008. GIS-based Urban Seismic Risk Assessment Using RISK.iitb. *ISET Journal of Earthquake Engineering*, **45** (3-4).

241. Smith, B. S. 1962. Lateral Stiffness of Infilled Frames. *ASCE Journal of Structural Division*, **88** (ST6):183-199.

242. Smith, B. S. 1967. Methods for Predicting the Lateral Stiffness and Strength of Multi-Storey Infilled Frames. *Building Science*, **2** (3):247-257.

243. Smith, B. S. 1968. Model Test Results of Vertical and Horizontal Loading of Infilled Frames. *Journal of the American Concrete Institute*, **65**:618-624.

244. Smith, B. S., and Carter, C. 1969. A method of Analysis for Infilled Frames. *Proceedings of the Institution of Civil Engineers*, **44**:31-48.

245. Smith, B. S., and Coull, A. 1991. *Tall Building Structures: Analysis and Design*, Wiley-Inter science.

246. Smith, B.S. 1966. Behaviour of Square Infilled Frames. *Journal of the Structural Division; American Society of Civil Engineers (ASCE)*, **92 (ST1)**:381-403.

247. Spence, R. J. S., Coburn, A. W., and Pomonis, A. 1992. Correlation of Ground Motion with Building Damage: The Definition of a New Damage-Based Seismic Intensity Scale. In *10th World Conference on Earthquake Engineering*, at Madrid, Spain.

248. Spence, R. J. S., Coburn, A. W., Sakai, S., and Pomonis, A. 1991. *A Parameterless Scale of Seismic Intensity for use in seismic risk analysis and vulnerability assessment*. Edited by S. o. E. a. C. E. Dynamics, *Earthquake Blast and Impact: Measurement and effects of vibration*. Amsterdam, Taylor & Francis.

249. Strasser, F. O., Bommer, J. J., Şeşetyan, K., Erdik, M., Çağnan, Z., Irizarry, J., Goula, X., Lucantoni, A., Sabetta, F., Bal, I. E., Crowley, H., and Lindholm, C. 2008. A Comparative Study of European Earthquake Loss Estimation Tools for a Scenario in Istanbul. *Journal of Earthquake Engineering*, **12** (sup2):246-256.

250. Syrmakezis, C. A., and Vratsanou, V. Y. 1986. Influence of Infill Walls to RC Frames Response. Paper read at Proc., 8th European Conf. on Earthquake Engineering Structures, at Istanbul, Turkey, 47-53.

251. Thiruvengadam, V. 1985. On the Natural Frequencies of Infilled Frames. . *Earthquake Engineering & Structural Dynamics*, **13**:401-419.

252. Townsend, W. H., and Hanson, R. D. 1973. Hysteresis Loops for Reinforced Concrete Beam-Column Connections. In the Proceedings of *5th World Conference on Earthquake Engineering*, 1131–1134.

253. UBC. 1994. *Uniform Building Code*. Whittier, California, International conference of building officials.

254. Unal, M., and Burak, B. 2012. Joint Shear Strength Prediction for Reinforced Concrete Beam-To-Column Connections. *Structural Engineering and Mechanics*, **41** (3):421-440.

255. Vamvatsikos, D. 2005a. Seismic Performance, Capacity and Reliability of Structures as Seen Through Incremental Dynamic Analysis, Ph.D. Thesis, Department of Civil and Environmental Engineering, Stanford University, Stanford, CA.

256. Vamvatsikos, D., and Cornell, C. A. 2002. Incremental Dynamic Analysis. *Earthquake Engineering & Structural Dynamic. 2002*, **31**:491-514.

257. Vamvatsikos, D., and Cornell, C. A. 2005b. Direct Estimation of the Seismic Demand and Capacity of MDOF systems through Incremental Dynamic Analysis of an SDOF approximation *Journal of Structural Engineering; American Society of Civil Engineers (ASCE)*, **131** (4):1-20.

258. Vamvatsikos, D., and Cornell, C. A. 2006. Direct Estimation of the Seismic Demand and Capacity of Oscillators with Multi-Linear Static Pushovers through IDA. *Earthquake Engineering & Structural Dynamics*, **35** (9):1097-1117.

259. Veletsos, A. S., and Newmark, N. M. 1960. Effect of Inelastic Behaviour on the Response of Simple Systems to Earthquake Motions. In *2nd World Conference on Earthquake Engineering*, 895-912.

260. Vidic, T., Fajfar, P., and Fischinger, M. 1994. Consistent inelastic design spectra: Strength and Displacement. *Earthquake Engineering & Structural Dynamics*, **23** (5):507-521.

261. Vollum, R. L., and Newman, J. B. 1999. Strut and Tie Models for Analysis/Design of External Beam-Column Joints. *Magazine of Concrete Research*, **51** (6):415-425.

262. Walker, S. G. 2001. Seismic Performance of Existing Reinforced Concrete Beam-Column Joints, Department of Civil and Environmental Engineering, University of Washington.

263. Wallace, J. W. 1999. Building Performance in the 17 August 1999 IZMIT (Kocaeli), Turkey Earthquake. In *CUREe Open Symposium*.

264. Wen, Y. K., Ellingwood, B. R., and Bracci, J. 2004. *Vulnerability Function Framework for Consequence-based Engineering*. Vol. DS-4, MAE Center Project DS-4 Report

265. Whitman, R. V., Reed, J. W., and Hong, S. T. 1973. Earthquake Damage Probability Matrices. In Proceedings of the *5th World Conference on Earthquake Engineering*, at Rome, Italy, 2531-2540.

266. Wood, R. H. 1978. Plasticity, Composite Action and Collapse Design of Unreinforced Shear Wall Panels in Frames. *ICE Proceedings*, **65** (2):381-411.

267. Xue, Q., and Chen, C.-C. 2003. Performance-based seismic design of structures: a direct displacement-based approach. *Engineering Structures*, **25** (14):1803-1813.

268. Yakut, A. 2004. Preliminary Seismic Performance Assessment Procedure for Existing RC Buildings. *Engineering Structures*, **26** (10):1447-1461.

269. Yeh, C. H., Loh, C. H., and Tsai, K. C. 2006. Overview of Taiwan Earthquake Loss Estimation System. *Natural Hazards*, **37** (1-2):23-37.

270. Youssef, M., and Ghobarah, A. 2001. Modelling of RC Beam-Column

Joints and Structural Walls. *Journal of Earthquake Engineering*, **5** (1):93-111.

271. Yuksel, E., Ilki, A., Erol, G., Demir, C. E. M., and Karadogan, H. F. 2006. Seismic Retrofit of Infilled Reinforced Concrete Frames With CFRP Composites. In *Advances in Earthquake Engineering for Urban Risk Reduction*, edited by S. T. Wasti and G. Ozcebe: Springer Netherlands.

272. Zarfam, P., and Mofid, M. 2009. Evaluation of modal incremental dynamic analysis, using input energy intensity and modified bilinear curve. *The Structural Design of Tall and Special Buildings*, **18** (5):573-586.

273. Zhuge, Y., Thambiratnam, D., and Corderoy, J. 1998. Nonlinear Dynamic Analysis of Unreinforced Masonry. *Journal of Structural Engineering*, **124** (3):270-277.

LIST OF PUBLICATIONS OF AUTHOR RELATED TO THE THESIS WORK

A. *REFEREED JOURNALS*

1. **Putul Haldar** and Yogendra Singh (2009), "Seismic Performance and Vulnerability of Indian Code Designed RC Frame Buildings," ***ISET Journal of Earthquake Engineering***, Paper No. 502, Vol. 46, No. 1, March 2009, pp. 29-45.

2. **Putul Haldar** and Yogendra Singh and D. K. Paul (2012), "Effect of URM Infills on Seismic Vulnerability of Indian Code Designed RC Frame Buildings", ***Earthquake Engineering and Engineering Vibration,*** Vol. 11, No. 2, June 2012, pp. 1-9.

3. **Putul Haldar** and Yogendra Singh (2012), "Modelling of URM Infills and their Effect on Seismic Behaviour of RC Frame Buildings," Special Issue on Advances in Infilled Framed Structures: Experimental & Modelling Aspects, in ***The Open Construction and Building Technology Journal***, Bentham Science Publishers, Vol. 6, (Suppl 1-M1), October 2012, pp. 35-41.

4. **Putul Haldar**, Yogendra Singh, Dominik. H. Lang and D. K. Paul (2013), "Comparison of Seismic Risk Assessment Based on Macroseismic Intensity and Spectrum Approaches using 'SeisVARA'", ***Soil Dynamics and Earthquake Engineering***, Vol. 48, May 2013, pp. 267-281.

5. **Putul Haldar**, Yogendra Singh and D. K. Paul (2013), "Identification of Failure Modes of URM Infilled RC Frame Buildings", ***Engineering Failure Analysis***, Vol. 33, pp. 97-118.

B. *REFEREED CONFERENCE PROCEEDINGS/SYMPOSIUMS*

1. **Putul Haldar** Yogendra Singh and D. K. Paul (2013), "Modeling of URM Infills and Their Effect on Seismic Vulnerability of RC Frame Buildings", ***Proceedings of the International Conference on Engineering Research, Innovation and Education*** **2013**, ICERIE 2013, 11− 13 January, SUST, Sylhet, Bangladesh, Paper No. ICERIE – 301.

2. **Putul Haldar** Yogendra Singh and D. K. Paul (2012), "Estimation of Capacity Curve Parameters for Indian RC Frame Buildings with URM Infills", ***15th World Conference on Earthquake Engineering***, September 24-28, Lisbon, Portugal.

3. **Putul Haldar**, Yogendra Singh, Domimik. H. Lang and D.K. Paul (2010), "IVARA – A Tool for Seismic Vulnerability and Risk Assessment of Indian Housing," ***14th Symposium on Earthquake Engineering***, Department of Earthquake Engineering, IIT, Roorkee, December 17-19, 2010, pp. 1405-1415.

4. **Putul Haldar**, Yogendra Singh and D.K. Paul (2009), "Seismic Vulnerability of URM Infilled RC Buildings," ***National Seminar on Research Activities for Disaster Mitigation in Housing in India***, August 22-23, Roorkee, India, pp. 230-242.

5. Yogendra Singh, Ratnesh Kumar and **Putul Haldar** (2009), "Earthquake Resistant Design & Construction Practices in India", ***Second India Disaster Management Congress – IDMC 2009***, November 4-6, Vigyan Bhaban, New Delhi, paper no. A1-SOA.

6. Yogendra Singh and **Putul Haldar** (2009), "Estimation of Seismic Performance of IS Code Designed RC Frame Buildings," ***Proc. Trends and Challenges in Structural Engineering and Construction Technology***, February 11-12, CBRI, Roorkee, India, pp. 534-535.

7. Yogendra Singh and **Putul Haldar** (2008), "Modern Trends in Earthquake Resistant Design of Structures," ***Proc. National Conference on Emerging Trends in Civil Engineering for Infrastructure Development,*** February 15-16, NIT Raipur, pp. 14-27.

C. ***ACADEMIC HONOR/AWARDS***

Received **Young Scientist Award** in ***5th Uttarakhand State Science and Technology Congress-2010***, under the discipline of Engineering Science and Technology.